RSALOP

Radionuclide Soil Action Levels Oversight Panel

RESRAD Documentation

Compiled by:

AIMSI

Advanced Integrated Management Services, Inc.
5460 Ward Road, Suite 370
Arvada, CO 80002
(303) 456-0884 fax. (303) 456-0858

1/22/1

1998/1999/2000

ANL/EAD/TM-84

External Exposure Model Used in the RESRAD Code for Various Geometries of Contaminated Soil

Environmental Assessment Division

Argonne National Laboratory

Operated by The University of Chicago,
under Contract W-31-109-Eng-38, for the

United States Department of Energy

Argonne National Laboratory

Argonne National Laboratory, with facilities in the states of Illinois and Idaho, is owned by the United States Government, and operated by the University of Chicago under the provisions of a contract with the Department of Energy.

This technical memo is a product of Argonne's Environmental Assessment Division (EAD). For information on the division's scientific and engineering activities, contact:

Director, Environmental Assessment Division
Argonne National Laboratory
Argonne, Illinois 60439-4815
Telephone (630) 252-3107

Presented in this technical memo are preliminary results of ongoing work or work that is more limited in scope and depth than that described in formal reports issued by the EAD.

Publishing support services were provided by Argonne's Information and Publishing Division (for more information, see IPD's home page: http://www.ipd.anl.gov/).

Disclaimer

Reproduced directly from the best available copy.

Available to DOE and DOE contractors from the Office of Scientific and Technical Information, P.O. Box 62, Oak Ridge, TN 37831; prices available from (423) 576-8401.

Available to the public from the National Technical Information Service, U.S. Department of Commerce, 5285 Port Royal Road, Springfield, VA 22161.

ANL/EAD/TM-84

External Exposure Model Used in the RESRAD Code for Various Geometries of Contaminated Soil

by S. Kamboj, C. Yu, and D.J. LePoire

Environmental Assessment Division,
Argonne National Laboratory, 9700 South Cass Avenue, Argonne, Illinois 60439

September 1998

Work sponsored by United States Department of Energy, Assistant Secretary for Environment, Safety and Health, Office of Environmental Policy and Assistance, and Assistant Secretary for Environmental Management, Office of Environmental Restoration

4

This report is printed on recycled paper.

CONTENTS

TABLES

TABLES (Cont.)

TABLES (Cont.)

FIGURES

FIGURES (Cont.)

ACKNOWLEDGMENTS

The authors would like to thank Harold Peterson, Alexander Williams, and Andrew Wallo of the U.S. Department of Energy for their support of the project and review of the final report. We would also like to thank Keith Eckerman of the Oak Ridge National Laboratory and Christopher Nelson of the U.S. Environmental Protection Agency for providing comments on an earlier draft report. Finally, we thank Argonne's Information and Publishing Division, in particular John DePue of Technical Communication Services for editorial assistance and the staff of Document Production for document preparation and publishing.

NOTATION

The following is a list of the acronyms, initialisms, and abbreviations (including units of measure) used in this document. Some acronyms used only in tables or equations are defined in the respective tables or equations.

ACRONYMS, INITIALISMS, AND ABBREVIATIONS

AP	anteroposterior
DCF	dose conversion factor
DOE	U.S. Department of Energy
EDE	effective dose equivalent
EPA	U.S. Environmental Protection Agency
$F_A(Ei)$	energy dependent area factor
F_a^{nuc}	radionuclide specific area factor
F_{CD}	cover-and-depth factor
F_D	depth factor
FGR-12	Federal Guidance Report No. 12
F_S	shape factor
ICRP	International Commission on Radiological Protection
ISO	isotropic
LAT	lateral
MCNP	Monte Carlo N-particle Transport Code
PA	posteroanterior
RESRAD	*res*idual *rad*ioactive material guideline computer code
ROT	rotational

UNITS OF MEASURE

Bq	becquerel(s)	m^2	square meter(s)
cm	centimeter(s)	m^3	cubic meter(s)
cm^2	square centimeter(s)	MeV	million electron volt(s)
cm^3	cubic centimeter(s)	mrem	millirem(s)
g	gram(s)	pCi	picocurie(s)
keV	kiloelectron volt(s)	s	second(s)
kg	kilogram(s)	Sv	sievert(s)
m	meter(s)	yr	year(s)

EXTERNAL EXPOSURE MODEL USED IN THE RESRAD CODE FOR VARIOUS GEOMETRIES OF CONTAMINATED SOIL

by

S. Kamboj, C. Yu, and D.J. LePoire

ABSTRACT

An external exposure model based on the U.S. Environmental Protection Agency's (EPA's) Federal Guidance Report No. 12 (FGR-12) dose conversion factors and the point kernel method has been developed for the *res*idual *radi*oactive (RESRAD) material guideline computer code. This model improves the external ground pathway dose estimation from that in earlier versions of the RESRAD code by extending FGR-12 data applicability to a wider range of source geometries. FGR-12 assumes that sources are infinite in lateral extent. In actual situations, soil contamination sources can have any depth, shape, cover, and size. A depth factor function was developed to express the attenuation of radionuclides by using regression analysis. Three independent, nuclei-specific parameters were determined by using the effective dose equivalent values from FGR-12. The depth factors derived with the new model were within 2% of the FGR-12 values for all depths for most of the radionuclides. A cover-and-depth factor function was derived on the basis of the depth factor function by considering both dose contribution and attenuation from different depths. The cover-and-depth factor was compared with FGR-12 computations for some representative radionuclides and source configurations. For thin cover thicknesses (1 cm), most of the values were within 2%; even for large cover thicknesses (5 to 15 cm), most of the values were within 10%. To further extend this model for actual geometries (finite irregular areas), area and shape factors were derived by using the point kernel method. These factors depend not only on the lateral extent of the contamination but also on source depth, cover thickness, and gamma energies. The area factor increases with source radius and approaches unity for source radii greater than 50 m. To test the integrity of FGR-12 data, effective dose equivalent values at the surface and four soil depths were compared with the Monte Carlo N-Particle (MCNP) transport code calculations for a few radionuclides. MCNP values were within 10% of the FGR values for the four soil depths. Depth and cover factors were also compared with MCNP calculations. Finally, overall comparisons were

made between the new RESRAD model (Versions 5.60 and later) and the old RESRAD model (Version 5.44 and earlier).

12

1 INTRODUCTION

An external exposure model has been developed for Version 5.60 of the *res*idual *radi*oactive (RESRAD) material guideline computer code (Yu et al. 1993a). This model, which is based on the dose conversion factors from the U.S. Environmental Protection Agency's (EPA's) Federal Guidance Report No. 12 (FGR-12) (Eckerman and Ryman 1993) and the point kernel method, improves the external ground pathway dose calculations from those in earlier versions of RESRAD (Version 5.44 and earlier) (Yu et al. 1993a) and extends the applicability of FGR-12 to soil contamination of any size, shape, depth, and density.

Dose conversion factors (or coefficients) for external exposure relate the concentrations of radionuclides in environmental media to the doses to organs and tissues of the body. These dose coefficients include the energy and angular distributions of the radiations incident upon the body and the transport of these radiations within the body.

FGR-12 gives the dose coefficients for external exposure to photons and electrons emitted by radionuclides distributed in soil. The values are given for surface and uniformly distributed volume sources at four specific thicknesses (1, 5, and 15 cm and effectively infinite) with a soil density of 1.6 g/cm^3. FGR-12 assumes that sources are infinite in lateral extent. In actual situations, sources can have any depth, shape, cover, and size. The soil density is also not fixed at 1.6 g/cm^3. It varies with soil type. The dry density of most soils varies within the range of 1.1 to 1.6 g/cm^3 (Yu et al. 1993b). A depth factor function was developed to express the attenuation of radionuclides by using regression analysis. Three independent, nuclei-specific parameters were determined by using the effective dose equivalent values of FGR-12 at different depths. A cover-and-depth factor function was derived on the basis of the depth factor function by considering both dose contribution and attenuation from different depths. To further extend this model for actual geometries (finite, irregular areas), an area-and-shape factor was derived by using the point kernel method (Kocher and Sjoreen 1985); this factor depends not only on the lateral extent of the contamination, but also on source depth, cover thickness, and gamma energies.

Section 2 describes FGR-12 methodology. Cover-and-depth factor functions are described in Section 3. Section 3 also compares depth factor and cover-and-depth factor results with FGR-12 results. Section 4 discusses area and shape factors. A comparison of RESRAD models (Version 5.44 and earlier vs. 5.60 and later) is provided in Section 5 for the following items: dose conversion factors, cover and depth factors, area factors, and dose calculations. Section 6 presents the conclusions drawn. Section 7 lists the references cited in the report, and the Appendix discusses application of the Monte Carlo N-Particle (MCNP) transport code (Briesmeister 1993), the external effective dose equivalent calculations, and the comparison of MCNP calculations with those of FGR-12 and the new RESRAD model.

2 FGR-12 METHODOLOGY

The EPA publication FGR-12 (Eckerman and Ryman 1993) gives the effective dose coefficients for exposure to soil with a density of 1.6 g/cm^3 contaminated to thicknesses of 1, 5, and 15 cm and effectively infinite. The organ dose coefficients for isotropic plane sources at six source depths (0, 0.04, 0.2, 1.0, 2.5, and 4.0 mean free paths in soil) were integrated over source depths to compute organ dose coefficients for uniformly distributed volume sources. Dose coefficient calculations involved use of energy and angular distribution of radiation incident on the body due to monoenergetic radiation sources in contaminated soil, and transport and energy deposition of these incident particles in different organs of the body, to calculate the organ and tissue dose for the incident source and to calculate the effective dose equivalent for a specific radionuclide. The latter calculations took into account the radionuclide's energies and intensities of radiation emitted during nuclear transformation and different organ weighting factors.

Doses were first calculated for monoenergetic photon and electron sources at 12 energy levels, from 0.01 to 5.0 MeV. The results of these calculations were then used to derive the dose coefficients, taking into account the detailed nuclear decay data of each radionuclide. For organ dose calculations, a modified Cristy adult hermaphrodite phantom was used (Cristy and Eckerman 1987). The head region was modified from the original phantom to include a neck and esophagus model. This phantom represents a standing adult of 179 cm height and 73 kg mass. The weighting factors used to calculate the effective dose equivalent were those recommended by the EPA in *Radiation Protection Guidance to Federal Agencies for Occupational Exposure* (EPA 1987).

The FGR-12 dose coefficients are compared with MCNP calculational results. As shown in the Appendix, the MCNP results are within 7 to 19% of the FGR-12 results. The FGR-12 dose coefficients are also compared with the dose coefficients used in the previous versions of the RESRAD code. The results are presented in Section 5.

3 DEPTH AND COVER-AND-DEPTH FACTORS

3.1 DEVELOPMENT

The depth factor (F_D) is based on the fits to the FGR-12 dose conversion factors (*DCF*s) as a function of depth according to the following function:

$$F_D = \frac{DCF(T_s = t_s)}{DCF(T_s = \infty)} = 1 - Ae^{-K_A \rho t_s} - Be^{-K_B \rho t_s} \quad , \tag{1}$$

where

$DCF\,(T_s = t_s)$ = FGR-12 *DCF* at different depths,

t_s = source depth (cm),

ρ = soil density (g/cm^3),

A, B = fit parameters (dimensionless), and

K_A, K_B = fit parameters (cm^2/g).

The following constraints were applied for the four fitting parameters:

- All the parameters are forced to be positive.
- $A + B = 1$.
- In the limit source depth $t_s \rightarrow$ zero, the *DCF* should be consistent with the contaminated surface *DCF*.

This method was used to determine the four unknown parameters (A, B, K_A, and K_B) for 84 radionuclides available in RESRAD (Table 1). RESRAD has two radionuclide libraries, one with the cutoff half-life of 6 months (67 radionuclides) and another with the cutoff half-life of 30 days (84 radionuclides). Progeny radionuclides with a half-life less than the cutoff half-life are assumed to be in secular equilibrium with the parent radionuclide. The symbol "+D" is used to indicate that the short-lived decay product radionuclides are in equilibrium with the parent radionuclide and that their dose factors have been added to the parent dose factor.

15

TABLE 1 Four Fitted Parameters (A, B, K_A, and K_B) to Calculate Cover-and-Depth Factor for 84 Radionuclides

Radionuclide[a]	A	B	K_A	K_B
H-3	0.00	0.00	0.00	0.00
C-14	6.421×10^{-1}	3.579×10^{-1}	2.940×10^{-1}	3.369
Na-22	9.263×10^{-1}	7.37×10^{-2}	8.74×10^{-2}	1.331
Al-26	9.276×10^{-1}	7.24×10^{-2}	7.94×10^{-2}	1.284
S-35	3.405×10^{-1}	6.595×10^{-1}	3.312	2.846×10^{-1}
Cl-36	8.885×10^{-1}	1.115×10^{-1}	1.325×10^{-1}	1.886
K-40	7.26×10^{-2}	9.274×10^{-1}	1.269	7.70×10^{-2}
Ca-41	0.00	0.00	0.00	0.00
Ca-45	2.519×10^{-1}	7.481×10^{-1}	2.743	2.259×10^{-1}
Sc-46	7.29×10^{-2}	9.271×10^{-1}	1.352	8.53×10^{-2}
Mn-54	8.48×10^{-2}	9.152×10^{-1}	1.215	8.79×10^{-2}
Fe-55	0.00	0.00	0.00	0.00
Fe-59	9.276×10^{-1}	7.24×10^{-2}	8.19×10^{-2}	1.314
Co-57	9.288×10^{-1}	7.12×10^{-2}	1.604×10^{-1}	1.671
Co-60	9.235×10^{-1}	7.65×10^{-2}	7.83×10^{-2}	1.263
Ni-59	0.00	0.00	0.00	0.00
Ni-63	0.00	0.00	0.00	0.00
Zn-65	9.271×10^{-1}	7.29×10^{-2}	8.37×10^{-2}	1.327
Ge-68+D	9.270×10^{-1}	7.30×10^{-2}	9.94×10^{-2}	1.412
Se-75	6.85×10^{-2}	9.315×10^{-1}	1.552	1.245×10^{-1}
Sr-85	7.210×10^{-2}	9.279×10^{-1}	1.441	9.99×10^{-2}
Sr-89	8.998×10^{-1}	1.002×10^{-1}	1.279×10^{-1}	1.763
Sr-90+D	9.074×10^{-1}	9.260×10^{-2}	1.202×10^{-1}	1.699
Nb-94	9.275×10^{-1}	7.250×10^{-2}	9.10×10^{-2}	1.378
Nb-95	7.480×10^{-2}	9.252×10^{-1}	1.363	9.12×10^{-2}
Zr-95+D	9.298×10^{-1}	7.020×10^{-2}	9.30×10^{-2}	1.445
Tc-99	7.871×10^{-1}	2.129×10^{-1}	2.106×10^{-1}	2.589
Ru-106	9.271×10^{-1}	7.290×10^{-2}	9.57×10^{-2}	1.409
Ag-108m	9.282×10^{-1}	7.180×10^{-2}	9.67×10^{-2}	1.442
Ag-110m+D	9.261×10^{-1}	7.390×10^{-2}	8.74×10^{-2}	1.339
Cd-109	6.534×10^{-1}	3.466×10^{-1}	2.047×10^{-1}	4.753
Sn-113+D	9.272×10^{-1}	7.28×10^{-2}	1.070×10^{-1}	1.652
Sb-124	1.109×10^{-1}	8.891×10^{-1}	9.478×10^{-1}	7.38×10^{-2}
Sb-125	9.273×10^{-1}	7.270×10^{-2}	1.005×10^{-1}	1.507
Te-125m	7.763×10^{-1}	2.237×10^{-1}	3.481	3.700×10^{-1}
I-125	8.540×10^{-1}	1.460×10^{-1}	3.451	4.422×10^{-1}
I-129	4.350×10^{-1}	5.650×10^{-1}	7.137×10^{-1}	3.555
Cs-134	9.266×10^{-1}	7.34×10^{-2}	9.26×10^{-2}	1.379
Cs-135	7.254×10^{-1}	2.746×10^{-1}	2.508×10^{-1}	3.030
Cs-137+D	9.281×10^{-1}	7.19×10^{-2}	9.47×10^{-2}	1.411
Ce-141	9.187×10^{-1}	8.13×10^{-2}	1.457×10^{-1}	1.683
Ce-144+D	9.116×10^{-1}	8.84×10^{-2}	9.38×10^{-2}	1.411
Pm-147	7.726×10^{-1}	2.274×10^{-1}	2.087×10^{-1}	2.780

TABLE 1 (Cont.)

Radionuclide[a]	A	B	K_A	K_B
Sm-147	0.00	0.00	0.00	0.00
Sm-151	3.310×10^{-2}	9.669×10^{-1}	8.270×10^{-1}	4.926
Eu-152	9.100×10^{-1}	9.000×10^{-2}	8.40×10^{-2}	1.185
Eu-154	8.939×10^{-1}	1.061×10^{-1}	8.25×10^{-1}	1.008
Eu-155	8.569×10^{-1}	1.431×10^{-1}	1.912×10^{-1}	1.486
Gd-152	0.00	0.00	0.00	0.00
Gd-153	8.226×10^{-1}	1.774×10^{-1}	1.986×10^{-1}	1.983
Ta-182	9.233×10^{-1}	7.670×10^{-2}	8.49×10^{-2}	1.337
Ir-192	9.306×10^{-1}	6.940×10^{-2}	1.078×10^{-1}	1.482
Au-195	8.772×10^{-1}	1.228×10^{-1}	2.380×10^{-1}	1.880
Tl-204	8.679×10^{-1}	1.321×10^{-1}	2.068×10^{-1}	1.923
Pb-210+D	7.502×10^{-1}	2.498×10^{-1}	1.753×10^{-1}	2.200
Po-210	9.269×10^{-1}	7.310×10^{-2}	9.04×10^{-2}	1.385
Bi-207	9.246×10^{-1}	7.540×10^{-2}	8.89×10^{-2}	1.350
Ra-226+D	9.272×10^{-1}	7.280×10^{-2}	8.35×10^{-2}	1.315
Ra-228+D	9.266×10^{-1}	7.340×10^{-2}	8.77×10^{-2}	1.371
Ac-227+D	9.229×10^{-1}	7.710×10^{-2}	1.172×10^{-1}	1.512
Th-228+D	9.277×10^{-1}	7.230×10^{-2}	7.55×10^{-2}	1.262
Th-229+D	9.130×10^{-1}	8.700×10^{-2}	1.130×10^{-1}	1.491
Th-230	8.628×10^{-1}	1.372×10^{-1}	1.871×10^{-1}	4.033
Th-232	8.152×10^{-1}	1.848×10^{-1}	2.082×10^{-1}	5.645
Pa-231	9.295×10^{-1}	7.050×10^{-2}	1.163×10^{-1}	2.014
U-232	8.086×10^{-1}	1.914×10^{-1}	1.754×10^{-1}	6.021
U-233	8.889×10^{-1}	1.112×10^{-1}	1.394×10^{-1}	4.179
U-234	7.229×10^{-1}	2.771×10^{-1}	1.937×10^{-1}	7.238
U-235	9.292×10^{-1}	7.080×10^{-2}	1.383×10^{-1}	1.813
U-236	5.932×10^{-1}	4.068×10^{-1}	1.980×10^{-1}	8.379
U-238+D	8.590×10^{-1}	1.410×10^{-1}	9.19×10^{-2}	1.111
Np-237+D	9.255×10^{-1}	7.450×10^{-2}	1.228×10^{-1}	1.671
Pu-238	2.972×10^{-1}	7.028×10^{-1}	1.958×10^{-1}	9.011
Pu-239	8.002×10^{-1}	1.998×10^{-1}	1.348×10^{-1}	6.550
Pu-240	2.977×10^{-1}	7.023×10^{-1}	2.176×10^{-1}	8.997
Pu-241	9.132×10^{-1}	8.680×10^{-2}	1.582×10^{-1}	2.027
Pu-242	3.314×10^{-1}	6.686×10^{-1}	2.109×10^{-1}	8.982
Pu-244	9.259×10^{-1}	7.410×10^{-2}	9.26×10^{-2}	1.431
Am-241	8.365×10^{-1}	1.635×10^{-1}	3.130×10^{-1}	2.883
Am-243+D	9.098×10^{-1}	9.020×10^{-2}	1.473×10^{-1}	1.642
Cm-243	9.247×10^{-1}	7.530×10^{-2}	1.350×10^{-1}	1.662
Cm-244	7.0×10^{-3}	9.930×10^{-1}	8.461×10^{2}	2.194
Cm-248	7.333×10^{-1}	2.667×10^{-1}	1.042×10^{1}	1.215
Cf-252	6.505×10^{-1}	3.495×10^{-1}	7.259	0.182

[a] +D means that associated decay product radionuclides with half-lives of less than 30 days are included.

On the basis of depth factor function, the following cover-and-depth factor (F_{CD}) was derived by considering both dose contribution and attenuation from different depths:

$$F_{CD} = \frac{DCF(T_c = t_c, T_s = t_s)}{DCF(T_c = 0, T_s = \infty)} = Ae^{-K_A\rho_c t_c}(1 - e^{-K_A\rho_s t_s}) + Be^{-K_B\rho_c t_c}(1 - e^{-K_B\rho_s t_s}) \quad , \qquad (2)$$

where

t_c = cover thickness (cm),

ρ_c = cover density (g/cm^3),

t_s = source depth (cm), and

ρ_s = source density (g/cm^3).

3.2 DEPTH FACTOR COMPARISON WITH FGR-12 RESULTS

Results obtained by using the fit parameters are compared with the FGR-12 data in Table 2 for 84 radionuclides for four source thicknesses. Four radionuclides (Cm-244, Cm-248, I-125, and Sm-151) showed less than 10% variation in *DCF* between 1 cm and infinite depth values. Among these four, Sm-151 showed the smallest variation (1%). The overall comparison shows that most of the fit data are within 3% of the FGR-12 data, except for eight points. For these eight points, fit values are mostly higher than FGR data (two are 5% higher, one is 3.2% lower, and five are 4% higher). A statistical analysis of the comparison is summarized in Table 3.

3.3 COVER-AND-DEPTH FACTOR COMPARISON WITH FGR-12 RESULTS

The results of dose calculations using the cover-and-depth factor for a few geometries are compared with FGR-12 radionuclide-specific dose calculations in Table 4. The comparisons were done for cadmium-109, cesium-137, cobalt-60, manganese-54, and aluminum-26. For the FGR-12 calculations, the effective dose equivalent for a source thickness of 4 cm with 1 cm cover, for example, was obtained by subtracting the value for a 1-cm-thick source from the value for a 5-cm-thick source. For a cover thickness of 1 cm, most values from RESRAD calculations were within 2% of the FGR-12 values, and the maximum difference was 5%. For cover thicknesses of 5 cm and 15 cm, most values were within 10%, and the maximum difference was less than 20%.

18

TABLE 2 Fitted *DCFs* for 84 Radionuclides at 1, 5, and 15 cm and Effectively Infinitely Thick Sources and the Ratio of the Fitted Values to the FGR-12 Values

	Fitted DCF [(mrem/yr)/(pCi/g)]				Fit/FGR-12 Ratio			
Radionuclide[a]	1 cm	5 cm	15 cm	Infinite	1 cm	5 cm	15 cm	Infinite
Ac-227+D	4.60×10^{-1}	1.29	1.91	2.02	1.00	1.00	1.01	1.00
Ag-108m+D	1.92	5.54	8.80	9.67	1.00	1.00	1.02	1.00
Ag-110m+D	3.19	9.26	1.52×10^{1}	1.72×10^{1}	9.97×10^{-1}	9.97×10^{-1}	1.03	1.00
Al-26	3.01	8.81	1.50×10^{1}	1.74×10^{1}	9.89×10^{-1}	9.93×10^{-1}	1.03	9.95×10^{-1}
Am-241	2.15×10^{-2}	4.08×10^{-2}	4.38×10^{-2}	4.38×10^{-2}	1.00	1.00	9.99×10^{-1}	1.00
Am-243+D	2.46×10^{-1}	6.45×10^{-1}	8.73×10^{-1}	8.97×10^{-1}	9.99×10^{-1}	9.99×10^{-1}	1.00	1.00
Au-195	8.21×10^{-2}	1.81×10^{-1}	2.07×10^{-1}	2.08×10^{-1}	1.00	1.00	9.98×10^{-1}	1.00
Bi-207	1.78	5.13	8.37	9.40	1.00	1.00	1.03	1.00
C-14	8.06×10^{-6}	1.27×10^{-5}	1.35×10^{-5}	1.35×10^{-5}	1.00	1.00	1.00	1.00
Ca-41	0.00	0.00	0.00	0.00	-	-	-	-
Ca-45	2.98×10^{-5}	5.49×10^{-5}	6.24×10^{-5}	6.26×10^{-5}	1.00	1.00	9.97×10^{-1}	1.00
Cd-109	7.78×10^{-3}	1.28×10^{-2}	1.46×10^{-2}	1.47×10^{-2}	9.99×10^{-1}	9.98×10^{-1}	9.92×10^{-1}	9.98×10^{-1}
Ce-141	8.49×10^{-2}	2.27×10^{-1}	3.09×10^{-1}	3.18×10^{-1}	9.99×10^{-1}	1.00	9.86×10^{-1}	9.99×10^{-1}
Ce-144+D	6.69×10^{-2}	1.85×10^{-1}	2.94×10^{-1}	3.25×10^{-1}	9.99×10^{-1}	1.00	1.04	1.00
Cf-252	1.30×10^{-4}	1.62×10^{-4}	1.75×10^{-4}	1.76×10^{-4}	9.99×10^{-1}	1.00	9.95×10^{-1}	1.00
Cl-36	6.62×10^{-4}	1.66×10^{-3}	2.31×10^{-3}	2.40×10^{-3}	1.00	1.00	1.01	1.00
Cm-243	1.46×10^{-1}	4.01×10^{-1}	5.63×10^{-1}	5.84×10^{-1}	9.99×10^{-1}	1.00	9.96×10^{-1}	1.00
Cm-244	1.22×10^{-4}	1.26×10^{-4}	1.26×10^{-4}	1.26×10^{-4}	9.98×10^{-1}	9.98×10^{-1}	9.98×10^{-1}	9.98×10^{-1}
Cm-248	8.47×10^{-5}	8.80×10^{-5}	8.80×10^{-5}	8.80×10^{-5}	1.00	1.00	1.00	1.00
Co-57	1.39×10^{-1}	3.72×10^{-1}	4.92×10^{-1}	5.02×10^{-1}	9.98×10^{-1}	9.99×10^{-1}	9.88×10^{-1}	1.00
Co-60	2.82	8.18	1.39×10^{1}	1.62×10^{1}	9.92×10^{-1}	9.82×10^{-1}	1.02	9.96×10^{-1}
Cs-134	1.83	5.31	8.55	9.49	1.00	1.00	1.02	1.00
Cs-135	1.97×10^{-5}	3.47×10^{-5}	3.83×10^{-5}	3.84×10^{-5}	1.00	1.00	9.98×10^{-1}	1.00
Cs-137+D	6.68×10^{-1}	1.94	3.10	3.42	1.00	1.00	1.02	1.00
Eu-152	1.34	3.76	6.17	7.02	1.02	9.89×10^{-1}	1.02	1.00
Eu-154	1.50	4.12	6.73	7.68	1.05	9.96×10^{-1}	1.02	9.99×10^{-1}
Eu-155	6.51×10^{-2}	1.49×10^{-1}	1.81×10^{-1}	1.83×10^{-1}	1.03	1.00	9.94×10^{-1}	1.00
Fe-55	0.00	0.00	0.00	0.00	-	-	-	-
Fe-59	1.35	3.96	6.65	7.63	9.98×10^{-1}	1.00	1.03	9.99×10^{-1}

TABLE 2 (Cont.)

	Fitted DCF [(mrem/yr)/(pCi/g)]				Fit/FGR-12 Ratio			
Radionuclide[a]	1 cm	5 cm	15 cm	Infinite	1 cm	5 cm	15 cm	Infinite
Gd-152	0.00	0.00	0.00	0.00	-	-	-	-
Gd-153	9.65×10^{-2}	2.04×10^{-1}	2.43×10^{-1}	2.45×10^{-1}	9.99×10^{-1}	1.00	9.92×10^{-1}	9.99×10^{-1}
Ge-68+D	1.13	3.27	5.15	5.63	9.96×10^{-1}	9.97×10^{-1}	1.01	9.99×10^{-1}
H-3	0.00	0.00	0.00	0.00	-	-	-	-
I-125	1.54×10^{-2}	1.65×10^{-2}	1.66×10^{-2}	1.66×10^{-2}	1.00	9.98×10^{-1}	1.00	1.00
I-129	1.12×10^{-2}	1.30×10^{-2}	1.30×10^{-2}	1.30×10^{-2}	1.00	1.00	1.00	1.00
Ir-192	9.72×10^{-1}	2.81	4.30	4.62	1.00	1.00	1.01	1.00
K-40	1.78×10^{-1}	5.19×10^{-1}	8.88×10^{-1}	1.04	9.99×10^{-1}	9.98×10^{-1}	1.04	9.96×10^{-1}
Mn-54	9.98×10^{-1}	2.83	4.60	5.17	1.02	1.00	1.02	1.00
Na-22	2.54	7.38	1.21×10^{1}	1.37×10^{1}	9.99×10^{-1}	9.97×10^{-1}	1.03	1.00
Nb-94	1.84	5.35	8.69	9.70	9.98×10^{-1}	1.00	1.02	1.00
Nb-95	9.00×10^{-1}	2.60	4.20	4.69	1.00	9.99×10^{-1}	1.02	1.00
Ni-59	0.00	0.00	0.00	0.00	-	-	-	-
Ni-63	0.00	0.00	0.00	0.00	-	-	-	-
Np-237+D	2.58×10^{-1}	7.19×10^{-1}	1.05	1.10	9.99×10^{-1}	1.00	1.00	1.00
Pa-231	4.29×10^{-2}	1.21×10^{-1}	1.80×10^{-1}	1.91×10^{-1}	9.97×10^{-1}	9.99×10^{-1}	1.00	1.00
Pb-210+D	2.58×10^{-3}	4.93×10^{-3}	5.98×10^{-3}	6.05×10^{-3}	1.00	9.88×10^{-1}	1.01	1.00
Pm-147	2.23×10^{-5}	4.29×10^{-5}	4.99×10^{-5}	5.02×10^{-5}	1.00	1.00	9.99×10^{-1}	1.00
Po-210	9.90×10^{-6}	2.87×10^{-5}	4.67×10^{-5}	5.23×10^{-5}	9.96×10^{-1}	9.97×10^{-1}	1.02	1.00
Pu-238	1.19×10^{-4}	1.43×10^{-4}	1.52×10^{-4}	1.52×10^{-4}	1.00	1.00	1.00	1.00
Pu-239	1.05×10^{-4}	2.16×10^{-4}	2.87×10^{-4}	2.96×10^{-4}	1.00	9.98×10^{-1}	1.01	1.00
Pu-240	1.16×10^{-4}	1.39×10^{-4}	1.47×10^{-4}	1.47×10^{-4}	1.00	1.00	1.00	1.00
Pu-241+D	5.44×10^{-6}	1.40×10^{-5}	1.85×10^{-5}	1.89×10^{-5}	9.99×10^{-1}	9.97×10^{-1}	9.89×10^{-1}	9.98×10^{-1}
Pu-242	9.78×10^{-5}	1.20×10^{-4}	1.28×10^{-4}	1.28×10^{-4}	9.98×10^{-1}	9.99×10^{-1}	9.96×10^{-1}	9.98×10^{-1}
Pu-244+D	1.50	4.32	6.94	7.73	9.94×10^{-1}	9.93×10^{-1}	1.02	1.00
Ra-226+D	2.01	5.85	9.78	1.12×10^{1}	9.97×10^{-1}	9.96×10^{-1}	1.03	9.98×10^{-1}
Ra-228+D	1.12	3.24	5.32	5.99	1.00	1.00	1.03	9.99×10^{-1}
Ru-106+D	2.55×10^{-1}	7.35×10^{-1}	1.17	1.29	1.00	9.99×10^{-1}	1.02	9.97×10^{-1}
S-35	8.64×10^{-6}	1.39×10^{-5}	1.49×10^{-5}	1.49×10^{-5}	1.00	1.00	1.00	1.00
Sb-124	2.18	5.95	9.94	1.17×10^{1}	1.05	9.82×10^{-1}	1.01	1.00

TABLE 2 (Cont.)

	Fitted DCF [(mrem/yr)/(pCi/g)]				Fit/FGR-12 Ratio			
Radionuclide[a]	1 cm	5 cm	15 cm	Infinite	1 cm	5 cm	15 cm	Infinite
Sb-125	4.99×10^{-1}	1.43	2.24	2.45	9.99×10^{-1}	9.99×10^{-1}	1.02	1.00
Sc-46	2.32	6.74	1.12×10^{1}	1.27×10^{1}	9.99×10^{-1}	9.99×10^{-1}	1.03	1.00
Se-75	4.57×10^{-1}	1.30	1.89	1.98	9.98×10^{-1}	9.98×10^{-1}	9.99×10^{-1}	1.00
Sm-147	0.00	0.00	0.00	0.00	-	-	-	-
Sm-151	9.78×10^{-7}	9.87×10^{-7}	9.87×10^{-7}	9.87×10^{-7}	1.00	1.00	1.00	1.00
Sn-113+D	3.12×10^{-1}	8.85×10^{-1}	1.36	1.46	9.97×10^{-1}	9.97×10^{-1}	1.00	9.97×10^{-1}
Sr-85	6.00×10^{-1}	1.73	2.72	2.97	1.00	1.00	1.01	1.00
Sr-89	2.37×10^{-3}	6.15×10^{-3}	8.70×10^{-3}	9.08×10^{-3}	1.00	1.00	1.01	1.00
Sr-90+D	6.06×10^{-3}	1.61×10^{-2}	2.34×10^{-2}	2.47×10^{-2}	1.00	1.00	1.01	1.00
Ta-182	1.47	4.23	6.99	7.93	1.00	1.00	1.04	9.99×10^{-1}
Tc-99	5.48×10^{-5}	1.08×10^{-4}	1.25×10^{-4}	1.26×10^{-4}	1.00	1.00	1.00	1.00
Te-125m	1.33×10^{-2}	1.50×10^{-2}	1.52×10^{-2}	1.52×10^{-2}	1.00	1.01	1.00	1.00
Th-228+D	1.71	5.00	8.62	1.02×10^{1}	9.91×10^{-1}	9.92×10^{-1}	1.04	9.94×10^{-1}
Th-229+D	3.63×10^{-1}	9.96×10^{-1}	1.48	1.58	1.00	1.00	1.02	9.99×10^{-1}
Th-230	4.36×10^{-4}	9.76×10^{-4}	1.20×10^{-3}	1.21×10^{-3}	9.98×10^{-1}	9.99×10^{-1}	1.00	9.99×10^{-1}
Th-232	2.17×10^{-4}	4.41×10^{-4}	5.19×10^{-4}	5.22×10^{-4}	9.99×10^{-1}	9.99×10^{-1}	9.97×10^{-1}	1.00
Tl-204	1.51×10^{-3}	3.39×10^{-3}	4.04×10^{-3}	4.06×10^{-3}	1.00	9.99×10^{-1}	1.00	9.99×10^{-1}
U-232	3.51×10^{-4}	7.24×10^{-4}	8.93×10^{-4}	9.04×10^{-4}	9.98×10^{-1}	9.99×10^{-1}	1.00	1.00
U-233	4.03×10^{-4}	9.91×10^{-4}	1.36×10^{-3}	1.40×10^{-3}	9.98×10^{-1}	9.99×10^{-1}	1.00	1.00
U-234	1.89×10^{-4}	3.41×10^{-4}	4.00×10^{-4}	4.03×10^{-4}	1.00	1.00	1.00	1.00
U-235+D	1.91×10^{-1}	5.25×10^{-1}	7.33×10^{-1}	7.59×10^{-1}	9.99×10^{-1}	9.99×10^{-1}	9.93×10^{-1}	1.00
U-236	1.22×10^{-4}	1.89×10^{-4}	2.14×10^{-4}	2.15×10^{-4}	9.99×10^{-1}	1.00	1.01	9.98×10^{-1}
U-238+D	3.08×10^{-2}	8.32×10^{-2}	1.23×10^{-1}	1.37×10^{-1}	1.04	9.68×10^{-1}	1.01	1.00
Zn-65	6.71×10^{-1}	1.95	3.25	3.71	1.00	1.00	1.03	1.00
Zr-95+D	8.67×10^{-1}	2.52	4.07	4.52	9.99×10^{-1}	9.99×10^{-1}	1.02	9.99×10^{-1}

[a] +D means that associated decay product radionuclides with half-lives less than 30 days are included.

TABLE 3 Statistical Analysis of the Fit/FGR-12 Ratio

	Fit/FGR-12 Ratio, by Source Thickness			
Statistical Parameter	1 cm	5 cm	15 cm	Infinite
Number of data points[a]	77	77	77	77
Average	1.00	0.998	1.01	0.999
Standard deviation	0.011	0.005	0.014	0.001
Maximum deviation	5% (Eu-155, Sb-124)	4% (U-238)	4% (Ce-144, K-40, Ta-182, Th-228)	1%

[a] Statistical analysis was done only for radionuclides with nonzero *DCFs* (the *DCFs* for Ca-41, Fe-55, Gd-152, H-3, Ni-59, Ni-63, and Sm-147 were zero).

TABLE 4 Comparison of Effective Dose Equivalent for Different Source Configurations Using the Fit Parameters with FGR-12 Values[a]

	Effective Dose Equivalent [(mrem/yr)/(pCi/g)]									
	Cd-109		Cs-137		Mn-54		Co-60		Al-26	
Source Configurations	Fit	FGR-12	Fit	FGR-12	Fit	FGR-12	Fit	FGR-12	Fit	FGR-12
Cover = 1 cm, source = 4 cm	0.0051	0.0051	1.26	1.26	1.83	1.85	5.37	5.47	5.83	5.83
Cover = 1 cm, source = 14 cm	0.0069	0.0069	2.42	2.36	3.59	3.51	11.1	10.7	12.0	11.4
Cover = 1 cm, source = infinite	0.0069	0.0069	2.75	2.75	4.16	4.18	13.4	13.4	14.4	14.4
Cover = 5 cm, source = 10 cm	0.0018	0.0019	1.16	1.10	1.76	1.66	5.72	5.23	6.15	5.59
Cover = 5 cm, source = infinite	0.0019	0.0019	1.48	1.48	2.34	2.34	8.00	7.90	8.56	8.56
Cover = 15 cm, source = infinite	0.000	0.000	0.33	0.39	0.57	0.67	2.29	2.67	2.40	2.97

[a] See Section 3.3 for calculation of the FGR-12 effective dose equivalents.

4 AREA AND SHAPE FACTORS

4.1 AREA FACTOR

The energy-dependent area factor, $F_A(Ei)$, can be derived by considering the point kernel dose integral, $D(R, t_a, t_c, t_s)$, over the source thickness (t_s), radius (R), distance from the receptor to the plane of the source and air interface (t_a), and thickness of the shielding material (t_c) for the rotational (ROT) geometry depicted in Figure 1. The area factor is the ratio of the dose integrals for the geometry being considered and the infinite slab geometry:

$$F_A(Ei) = \frac{D(R = r,\ T_a = 1\text{m},\ T_c = t_c,\ T_s = t_s)}{D(R = \infty,\ T_a = 1\text{m},\ T_c = t_c,\ T_s = t_s)} \quad , \tag{3}$$

where the function D is the dose evaluated by using the point kernel method (Figure 2):

$$D(R,\ t_a,\ t_c,\ t_s) = K \int_{V_s} e^{-z} \frac{B(z)}{4\pi l^2}\, dV_S \quad , \tag{4}$$

where

$$z = \frac{\mu_a t_a + \mu_c t_c + \mu_s t}{t_a + t_c + t}\, l \quad ;$$

$$l^2 = r^2 + (t_a + t_c + t)^2 \quad ;$$

$$dV_S = 2\pi\, r t\, dr\, dt \quad ;$$

μ_a = attenuation coefficient for air (cm^{-1});

μ_c = attenuation coefficient for the cover material (cm^{-1});

μ_s = attenuation coefficient of the source material (cm^{-1});

$B(z)$ = buildup factor (G-P Method [Trubey 1991]) for length measured in mean free paths, z; and

K = energy-dependent conversion factor.

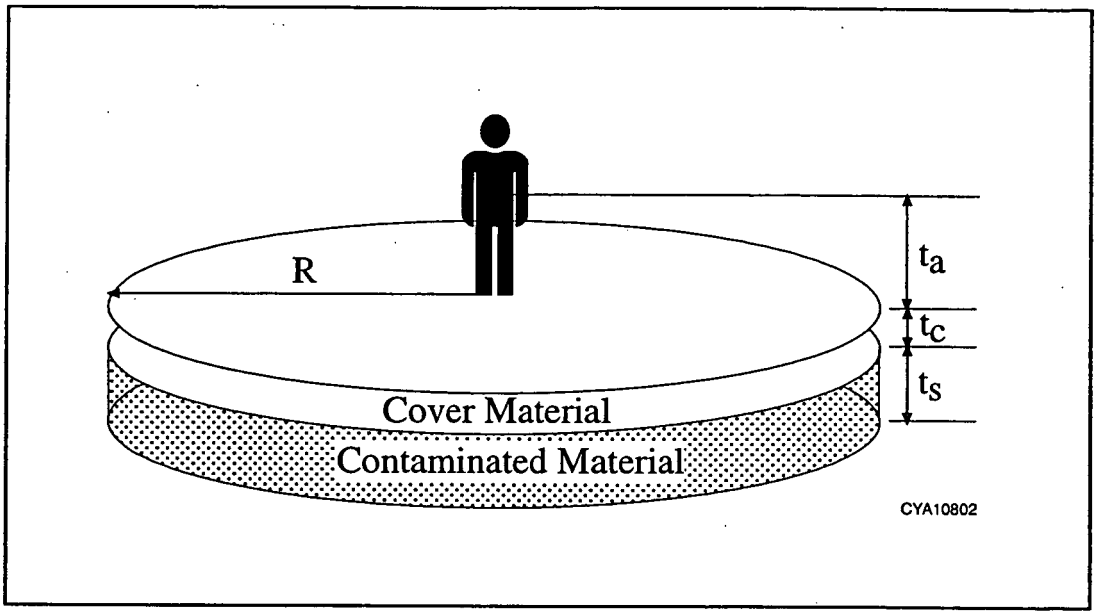

FIGURE 1 Exposure Geometry Considered for Area Factor Calculation

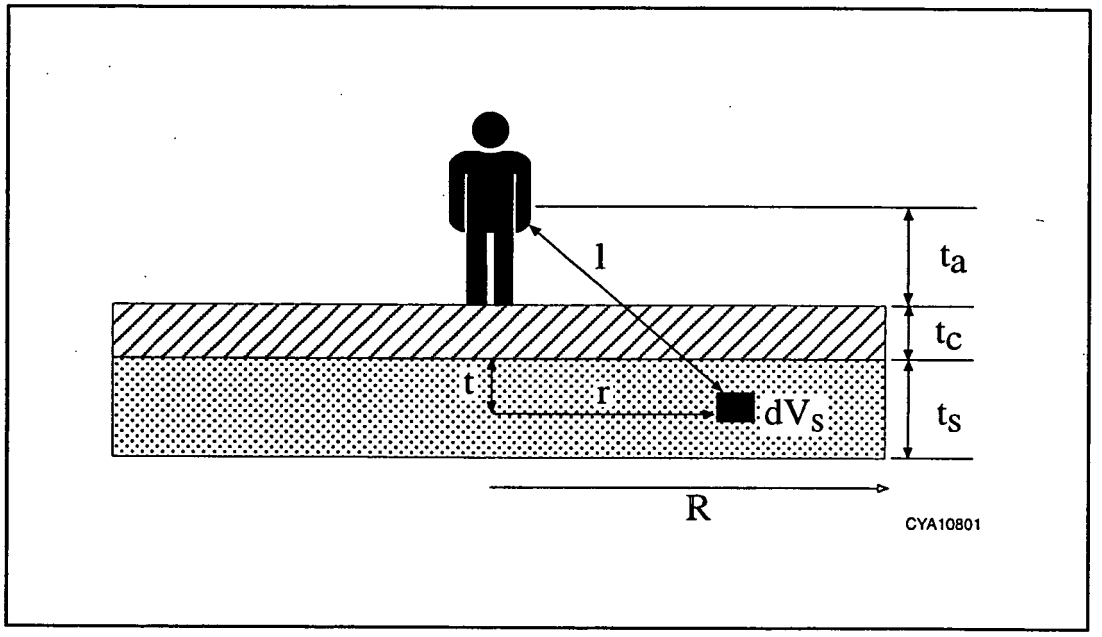

FIGURE 2 Cross Section of Exposure Geometry Showing Element of Integration for Area Factor Calculation

The volume integral can be written more explicitly as:

$$\int_0^{t_s} dt \int_0^{R} \frac{e^{-z}B(z)}{4\pi l^2} 2\pi r \, dr \quad . \tag{5}$$

Or, noticing that in the inner integral:

$$\frac{dz}{z} = \frac{dl}{l} = \frac{r\,dr}{l^2} \quad , \tag{6}$$

then the volume integral can be written:

$$\frac{1}{2} \int_0^{t_s} dt \int_{z_0}^{z_f} \frac{e^{-z}B(z)}{z} dz \quad , \tag{7}$$

where

$$z_0 = \mu_a t_a + \mu_c t_c + \mu_s t \quad ; \quad \text{and}$$

$$z_f = z_0 \sqrt{1 + \frac{R^2}{(t_a + t_c + t)^2}} \quad .$$

To conserve computational time without sacrificing too much accuracy, the International Commission on Radiological Protection (ICRP) Publication 38 (ICRP 1983) photon energies and yields were condensed into a smaller number of energies and yields for each radionuclide. The spectra-condensing algorithms, which conserve energy, repeatedly combine the photons that are closest in their energies (using their ratio). The yield of the resultant photon is the sum of the yields of the two photons, and the energy is the yield-weighted energy of the two photons. This combining of pairs of photons was repeated until individual photon energy was more than a factor of 3 apart from any other photon energy. This process resulted in four or fewer collapsed photons for all radionuclides processed. It was found that adding extra energy groups beyond four groups would not change area factor more than 5% for all radionuclides included in the RESRAD database. Even when there are four energy groups, the external dose routine in the RESRAD code is the most time-consuming routine for most radionuclides. The resultant collapsed gamma energies with their respective fractions for 84 radionuclides are shown in Table 5.

TABLE 5 Number of Collapsed Gammas (NPT), Energies (EPTs) (in MeV), and Their Respective Gamma Fractions (FPTs) for 84 Radionuclides

Radionuclide[a]	NPT	EPT(1)	EPT(2)	EPT(3)	EPT(4)	FPT(1)	FPT(2)	FPT(3)	FPT(4)
H-3	0	0.00	0.00	0.00	0.00	0.00	0.00	0.00	0.00
C-14	0	0.00	0.00	0.00	0.00	0.00	0.00	0.00	0.00
Na-22	2	8.49×10^{-4}	7.84×10^{-1}	0.00	0.00	1.25×10^{-3}	2.80	0.00	0.00
Al-26	2	5.11×10^{-1}	1.80	0.00	0.00	1.64	1.03	0.00	0.00
S-35	0	0.00	0.00	0.00	0.00	0.00	0.00	0.00	0.00
Cl-36	2	2.31×10^{-3}	5.11×10^{-1}	0.00	0.00	1.23×10^{-3}	2.97×10^{-4}	0.00	0.00
K-40	2	2.98×10^{-3}	1.46	0.00	0.00	9.59×10^{-3}	1.07×10^{-1}	0.00	0.00
Ca-41	1	3.31×10^{-3}	0.00	0.00	0.00	1.23×10^{-1}	0.00	0.00	0.00
Ca-45	2	4.13×10^{-3}	1.25×10^{-2}	0.00	0.00	2.49×10^{-6}	2.66×10^{-6}	0.00	0.00
Sc-46	1	1.01	0.00	0.00	0.00	2.00	0.00	0.00	0.00
Mn-54	1	8.35×10^{-1}	0.00	0.00	0.00	1.00	0.00	0.00	0.00
Fe-55	1	5.97×10^{-3}	0.00	0.00	0.00	2.83×10^{-1}	0.00	0.00	0.00
Fe-59	2	1.80×10^{-1}	1.18	0.00	0.00	4.00×10^{-2}	9.97×10^{-1}	0.00	0.00
Co-57	3	7.58×10^{-3}	1.24×10^{-1}	6.92×10^{-1}	0.00	6.63×10^{-1}	9.62×10^{-1}	1.60×10^{-3}	0.00
Co-60	1	1.25	0.00	0.00	0.00	2.00	0.00	0.00	0.00
Ni-59	1	7.01×10^{-3}	0.00	0.00	0.00	3.43×10^{-1}	0.00	0.00	0.00
Ni-63	0	0.00	0.00	0.00	0.00	0.00	0.00	0.00	0.00
Zn-65	2	8.04×10^{-3}	1.08	0.00	0.00	3.41×10^{-1}	5.36×10^{-1}	0.00	0.00
Ge-68+D	2	9.24×10^{-3}	5.23×10^{-1}	0.00	0.00	3.86×10^{-1}	1.82	0.00	0.00
Se-75	2	1.06×10^{-2}	2.14×10^{-1}	0.00	0.00	5.28×10^{-1}	1.82	0.00	0.00
Sr-85	2	1.35×10^{-2}	5.14×10^{-1}	0.00	0.00	5.52×10^{-1}	9.80×10^{-1}	0.00	0.00
Sr-89	1	9.09×10^{-1}	0.00	0.00	0.00	9.30×10^{-5}	0.00	0.00	0.00
Sr-90+D	2	2.08×10^{-3}	1.61×10^{-2}	0.00	0.00	3.90×10^{-6}	1.05×10^{-4}	0.00	0.00
Zr-95+D	3	1.69×10^{-2}	2.35×10^{-1}	7.42×10^{-1}	0.00	3.11×10^{-3}	1.81×10^{-3}	9.95×10^{-1}	0.00
Nb-94	1	7.87×10^{-1}	0.00	0.00	0.00	2.00	0.00	0.00	0.00
Nb-95	1	7.66×10^{-1}	0.00	0.00	0.00	1.00	0.00	0.00	0.00
Tc-99	0	0.00	0.00	0.00	0.00	0.00	0.00	0.00	0.00
Ru-106	1	5.93×10^{-1}	0.00	0.00	0.00	3.39×10^{-1}	0.00	0.00	0.00
Ag-108m	3	2.11×10^{-2}	7.92×10^{-2}	5.91×10^{-1}	0.00	5.30×10^{-1}	6.78×10^{-2}	2.72	0.00
Ag-110m+D	1	8.57×10^{-1}	0.00	0.00	0.00	3.19	0.00	0.00	0.00
Cd-109	2	2.26×10^{-2}	8.80×10^{-2}	0.00	0.00	1.01	3.61×10^{-2}	0.00	0.00
Sn-113+D	2	2.47×10^{-2}	3.88×10^{-1}	0.00	0.00	9.62×10^{-1}	6.61×10^{-1}	0.00	0.00
Sb-124	1	9.83×10^{-1}	0.00	0.00	0.00	1.83	0.00	0.00	0.00
Sb-125	2	2.87×10^{-2}	4.88×10^{-1}	0.00	0.00	5.13×10^{-1}	8.49×10^{-1}	0.00	0.00
Te-125m	2	2.85×10^{-2}	1.09×10^{-1}	0.00	0.00	1.22	2.74×10^{-3}	0.00	0.00
I-125	1	2.84×10^{-2}	0.00	0.00	0.00	1.46	0.00	0.00	0.00
I-129	2	4.29×10^{-3}	3.13×10^{-2}	0.00	0.00	6.60×10^{-2}	7.75×10^{-1}	0.00	0.00
Cs-134	1	6.98×10^{-1}	0.00	0.00	0.00	2.23	0.00	0.00	0.00
Cs-135	0	0.00	0.00	0.00	0.00	0.00	0.00	0.00	0.00
Cs-137+D	2	3.21×10^{-2}	6.62×10^{-1}	0.00	0.00	5.72×10^{-2}	8.50×10^{-1}	0.00	0.00
Ce-141	2	3.69×10^{-2}	1.45×10^{-1}	0.00	0.00	1.70×10^{-1}	4.80×10^{-1}	0.00	0.00
Ce-144+D	3	3.70×10^{-2}	1.24×10^{-1}	1.24	0.00	1.17×10^{-1}	1.33×10^{-1}	2.56×10^{-2}	0.00
Pm-147	1	8.64×10^{-2}	0.00	0.00	0.00	5.03×10^{-5}	0.00	0.00	0.00
Sm-147	0	0.00	0.00	0.00	0.00	0.00	0.00	0.00	0.00
Sm-151	2	6.49×10^{-3}	2.15×10^{-2}	0.00	0.00	1.10×10^{-3}	2.93×10^{-4}	0.00	0.00
Eu-152	2	6.34×10^{-2}	8.47×10^{-1}	0.00	0.00	1.03	1.27	0.00	0.00
Eu-154	3	4.33×10^{-2}	1.41×10^{-1}	1.01	0.00	2.48×10^{-1}	4.71×10^{-1}	1.14	0.00
Eu-155	2	6.42×10^{-3}	7.76×10^{-2}	0.00	0.00	6.34×10^{-2}	7.75×10^{-1}	0.00	0.00
Gd-152	0	0.00	0.00	0.00	0.00	0.00	0.00	0.00	0.00
Gd-153	1	5.95×10^{-2}	0.00	0.00	0.00	1.75	0.00	0.00	0.00
Ta-182	2	1.01×10^{-1}	1.18	0.00	0.00	1.27	9.85×10^{-1}	0.00	0.00
Ir-192	2	6.55×10^{-2}	3.72×10^{-1}	0.00	0.00	9.43×10^{-2}	2.16	0.00	0.00
Au-195	1	7.16×10^{-2}	0.00	0.00	0.00	1.10	0.00	0.00	0.00
Tl-204	1	7.24×10^{-2}	0.00	0.00	0.00	1.45×10^{-2}	0.00	0.00	0.00
Pb-210+D	2	1.24×10^{-2}	4.65×10^{-2}	0.00	0.00	2.37×10^{-1}	4.05×10^{-2}	0.00	0.00
Bi-207	2	7.66×10^{-2}	8.22×10^{-1}	0.00	0.00	7.44×10^{-1}	1.80	0.00	0.00
Po-210	1	8.02×10^{-1}	0.00	0.00	0.00	1.06×10^{-5}	0.00	0.00	0.00
Ra-226+D	4	2.67×10^{-2}	9.30×10^{-2}	4.81×10^{-1}	1.53	1.38×10^{-1}	2.46×10^{-1}	1.27	6.79×10^{-1}
Ra-228+D	3	1.49×10^{-2}	3.01×10^{-1}	1.01	0.00	3.58×10^{-1}	4.92×10^{-1}	7.66×10^{-1}	0.00
Ac-227+D	3	1.40×10^{-2}	9.42×10^{-2}	3.30×10^{-1}	0.00	6.41×10^{-1}	9.06×10^{-1}	8.60×10^{-1}	0.00
Th-228+D	4	1.36×10^{-2}	1.77×10^{-1}	6.54×10^{-1}	2.55	3.14×10^{-1}	9.47×10^{-1}	6.03×10^{-1}	3.87×10^{-1}
Th-229+D	4	1.97×10^{-2}	1.16×10^{-1}	4.51×10^{-1}	1.57	1.37	1.16	3.10×10^{-1}	2.12×10^{-2}
Th-230	2	1.45×10^{-2}	8.27×10^{-2}	0.00	0.00	8.10×10^{-2}	4.50×10^{-3}	0.00	0.00
Th-232	2	1.45×10^{-2}	7.21×10^{-2}	0.00	0.00	8.00×10^{-2}	2.46×10^{-3}	0.00	0.00
Pa-231	3	1.62×10^{-2}	9.09×10^{-2}	2.83×10^{-1}	0.00	7.87×10^{-1}	6.95×10^{-3}	1.30×10^{-1}	0.00

TABLE 5 (Cont.)

Radionuclide[a]	NPT	EPT(1)	EPT(2)	EPT(3)	EPT(4)	FPT(1)	FPT(2)	FPT(3)	FPT(4)
U-232	3	1.53×10^{-2}	7.75×10^{-2}	2.98×10^{-1}	0.00	1.26×10^{-1}	3.03×10^{-3}	7.20×10^{-5}	0.00
U-233	2	1.59×10^{-2}	1.58×10^{-1}	0.00	0.00	6.66×10^{-2}	1.60×10^{-3}	0.00	0.00
U-234	2	1.53×10^{-2}	7.13×10^{-2}	0.00	0.00	1.05×10^{-1}	1.66×10^{-3}	0.00	0.00
U-235	2	1.68×10^{-2}	1.59×10^{-1}	0.00	0.00	1.14	1.01	0.00	0.00
U-236	2	1.53×10^{-2}	6.25×10^{-2}	0.00	0.00	9.87×10^{-2}	9.85×10^{-4}	0.00	0.00
U-238+D	3	1.55×10^{-2}	8.27×10^{-2}	9.15×10^{-1}	0.00	1.91×10^{-1}	1.02×10^{-1}	1.46×10^{-2}	0.00
Np-237+D	3	1.76×10^{-2}	9.70×10^{-2}	3.17×10^{-1}	0.00	1.15	5.87×10^{-1}	5.06×10^{-1}	0.00
Pu-238	2	1.61×10^{-2}	5.26×10^{-2}	0.00	0.00	1.11×10^{-1}	4.64×10^{-4}	0.00	0.00
Pu-239	4	7.30×10^{-5}	1.61×10^{-2}	4.88×10^{-2}	1.87×10^{-1}	9.99×10^{-1}	4.17×10^{-2}	2.67×10^{-4}	2.09×10^{-4}
Pu-240	2	1.61×10^{-2}	5.32×10^{-2}	0.00	0.00	1.06×10^{-1}	5.20×10^{-4}	0.00	0.00
Pu-241	2	1.62×10^{-2}	1.12×10^{-1}	0.00	0.00	7.90×10^{-5}	4.23×10^{-5}	0.00	0.00
Pu-242	2	1.61×10^{-2}	5.54×10^{-2}	0.00	0.00	8.81×10^{-2}	4.39×10^{-4}	0.00	0.00
Pu-244	2	5.46×10^{-2}	6.48×10^{-1}	0.00	0.00	2.09×10^{-2}	4.99×10^{-1}	0.00	0.00
Am-241	2	1.68×10^{-2}	5.95×10^{-2}	0.00	0.00	6.65×10^{-1}	3.57×10^{-1}	0.00	0.00
Am-243+D	2	1.92×10^{-2}	1.24×10^{-1}	0.00	0.00	8.18×10^{-1}	1.71	0.00	0.00
Cm-243	2	1.67×10^{-2}	1.60×10^{-1}	0.00	0.00	5.72×10^{-1}	7.75×10^{-1}	0.00	0.00
Cm-244	1	1.69×10^{-2}	0.00	0.00	0.00	1.00×10^{-1}	0.00	0.00	0.00
Cm-248	1	4.40×10^{-2}	0.00	0.00	0.00	2.02×10^{-4}	0.00	0.00	0.00
Cf-252	1	7.55×10^{-2}	0.00	0.00	0.00	2.93×10^{-4}	0.00	0.00	0.00

[a] +D means that gamma energies of the associated progeny radionuclides with half-lives less than 30 days are included.

The radionuclide-specific area factor for a circular area x, $F_A^{nuc}(x)$, is obtained by combining the energy-dependent area factors weighted by their photon fraction, FPT_i, and dose contribution at the reference point:

$$F_A^{nuc}(x) = \frac{\sum_i F_A(EPT_i)\, FPT_i\, D_{slab}(EPT_i)}{\sum_i FPT_i\, D_{slab}(EPT_i)} \quad , \tag{8}$$

where

$D_{slab}(EPT_i)$ = effective dose equivalent from the infinite slab geometry.

4.2 SHAPE FACTOR

A shape factor, F_S, is used to correct a noncircular-shaped contaminated area on the basis of an ideally circular zone. The shape factor of a circular contaminated area is 1.0. For an irregularly shaped contaminated area, the shape factor is obtained by enclosing the irregularly shaped contaminated area in a circle, multiplying the area factor of each annulus by the fraction of the

annulus area that is contaminated, summing the products, and dividing by the area factor of a circular contaminated zone that is equivalent in area:

$$F_s = \frac{\sum_{i=0}^{n} f_i\left[F_A^{nuc}(A_i) - F_A^{nuc}(A_{i-1})\right]}{F_A^{nuc}\left(\sum_{i=0}^{n} f_i(A_i - A_{i-1})\right)}, \quad (9)$$

where

f_i = fraction of annular area that is contaminated and

$F_A^{nuc}(x)$ = radionuclide specific area factor for an area x.

5 COMPARISON OF RESRAD MODELS (VERSION 5.44 AND EARLIER VS. 5.60 AND LATER)

The contribution to the effective dose equivalent (*EDE*) rate from the external ground radiation of the source of any depth, shape, cover, and size for a single radionuclide can be given by the equation:

$$EDE = Source\ Activity \times DCF \times F_{CD} \times F_A^{nuc} \times F_S\ , \qquad (10)$$

where *DCF* is the dose conversion factor for the radionuclide present at the unit concentration in a uniformly contaminated zone of infinite depth and lateral extent. The *DCF* multiplied by the source activity gives the *EDE* for the given activity. When this value is multiplied by F_{CD}, the dose equivalent is obtained for a geometry with a given source depth and cover thickness but still of an infinite lateral extent. F_A^{nuc} accounts for the finite radius source, but the source is still assumed to be circular. F_S accounts for irregular source shapes. If many radionuclides are present, the *EDE* can be calculated separately for each radionuclide and summed to get the total *EDE*.

5.1 DOSE CONVERSION FACTORS

Table 6 compares the infinite thickness *DCF*s used in the FGR-12 report with those used in the previous RESRAD model for the 67 (six-month equilibration) and 84 (30-day equilibration) radionuclides. The *DCF*s used in RESRAD 5.44 and earlier versions were based on U.S. Department of Energy (DOE) report EH-0070 (DOE 1988) and the methods of Kocher and Sjoreen (1985) and Chen (1991). The "Ratio" columns represent the ratio of previous RESRAD *DCF*s divided by the FGR-12 *DCF*s. In the table, "BZ" indicates cases in which both values are zero, "INF" indicates radionuclides for which the FGR values are zero and RESRAD has finite values, and "ZERO" indicates radionuclides for which only RESRAD values are zero.

The following comparisons are made:

- For Ca-41, Fe-55, and Ni-59, FGR-12 *DCF*s are zero, and the previous RESRAD model had nonzero values.
- For C-14, S-35, Sr-90, and Cs-135, FGR-12 assigns some finite *DCF*, whereas the previous RESRAD model had zero values.
- For H-3, Ni-63, Sm-147, and Gd-152, *DCF*s are zero in both cases.
- For 38 out of 84 radionuclides, differences are equal to or less than 20%.

TABLE 6 Comparison of Infinite Thickness *DCFs* [(mrem/year)/(pCi/g)] between the Previous RESRAD Model and FGR-12

	6-Month Equilibration				30-Day Equilibration		
Radionuclide	RESRAD	FGR-12	Ratio[a]	Radionuclide	RESRAD	FGR-12	Ratio[a]
H-3	0.00	0.00	BZ[b]	H-3	0.00	0.00	BZ
C-14	0.00	1.34×10^{-5}	ZERO[c]	C-14	0.00	1.34×10^{-5}	ZERO
Na-22	1.54×10^{1}	1.37×10^{1}	1.12	Na-22	1.54×10^{1}	1.37×10^{1}	1.12
Al-26	2.00×10^{1}	1.74×10^{1}	1.15	Al-26	2.00×10^{1}	1.74×10^{1}	1.15
Cl-36	1.02×10^{-3}	2.39×10^{-3}	4.31×10^{-1}	S-35	0.00	1.49×10^{-5}	ZERO
K-40	1.17	1.04	1.13	Cl-36	1.02×10^{-3}	2.39×10^{-3}	4.31×10^{-1}
Ca-41	1.94×10^{-6}	0.00	INF[d]	K-40	1.17	1.04	1.13
Mn-54	5.88	5.16	1.14	Ca-41	1.94×10^{-6}	0.00	INF[d]
Fe-55	4.44×10^{-6}	0.00	INF	Ca-45	2.53E-10	6.26×10^{-5}	4.04×10^{-6}
Co-57	5.03×10^{-1}	5.01×10^{-1}	1.00	Sc-46	1.33×10^{1}	1.27×10^{1}	1.05
Co-60	2.27×10^{1}	1.62×10^{1}	1.40	Mn-54	5.88	5.16	1.14
Ni-59	5.38×10^{-6}	0.00	INF	Fe-55	4.44×10^{-6}	0.00	INF
Ni-63	0.00	0.00	BZ	Fe-59	7.99	7.64	1.05
Zn-65	3.71	3.70	1.00	Co-57	5.03×10^{-1}	5.01×10^{-1}	1.00
Ge-68+D180[e]	6.39	5.62	1.14	Co-60	2.27×10^{1}	1.62×10^{1}	1.40
Sr-90+D180	0.00	2.46×10^{-2}	ZERO	Ni-59	5.38×10^{-6}	0.00	INF
Nb-94	1.42×10^{1}	9.68	1.46	Ni-63	0.00	0.00	BZ
Tc-99	1.68×10^{-6}	1.26×10^{-4}	1.33×10^{-2}	Zn-65	3.71	3.70	1.00
Ru-106	1.35	1.29	1.05	Ge-68+D30[f]	6.39	5.62	1.14
Ag-108m	1.11×10^{1}	9.65	1.15	Se-75	2.17	1.98	1.10
Ag-110m	1.92×10^{1}	1.72×10^{1}	1.12	Sr-85	3.40	2.97	1.14
Cd-109	1.17×10^{-2}	1.47×10^{-2}	7.96×10^{-1}	Sr-89	5.77×10^{-4}	9.08×10^{-3}	6.35×10^{-2}
Sb-125+D180	2.81	2.45	1.15	Sr-90+D30	0.00	2.46×10^{-2}	ZERO
I-129	3.24×10^{-2}	1.29×10^{-2}	2.51	Zr-95+D30	5.15	4.52	1.14
Cs-134	1.08×10^{1}	9.47	1.14	Nb-94	1.42×10^{1}	9.68	1.47
Cs-135	0.00	3.83×10^{-5}	ZERO	Nb-95	5.36	4.69	1.14
Cs-137+D180	5.03	3.41	1.48	Tc-99	1.68×10^{-6}	1.26×10^{-4}	1.33×10^{-2}
Ce-144+D180	3.12×10^{-1}	3.20×10^{-1}	9.75×10^{-1}	Ru-106+D30	1.35	1.29	1.05
Pm-147	1.47×10^{-5}	5.01×10^{-5}	2.93×10^{-1}	Ag-108m+D30	1.11×10^{1}	9.65	1.15
Sm-147	0.00	0.00	BZ	Ag-110m+D30	1.92×10^{1}	1.72×10^{1}	1.12
Sm-151	5.45×10^{-7}	9.84×10^{-7}	5.54×10^{-1}	Cd-109	1.17×10^{-2}	1.47×10^{-2}	7.96×10^{-1}
Eu-152	9.91	7.01	1.41	Sn-113+D30	1.73	1.46	1.18
Eu-154	1.10×10^{1}	7.68	1.43	Sb-124	1.32×10^{1}	1.17×10^{1}	1.13
Eu-155	1.65×10^{-1}	1.82×10^{-1}	9.07×10^{-1}	Sb-125	2.81	2.45	1.15
Gd-152	0.00	0.00	BZ	Te-125m	8.80×10^{-3}	1.51×10^{-2}	5.83×10^{-1}
Gd-153	2.12×10^{-1}	2.45×10^{-1}	8.65×10^{-1}	I-125	9.07×10^{-3}	1.66×10^{-2}	5.46×10^{-1}
Au-195	1.67×10^{-1}	2.07×10^{-1}	8.07×10^{-1}	I-129	3.24×10^{-2}	1.29×10^{-2}	2.51
Tl-204	2.20×10^{-3}	4.05×10^{-3}	5.43×10^{-1}	Cs-134	1.08×10^{1}	9.47	1.14
Pb-210+D180	4.87×10^{-3}	6.12×10^{-3}	7.96×10^{-1}	Cs-135	0.00	3.83×10^{-5}	ZERO
Bi-207	9.72	9.38	1.04	Cs-137+D30	5.03	3.41	1.48
Ra-226+D180	1.55×10^{1}	1.12×10^{1}	1.38	Ce-141	3.20×10^{-1}	3.18×10^{-1}	1.01
Ra-228+D180	8.18	5.98	1.37	Ce-144+D30	3.12×10^{-1}	3.20×10^{-1}	9.75×10^{-1}
Ac-227+D180	2.76	2.01	1.37	Pm-147	1.47×10^{-5}	5.01×10^{-5}	2.93×10^{-1}
Th-228+D180	1.33×10^{1}	1.02×10^{1}	1.30	Sm-147	0.00	0.00	BZ
Th-229+D180	2.20	1.60	1.38	Sm-151	5.45×10^{-7}	9.84×10^{-7}	5.54×10^{-1}
Th-230	2.11×10^{-3}	1.21×10^{-3}	1.74	Eu-152	9.91	7.01	1.41
Th-232	1.35×10^{-3}	5.21×10^{-4}	2.59	Eu-154	1.10×10^{1}	7.68	1.43
Pa-231	2.21×10^{-1}	1.91×10^{-1}	1.16	Eu-155	1.65×10^{-1}	1.82×10^{-1}	9.07×10^{-1}

TABLE 6 (Cont.)

Radionuclide	6-Month Equilibration RESRAD	FGR-12	Ratio[a]	Radionuclide	30-Day Equilibration RESRAD	FGR-12	Ratio[a]
U-232	2.19×10^{-3}	9.02×10^{-4}	2.43	Gd-152	0.00	0.00	BZ
U-233	1.40×10^{-3}	1.40×10^{-3}	1.00	Gd-153	2.12×10^{-1}	2.45×10^{-1}	8.65×10^{-1}
U-234	1.58×10^{-3}	4.02×10^{-4}	3.92	Ta-182	8.26	7.94	1.04
U-235+D180	8.94×10^{-1}	7.57×10^{-1}	1.18	Ir-192	5.22	4.61	1.13
U-236	1.35×10^{-3}	2.15×10^{-4}	6.28	Au-195	1.67×10^{-1}	2.07×10^{-1}	8.07×10^{-1}
U-238+D180	1.27×10^{-1}	1.37×10^{-1}	9.27×10^{-1}	Tl-204	2.20×10^{-3}	4.05×10^{-3}	5.43×10^{-1}
Np-237+D180	1.61	1.10	1.46	Pb-210+D30	4.81×10^{-3}	6.05×10^{-3}	7.95×10^{-1}
Pu-238	1.56×10^{-3}	1.51×10^{-4}	1.03×10^{1}	Bi-207	9.72	9.38	1.04
Pu-239	8.14×10^{-4}	2.95×10^{-4}	2.75	Po-210	5.98×10^{-5}	5.23×10^{-5}	1.14
Pu-240	1.48×10^{-3}	1.47×10^{-4}	1.01×10^{1}	Ra-226+D30	1.55×10^{1}	1.12×10^{1}	1.38
Pu-241+D180	1.88×10^{-5}	1.89×10^{-5}	9.95×10^{-1}	Ra-228+D30	8.18	5.98	1.37
Pu-242	1.24×10^{-3}	1.28×10^{-4}	9.69	Ac-227+D30	2.76	2.01	1.37
Pu-244+D180	2.23	7.73	2.88×10^{-1}	Th-228+D30	1.33×10^{1}	1.02×10^{1}	1.30
Am-241	4.79×10^{-2}	4.37×10^{-2}	1.10	Th-229+D30	2.20	1.60	1.38
Am-243+D180	1.08	8.95×10^{-1}	1.21	Th-230	2.11×10^{-3}	1.21×10^{-3}	1.74
Cm-243	7.26×10^{-1}	5.83×10^{-1}	1.25	Th-232	1.35×10^{-3}	5.21×10^{-4}	2.59
Cm-244	1.51×10^{-3}	1.26×10^{-4}	1.20×10^{1}	Pa-231	2.21×10^{-1}	1.91×10^{-1}	1.16
Cm-248	6.10×10^{-6}	8.78×10^{-5}	6.95×10^{-2}	U-232	2.19×10^{-3}	9.02×10^{-4}	2.43
Cf-252	6.32×10^{-5}	1.76×10^{-4}	3.59×10^{-1}	U-233	1.40×10^{-3}	1.40×10^{-3}	1.00
				U-234	1.58×10^{-3}	4.02×10^{-4}	3.93
				U-235+D30	8.94×10^{-1}	7.57×10^{-1}	1.18
				U-236	1.35×10^{-3}	2.15×10^{-4}	6.28
				U-238+D30	1.27×10^{-1}	1.37×10^{-1}	9.27×10^{-1}
				Np-237+D30	1.61	1.10	1.46
				Pu-238	1.56×10^{-3}	1.51×10^{-4}	1.03×10^{1}
				Pu-239	8.14×10^{-4}	2.95×10^{-4}	2.76
				Pu-240	1.48×10^{-3}	1.47×10^{-4}	1.01×10^{1}
				Pu-241+D30	1.88×10^{-5}	1.89×10^{-5}	9.95×10^{-1}
				Pu-242	1.24×10^{-3}	1.28×10^{-4}	9.69
				Pu-244+D30	2.23	7.73	2.88×10^{-1}
				Am-241	4.79×10^{-2}	4.37×10^{-2}	1.10
				Am-243+D30	1.08	8.95×10^{-1}	1.21
				Cm-243	7.26×10^{-1}	5.83×10^{-1}	1.25
				Cm-244	1.51×10^{-3}	1.26×10^{-4}	1.20×10^{1}
				Cm-248	6.10×10^{-6}	8.78×10^{-5}	6.95×10^{-2}
				Cf-252	6.32×10^{-5}	1.76×10^{-4}	3.59×10^{-1}

[a] Ratio: represents the ratio of previous RESRAD *DCFs* divided by the FGR-12 *DCFs*.

[b] BZ: cases in which both values are zero.

[c] ZERO: cases in which only RESRAD *DCFs* are zero.

[d] INF: cases in which only FGR-12 *DCFs* are zero.

[e] +D180: associated radionuclides with half-lives less than 6 months are included.

[f] +D30: associated radionuclides with half-lives less than 30 days are included.

- For Ca-45, Sr-89, Tc-99, Pu-238, Pu-240, Pu-242, Cm-244, and Cm-248, *DCF*s differ by an order of magnitude. Previous RESRAD values are higher in most of these cases.

- For Co-60, Cs-137, Eu-152, Eu-154, Ra-226, Ra-228, Ac-227, Th-228, Th-229, and Np-237, differences in *DCF*s are between 20 and 50%.

Table 7 shows the differences in the ratio of the *DCF*s between the previous RESRAD model and FGR-12 as they increase. "BZ" indicates both values are zero, <20% means less than 20% difference in the ratio, 20-100% means the differences are between 20 and 100%, >2 represents differences greater than a factor of 2 but less than a factor of 10, and >10 means differences are greater than an order of magnitude.

5.2 COVER AND DEPTH FACTORS

Cover and depth factors for the new RESRAD model were compared with the previous model. In these comparisons, the source area was assumed to be of infinite extent, with a density of 1.6 g/cm^3, and only source depths and cover thicknesses were changed. The comparisons were made for Co-60, U-234, U-235, U-238, Mn-54, Al-26, Co-57, and Cs-137. These radionuclides were chosen because of the differences in their average energies.

Table 8 compares the depth factors of the old (version 5.44 and earlier) and new (version 5.60 and later) RESRAD models, and Table 9 gives the depth factor ratio for the old and new models. Figure 3a shows the depth factor as a function of source depth for Co-60, U-234, U-235, U-238, and Mn-54. In this illustration, "n" always represents the results with the new model. Figure 3b illustrates the variation of ratio with source depth. Figure 3 shows that no significant difference exists between the old and new RESRAD models for source depths greater than 30 cm; however, thin sources show major differences. The new model gives a higher depth factor for thin sources, which means that the dose calculated with the new model will be higher in these cases.

Table 10 shows the cover-and-depth factor comparisons between the old and new RESRAD models at different source depths. Cover thickness varies from 0.001 to 50 cm. Comparisons are made for Co-60, Mn-54, Al-26, U-234, U-235, U-238, and Co-57. Figure 4a shows the cover factor variations with cover thickness for different source depths of Co-60. To get only the cover factor variations, values were divided by the zero cover thickness for the respective source depths. Figure 4b gives the ratio of cover factor for old to new models as a function of cover thickness. Figure 5a shows the cover-and-depth factor variations with cover thickness for source depths of 1, 5, 15, and 50 cm. Figure 5b gives the ratio of cover-and-depth factor variations for a Co-60 source.

TABLE 7 Comparison of the Ratio of the *DCFs* between the Previous RESRAD Model and FGR-12 for 30-Day Equilibration Radionuclides

Ratio[a]	Number	Radionuclides
BZ	4	H-3, N-63, Sm-147, Gd-152
<20%	37	Na-22, Al-26, K-40, Sc-46, Mn-54, Fe-59, Co-57, Zn-65, Ge-68+D, Se-75, Sr-85, Zr-95+D, Nb-95, Ru-106+D, Ag-108m+D, Ag-110m+D, Cd-108, Sn-113+D, Sb-124, Sb-125, Cs-134, Ce-141, Ce-144+D, Eu-155, Gd-153, Ta-182, Ir-192, Au-195, Pb-210+D, Bi-207, Po-210, Pa-231, U-233, U-235+D, U-238+D, Pu-241+D, Am-241
20-100%	18	Co-60, Nb-94, Te-125m, I-125, Cs-137+D, Sm-151, Eu-152,Eu-154, Tl-204, Ra-226+D, Ra-228+D, Ac-227+D, Th-228+D, Th-229+D, Th-230, Np-237+D, Am-243+D, Cm-243
>2	11	Cl-36, I-129, Pm-147, Th-232, U-232, U-234, U-236, Pu-239, Pu-242, Pu-244+D, Cf-252
>10	7	Ca-45, Sr-89, Tc-99, Pu-238, Pu-240, Cm-244, Cm-248
INF	3	Ca-41, Fe-55, Ni-59
ZERO	4	C-14, S-35, Sr-90+D, Cs-135

[a] Notation: BZ: both zero; INF: cases in which only FGR-12 *DCFs* are zero; ZERO: cases in which only RESRAD *DCFs* are zero; <20%: less than 20% difference in ratio; 20-100%: differences between 20 and 100%; >2: differences greater than a factor of 2 but less than factor of 10; >10: differences greater than a factor of ten.

Table 10 shows that for all radionuclides considered, while the old RESRAD cover factor was independent of source thickness, the new model yields a sharper decrease in cover factor with an increase in cover thickness at small cover. The cover factor comparison shows that the maximum differences occur for a large cover thickness and small source depths. Figure 4b shows that the ratio of the old to new models varies from 1 to 3 with an increase in the cover thickness. The cover-and-depth factor comparisons in Figure 5 show that large differences are observed for thin sources without any cover and for sources with very thick covers. For all source depths with a cover between 0.5 and 10 cm, the ratio is between 0.8 and 1.2.

5.3 AREA FACTOR

In the old RESRAD model, a radionuclide-independent area factor was used (Napier et al. 1984). Measurements were made for surface sources of maximum area 1,222 m^2 (equivalent to 19.72-m radius). Values at different areas were divided by the maximum value to get the area factor. It was assumed that there was no contribution from regions beyond 19.72-m radius. All the sources used had average energies greater than 100 keV. In that study, it was observed that when plotted against area, the exposure rate was parallel for all isotopes, which suggests that the area factor does

TABLE 8 Comparison of Depth Factors for Old and New RESRAD Models for Co-60, U-234, U-235, U-238, Mn-54, Al-26, Co-57, and Cs-137

Source Depth (cm)	Co-60		U-234		U-235		U-238	
	Old	New	Old	New	Old	New	Old	New
1	1.06×10^{-1}	1.75×10^{-1}	2.18×10^{-1}	4.70×10^{-1}	2.04×10^{-1}	2.51×10^{-1}	1.21×10^{-1}	2.35×10^{-1}
3	2.86×10^{-1}	3.65×10^{-1}	5.22×10^{-1}	7.15×10^{-1}	4.96×10^{-1}	5.21×10^{-1}	3.20×10^{-1}	4.47×10^{-1}
5	4.30×10^{-1}	5.06×10^{-1}	7.08×10^{-1}	8.47×10^{-1}	6.81×10^{-1}	6.92×10^{-1}	4.75×10^{-1}	5.88×10^{-1}
10	6.75×10^{-1}	7.36×10^{-1}	9.15×10^{-1}	9.68×10^{-1}	8.98×10^{-1}	8.98×10^{-1}	7.24×10^{-1}	8.03×10^{-1}
15	8.15×10^{-1}	8.59×10^{-1}	9.75×10^{-1}	9.93×10^{-1}	9.68×10^{-1}	9.66×10^{-1}	8.55×10^{-1}	9.05×10^{-1}
30	9.66×10^{-1}	9.79×10^{-1}	9.99×10^{-1}	1.00	9.99×10^{-1}	9.99×10^{-1}	9.79×10^{-1}	9.90×10^{-1}
50	9.96×10^{-1}	9.98×10^{-1}	1.00	1.00	1.00	1.00	9.98×10^{-1}	9.99×10^{-1}
100	1.00	1.00	1.00	1.00	1.00	1.00	1.00	1.00

Source Depth (cm)	Mn-54		Al-26		Co-57		Cs-137	
	Old	New	Old	New	Old	New	Old	New
1	1.10×10^{-1}	1.93×10^{-1}	9.91×10^{-2}	1.73×10^{-1}	2.01×10^{-1}	2.76×10^{-1}	1.24×10^{-1}	1.95×10^{-1}
3	2.95×10^{-1}	4.00×10^{-1}	2.69×10^{-1}	3.65×10^{-1}	4.90×10^{-1}	5.69×10^{-1}	3.28×10^{-1}	4.12×10^{-1}
5	4.42×10^{-1}	5.47×10^{-1}	4.07×10^{-1}	5.07×10^{-1}	6.75×10^{-1}	7.42×10^{-1}	4.84×10^{-1}	5.66×10^{-1}
10	6.88×10^{-1}	7.76×10^{-1}	6.48×10^{-1}	7.38×10^{-1}	8.94×10^{-1}	9.28×10^{-1}	7.34×10^{-1}	7.97×10^{-1}
15	8.26×10^{-1}	8.89×10^{-1}	7.91×10^{-1}	8.61×10^{-1}	9.66×10^{-1}	9.80×10^{-1}	8.63×10^{-1}	9.05×10^{-1}
30	9.70×10^{-1}	9.87×10^{-1}	9.56×10^{-1}	9.79×10^{-1}	9.99×10^{-1}	1.00	9.81×10^{-1}	9.90×10^{-1}
50	9.97×10^{-1}	9.99×10^{-1}	9.95×10^{-1}	9.98×10^{-1}	1.00	1.00	9.99×10^{-1}	1.00
100	1.00	1.00	1.00	1.00	1.00	1.00	1.00	1.00

TABLE 9 Depth Factor Ratio of Old to New RESRAD Models for Different Source Depths for Co-60, U-234, U-235, U-238, Mn-54, Al-26, Co-57, and Cs-137

Source Depth (cm)	Depth Factor Ratio of Old Model/New Model							
	Co-60	U-234	U-235	U-238	Mn-54	Al-26	Co-57	Cs-137
1	6.08×10^{-1}	4.64×10^{-1}	8.13×10^{-1}	5.15×10^{-1}	5.71×10^{-1}	5.71×10^{-1}	7.27×10^{-1}	6.36×10^{-1}
3	7.83×10^{-1}	7.30×10^{-1}	9.52×10^{-1}	7.17×10^{-1}	7.39×10^{-1}	7.35×10^{-1}	8.60×10^{-1}	7.98×10^{-1}
5	8.50×10^{-1}	8.36×10^{-1}	9.84×10^{-1}	8.07×10^{-1}	8.08×10^{-1}	8.00×10^{-1}	9.08×10^{-1}	8.57×10^{-1}
10	9.17×10^{-1}	9.45×10^{-1}	1.00	9.02×10^{-1}	8.87×10^{-1}	8.76×10^{-1}	9.63×10^{-1}	9.22×10^{-1}
15	9.49×10^{-1}	9.82×10^{-1}	1.00	9.44×10^{-1}	9.29×10^{-1}	9.18×10^{-1}	9.85×10^{-1}	9.54×10^{-1}
30	9.87×10^{-1}	9.99×10^{-1}	1.00	9.89×10^{-1}	9.83×10^{-1}	9.76×10^{-1}	9.99×10^{-1}	9.91×10^{-1}
50	9.98×10^{-1}	1.00	1.00	9.99×10^{-1}	9.98×10^{-1}	9.96×10^{-1}	1.00	9.99×10^{-1}
100	1.00	1.00	1.00	1.00	1.00	1.00	1.00	1.00

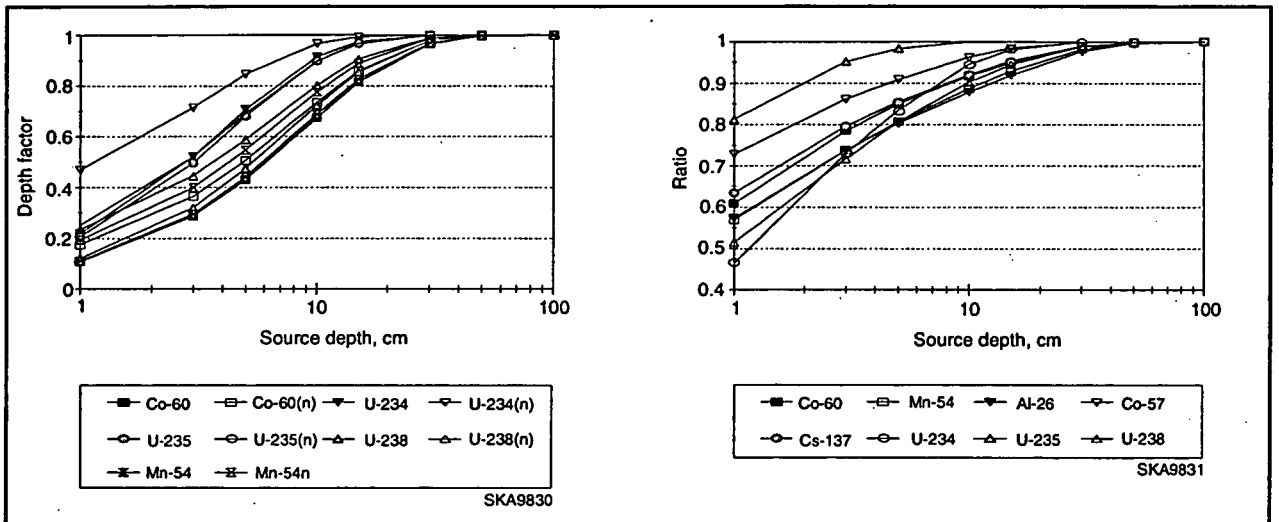

(a) Actual depth for old (solid) and new (open) RESRAD models

(b) Ratio of depth factor for RESRAD models

FIGURE 3 Depth Factor Comparison as a Function of Depth for a Set of Radionuclides

TABLE 10 Cover-and-Depth Factor Comparison of Old and New RESRAD Models for Various Radionuclides at Source Depths of 1, 5, 15, and 50 cm

Cover Thickness (cm)	Cover-and-Depth Factor by Source Depth							
	1 cm		5 cm		15 cm		50 cm	
	Old	New	Old	New	Old	New	Old	New
Co-60								
0.001	1.06×10^{-1}	1.75×10^{-1}	4.30×10^{-1}	5.06×10^{-1}	8.15×10^{-1}	8.59×10^{-1}	9.96×10^{-1}	9.98×10^{-1}
0.5	1.01×10^{-1}	1.26×10^{-1}	4.07×10^{-1}	4.32×10^{-1}	7.70×10^{-1}	7.63×10^{-1}	9.42×10^{-1}	8.94×10^{-1}
1	9.50×10^{-2}	1.05×10^{-1}	3.84×10^{-1}	3.90×10^{-1}	7.28×10^{-1}	7.01×10^{-1}	8.90×10^{-1}	8.24×10^{-1}
2	8.49×10^{-2}	8.59×10^{-2}	3.44×10^{-1}	3.36×10^{-1}	6.51×10^{-1}	6.11×10^{-1}	7.96×10^{-1}	7.19×10^{-1}
5	6.06×10^{-2}	5.82×10^{-2}	2.45×10^{-1}	2.30×10^{-1}	4.64×10^{-1}	4.19×10^{-1}	5.68×10^{-1}	4.93×10^{-1}
10	3.45×10^{-2}	3.11×10^{-2}	1.40×10^{-1}	1.23×10^{-1}	2.65×10^{-1}	2.24×10^{-1}	3.23×10^{-1}	2.64×10^{-1}
15	1.96×10^{-2}	1.66×10^{-2}	7.95×10^{-2}	6.57×10^{-2}	1.51×10^{-1}	1.20×10^{-1}	1.84×10^{-1}	1.41×10^{-1}
20	1.12×10^{-2}	8.88×10^{-3}	4.53×10^{-2}	3.51×10^{-2}	8.59×10^{-2}	6.39×10^{-2}	1.05×10^{-1}	7.53×10^{-2}
25	6.39×10^{-3}	4.75×10^{-3}	2.58×10^{-2}	1.88×10^{-2}	4.89×10^{-2}	3.42×10^{-2}	5.98×10^{-2}	4.02×10^{-2}
30	3.64×10^{-3}	2.54×10^{-3}	1.47×10^{-2}	1.00×10^{-2}	2.78×10^{-2}	1.83×10^{-2}	3.40×10^{-2}	2.15×10^{-2}
40	1.18×10^{-3}	7.25×10^{-4}	4.78×10^{-3}	2.87×10^{-3}	9.05×10^{-3}	5.22×10^{-3}	1.10×10^{-2}	6.15×10^{-3}
50	3.84×10^{-4}	2.07×10^{-4}	1.55×10^{-3}	8.19×10^{-4}	2.94×10^{-3}	1.49×10^{-3}	3.60×10^{-3}	1.76×10^{-3}
Mn-54								
0.001	1.10×10^{-1}	1.93×10^{-1}	4.42×10^{-1}	5.47×10^{-1}	8.26×10^{-1}	8.89×10^{-1}	9.97×10^{-1}	9.99×10^{-1}
0.5	1.04×10^{-1}	1.40×10^{-1}	4.17×10^{-1}	4.63×10^{-1}	7.79×10^{-1}	7.82×10^{-1}	9.41×10^{-1}	8.84×10^{-1}
1	9.79×10^{-2}	1.15×10^{-1}	3.93×10^{-1}	4.14×10^{-1}	7.35×10^{-1}	7.11×10^{-1}	8.87×10^{-1}	8.06×10^{-1}
2	8.71×10^{-2}	9.22×10^{-2}	3.50×10^{-1}	3.51×10^{-1}	6.54×10^{-1}	6.09×10^{-1}	7.90×10^{-1}	6.92×10^{-1}
5	6.14×10^{-2}	5.94×10^{-2}	2.47×10^{-1}	2.29×10^{-1}	4.61×10^{-1}	3.98×10^{-1}	5.57×10^{-1}	4.52×10^{-1}
10	3.42×10^{-2}	2.94×10^{-2}	1.38×10^{-1}	1.13×10^{-1}	2.57×10^{-1}	1.97×10^{-1}	3.11×10^{-1}	2.24×10^{-1}
15	1.91×10^{-2}	1.45×10^{-2}	7.68×10^{-2}	5.60×10^{-2}	1.44×10^{-1}	9.73×10^{-2}	1.73×10^{-1}	1.11×10^{-1}
20	1.06×10^{-2}	7.19×10^{-3}	4.29×10^{-2}	2.77×10^{-2}	8.02×10^{-2}	4.81×10^{-2}	9.68×10^{-2}	5.47×10^{-2}
25	5.97×10^{-3}	3.56×10^{-3}	2.39×10^{-2}	1.37×10^{-2}	4.47×10^{-2}	2.38×10^{-2}	5.40×10^{-2}	2.71×10^{-2}
30	3.33×10^{-3}	1.76×10^{-3}	1.33×10^{-2}	6.77×10^{-3}	2.50×10^{-2}	1.18×10^{-2}	3.01×10^{-2}	1.34×10^{-2}
40	1.04×10^{-3}	4.30×10^{-4}	4.17×10^{-3}	1.68×10^{-3}	7.79×10^{-3}	2.88×10^{-3}	9.41×10^{-3}	3.27×10^{-3}
50	3.24×10^{-4}	1.05×10^{-4}	1.30×10^{-3}	4.05×10^{-4}	2.43×10^{-3}	7.05×10^{-4}	2.93×10^{-3}	8.01×10^{-4}

TABLE 10 (Cont.)

Cover Thickness (cm)	Cover-and-Depth Factor by Source Depth							
	1 cm		5 cm		15 cm		50 cm	
	Old	New	Old	New	Old	New	Old	New
Al-26								
0.001	9.91×10^{-2}	1.73×10^{-1}	4.07×10^{-1}	5.07×10^{-1}	7.91×10^{-1}	8.61×10^{-1}	9.95×10^{-1}	9.98×10^{-1}
0.5	9.41×10^{-2}	1.26×10^{-1}	3.86×10^{-1}	4.34×10^{-1}	7.51×10^{-1}	7.66×10^{-1}	9.44×10^{-1}	8.96×10^{-1}
1	8.93×10^{-2}	1.05×10^{-1}	3.66×10^{-1}	3.92×10^{-1}	7.13×10^{-1}	7.04×10^{-1}	8.96×10^{-1}	8.26×10^{-1}
2	8.04×10^{-2}	8.66×10^{-2}	3.30×10^{-1}	3.39×10^{-1}	6.42×10^{-1}	6.14×10^{-1}	8.07×10^{-1}	7.21×10^{-1}
5	5.88×10^{-2}	5.86×10^{-2}	2.41×10^{-1}	2.31×10^{-1}	4.69×10^{-1}	4.19×10^{-1}	5.90×10^{-1}	4.92×10^{-1}
10	3.48×10^{-2}	3.11×10^{-2}	1.43×10^{-1}	1.23×10^{-1}	2.78×10^{-1}	2.23×10^{-1}	3.50×10^{-1}	2.61×10^{-1}
15	2.07×10^{-2}	1.66×10^{-2}	8.49×10^{-2}	6.53×10^{-2}	1.65×10^{-1}	1.18×10^{-1}	2.08×10^{-1}	1.39×10^{-1}
20	1.22×10^{-2}	8.80×10^{-3}	5.03×10^{-2}	3.47×10^{-2}	9.79×10^{-2}	6.30×10^{-2}	1.23×10^{-1}	7.39×10^{-2}
25	7.29×10^{-3}	4.68×10^{-3}	2.98×10^{-2}	1.84×10^{-2}	5.81×10^{-2}	3.35×10^{-2}	7.30×10^{-2}	3.93×10^{-2}
30	4.32×10^{-3}	2.49×10^{-3}	1.77×10^{-2}	9.80×10^{-3}	3.44×10^{-2}	1.78×10^{-2}	4.33×10^{-2}	2.09×10^{-2}
40	1.52×10^{-3}	7.02×10^{-4}	6.24×10^{-3}	2.77×10^{-3}	1.21×10^{-2}	5.02×10^{-3}	1.52×10^{-2}	5.90×10^{-3}
50	5.35×10^{-4}	1.98×10^{-4}	2.20×10^{-3}	7.83×10^{-4}	4.27×10^{-3}	1.42×10^{-3}	5.37×10^{-3}	1.67×10^{-3}
U-234								
0.001	2.18×10^{-1}	4.67×10^{-1}	7.08×10^{-1}	8.44×10^{-1}	9.75×10^{-1}	9.90×10^{-1}	1.00	9.97×10^{-1}
0.5	1.93×10^{-1}	1.66×10^{-1}	6.26×10^{-1}	4.89×10^{-1}	8.62×10^{-1}	6.14×10^{-1}	8.84×10^{-1}	6.20×10^{-1}
1	1.71×10^{-1}	1.41×10^{-1}	5.53×10^{-1}	4.18×10^{-1}	7.63×10^{-1}	5.25×10^{-1}	7.82×10^{-1}	5.30×10^{-1}
2	1.33×10^{-1}	1.04×10^{-1}	4.33×10^{-1}	3.06×10^{-1}	5.96×10^{-1}	3.85×10^{-1}	6.12×10^{-1}	3.89×10^{-1}
5	6.37×10^{-2}	4.09×10^{-2}	2.07×10^{-1}	1.21×10^{-1}	2.85×10^{-1}	1.52×10^{-1}	2.92×10^{-1}	1.53×10^{-1}
10	1.86×10^{-2}	8.66×10^{-3}	6.05×10^{-2}	2.56×10^{-2}	8.34×10^{-2}	3.21×10^{-2}	8.55×10^{-2}	3.24×10^{-2}
15	5.45×10^{-3}	1.83×10^{-3}	1.77×10^{-2}	5.42×10^{-3}	2.44×10^{-2}	6.81×10^{-3}	2.50×10^{-2}	6.87×10^{-3}
20	1.59×10^{-3}	3.88×10^{-4}	5.17×10^{-3}	1.15×10^{-3}	7.13×10^{-3}	1.44×10^{-3}	7.31×10^{-3}	1.46×10^{-3}
25	4.66×10^{-4}	8.23×10^{-5}	1.51×10^{-3}	2.43×10^{-4}	2.08×10^{-3}	3.05×10^{-4}	2.14×10^{-3}	3.08×10^{-4}
30	1.36×10^{-4}	1.74×10^{-5}	4.42×10^{-4}	5.15×10^{-5}	6.09×10^{-4}	6.47×10^{-5}	6.25×10^{-4}	6.53×10^{-5}

TABLE 10 (Cont.)

Cover Thickness (cm)	Cover-and-Depth Factor by Source Depth							
	1 cm		5 cm		15 cm		50 cm	
	Old	New	Old	New	Old	New	Old	New
U-235								
0.001	2.04×10^{-1}	2.51×10^{-1}	6.81×10^{-1}	6.92×10^{-1}	9.67×10^{-1}	9.66×10^{-1}	1.00	1.00
0.5	1.82×10^{-1}	1.81×10^{-1}	6.07×10^{-1}	5.73×10^{-1}	8.63×10^{-1}	8.13×10^{-1}	8.92×10^{-1}	8.49×10^{-1}
1	1.62×10^{-1}	1.51×10^{-1}	5.42×10^{-1}	5.02×10^{-1}	7.70×10^{-1}	7.22×10^{-1}	7.96×10^{-1}	7.49×10^{-1}
2	1.29×10^{-1}	1.19×10^{-1}	4.31×10^{-1}	4.00×10^{-1}	6.13×10^{-1}	5.76×10^{-1}	6.33×10^{-1}	5.98×10^{-1}
5	6.52×10^{-2}	6.10×10^{-2}	2.17×10^{-1}	2.06×10^{-1}	3.09×10^{-1}	2.97×10^{-1}	3.19×10^{-1}	3.08×10^{-1}
10	2.08×10^{-2}	2.02×10^{-2}	6.93×10^{-2}	6.83×10^{-2}	9.85×10^{-2}	9.84×10^{-2}	1.02×10^{-1}	1.02×10^{-1}
15	6.64×10^{-3}	6.71×10^{-3}	2.21×10^{-2}	2.26×10^{-2}	3.14×10^{-2}	3.26×10^{-2}	3.25×10^{-2}	3.39×10^{-2}
20	2.12×10^{-3}	2.22×10^{-3}	7.06×10^{-3}	7.50×10^{-3}	1.00×10^{-2}	1.08×10^{-2}	1.04×10^{-2}	1.12×10^{-2}
25	6.76×10^{-4}	7.37×10^{-4}	2.25×10^{-3}	2.49×10^{-3}	3.20×10^{-3}	3.59×10^{-3}	3.31×10^{-3}	3.72×10^{-3}
30	2.16×10^{-4}	2.44×10^{-4}	7.19×10^{-4}	8.25×10^{-4}	1.02×10^{-3}	1.19×10^{-3}	1.06×10^{-3}	1.23×10^{-3}
40	2.20×10^{-5}	2.69×10^{-5}	7.33×10^{-5}	9.07×10^{-5}	1.04×10^{-4}	1.31×10^{-4}	1.08×10^{-4}	1.36×10^{-4}
50	2.24×10^{-6}	2.95×10^{-6}	7.46×10^{-6}	9.97×10^{-6}	1.06×10^{-5}	1.44×10^{-5}	1.10×10^{-5}	1.49×10^{-5}
U-238								
0.001	1.21×10^{-1}	2.34×10^{-1}	4.80×10^{-1}	5.88×10^{-1}	8.55×10^{-1}	9.05×10^{-1}	9.98×10^{-1}	9.99×10^{-1}
0.5	1.13×10^{-1}	1.57×10^{-1}	4.45×10^{-1}	4.74×10^{-1}	8.02×10^{-1}	7.68×10^{-1}	9.36×10^{-1}	8.56×10^{-1}
1	1.06×10^{-1}	1.21×10^{-1}	4.17×10^{-1}	4.10×10^{-1}	7.52×10^{-1}	6.84×10^{-1}	8.78×10^{-1}	7.65×10^{-1}
2	9.34×10^{-2}	9.09×10^{-2}	3.67×10^{-1}	3.37×10^{-1}	6.61×10^{-1}	5.74×10^{-1}	7.72×10^{-1}	6.44×10^{-1}
5	6.35×10^{-2}	5.63×10^{-2}	2.49×10^{-1}	2.14×10^{-1}	4.49×10^{-1}	3.67×10^{-1}	5.25×10^{-1}	4.12×10^{-1}
10	3.33×10^{-2}	2.70×10^{-2}	1.31×10^{-1}	1.03×10^{-1}	2.36×10^{-1}	1.76×10^{-1}	2.76×10^{-1}	1.97×10^{-1}
15	1.75×10^{-2}	1.29×10^{-2}	6.88×10^{-2}	4.93×10^{-2}	1.24×10^{-1}	8.42×10^{-2}	1.45×10^{-1}	9.46×10^{-2}
20	9.20×10^{-3}	6.21×10^{-3}	3.62×10^{-2}	2.36×10^{-2}	6.51×10^{-2}	4.04×10^{-2}	7.61×10^{-2}	4.54×10^{-2}
25	4.83×10^{-3}	2.98×10^{-3}	1.90×10^{-2}	1.13×10^{-2}	3.42×10^{-2}	1.94×10^{-2}	4.00×10^{-2}	2.17×10^{-2}
30	2.54×10^{-3}	1.43×10^{-3}	1.00×10^{-2}	5.43×10^{-3}	1.80×10^{-2}	9.28×10^{-3}	2.10×10^{-2}	1.04×10^{-2}
40	7.01×10^{-4}	3.28×10^{-4}	2.75×10^{-3}	1.25×10^{-3}	4.96×10^{-3}	2.13×10^{-3}	5.79×10^{-3}	2.40×10^{-3}
50	1.94×10^{-4}	7.53×10^{-5}	7.60×10^{-4}	2.87×10^{-4}	1.37×10^{-4}	4.90×10^{-4}	1.60×10^{-3}	5.51×10^{-4}

TABLE 10 (Cont.)

Cover Thickness (cm)	Cover-and-Depth Factor by Source Depth							
	1 cm		5 cm		15 cm		50 cm	
	Old	New	Old	New	Old	New	Old	New
Co-57								
0.001	2.01×10^{-1}	2.76×10^{-1}	6.74×10^{-1}	7.42×10^{-1}	9.65×10^{-1}	9.80×10^{-1}	1.00	1.00
0.5	1.80×10^{-1}	2.02×10^{-1}	6.03×10^{-1}	6.09×10^{-1}	8.63×10^{-1}	8.19×10^{-1}	8.94×10^{-1}	8.36×10^{-1}
1	1.61×10^{-1}	1.67×10^{-1}	5.39×10^{-1}	5.24×10^{-1}	7.71×10^{-1}	7.09×10^{-1}	7.99×10^{-1}	7.24×10^{-1}
2	1.28×10^{-1}	1.26×10^{-1}	4.31×10^{-1}	4.02×10^{-1}	6.16×10^{-1}	5.45×10^{-1}	6.38×10^{-1}	5.57×10^{-1}
5	6.54×10^{-2}	5.83×10^{-2}	2.20×10^{-1}	1.87×10^{-1}	3.14×10^{-1}	2.53×10^{-1}	3.26×10^{-1}	2.58×10^{-1}
10	2.13×10^{-2}	1.62×10^{-2}	7.14×10^{-2}	5.19×10^{-2}	1.02×10^{-1}	7.03×10^{-2}	1.06×10^{-1}	7.18×10^{-2}
15	6.93×10^{-3}	4.51×10^{-3}	2.32×10^{-2}	1.44×10^{-2}	3.33×10^{-2}	1.95×10^{-2}	3.45×10^{-2}	2.00×10^{-2}
20	2.26×10^{-3}	1.25×10^{-3}	7.57×10^{-3}	4.01×10^{-3}	1.08×10^{-2}	5.43×10^{-3}	1.12×10^{-2}	5.55×10^{-3}
25	7.35×10^{-4}	3.49×10^{-4}	2.47×10^{-3}	1.11×10^{-3}	3.53×10^{-3}	1.51×10^{-3}	3.66×10^{-3}	1.54×10^{-3}
30	2.39×10^{-4}	9.69×10^{-5}	8.03×10^{-4}	3.10×10^{-4}	1.15×10^{-3}	4.20×10^{-4}	1.19×10^{-3}	4.29×10^{-4}

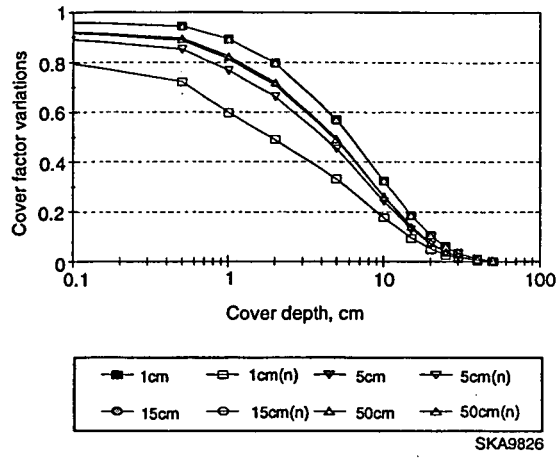

(a) Actual cover factor for old (solid) and new (open) RESRAD models

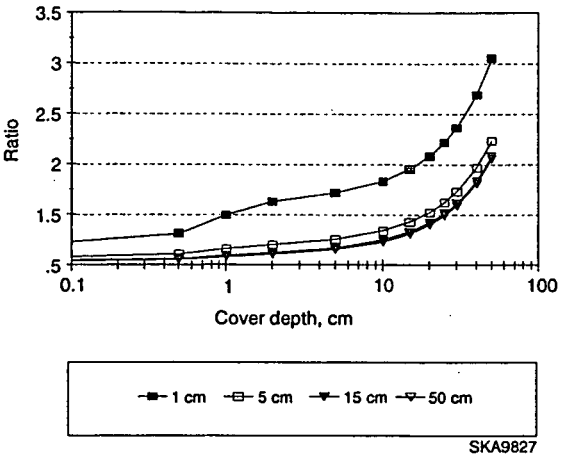

(b) Ratio of cover factor for RESRAD models

FIGURE 4 Cover Factor Comparison as a Function of Cover Depth for a Set of Co-60-Contaminated Source Depths

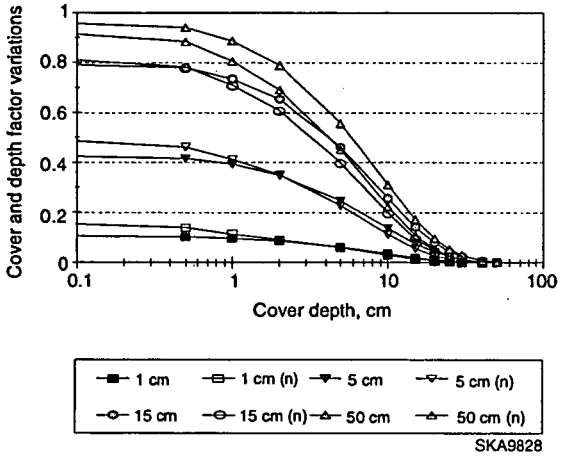

(a) Actual cover-and-depth factor for old (solid) and new (open) RESRAD models

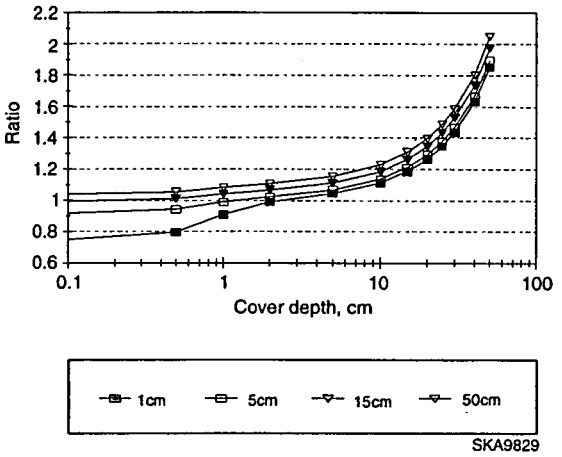

(b) Radio of cover-and-depth factor for RESRAD models

FIGURE 5 Cover-and-Depth Factor Comparison as a Function of Cover Depth for a Set of Co-60-Contaminated Source Depths

not depend on energy. Therefore, a uniform correction was applied for all energies. The area factor correction curve was approximated as the sum of four line segments:

$$y = 0.016\,A \text{ for } 0 < A < 25 \text{ m}^2,$$

$$y = 0.35 + 0.002\,A \text{ for } 25 < A < 100 \text{ m}^2,$$

$$y = 0.48 + 0.00065\,A \text{ for } 100 < A < 500 \text{ m}^2,$$

$$y = 0.67 + 0.00027\,A \text{ for } 500 < A < 1{,}222 \text{ m}^2, \text{ and}$$

$$y = 1 \text{ for } A \geq 1{,}222 \text{ m}^2.$$

The results from comparison of the old and new methods are discussed here. The area factor is plotted against the source radius for different energies and is calculated for different source depths. Table 11 gives the area factor, $F_A(Ei)$, for different source depths. Sources are assumed to be of different energies (10, 30, 60, 100, 300, 600, 1,000, 3,000, 6,000, and 10,000 keV), and the source radius varies from 0.56 to 1,000 m. Different columns give area factors for different energies. Different rows give the area factors at different source radii. Figure 6 shows the area factor variations for different source depths (0.1, 1.0, 10.0, and 100 cm). Each curve in the figures represents the variation with source radius for a particular energy.

As shown in Figure 6, the area factor increases with source radius and approaches unity for radii greater than 50 m. The area factor is always larger in the new model for small source radii for all energies. For the 100-cm-thick source, the area factor is larger up to a source radius of 13 m; for the 1-cm-thick source, it is larger up to a 2-m source radius. The area factor decreases with increasing energy, with sharp decreases when the energy changes from 10 to 60 keV, and varies slightly with higher energy. The area factor also increases with increasing source depth. Comparisons show that the area factor of sources with depths greater than 10 cm are always greater in the new model. For very thin sources (0.1 cm depth), the old RESRAD model values are higher except for energies under 30 keV, for which the new model gives higher values. Values compare reasonably well in the two models at a source depth of 1 cm for energies above 30 keV.

Tables 12 through 14 show the variation of area factor with cover thickness. Computations are made for three energy levels (10, 100, and 1,000 keV) and four source depths (0.1, 1, 10, and 100 cm). Source radius varies from 0.56 to 1,000 m, and cover thickness varies from 0 to 50 cm for each set.

Table 12 shows the variation of the area factor with cover material at 10 keV. The area factor increases with the source radius for all source depths when there is no cover. With some cover (greater than 0.5 cm), the area factor becomes unity and is independent of source dimension.

TABLE 11 Area Factors for Source Depths of 0.1, 1, 10, and 100 cm at Different Energies

Radius (m)	Area Factor, F_A, by Energy Level										
	10 keV	30 keV	60 keV	100 keV	300 keV	600 keV	1 MeV	3 MeV	6 MeV	10 MeV	Old Model
Source Depth = 0.1 cm											
0.56	0.246	0.0527	0.0234	0.0218	0.0265	0.0275	0.0278	0.0266	0.0259	0.0257	0.0160
1	0.528	0.134	0.0599	0.0556	0.0672	0.0697	0.0705	0.0676	0.0657	0.0652	0.0500
1.5	0.742	0.229	0.103	0.0951	0.115	0.119	0.120	0.115	0.112	0.111	0.113
2	0.859	0.312	0.142	0.131	0.156	0.162	0.164	0.157	0.153	0.151	0.200
2.8	0.944	0.421	0.196	0.178	0.212	0.219	0.222	0.212	0.207	0.205	0.400
3.5	0.974	0.497	0.235	0.213	0.251	0.260	0.263	0.252	0.245	0.243	0.427
4.5	0.991	0.582	0.283	0.254	0.297	0.307	0.311	0.297	0.289	0.287	0.477
5.6	0.997	0.654	0.328	0.292	0.339	0.349	0.353	0.338	0.329	0.326	0.550
7	0.999	0.723	0.377	0.333	0.381	0.392	0.397	0.380	0.369	0.366	0.580
9	1.00	0.792	0.436	0.381	0.431	0.442	0.447	0.428	0.416	0.412	0.645
11	1.00	0.841	0.485	0.421	0.470	0.482	0.486	0.466	0.453	0.449	0.727
13	1.00	0.876	0.528	0.457	0.504	0.515	0.519	0.497	0.483	0.479	0.800
15	1.00	0.902	0.566	0.488	0.532	0.543	0.547	0.524	0.510	0.505	0.860
17.5	1.00	0.925	0.608	0.523	0.564	0.574	0.578	0.553	0.538	0.533	0.929
20	1.00	0.942	0.645	0.554	0.591	0.600	0.604	0.578	0.562	0.557	1.00
50	1.00	0.994	0.881	0.789	0.781	0.777	0.776	0.742	0.722	0.715	1.00
100	1.00	1.00	0.979	0.939	0.909	0.894	0.889	0.852	0.830	0.822	1.00
200	1.00	1.00	1.00	0.998	0.986	0.972	0.966	0.936	0.917	0.909	1.00
500	1.00	1.00	1.00	1.00	1.00	1.00	0.999	0.992	0.984	0.978	1.00
1000	1.00	1.00	1.00	1.00	1.00	1.00	1.00	1.00	1.00	0.998	1.00
Source Depth = 1 cm											
0.56	0.246	0.117	0.0417	0.0319	0.0361	0.0376	0.0378	0.0358	0.0347	0.0345	0.0160
1	0.528	0.281	0.109	0.0826	0.0921	0.0956	0.0961	0.0908	0.0881	0.0876	0.0500
1.5	0.741	0.442	0.190	0.144	0.157	0.163	0.164	0.155	0.150	0.149	0.113
2	0.858	0.561	0.265	0.200	0.216	0.222	0.223	0.211	0.204	0.203	0.200
2.8	0.943	0.686	0.369	0.279	0.293	0.301	0.302	0.285	0.276	0.274	0.400
3.5	0.973	0.755	0.444	0.338	0.349	0.357	0.357	0.337	0.327	0.325	0.427
4.5	0.990	0.819	0.531	0.410	0.415	0.422	0.421	0.397	0.385	0.382	0.477
5.6	0.997	0.862	0.606	0.476	0.473	0.479	0.477	0.450	0.436	0.433	0.550
7	0.999	0.898	0.680	0.546	0.534	0.537	0.534	0.504	0.489	0.485	0.580
9	1.00	0.935	0.754	0.625	0.603	0.603	0.598	0.564	0.547	0.543	0.645
11	1.00	0.956	0.806	0.687	0.657	0.654	0.648	0.611	0.593	0.588	0.727
13	1.00	0.960	0.843	0.736	0.701	0.695	0.6878	0.649	0.630	0.625	0.800
15	1.00	0.968	0.869	0.775	0.737	0.729	0.721	0.681	0.661	0.655	0.860
17.5	1.00	0.978	0.894	0.813	0.774	0.763	0.755	0.714	0.693	0.687	0.929
20	1.00	0.984	0.913	0.843	0.804	0.792	0.783	0.741	0.721	0.714	1.00
50	1.00	0.997	0.982	0.962	0.945	0.934	0.928	0.894	0.876	0.869	1.00
100	1.00	1.00	0.997	0.992	0.985	0.980	0.977	0.961	0.948	0.941	1.00
200	1.00	1.00	1.00	0.999	0.998	0.996	0.995	0.988	0.982	0.980	1.00
500	1.00	1.00	1.00	1.00	1.00	1.00	1.00	1.00	0.998	0.997	1.00
1000	1.00	1.00	1.00	1.00	1.00	1.00	1.00	1.00	1.00	1.00	1.00

TABLE 11 (Cont.)

Radius (m)	Area Factor, F_A, by Energy Level										
	10 keV	30 keV	60 keV	100 keV	300 keV	600 keV	1 MeV	3 MeV	6 MeV	10 MeV	Old Model
Source Depth = 10 cm											
0.56	0.246	0.133	0.117	0.0917	0.0781	0.0749	0.072	0.0641	0.0604	0.0595	0.0160
1	0.528	0.305	0.280	0.231	0.198	0.190	0.182	0.163	0.153	0.151	0.0500
1.5	0.741	0.464	0.438	0.380	0.333	0.319	0.306	0.275	0.260	0.256	0.113
2	0.858	0.575	0.553	0.498	0.445	0.427	0.411	0.371	0.351	0.346	0.200
2.8	0.943	0.687	0.671	0.628	0.577	0.555	0.537	0.489	0.465	0.458	0.400
3.5	0.973	0.747	0.737	0.702	0.656	0.634	0.615	0.567	0.540	0.533	0.427
4.5	0.990	0.806	0.796	0.769	0.733	0.713	0.695	0.648	0.620	0.612	0.477
5.6	0.997	0.847	0.838	0.816	0.787	0.770	0.754	0.712	0.684	0.676	0.550
7	0.999	0.868	0.873	0.860	0.835	0.819	0.806	0.768	0.743	0.735	0.580
9	1.00	0.894	0.902	0.894	0.875	0.860	0.849	0.820	0.800	0.792	0.645
11	1.00	0.910	0.920	0.916	0.900	0.887	0.879	0.854	0.835	0.831	0.727
13	1.00	0.922	0.934	0.930	0.918	0.905	0.899	0.881	0.864	0.859	0.800
15	1.00	0.931	0.944	0.941	0.931	0.918	0.913	0.899	0.884	0.877	0.860
17.5	1.00	0.941	0.946	0.951	0.940	0.932	0.925	0.915	0.901	0.896	0.929
20	1.00	0.949	0.949	0.958	0.948	0.941	0.935	0.927	0.914	0.909	1.00
50	1.00	0.990	0.973	0.979	0.981	0.979	0.976	0.974	0.970	0.968	1.00
100	1.00	0.999	0.991	0.990	0.989	0.988	0.988	0.987	0.986	0.985	1.00
200	1.00	1.00	1.00	0.998	0.996	0.995	0.995	0.994	0.993	0.992	1.00
500	1.00	1.00	1.00	1.00	1.00	1.00	0.999	0.999	0.998	0.998	1.00
1000	1.00	1.00	1.00	1.00	1.00	1.00	1.00	1.00	1.00	1.00	1.00
Source Depth = 100 cm											
0.56	0.246	0.133	0.121	0.114	0.106	0.100	0.0960	0.0860	0.0820	0.0800	0.0160
1	0.528	0.305	0.286	0.274	0.258	0.246	0.236	0.215	0.208	0.203	0.0500
1.5	0.741	0.464	0.443	0.432	0.411	0.393	0.380	0.353	0.345	0.34	0.113
2	0.858	0.575	0.555	0.546	0.524	0.503	0.487	0.459	0.454	0.448	0.200
2.8	0.943	0.687	0.670	0.664	0.641	0.617	0.600	0.573	0.571	0.567	0.400
3.5	0.973	0.747	0.734	0.729	0.705	0.68	0.662	0.636	0.638	0.635	0.427
4.5	0.99	0.806	0.791	0.788	0.765	0.737	0.719	0.694	0.698	0.697	0.477
5.6	0.997	0.847	0.831	0.831	0.804	0.777	0.758	0.734	0.740	0.739	0.550
7	0.999	0.868	0.863	0.862	0.837	0.810	0.789	0.765	0.774	0.774	0.580
9	1.00	0.894	0.887	0.890	0.864	0.836	0.816	0.793	0.805	0.805	0.645
11	1.00	0.910	0.901	0.904	0.881	0.852	0.832	0.811	0.822	0.824	0.727
13	1.00	0.922	0.908	0.911	0.89	0.863	0.844	0.824	0.835	0.837	0.800
15	1.00	0.931	0.913	0.915	0.895	0.869	0.851	0.833	0.845	0.847	0.860
17.5	1.00	0.941	0.918	0.919	0.901	0.876	0.86	0.842	0.854	0.856	0.929
20	1.00	0.949	0.923	0.923	0.906	0.883	0.867	0.850	0.861	0.863	1.00
50	1.00	0.990	0.960	0.953	0.940	0.925	0.915	0.900	0.905	0.906	1.00
100	1.00	0.999	0.986	0.978	0.967	0.955	0.948	0.936	0.937	0.936	1.00
200	1.00	1.00	0.999	0.996	0.989	0.981	0.977	0.967	0.964	0.963	1.00
500	1.00	1.00	1.00	1.00	1.00	0.999	0.998	0.993	0.990	0.988	1.00
1000	1.00	1.00	1.00	1.00	1.00	1.00	1.00	1.00	0.999	0.998	1.00

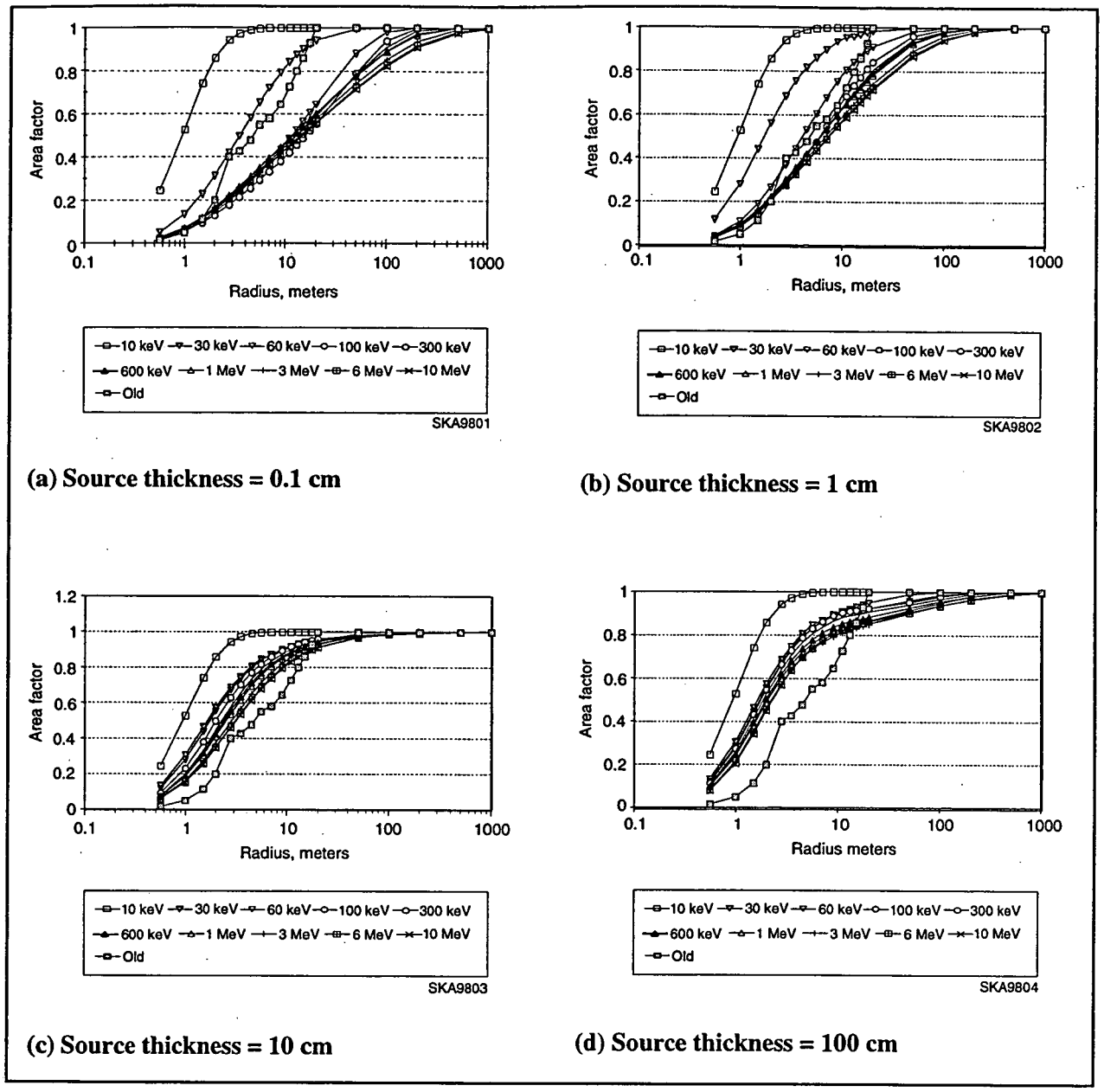

FIGURE 6 Area Factor Versus Source Radius for a Set of Gamma Energies with No Cover

TABLE 12 Area Factor Variations with Cover Thickness for Different Source Radii at an Energy of 10 keV and Source Depths of 0.1, 1, 10, and 100 cm

Cover Thickness (cm)	Area Factor, F_A, by Source Radius									
	0.56 m	1.0 m	2.8 m	5.6 m	13 m	20 m	50 m	200 m	500 m	1,000 m
Source Depth = 0.1 cm										
0	2.46×10^{-1}	5.28×10^{-1}	9.44×10^{-1}	9.97×10^{-1}	1.00	1.00	1.00	1.00	1.00	1.00
0.5	1.00	1.00	1.00	1.00	1.00	1.00	1.00	1.00	1.00	1.00
2	1.00	1.00	1.00	1.00	1.00	1.00	1.00	1.00	1.00	1.00
4	1.00	1.00	1.00	1.00	1.00	1.00	1.00	1.00	1.00	1.00
6	1.00	1.00	1.00	1.00	1.00	1.00	1.00	1.00	1.00	1.00
8	1.00	1.00	1.00	1.00	1.00	1.00	1.00	1.00	1.00	1.00
10	1.00	1.00	1.00	1.00	1.00	1.00	1.00	1.00	1.00	1.00
15	1.00	1.00	1.00	1.00	1.00	1.00	1.00	1.00	1.00	1.00
20	1.00	1.00	1.00	1.00	1.00	1.00	1.00	1.00	1.00	1.00
50	1.00	1.00	1.00	1.00	1.00	1.00	1.00	1.00	1.00	1.00
Source Depth = 1 cm										
0	2.46×10^{-1}	5.28×10^{-1}	9.43×10^{-1}	9.97×10^{-1}	1.00	1.00	1.00	1.00	1.00	1.00
0.5	1.00	1.00	1.00	1.00	1.00	1.00	1.00	1.00	1.00	1.00
2	1.00	1.00	1.00	1.00	1.00	1.00	1.00	1.00	1.00	1.00
4	1.00	1.00	1.00	1.00	1.00	1.00	1.00	1.00	1.00	1.00
6	1.00	1.00	1.00	1.00	1.00	1.00	1.00	1.00	1.00	1.00
8	1.00	1.00	1.00	1.00	1.00	1.00	1.00	1.00	1.00	1.00
10	1.00	1.00	1.00	1.00	1.00	1.00	1.00	1.00	1.00	1.00
15	1.00	1.00	1.00	1.00	1.00	1.00	1.00	1.00	1.00	1.00
20	1.00	1.00	1.00	1.00	1.00	1.00	1.00	1.00	1.00	1.00
50	1.00	1.00	1.00	1.00	1.00	1.00	1.00	1.00	1.00	1.00

TABLE 12 (Cont.)

Cover Thickness (cm)	Area Factor, F_A, by Source Radius									
	0.56 m	1.0 m	2.8 m	5.6 m	13 m	20 m	50 m	200 m	500 m	1,000 m
Source Depth = 10 cm										
0	2.46×10^{-1}	5.28×10^{-1}	9.43×10^{-1}	9.97×10^{-1}	1.00	1.00	1.00	1.00	1.00	1.00
0.5	1.00	1.00	1.00	1.00	1.00	1.00	1.00	1.00	1.00	1.00
2	1.00	1.00	1.00	1.00	1.00	1.00	1.00	1.00	1.00	1.00
4	1.00	1.00	1.00	1.00	1.00	1.00	1.00	1.00	1.00	1.00
6	1.00	1.00	1.00	1.00	1.00	1.00	1.00	1.00	1.00	1.00
8	1.00	1.00	1.00	1.00	1.00	1.00	1.00	1.00	1.00	1.00
10	1.00	1.00	1.00	1.00	1.00	1.00	1.00	1.00	1.00	1.00
15	1.00	1.00	1.00	1.00	1.00	1.00	1.00	1.00	1.00	1.00
20	1.00	1.00	1.00	1.00	1.00	1.00	1.00	1.00	1.00	1.00
50	1.00	1.00	1.00	1.00	1.00	1.00	1.00	1.00	1.00	1.00
Source Depth = 100 cm										
0	2.46×10^{-1}	5.28×10^{-1}	9.43×10^{-1}	9.97×10^{-1}	1.00	1.00	1.00	1.00	1.00	1.00
0.5	1.00	1.00	1.00	1.00	1.00	1.00	1.00	1.00	1.00	1.00
2	1.00	1.00	1.00	1.00	1.00	1.00	1.00	1.00	1.00	1.00
4	1.00	1.00	1.00	1.00	1.00	1.00	1.00	1.00	1.00	1.00
6	1.00	1.00	1.00	1.00	1.00	1.00	1.00	1.00	1.00	1.00
8	1.00	1.00	1.00	1.00	1.00	1.00	1.00	1.00	1.00	1.00
10	1.00	1.00	1.00	1.00	1.00	1.00	1.00	1.00	1.00	1.00
15	1.00	1.00	1.00	1.00	1.00	1.00	1.00	1.00	1.00	1.00
20	1.00	1.00	1.00	1.00	1.00	1.00	1.00	1.00	1.00	1.00
50	1.00	1.00	1.00	1.00	1.00	1.00	1.00	1.00	1.00	1.00

TABLE 13 Area Factor Variations with Cover Thickness for Different Source Radii at an Energy of 100 keV and Source Depths of 0.1, 1, 10, and 100 cm

Cover Thickness (cm)	Area Factor, F_A, by Source Radius									
	0.56 m	1.0 m	2.8 m	5.6 m	13 m	20 m	50 m	200 m	500 m	1,000 m
Source Depth = 0.1 cm										
0	2.18×10^{-2}	5.56×10^{-2}	1.78×10^{-1}	2.92×10^{-1}	4.57×10^{-1}	5.54×10^{-1}	7.89×10^{-1}	9.98×10^{-1}	1.00	1.00
0.5	3.43×10^{-2}	8.88×10^{-2}	3.03×10^{-1}	5.24×10^{-1}	8.22×10^{-1}	9.39×10^{-1}	1.00	1.00	1.00	1.00
2	6.69×10^{-2}	1.75×10^{-1}	5.86×10^{-1}	8.85×10^{-1}	1.00	1.00	1.00	1.00	1.00	1.00
4	1.11×10^{-1}	2.84×10^{-1}	8.15×10^{-1}	1.00	1.00	1.00	1.00	1.00	1.00	1.00
6	1.54×10^{-1}	3.81×10^{-1}	9.21×10^{-1}	1.00	1.00	1.00	1.00	1.00	1.00	1.00
8	1.93×10^{-1}	4.64×10^{-1}	9.72×10^{-1}	1.00	1.00	1.00	1.00	1.00	1.00	1.00
10	2.30×10^{-1}	5.34×10^{-1}	9.96×10^{-1}	1.00	1.00	1.00	1.00	1.00	1.00	1.00
15	3.09×10^{-1}	6.65×10^{-1}	1.00	1.00	1.00	1.00	1.00	1.00	1.00	1.00
20	3.73×10^{-1}	7.51×10^{-1}	1.00	1.00	1.00	1.00	1.00	1.00	1.00	1.00
50	5.64×10^{-1}	9.24×10^{-1}	1.00	1.00	1.00	1.00	1.00	1.00	1.00	1.00
Source Depth = 1 cm										
0	3.19×10^{-2}	8.26×10^{-2}	2.79×10^{-1}	4.76×10^{-1}	7.36×10^{-1}	8.43×10^{-1}	9.62×10^{-1}	9.99×10^{-1}	1.00	1.00
0.5	4.33×10^{-2}	1.13×10^{-1}	3.91×10^{-1}	6.58×10^{-1}	9.29×10^{-1}	9.87×10^{-1}	1.00	1.00	1.00	1.00
2	7.64×10^{-2}	1.99×10^{-1}	6.46×10^{-1}	9.26×10^{-1}	1.00	1.00	1.00	1.00	1.00	1.00
4	1.20×10^{-1}	3.06×10^{-1}	8.43×10^{-1}	1.00	1.00	1.00	1.00	1.00	1.00	1.00
6	1.62×10^{-1}	4.00×10^{-1}	9.35×10^{-1}	1.00	1.00	1.00	1.00	1.00	1.00	1.00
8	2.02×10^{-1}	4.80×10^{-1}	9.79×10^{-1}	1.00	1.00	1.00	1.00	1.00	1.00	1.00
10	2.37×10^{-1}	5.47×10^{-1}	9.98×10^{-1}	1.00	1.00	1.00	1.00	1.00	1.00	1.00
15	3.15×10^{-1}	6.74×10^{-1}	1.00	1.00	1.00	1.00	1.00	1.00	1.00	1.00
20	3.78×10^{-1}	7.57×10^{-1}	1.00	1.00	1.00	1.00	1.00	1.00	1.00	1.00
50	5.65×10^{-1}	9.25×10^{-1}	1.00	1.00	1.00	1.00	1.00	1.00	1.00	1.00

TABLE 13 (Cont.)

Cover Thickness (cm)	Area Factor, F_A, by Source Radius									
	0.56 m	1.0 m	2.8 m	5.6 m	13 m	20 m	50 m	200 m	500 m	1,000 m
Source Depth = 10 cm										
0	9.17×10^{-2}	2.31×10^{-1}	6.28×10^{-1}	8.16×10^{-1}	9.30×10^{-1}	9.58×10^{-1}	9.79×10^{-1}	9.98×10^{-1}	1.00	1.00
0.5	1.05×10^{-1}	2.62×10^{-1}	7.02×10^{-1}	8.93×10^{-1}	9.84×10^{-1}	9.96×10^{-1}	1.00	1.00	1.00	1.00
2	1.38×10^{-1}	3.39×10^{-1}	8.38×10^{-1}	9.83×10^{-1}	1.00	1.00	1.00	1.00	1.00	1.00
4	1.78×10^{-1}	4.28×10^{-1}	9.32×10^{-1}	1.00	1.00	1.00	1.00	1.00	1.00	1.00
6	2.16×10^{-1}	5.03×10^{-1}	9.75×10^{-1}	1.00	1.00	1.00	1.00	1.00	1.00	1.00
8	2.50×10^{-1}	5.66×10^{-1}	9.94×10^{-1}	1.00	1.00	1.00	1.00	1.00	1.00	1.00
10	2.82×10^{-1}	6.20×10^{-1}	1.00	1.00	1.00	1.00	1.00	1.00	1.00	1.00
15	3.51×10^{-1}	7.21×10^{-1}	1.00	1.00	1.00	1.00	1.00	1.00	1.00	1.00
20	4.06×10^{-1}	7.88×10^{-1}	1.00	1.00	1.00	1.00	1.00	1.00	1.00	1.00
50	5.72×10^{-1}	9.29×10^{-1}	1.00	1.00	1.00	1.00	1.00	1.00	1.00	1.00
Source Depth = 100 cm										
0	1.14×10^{-1}	2.74×10^{-1}	6.64×10^{-1}	8.31×10^{-1}	9.11×10^{-1}	9.23×10^{-1}	9.53×10^{-1}	9.96×10^{-1}	1.00	1.00
0.5	1.28×10^{-1}	3.08×10^{-1}	7.37×10^{-1}	9.05×10^{-1}	9.77×10^{-1}	9.91×10^{-1}	1.00	1.00	1.00	1.00
2	1.60×10^{-1}	3.80×10^{-1}	8.57×10^{-1}	9.84×10^{-1}	1.00	1.00	1.00	1.00	1.00	1.00
4	1.98×10^{-1}	4.61×10^{-1}	9.41×10^{-1}	1.00	1.00	1.00	1.00	1.00	1.00	1.00
6	2.34×10^{-1}	5.31×10^{-1}	9.78×10^{-1}	1.00	1.00	1.00	1.00	1.00	1.00	1.00
8	2.66×10^{-1}	5.89×10^{-1}	9.94×10^{-1}	1.00	1.00	1.00	1.00	1.00	1.00	1.00
10	2.97×10^{-1}	6.39×10^{-1}	1.00	1.00	1.00	1.00	1.00	1.00	1.00	1.00
15	3.62×10^{-1}	7.34×10^{-1}	1.00	1.00	1.00	1.00	1.00	1.00	1.00	1.00
20	4.14×10^{-1}	7.97×10^{-1}	1.00	1.00	1.00	1.00	1.00	1.00	1.00	1.00
50	5.74×10^{-1}	9.30×10^{-1}	1.00	1.00	1.00	1.00	1.00	1.00	1.00	1.00

TABLE 14 Area Factor Variations with Cover Thickness for Different Source Radii at an Energy of 1 MeV and Source Depths of 0.1, 1, 10, and 100 cm

Cover Thickness (cm)	Area Factor, F_A, by Source Radius									
	0.56 m	1.0 m	2.8 m	5.6 m	13 m	20 m	50 m	200 m	500 m	1,000 m
Source Depth = 0.1 cm										
0	2.78×10^{-2}	7.05×10^{-2}	2.22×10^{-1}	3.53×10^{-1}	5.19×10^{-1}	6.04×10^{-1}	7.76×10^{-1}	9.66×10^{-1}	9.99×10^{-1}	1.00
0.5	4.05×10^{-2}	1.03×10^{-1}	3.23×10^{-1}	5.11×10^{-1}	7.36×10^{-1}	8.36×10^{-1}	9.71×10^{-1}	1.00	1.00	1.00
2	5.98×10^{-2}	1.52×10^{-1}	4.71×10^{-1}	7.18×10^{-1}	9.26×10^{-1}	9.85×10^{-1}	1.00	1.00	1.00	1.00
4	8.11×10^{-2}	2.06×10^{-1}	6.17×10^{-1}	8.77×10^{-1}	9.99×10^{-1}	1.00	1.00	1.00	1.00	1.00
6	9.84×10^{-2}	2.49×10^{-1}	7.14×10^{-1}	9.61×10^{-1}	1.00	1.00	1.00	1.00	1.00	1.00
8	1.14×10^{-1}	2.87×10^{-1}	7.88×10^{-1}	9.76×10^{-1}	1.00	1.00	1.00	1.00	1.00	1.00
10	1.29×10^{-1}	3.22×10^{-1}	8.38×10^{-1}	9.92×10^{-1}	1.00	1.00	1.00	1.00	1.00	1.00
15	1.61×10^{-1}	3.94×10^{-1}	9.18×10^{-1}	1.00	1.00	1.00	1.00	1.00	1.00	1.00
20	1.87×10^{-1}	4.52×10^{-1}	9.57×10^{-1}	1.00	1.00	1.00	1.00	1.00	1.00	1.00
50	2.77×10^{-1}	6.24×10^{-1}	1.00	1.00	1.00	1.00	1.00	1.00	1.00	1.00
Source Depth = 1 cm										
0	3.78×10^{-2}	9.61×10^{-2}	3.02×10^{-1}	4.77×10^{-1}	6.88×10^{-1}	7.83×10^{-1}	9.28×10^{-1}	9.95×10^{-1}	9.98×10^{-1}	1.00
0.5	4.73×10^{-2}	1.20×10^{-1}	3.76×10^{-1}	5.89×10^{-1}	8.23×10^{-1}	9.11×10^{-1}	9.94×10^{-1}	1.00	1.00	1.00
2	6.56×10^{-2}	1.67×10^{-1}	5.14×10^{-1}	7.72×10^{-1}	9.68×10^{-1}	1.00	1.00	1.00	1.00	1.00
4	8.45×10^{-2}	2.15×10^{-1}	6.37×10^{-1}	8.91×10^{-1}	1.00	1.00	1.00	1.00	1.00	1.00
6	1.02×10^{-1}	2.58×10^{-1}	7.32×10^{-1}	9.58×10^{-1}	1.00	1.00	1.00	1.00	1.00	1.00
8	1.17×10^{-1}	2.95×10^{-1}	7.99×10^{-1}	9.81×10^{-1}	1.00	1.00	1.00	1.00	1.00	1.00
10	1.32×10^{-1}	3.29×10^{-1}	8.47×10^{-1}	9.94×10^{-1}	1.00	1.00	1.00	1.00	1.00	1.00
15	1.63×10^{-1}	4.00×10^{-1}	9.23×10^{-1}	1.00	1.00	1.00	1.00	1.00	1.00	1.00
20	1.89×10^{-1}	4.56×10^{-1}	9.60×10^{-1}	1.00	1.00	1.00	1.00	1.00	1.00	1.00
50	2.78×10^{-1}	6.25×10^{-1}	1.00	1.00	1.00	1.00	1.00	1.00	1.00	1.00

TABLE 14 (Cont.)

Cover Thickness (cm)	Area Factor, F_A, by Source Radius									
	0.56 m	1.0 m	2.8 m	5.6 m	13 m	20 m	50 m	200 m	500 m	1,000 m
Source Depth = 10 cm										
0	7.20×10^{-2}	1.82×10^{-1}	5.37×10^{-1}	7.54×10^{-1}	8.99×10^{-1}	9.35×10^{-1}	9.76×10^{-1}	9.95×10^{-1}	9.99×10^{-1}	1.00
0.5	8.02×10^{-2}	2.03×10^{-1}	5.92×10^{-1}	8.21×10^{-1}	9.54×10^{-1}	9.81×10^{-1}	9.99×10^{-1}	1.00	1.00	1.00
2	9.51×10^{-2}	2.40×10^{-1}	6.79×10^{-1}	9.00×10^{-1}	9.93×10^{-1}	9.99×10^{-1}	1.00	1.00	1.00	1.00
4	1.13×10^{-1}	2.82×10^{-1}	7.65×10^{-1}	9.59×10^{-1}	1.00	1.00	1.00	1.00	1.00	1.00
6	1.28×10^{-1}	3.19×10^{-1}	8.26×10^{-1}	9.84×10^{-1}	1.00	1.00	1.00	1.00	1.00	1.00
8	1.42×10^{-1}	3.51×10^{-1}	8.69×10^{-1}	9.95×10^{-1}	1.00	1.00	1.00	1.00	1.00	1.00
10	1.54×10^{-1}	3.80×10^{-1}	9.01×10^{-1}	9.99×10^{-1}	1.00	1.00	1.00	1.00	1.00	1.00
15	1.82×10^{-1}	4.41×10^{-1}	9.49×10^{-1}	1.00	1.00	1.00	1.00	1.00	1.00	1.00
20	2.05×10^{-1}	4.89×10^{-1}	9.74×10^{-1}	1.00	1.00	1.00	1.00	1.00	1.00	1.00
50	2.84×10^{-1}	6.34×10^{-1}	1.00	1.00	1.00	1.00	1.00	1.00	1.00	1.00
Source Depth = 100 cm										
0	9.55×10^{-2}	2.36×10^{-1}	6.00×10^{-1}	7.58×10^{-1}	8.44×10^{-1}	8.67×10^{-1}	9.15×10^{-1}	9.77×10^{-1}	9.98×10^{-1}	1.00
0.5	1.10×10^{-1}	2.71×10^{-1}	6.84×10^{-1}	8.56×10^{-1}	9.41×10^{-1}	9.63×10^{-1}	9.94×10^{-1}	1.00	1.00	1.00
2	1.26×10^{-1}	3.11×10^{-1}	7.66×10^{-1}	9.29×10^{-1}	9.86×10^{-1}	9.97×10^{-1}	1.00	1.00	1.00	1.00
4	1.43×10^{-1}	3.50×10^{-1}	8.34×10^{-1}	9.72×10^{-1}	1.00	1.00	1.00	1.00	1.00	1.00
6	1.57×10^{-1}	3.82×10^{-1}	8.77×10^{-1}	9.92×10^{-1}	1.00	1.00	1.00	1.00	1.00	1.00
8	1.69×10^{-1}	4.09×10^{-1}	9.09×10^{-1}	9.97×10^{-1}	1.00	1.00	1.00	1.00	1.00	1.00
10	1.89×10^{-1}	4.34×10^{-1}	9.31×10^{-1}	9.99×10^{-1}	1.00	1.00	1.00	1.00	1.00	1.00
15	2.04×10^{-1}	4.84×10^{-1}	9.65×10^{-1}	1.00	1.00	1.00	1.00	1.00	1.00	1.00
20	2.24×10^{-1}	5.25×10^{-1}	9.83×10^{-1}	1.00	1.00	1.00	1.00	1.00	1.00	1.00
50	2.90×10^{-1}	6.45×10^{-1}	1.00	1.00	1.00	1.00	1.00	1.00	1.00	1.00

Figure 7a shows the area factor variation with cover thickness for a 10-keV source at depths of 0.1, 1.0, 10.0, and 100.0 cm. As shown, for a 10-keV source, the area factor is independent of source depth.

Table 13 gives the area factor variation at 100 keV. The cover thickness varies from 0 to 50 cm, and the area factor is calculated at different source radii (0.56, 1.0, 2.8, 5.6, 13.0, 20.0, 50.0, 200.0, 500.0, and 1000 m). Results are shown in Figures 7b through 7e. Table 13 shows that for source radii greater than 200 m, the area factor is always 1. As the cover thickness increases, the area factor approaches unity at smaller source radii. Table 14 shows the area factor variation at 1 MeV.

Tables 12 to 14 and Figure 7 show that for very low energy (10 keV), the area factor is a function of source radii; however, with a very small cover, the area factor becomes independent of source radii and becomes unity. For energies in the range of 100 to 1,000 keV, the area factor increases with source radius and cover thickness. As the cover thickness increases, the area factor saturates at a smaller source radius.

5.4 DOSE CALCULATIONS

Doses were calculated for four source depths (1, 5, 15, and 50 cm) with the old and new RESRAD models for selected radionuclides without any cover. Table 15 compares results of the new dose model with those of the old model for Cs-137, Co-60, Mn-54, Co-57, U-234, U-235, U-238, and Al-26. In these calculations, the source radius varies from 0.56 to 1,000 m. Doses [(mrem/yr)/(pCi/g)] are compared only for the external pathway at time zero. The following RESRAD parameters were used in the calculations:

- Density of contaminated zone = 1.6 g/cm^3,
- Cover density = 1.6 g/cm^3,
- Initial concentration of radionuclides = 1 pCi/g,
- Exposure duration = 30 years,
- External shielding factor = 1,
- Time fraction for outdoors = 1, and
- Time fraction for indoors = 0.

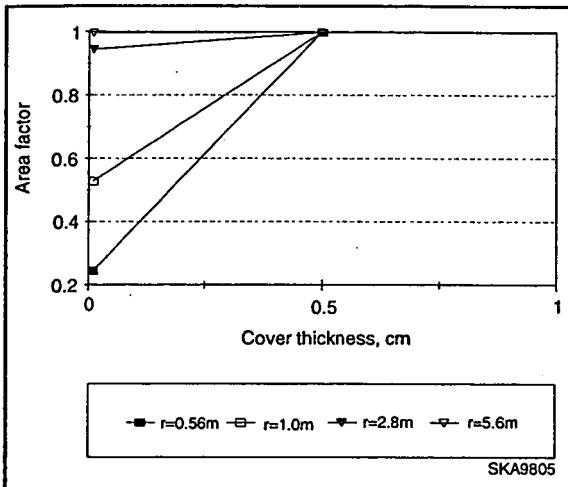

(a) Source Depths of 0.1, 1.0, 10.0, and 100.0 cm and Energy of 10 keV

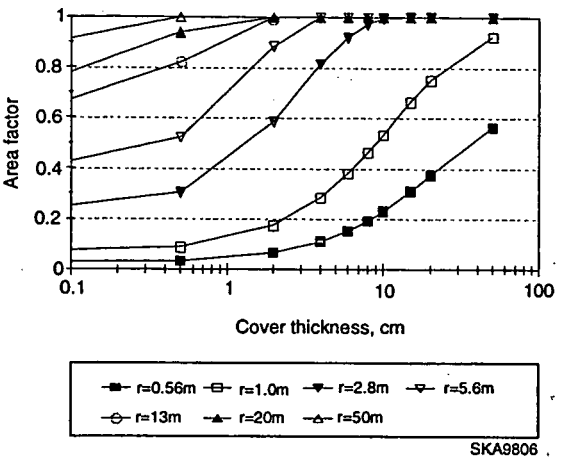

(b) Source Depth of 0.1 cm and Energy of 100 KeV

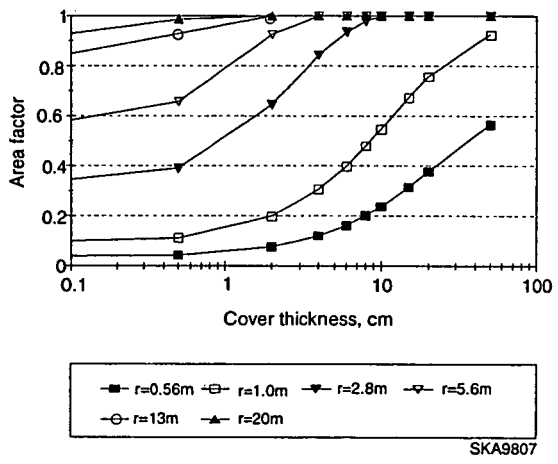

(c) Source Depth of 1.0 cm and Energy of 100 keV

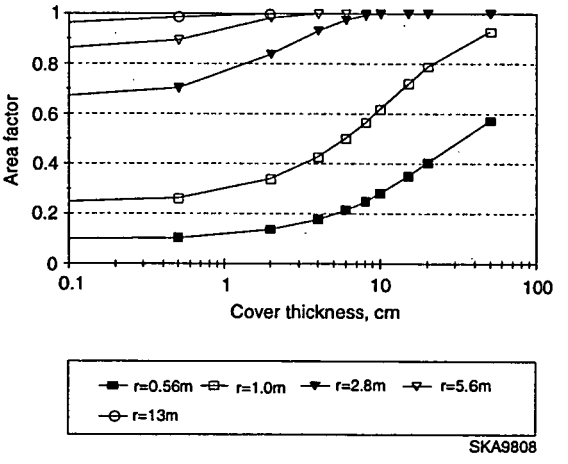

(d) Source Depth of 10.0 cm and Energy of 100 keV

FIGURE 7 Area Factor as a Function of Cover Thickness for a Set of Source Radii

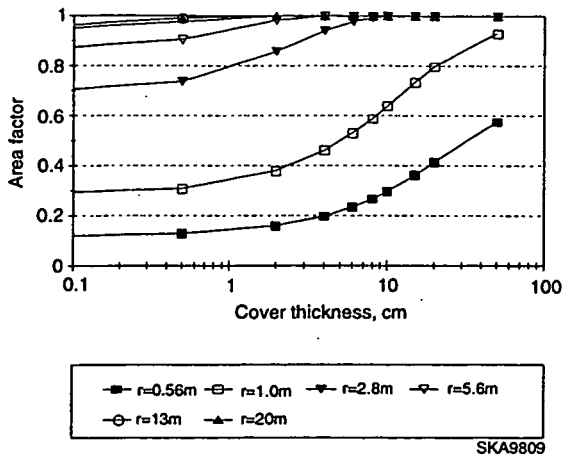

(e) Source Depth of 100.0 cm and Energy of 100 keV

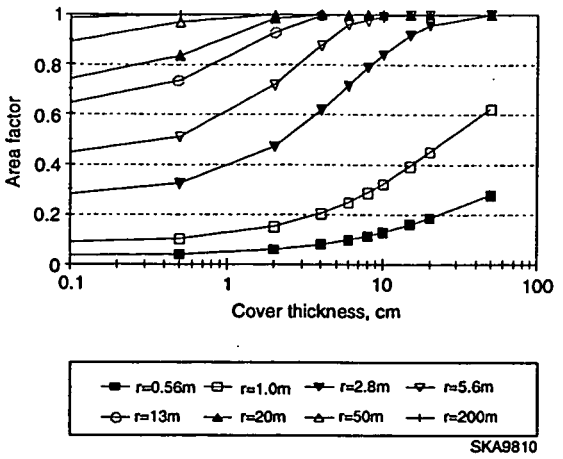

(f) Source Depth of 0.1 cm and Energy of 1 MeV

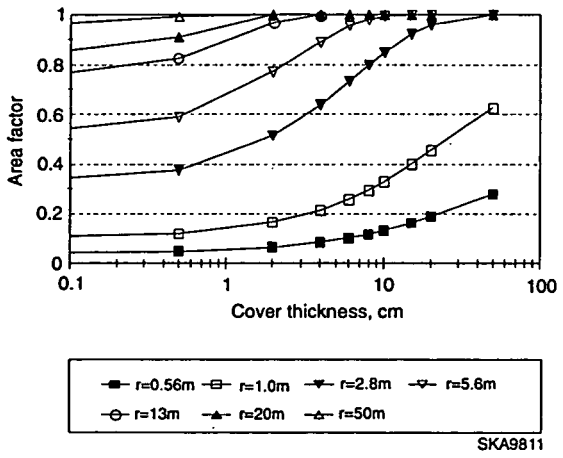

(g) Source Depth of 1.0 cm and Energy of 1 MeV

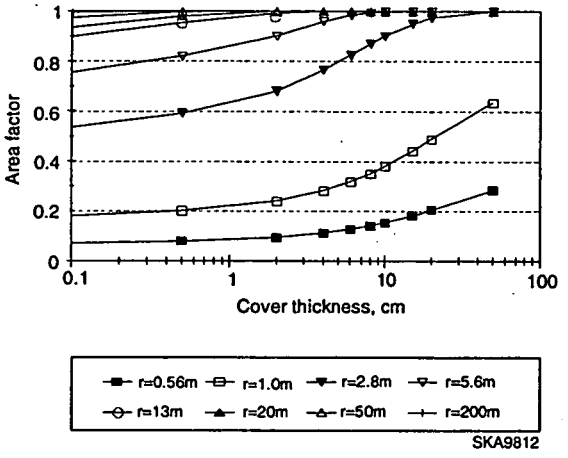

(h) Source Depth of 10.0 cm and Energy of 1 MeV

FIGURE 7 (Cont.)

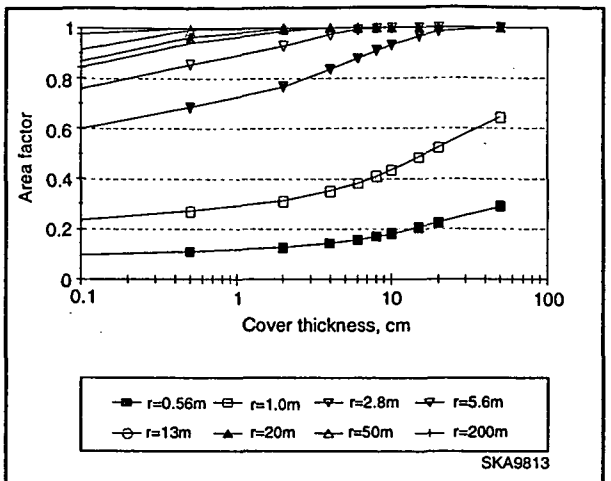

(i) Source Depth of 100.0 cm and Energy of 1 MeV

FIGURE 7 (Cont.)

Contaminated zone parameters, such as erosion rate, total porosity, effective porosity, hydraulic conductivity, *b* parameter, evapotranspiration coefficient, precipitation, irrigation mode, and runoff coefficients, will not affect these calculations.

Figures 8a through 8h compare doses between the old and new RESRAD models for Cs-137, Co-60, Co-57, Mn-54, U-234, U-235, U-238, and Al-26. These figures show the combined effects of depth factor, area factor, and *DCF* differences in the two models on dose calculations. For a small radius and 50-cm-thick source, differences are due to the area factor and *DCF*; however, at a large radius, the difference arises only because of the *DCF*.

Figure 8a compares Cs-137 doses in the two models. With the new model, the *DCF* is 3.42 mrem/yr; with the old model, it is 5.03. This change of about 47% is reflected in the dose value for a source depth of 50 cm and a 1,000-m radius. Based solely on the *DCF* difference, all the values at a source depth of 50 cm in the old RESRAD model should have been larger; however, it is not so because of differences in area factor. The new model always gives a large area factor at a small radius compared with the old model; this fact is reflected in dose values at a small radius. In Figures 8a through 8h, dose values at 0.56-m radius are always higher for the new model. The ratio in the new model at 0.56-m radius increases as the source thickness increases. The old model dose values do not change beyond a 20-m radius; for the new model, saturation occurs beyond a 20-m radius and depends on source energy. For Co-57, dose values change as much as 5 to 24%, depending on the source thickness, when the radius is increased beyond 20 m. For Al-26, this change is 10 to 32%.

TABLE 15 Dose (mrem/yr) Comparisons for Radionuclides at Source Depths (T_s) of 1, 5, 15, and 50 cm for New and Old RESRAD Models

Radius (m)	New Model				Old Model			
	Ts = 1 cm	*Ts* = 5 cm	*Ts* = 15 cm	*Ts* = 50 cm	*Ts* = 1 cm	*Ts* = 5 cm	*Ts* = 15 cm	*Ts* = 50 cm
Cs-137								
0.56	2.54×10^{-2}	1.16×10^{-1}	2.69×10^{-1}	3.48×10^{-1}	1.01×10^{-2}	3.92×10^{-2}	7.00×10^{-2}	8.10×10^{-2}
2.8	1.96×10^{-1}	8.78×10^{-1}	1.82	2.09	2.51×10^{-1}	9.81×10^{-1}	1.75	2.03
5.6	3.15×10^{-1}	1.33	2.45	2.67	3.49×10^{-1}	1.36	2.43	2.81
13	4.55×10^{-1}	1.69	2.82	2.97	5.16×10^{-1}	2.01	3.59	4.16
20	5.11×10^{-1}	1.78	2.91	3.04	6.37×10^{-1}	2.49	4.44	5.14
564.19	6.66×10^{-1}	1.93	3.09	3.41	6.37×10^{-1}	2.49	4.44	5.14
Co-60								
0.56	1.08×10^{-1}	4.76×10^{-1}	1.16	1.60	3.89×10^{-2}	1.57×10^{-1}	2.98×10^{-1}	3.65×10^{-1}
2.8	8.33×10^{-1}	3.64	8.02	9.88	9.74×10^{-1}	3.94	7.46	9.12
5.6	1.33	5.55	1.10×10^{1}	1.27×10^{1}	1.35	5.46	1.04×10^{1}	1.27×10^{1}
13	1.91	7.10	1.27×10^{1}	1.42×10^{1}	2.00	8.08	1.53×10^{1}	1.87×10^{1}
20	2.15	7.49	1.31×10^{1}	1.45×10^{1}	2.47	9.99	1.89×10^{1}	2.31×10^{1}
564.19	2.83	8.20	1.39×10^{1}	1.62×10^{1}	2.47	9.99	1.89×10^{1}	2.31×10^{1}
Co-57								
0.56	4.44×10^{-3}	2.45×10^{-2}	5.24×10^{-2}	5.75×10^{-2}	1.64×10^{-3}	5.51×10^{-3}	7.89×10^{-3}	8.18×10^{-3}
2.8	3.78×10^{-2}	1.94×10^{-1}	3.19×10^{-1}	3.28×10^{-1}	4.11×10^{-2}	1.38×10^{-1}	1.97×10^{-1}	2.04×10^{-1}
5.6	6.43×10^{-2}	2.83×10^{-1}	4.08×10^{-1}	4.16×10^{-1}	5.70×10^{-2}	1.91×10^{-1}	2.74×10^{-1}	2.84×10^{-1}
13	9.77×10^{-2}	3.38×10^{-1}	4.57×10^{-1}	4.57×10^{-1}	8.43×10^{-2}	2.83×10^{-1}	4.05×10^{-1}	4.20×10^{-1}
20	1.11×10^{-1}	3.51×10^{-1}	4.67×10^{-1}	4.62×10^{-1}	1.04×10^{-1}	3.50×10^{-1}	5.01×10^{-1}	5.19×10^{-1}
564.19	1.38×10^{-1}	3.72×10^{-1}	4.91×10^{-1}	5.01×10^{-1}	1.04×10^{-1}	3.50×10^{-1}	5.01×10^{-1}	5.19×10^{-1}
Mn-54								
0.56	3.79×10^{-2}	1.67×10^{-1}	3.90×10^{-1}	5.21×10^{-1}	1.05×10^{-2}	4.22×10^{-2}	7.89×10^{-2}	9.52×10^{-2}
2.8	2.94×10^{-1}	1.27	2.68	3.16	2.63×10^{-1}	1.06	1.97	2.38
5.6	4.72×10^{-1}	1.93	3.65	4.05	3.65×10^{-1}	1.46	2.74	3.31
13	6.78×10^{-1}	2.46	4.19	4.52	5.39×10^{-1}	2.17	4.05	4.89
20	7.63×10^{-1}	2.59	4.32	4.62	6.67×10^{-1}	2.68	5.00	6.04
564.19	9.96×10^{-1}	2.83	4.59	5.16	6.67×10^{-1}	2.68	5.00	6.04

TABLE 15 (Cont.)

Radius (m)	New Model				Old Model			
	Ts = 1 cm	*Ts* = 5 cm	*Ts* = 15 cm	*Ts* = 50 cm	*Ts* = 1 cm	*Ts* = 5 cm	*Ts* = 15 cm	*Ts* = 50 cm
U-234								
0.56	1.44×10^{-5}	3.64×10^{-5}	5.13×10^{-5}	5.17×10^{-5}	4.70×10^{-6}	1.53×10^{-5}	2.10×10^{-5}	2.16×10^{-5}
2.8	8.91×10^{-5}	2.21×10^{-4}	2.71×10^{-4}	2.73×10^{-4}	1.18×10^{-4}	3.82×10^{-4}	5.26×10^{-4}	5.39×10^{-4}
5.6	1.28×10^{-4}	2.86×10^{-4}	3.38×10^{-4}	3.40×10^{-4}	1.63×10^{-4}	5.30×10^{-4}	7.30×10^{-4}	7.49×10^{-4}
13	1.62×10^{-4}	3.21×10^{-4}	3.68×10^{-4}	3.69×10^{-4}	2.41×10^{-4}	7.83×10^{-4}	1.08×10^{-3}	1.11×10^{-3}
20	1.72×10^{-4}	3.28×10^{-4}	3.73×10^{-4}	3.75×10^{-4}	2.98×10^{-4}	9.68×10^{-4}	1.33×10^{-3}	1.37×10^{-3}
564.19	1.89×10^{-4}	3.40×10^{-4}	3.99×10^{-4}	4.02×10^{-4}	2.98×10^{-4}	9.68×10^{-4}	1.33×10^{-3}	1.37×10^{-3}
U-235								
0.56	6.28×10^{-3}	3.20×10^{-2}	7.25×10^{-2}	8.41×10^{-2}	2.93×10^{-3}	9.78×10^{-3}	1.39×10^{-2}	1.44×10^{-2}
2.8	5.16×10^{-2}	2.55×10^{-1}	4.63×10^{-1}	4.91×10^{-1}	7.33×10^{-2}	2.45×10^{-1}	3.47×10^{-1}	3.59×10^{-1}
5.6	8.62×10^{-2}	3.85×10^{-1}	6.02×10^{-1}	6.23×10^{-1}	1.02×10^{-1}	3.39×10^{-1}	4.82×10^{-1}	4.98×10^{-1}
13	1.30×10^{-1}	4.70×10^{-1}	6.79×10^{-1}	6.86×10^{-1}	1.51×10^{-1}	5.02×10^{-1}	7.13×10^{-1}	7.37×10^{-1}
20	1.48×10^{-1}	4.91×10^{-1}	6.96×10^{-1}	6.95×10^{-1}	1.86×10^{-1}	6.20×10^{-1}	8.82×10^{-1}	9.11×10^{-1}
564.19	1.90×10^{-1}	5.24×10^{-1}	7.31×10^{-1}	7.57×10^{-1}	1.86×10^{-1}	6.20×10^{-1}	8.82×10^{-1}	9.11×10^{-1}
U-238								
0.56	1.19×10^{-3}	5.12×10^{-3}	1.13×10^{-2}	1.43×10^{-2}	2.47×10^{-4}	9.69×10^{-4}	1.75×10^{-3}	2.04×10^{-3}
2.8	9.50×10^{-3}	3.87×10^{-2}	7.43×10^{-2}	8.51×10^{-2}	6.17×10^{-3}	2.42×10^{-2}	4.37×10^{-2}	5.10×10^{-2}
5.6	1.55×10^{-2}	5.74×10^{-2}	9.95×10^{-2}	1.09×10^{-1}	8.56×10^{-3}	3.36×10^{-2}	6.06×10^{-2}	7.08×10^{-2}
13	2.25×10^{-2}	7.12×10^{-2}	1.14×10^{-1}	1.21×10^{-1}	1.27×10^{-2}	4.97×10^{-2}	8.96×10^{-2}	1.05×10^{-1}
20	2.53×10^{-2}	7.46×10^{-2}	1.17×10^{-1}	1.23×10^{-1}	1.57×10^{-2}	6.15×10^{-2}	1.11×10^{-1}	1.29×10^{-1}
564.19	3.21×10^{-2}	8.06×10^{-2}	1.24×10^{-1}	1.37×10^{-1}	1.57×10^{-2}	6.15×10^{-2}	1.11×10^{-1}	1.29×10^{-1}
Al-26								
0.56	1.12×10^{-1}	5.12×10^{-1}	1.23	1.71	3.22×10^{-2}	1.32×10^{-1}	2.57×10^{-1}	3.23×10^{-1}
2.8	8.75×10^{-1}	3.88	8.55	1.06×10^{1}	8.04×10^{-1}	3.30	6.42	8.07
5.6	1.40	5.92	1.18×10^{1}	1.37×10^{1}	1.12	4.58	8.91	1.12×10^{1}
13	2.02	7.60	1.37×10^{1}	1.53×10^{1}	1.65	6.77	1.32×10^{1}	1.66×10^{1}
20	2.27	8.03	1.41×10^{1}	1.56×10^{1}	2.04	8.37	1.63×10^{1}	2.05×10^{1}
564.19	3.01	8.81	1.50×10^{1}	1.73×10^{1}	2.04	8.37	1.63×10^{1}	2.05×10^{1}

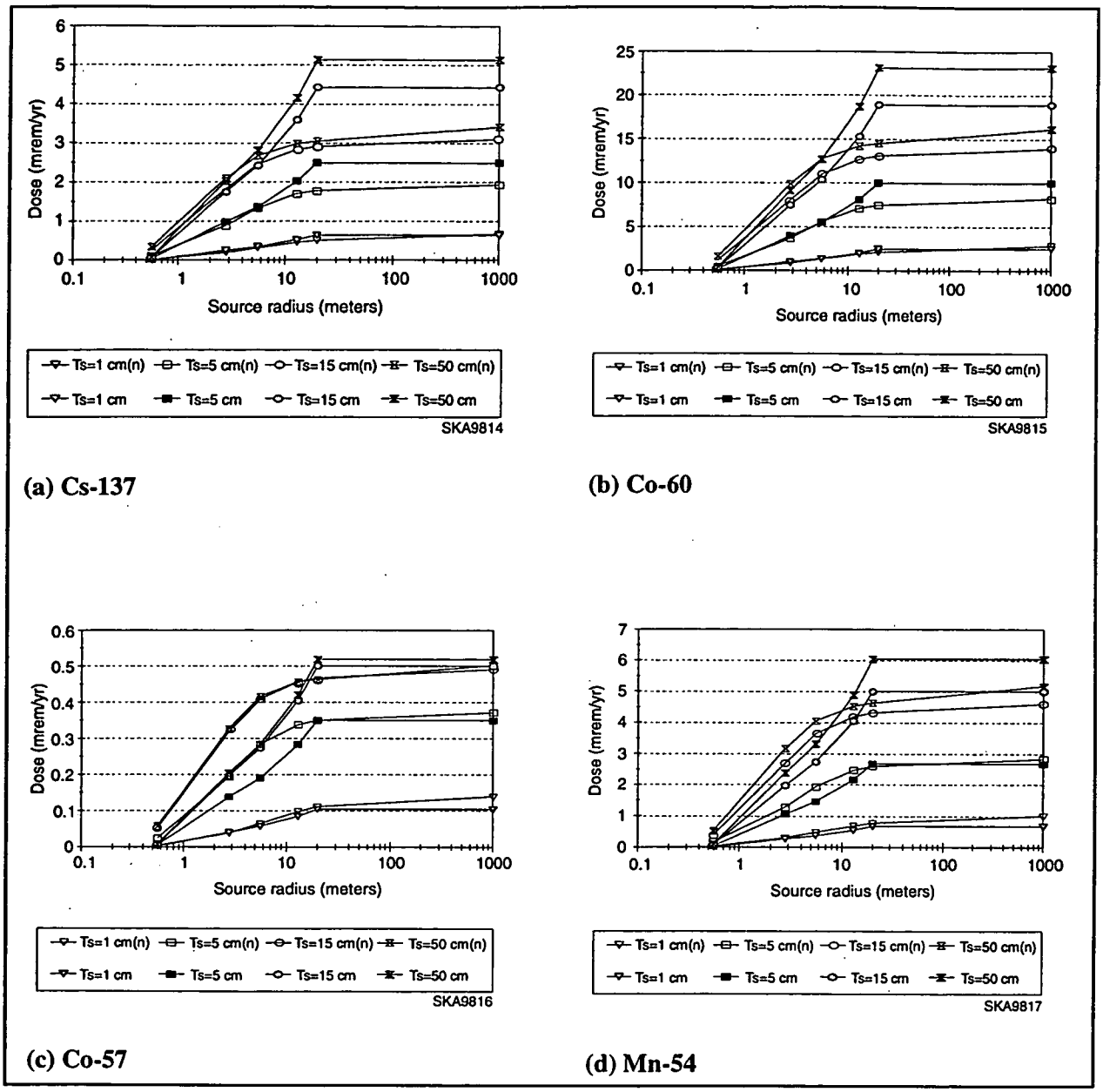

FIGURE 8 Dose Comparison as a Function of Source Radius for a Set of Source Depths with No Cover (Depths: 1 to 50 cm) (Note: (n) in legends denotes results for new RESRAD model.)

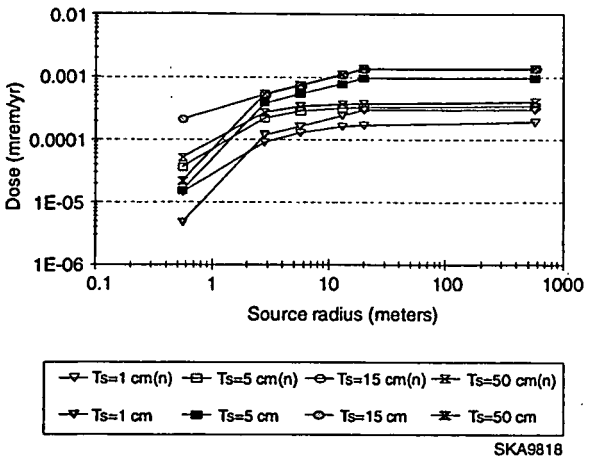

(e) U-234

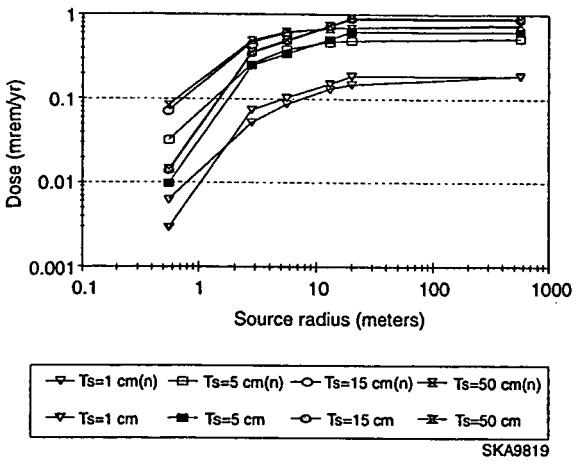

(f) U-235

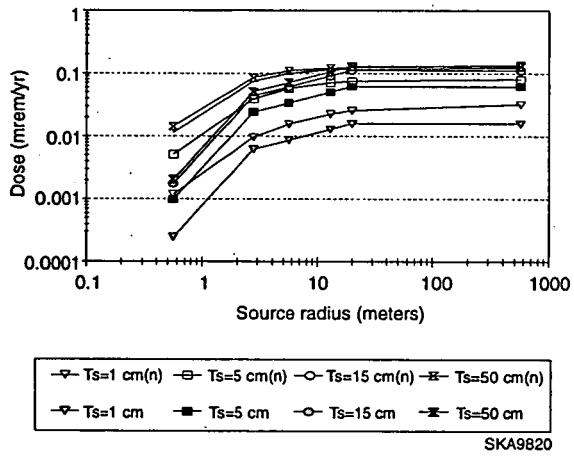

(g) U-238

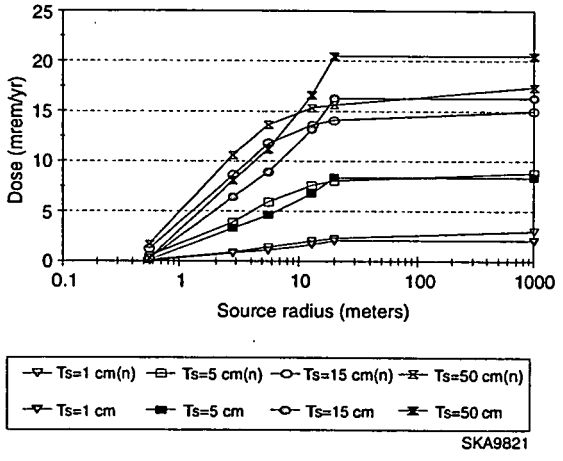

(h) Al-26

FIGURE 8 (Cont.)

Figure 8c compares Co-57 doses; in both models the values are the same, and differences only occur because of depth and area factors. For Co-57, at a small radius (under 13 m), the new model always gives higher dose values. For thick sources with a radius over 13 m, values are close in the two models.

Table 16 and Figure 9 give the dose comparison at four radii (0.56, 2.8, 13.0, and 564.19 m) for Co-60 source as a function of source depth. Table 17 gives the dose comparison at four radii for Co-60 source as a function of cover thickness for a source depth of 50 cm; Figure 9 shows the results.

TABLE 16 Dose (mrem/yr) Comparison for Co-60 as a Function of Source Depth at Different Radii (0.56, 2.8, 13.0, and 564.19 m) for New and Old RESRAD Models

Source Depth (cm)	New Model				Old Model			
	$r = 0.56$ m	$r = 2.8$ m	$r = 13.0$ m	$r = 564.19$ m	$r = 0.56$ m	$r = 2.8$ m	$r = 13.0$ m	$r = 564.19$ m
1.0	1.08×10^{-1}	8.33×10^{-1}	1.91	2.83	3.89×10^{-2}	9.74×10^{-1}	2.00	2.47
2.0	2.01×10^{-1}	1.55	3.41	4.53	7.37×10^{-2}	1.84	3.78	4.68
3.0	2.89×10^{-1}	2.23	4.68	5.92	1.05×10^{-1}	2.62	5.38	6.65
5.0	4.76×10^{-1}	3.64	7.10	8.20	1.57×10^{-1}	3.94	8.08	9.99
10.0	8.41×10^{-1}	6.09	1.06×10^{1}	1.19×10^{1}	2.47×10^{-1}	6.18	1.27×10^{1}	1.57×10^{1}
15.0	1.16	8.02	1.27×10^{1}	1.39×10^{1}	2.98×10^{-1}	7.46	1.53×10^{1}	1.89×10^{1}
25.0	1.36	9.12	1.40×10^{1}	1.55×10^{1}	3.44×10^{-1}	8.60	1.77×10^{1}	2.18×10^{1}
35.0	1.48	9.55	1.43×10^{1}	1.60×10^{1}	3.59×10^{-1}	8.97	1.84×10^{1}	2.28×10^{1}
50.0	1.60	9.88	1.42×10^{1}	1.62×10^{1}	3.65×10^{-1}	9.12	1.87×10^{1}	2.31×10^{1}

TABLE 17 Dose (mrem/yr) Comparison for Co-60 (50-cm depth) as a Function of Cover Thickness at Different Radii (0.56, 2.8, 13.0, and 564.19 m) for New and Old RESRAD Models

Cover Thick-ness (cm)	New Model				Old Model			
	$r = 0.56$ m	$r = 2.8$ m	$r = 13.0$ m	$r = 564.19$ m	$r = 0.56$ m	$r = 2.8$ m	$r = 13.0$ m	$r = 564.19$ m
0.0	1.60	9.88	1.42×10^{1}	1.62×10^{1}	3.65×10^{-1}	9.12	1.87×10^{1}	2.31×10^{1}
0.5	1.62	9.85	1.38×10^{1}	1.45×10^{1}	3.45×10^{-1}	8.62	1.77×10^{1}	2.19×10^{1}
1.0	1.57	9.45	1.30×10^{1}	1.34×10^{1}	3.26×10^{-1}	8.15	1.67×10^{1}	2.07×10^{1}
2.0	1.48	8.76	1.15×10^{1}	1.17×10^{1}	2.91×10^{-1}	7.28	1.49×10^{1}	1.85×10^{1}
3.0	1.38	8.01	1.02×10^{1}	1.03×10^{1}	2.60×10^{-1}	6.51	1.34×10^{1}	1.65×10^{1}
5.0	1.20	6.70	7.99	7.99	2.08×10^{-1}	5.20	1.07×10^{1}	1.32×10^{1}
10.0	7.60×10^{-1}	3.83	4.27	4.27	1.18×10^{-1}	2.96	6.08	7.51
15.0	4.70×10^{-1}	2.18	2.28	2.28	6.75×10^{-2}	1.69	3.46	4.28
20.0	2.66×10^{-1}	1.17	1.22	1.22	3.84×10^{-2}	9.61×10^{-1}	1.97	2.44
25.0	1.51×10^{-1}	6.30×10^{-1}	6.52×10^{-1}	6.52×10^{-1}	2.97×10^{-2}	5.48×10^{-1}	1.12	1.39

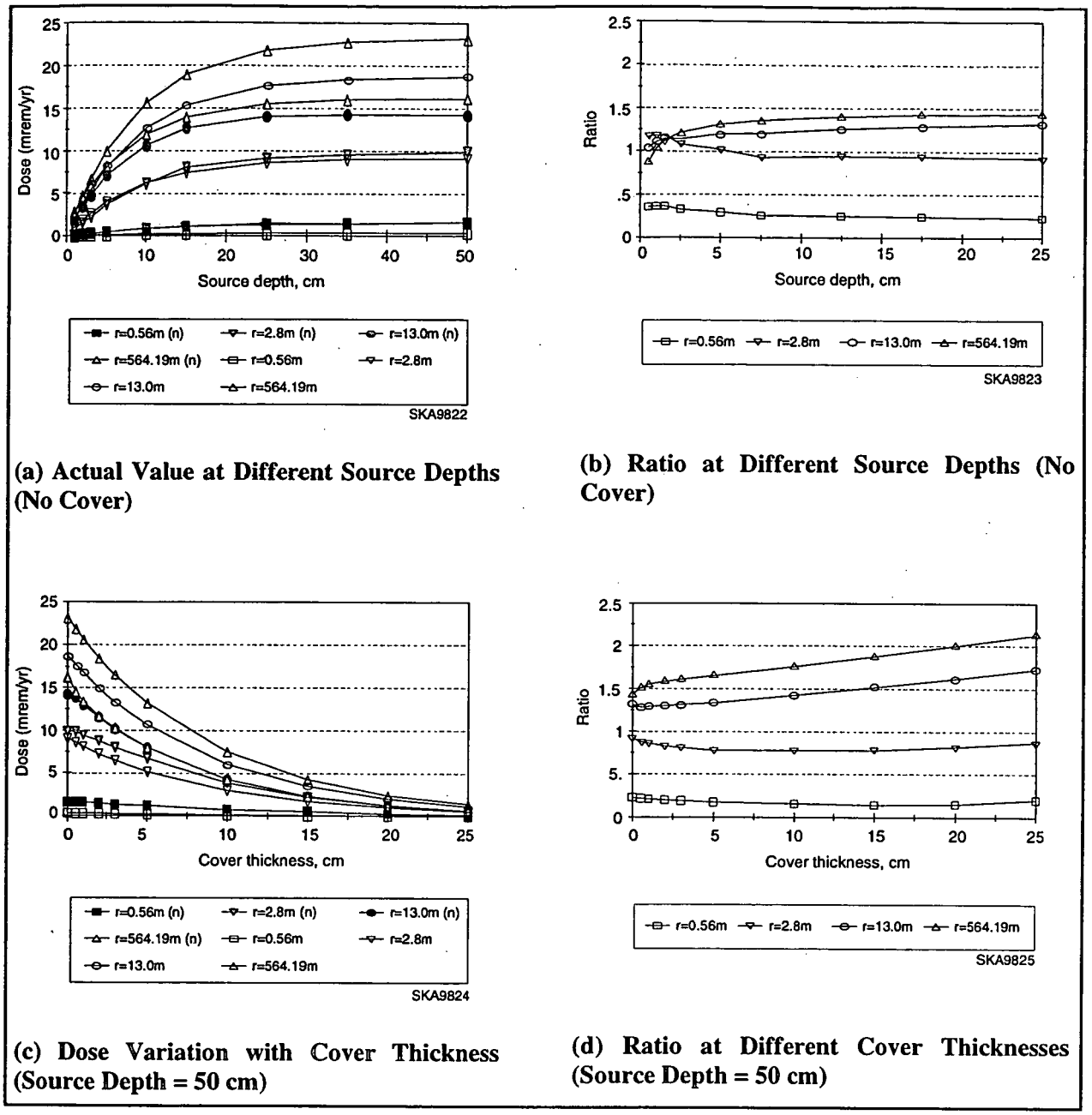

(a) Actual Value at Different Source Depths (No Cover)

(b) Ratio at Different Source Depths (No Cover)

(c) Dose Variation with Cover Thickness (Source Depth = 50 cm)

(d) Ratio at Different Cover Thicknesses (Source Depth = 50 cm)

FIGURE 9 Dose Comparison of Old and New RESRAD Models as a Function of Various Dependent Parameters for a Set of Co-60-Contaminated Source Radii (Note: (n) in legends denotes results for new RESRAD model.)

6 CONCLUSIONS

A new external exposure model, based on dose conversion factors from FGR-12 (Eckerman and Ryman 1993) and the point kernel method, has been developed for use in the RESRAD code. This model improves the external ground pathway dose estimation from the earlier version of the RESRAD code by extending FGR-12 data applicability to a wider range of source geometries. FGR-12 provides the dose coefficients for external exposure to photons and electrons emitted by radionuclides distributed in soil; tabulated values are given for surface and uniformly distributed volume sources at four specific thicknesses (1, 5, and 15 cm and effectively infinite) of soil with a density of 1.6 g/cm^3.

Differences in the calculated doses between the old and new RESRAD models arise because of differences in the dose conversion coefficients between FGR-12 and the old RESRAD, differences in the cover-and-depth factor in the two methods, and differences in the area factor. The area factor in the new model depends on energy, source area, source depth, and cover thickness. The old RESRAD model assumed that area factor is a function of area only. In addition to the differences in DCFs, the major differences between the old and new models will occur for small energies, small source radii, small source depths, and small cover thicknesses.

Comparison of the derived depth factor function with FGR-12 values shows that the factors are within 2% for all depths for most radionuclides. The cover-and-depth factor comparison shows that for small cover thicknesses, most values are within 2%, and for large covers (5 cm, 15 cm), most values are within 10%. Comparison of the old and new RESRAD model depth factors shows no significant difference at depths greater than 30 cm, but major differences occur for thin sources. The new model gives higher depth factors for thin sources, which means that the new model will predict higher doses for thin sources. The cover-and-depth factor comparisons show large differences for thin sources without any cover and for any sources with very thick covers. For all source depths with covers between 0.5 and 10 cm, the ratio of the cover-and-depth factor of the old to new RESRAD models is within 0.8 and 1.2.

The area factor increases with the source radius and approaches unity for a radius greater than 50 m. The area factor decreases with increasing energy, with sharp decreases when the energy changes from 10 to 60 keV and slight variations when the energy is higher. The area factor also increases with increasing source depth. The area factors of sources with depths greater than 10 cm were always greater in the new model. For very thin sources (0.1-cm depth) the old RESRAD model values are higher except for energies below 30 keV, for which the new model gives higher values. Values compare reasonably well in the two models at a source depth of 10 cm for energies above 30 keV.

7 REFERENCES

Briesmeister, J.F. (editor), 1993, *MCNP — A General Monte Carlo N-Particle Transport Code, Version 4A*, LA-12625, Los Alamos National Laboratory, Los Alamos, N.M.

Chen, S.Y., 1991, "Calculation of Effective Dose Equivalent Responses for External Exposure from Residual Photon Emitters in Soil," *Health Physics* 60:411-426.

Cristy, M., and K.F. Eckerman, 1987, *Specific Absorbed Fractions of Energy at Various Ages from Internal Photon Sources, I. Methods*, ORNL/TM-8381/VI, Oak Ridge National Laboratory, Oak Ridge, Tenn.

DOE: See U.S. Department of Energy.

Eckerman, K.F., and J.C. Ryman, 1993, *External Exposure to Radionuclides in Air, Water, and Soil, Exposure to Dose Coefficients for General Application, Based on the 1987 Federal Radiation Protection Guidance*, Federal Guidance Report No. 12, EPA 402-R-93-081, prepared by Oak Ridge National Laboratory, Oak Ridge, Tenn., for U.S. Environmental Protection Agency, Office of Radiation and Indoor Air, Washington, D.C.

EPA: See U.S. Environmental Protection Agency.

ICRP: See International Commission on Radiological Protection.

International Commission on Radiological Protection, 1983, *Radionuclide Transformations: Energy and Intensity of Emissions*, ICRP Publication 38, Annals of the ICRP, Vols. 11-13, Pergamon Press, New York, N.Y.

Kocher, D.C., and A.L. Sjoreen, 1985, "Dose-Rate Conversion Factors for External Exposure to Photon Emitters in Soil," *Health Physics* 28:193-205.

Napier, B.A., et al., 1984, *Intruder Dose Pathway Analysis for the Onsite Disposal of Radioactive Wastes: The ONSITE/MAxI1 Computer Program*, NUREG/CR-3620, PNL-4054, prepared by Pacific Northwest Laboratory, Richland, Wash., for U.S. Nuclear Regulatory Commission, Division of Waste Management, Washington, D.C.

Trubey, D.K., 1991, *New Gamma-Ray Buildup Factor Data for Point Kernel Calculations: ANS-6.4.3 Standard Reference Data*, NUREG-5740, ORNL/RSIC-49, prepared by Oak Ridge National Laboratory, Oak Ridge, Tenn., for U.S. Nuclear Regulatory Commission, Washington, D.C., Aug.

U.S. Department of Energy, 1988, *External Dose-Rate Conversion Factors for Calculation of Dose to the Public*, DOE/EH-0070, Assistant Secretary for Environment, Safety and Health, Washington, D.C.

U.S. Environmental Protection Agency, 1987, "Radiation Protection Guidance to Federal Agencies for Occupational Exposure," *Federal Register* 52(17):2822; with corrections published in the *Federal Register* on Friday, Jan. 30, and Wednesday, Feb. 4, 1987.

Yu, C., et al., 1993a, *Manual for Implementing Residual Radioactive Material Guidelines Using RESRAD, Version 5.0*, Draft, ANL/EAD/LD-2, Argonne National Laboratory, Argonne, Ill., Sept.

Yu, C., et al., 1993b, *Data Collection Handbook to Support Modeling the Impacts of Radioactive Material in Soil*, ANL/EAIS-8, Argonne National Laboratory, Argonne, Ill.

APPENDIX:

EXTERNAL EFFECTIVE DOSE EQUIVALENT CALCULATIONS FOR CONTAMINATED SOIL WITH THE MONTE CARLO N-PARTICLE TRANSPORT CODE

APPENDIX:

EXTERNAL EFFECTIVE DOSE EQUIVALENT CALCULATIONS FOR CONTAMINATED SOIL WITH THE MONTE CARLO N-PARTICLE TRANSPORT CODE

The Monte Carlo N-Particle (MCNP) Transport Code (Briesmeister 1993) is used to calculate the external effective dose equivalent at a distance of 1 m from contaminated soil of varying thicknesses. The calculated results are then compared with values from the Federal Guidance Report No. 12 (FGR-12) (Eckerman and Ryman 1993) for different isotopes.

A.1 MCNP CALCULATIONS

MCNP is a general-purpose, continuous energy, generalized geometry, time-dependent code that can be used for neutron, photon, electron, or coupled neutron/photon/electron transport. The photon and electron energy regimes are from 1 keV to 1,000 MeV. Photon interaction tables exist for all elements from atomic numbers 1 through 94. The data in the photon interaction tables allow MCNP to account for coherent and incoherent scattering, photoelectric absorption and the possibility of fluorescent emission, and pair production. Scattering angular distributions are modified by atomic form factors and incoherent scattering functions. To run a problem, an input file is prepared that contains such information as the geometry specification, the description of the materials and selection of cross-section evaluations, the location and characteristics of the source, the type of answers or tallies desired, and variance reduction techniques used to improve efficiency.

For MCNP calculations, gamma energies and their respective abundances were taken from the International Commission on Radiological Protection (ICRP) Publication 38 (ICRP 1983) (Table A.1). Flux is calculated at a height of 100 cm from the contaminated source by using a point detector next-event estimator. A point detector is known as a "next event estimator" because it is a tally of the flux at a point if the next event is a trajectory directly to the point detector without further collision. A point detector is a deterministic estimate (from the current event point) of the flux at a point in space. The contributions to the point detector are made at source and collision events throughout the random walk. Flux at the detector is given by:

$$\Psi(r,E,t,\mu) = \frac{Wp(\mu)e^{-\lambda}}{2\pi R^2} \quad \text{and} \tag{A.1}$$

$$\lambda = \int_0^R \Sigma_t(s)ds \quad ,$$

TABLE A.1 Gamma Energies and Yield

Isotope	Energy (keV)	Yield (%)
Co-60	1.173×10^3	1.00×10^2
	1.332×10^3	1.00×10^2
Mn-54	8.348×10^2	1.00×10^2
Ra-226	2.623×10^2	5.40×10^{-3}
	1.860×10^2	3.28
	9.771×10^1	3.36×10^{-2}
	9.487×10^1	6.79×10^{-2}
	9.424×10^1	3.55×10^{-2}
	8.378×10^1	2.98×10^{-1}
	8.107×10^1	1.79×10^{-1}
	1.688×10^1	9.04×10^{-2}
	1.428×10^1	4.05×10^{-1}
	1.171×10^1	2.53×10^{-1}
U-238	4.955×10^1	6.79×10^{-2}
	1.909×10^1	1.02
	1.610×10^1	4.47
	1.451×10^1	9.20×10^{-2}
	1.295×10^1	2.96
	1.112×10^1	1.41×10^{-1}
Al-26	5.110×10^2	1.64×10^2
	1.130×10^3	2.50
	1.809×10^3	9.98×10^1
	2.938×10^3	2.40×10^{-1}

Source: ICRP (1983).

where

W = particle weight,

λ = total number of mean free paths integrated over the trajectory from the source or collision point to the detector,

s = measured distance along the direction from the collision or source point to the detector,

$\Sigma_t(s)$ = macroscopic total cross section at s,

R = distance from source or collision event to detector, and

$p(\mu)$ = value of probability density function at μ, the cosine of the angle between the particle trajectory and the direction to the detector.

The $e^{-\lambda}$ term accounts for attenuation between the present event and the detector point. The $1/2\pi R^2$ term accounts for the solid angle effect. The $p(\mu)$ term accounts for the probability of scattering toward the detector instead of in the direction selected in the random walk. Each contribution to the detector can be thought of as the transport of a pseudoparticle to the detector.

This flux is used to calculate the effective dose equivalent by using the conversion coefficients between effective dose equivalent and fluence values (Table A.2). Table A.2 lists conversion coefficients for anteroposterior (AP), posteroanterior (PA), lateral (LAT), rotational (ROT), and isotropic (ISO) geometries. For the calculations, ROT symmetry is assumed. These values are taken from ICRP Publication 51 (ICRP 1987).

For MCNP computations, cylindrical sources with a 10,000-cm radius and of different thicknesses were used for flux estimation. Soil and air composition was taken from FGR-12 (Eckerman and Ryman 1993). These values are shown in Tables A.3 and A.4, respectively. A soil density of 1.6 g/cm^3 was used.

Results obtained with MCNP are in units of Sv/gamma. These values were multiplied by gamma abundance and source volume to get the effective dose equivalent in units of (Sv/s)/(Bq/m^3) for volume sources and were multiplied by gamma abundance and surface area to get the effective dose equivalent in units of (Sv/s)/(Bq/m^2) for surface sources.

A.2 COMPARISON OF FGR-12 AND MCNP RESULTS

Effective dose equivalents for source depths of 1, 5, 15, 50, and 100 cm calculated with MCNP are compared with FGR values for Co-60, Mn-54, Ra-226, U-238, and Al-26 in Table A.5. Source sizes used in the MCNP calculations are also shown. Table A.6 gives the surface dose comparison.

Figure A.1 compares FGR-12 dose values with MCNP calculations for Co-60, Mn-54, Ra-226, U-238, and Al-26 at different source thicknesses. Figure A.2 compares the values for surface sources. A comparison of the volume sources shows that the ratio in all cases is between 0.93 and 1.10, and in most cases it is between 0.95 and 1.05. However, for the surface sources, FGR-12 results are always higher. One reason for this difference could be beta activity, which is not taken into account in MCNP calculations. Statistical uncertainty in MCNP calculations is less than 5% at 1 σ.

TABLE A.2 Effective Dose Equivalent per Unit Fluence for Photons Incident in Various Geometries on an Anthropomorphic Phantom

Photon Energy (MeV)	Conversion Coefficient[a] (10^{-12} Sv cm^2)				
	AP	PA	LAT	ROT	ISO
0.010	0.062	0.0	0.02	0.029	0.022
0.015	0.157	0.0310	0.0330	0.0710	0.0570
0.020	0.238	0.0868	0.0491	0.110	0.0912
0.030	0.329	0.161	0.0863	0.166	0.138
0.040	0.365	0.222	0.123	0.199	0.163
0.050	0.384	0.260	0.152	0.222	0.180
0.060	0.400	0.286	0.170	0.240	0.196
0.080	0.451	0.344	0.212	0.293	0.237
0.100	0.533	0.418	0.258	0.357	0.284
0.150	0.777	0.624	0.396	0.534	0.436
0.200	1.03	0.844	0.557	0.731	0.602
0.300	1.56	1.30	0.891	1.14	0.949
0.400	2.06	1.76	1.24	1.55	1.30
0.500	2.54	2.20	1.58	1.96	1.64
0.600	2.99	2.62	1.92	2.34	1.98
0.800	3.83	3.43	2.60	3.07	2.64
1.000	4.60	4.18	3.24	3.75	3.27
1.500	6.24	5.80	4.70	5.24	4.68
2.000	7.66	7.21	6.02	6.56	5.93
3.000	10.2	9.71	8.40	8.90	8.19
4.000	12.5	12.0	10.6	11.0	10.2
5.000	14.7	14.1	12.6	13.0	12.1
6.000	16.7	16.2	14.6	14.9	14.0
8.000	20.8	20.2	18.5	18.9	17.8
10.00	24.7	24.2	22.3	22.9	21.6

[a] The geometries are as follows: AP = anteroposterior, PA = posteroanterior, LAT = lateral, ROT = rotational, ISO = isotropic.

Source: ICRP (1987).

69

A.3 COMPARISON OF COVER-AND-DEPTH FACTOR WITH MCNP

Doses were compared between MCNP and the new RESRAD model for different source depths and cover thicknesses for Co-60 and Mn-54. These two radionuclides were chosen because of their relatively simple decay. Table A.7 gives the source depth factor comparison. Source depths were varied from 0.5 to 100.0 cm.

Figure A.3 shows the depth factor comparison of the new model with MCNP calculations. The ratio of new model to MCNP varies between 1.12 and 0.93; in most cases, differences are less than 7%.

Table A.8 gives the cover factor comparison for source depths of 1, 5, 15, and 50 cm. The cover thickness varies from 0.0 to 25.0 cm. These results are shown in Figure A.4.

Table A.9 and Figure A.5 show the ratio of the new model cover-and-depth factor results compared with MCNP calculations for Co-60 and Mn-54. Comparisons were made for source depths of 1, 5, 15, and 50 cm.

TABLE A.3 Soil Composition

Element	Mass Fraction
H	0.021
C	0.016
O	0.577
Al	0.050
Si	0.271
K	0.013
Ca	0.041
Fe	0.011
Total	1.000

Source: Eckerman and Ryman (1993).

TABLE A.4 Air Composition

Element	Mass Fraction
H	0.00064
C	0.00014
N	0.75086
O	0.23555
Ar	0.01281
Total	1.00000

Source: Eckerman and Ryman (1993).

Tables A.8 and A.9 and Figures A.4 and A.5 show that the ratios of new model to MCNP values are close to unity for small cover thicknesses (less than 25 cm). Large differences are observed for cover thicknesses greater than 10 cm and at source depths greater than 15 cm. For cover thicknesses greater than 10 cm at source depths greater than 15 cm, the resultant dose, which is calculated as the difference between the doses for sources greater than 25 cm deep and sources greater than 15 cm deep, is small. As one example, for a Co-60 source at a depth of 15 cm without any cover, the dose is 13.9 mrem/yr (Table A.8), but the dose decreases to 0.55 mrem/yr with 25 cm of cover (a decrease by a factor of more than 20). Although the absolute difference between the two results (the MCNP and the new RESRAD model) is small (0.91 vs. 0.55 mrem/yr, Table A.8). the relative difference can appear large; that is, the uncertainty factor is amplified. However, because the doses are so small for these conditions, the differences between the model results are not of significant concern.

TABLE A.5 Comparison of MCNP and FGR-12 Dose Conversion Factors for Various Radionuclides

Isotope	Thickness (cm)	Radius (cm)	Volume (m^3)	Dose Conversion Factor $[(Sv/s)/(Bq/m^3) \times 10^{-18}]$ MCNP	FGR-12	Ratio FGR/MCNP
Co-60	1.0	1.0×10^4	3.14×10^2	1.42×10^1	1.52×10^1	1.07
	5.0	1.0×10^4	1.57×10^3	4.43×10^1	4.45×10^1	1.00
	1.5×10^1	1.0×10^4	4.71×10^3	7.25×10^1	7.25×10^1	1.00
	5.0×10^1	1.0×10^4	1.57×10^4	8.95×10^1	8.68×10^1	9.70×10^{-1}
	1.0×10^2	1.0×10^4	3.14×10^4	8.73×10^1	8.68×10^1	9.94×10^{-1}
Mn-54	1.0	1.0×10^4	3.14×10^2	4.96	5.21	1.05
	5.0	1.0×10^4	1.57×10^3	1.51×10^1	1.51×10^1	1.00
	1.5×10^1	1.0×10^4	4.71×10^3	2.38×10^1	2.40×10^1	1.01
	5.0×10^1	1.0×10^4	1.57×10^4	2.97×10^1	2.76×10^1	9.29×10^{-1}
	1.0×10^2	1.0×10^4	3.14×10^4	2.77×10^1	2.76×10^1	9.96×10^{-1}
Ra-226	1.0	1.0×10^4	3.14×10^2	4.13×10^{-2}	4.15×10^{-2}	1.00
	5.0	1.0×10^4	1.57×10^3	1.20×10^{-1}	1.16×10^{-1}	9.67×10^{-1}
	1.5×10^1	1.0×10^4	4.71×10^3	1.71×10^{-1}	1.65×10^{-1}	9.65×10^{-1}
	5.0×10^1	1.0×10^4	1.57×10^4	1.86×10^{-1}	1.70×10^{-1}	9.14×10^{-1}
U-238	1.0	1.0×10^4	3.14×10^2	4.03×10^{-4}	4.42×10^{-4}	1.10
	5.0	1.0×10^4	1.57×10^3	5.71×10^{-4}	5.45×10^{-4}	9.54×10^{-1}
	1.5×10^1	1.0×10^4	4.71×10^3	5.76×10^{-4}	5.52×10^{-4}	9.58×10^{-1}
Al-26	1.0	1.0×10^4	3.14×10^2	1.54×10^1	1.62×10^1	1.05
	5.0	1.0×10^4	1.57×10^3	4.77×10^1	4.74×10^1	9.94×10^{-1}
	1.5×10^1	1.0×10^4	4.71×10^3	7.96×10^1	7.73×10^1	9.71×10^{-1}
	5.0×10^1	1.0×10^4	1.57×10^4	1.00×10^2	9.32×10^1	9.32×10^{-1}
	1.0×10^2	1.0×10^4	3.14×10^4	9.04×10^1	9.32×10^1	1.03

TABLE A.6 Surface Dose Comparison of MCNP and FGR-12 Values

	Surface Dose $[(Sv/s)/(Bq/m^2) \times 10^{-18}]$				
	Co-60	Mn-54	Ra-226	U-238	Al-26
FGR-12	2.35×10^3	8.10×10^2	6.44	5.15×10^{-1}	2.49×10^3
MCNP	2.05×10^3	7.25×10^2	6.16	4.31×10^{-1}	2.21×10^3
Ratio (FGR/MCNP)	1.15	1.12	1.05	1.19	1.13

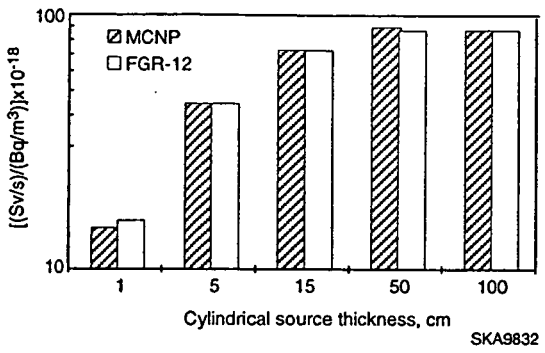

(a) Co-60

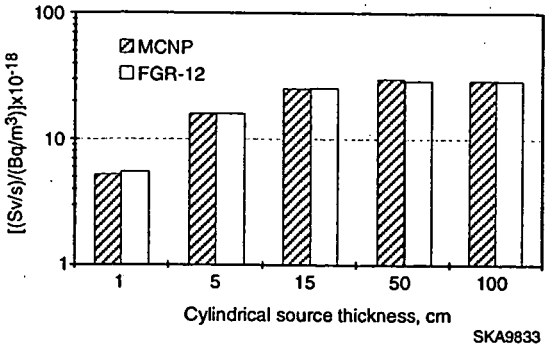

(b) Mn-54

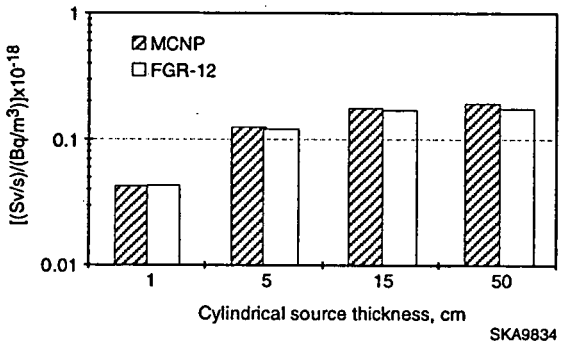

(c) Ra-226

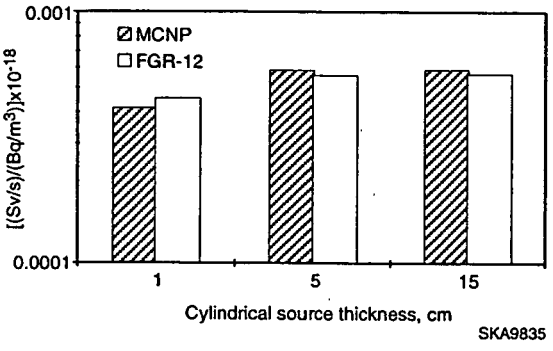

(d) U-238

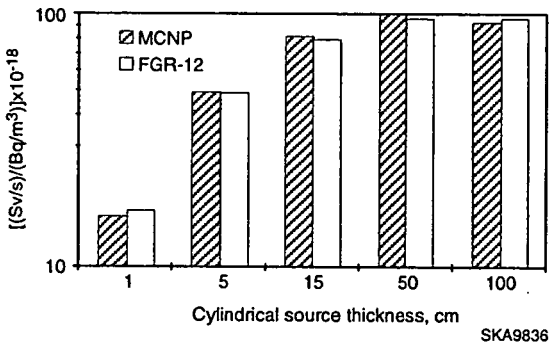

(e) Al-26

FIGURE A.1 Comparison of MCNP and FGR-12 Dose Values for Various Radionuclides

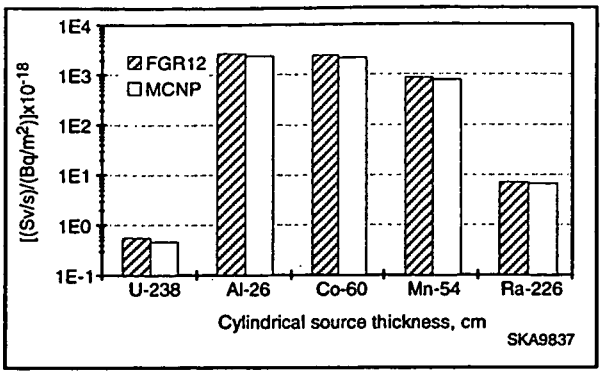

FIGURE A.2 Comparison of FGR-12 and MCNP Dose Values for Surface Sources

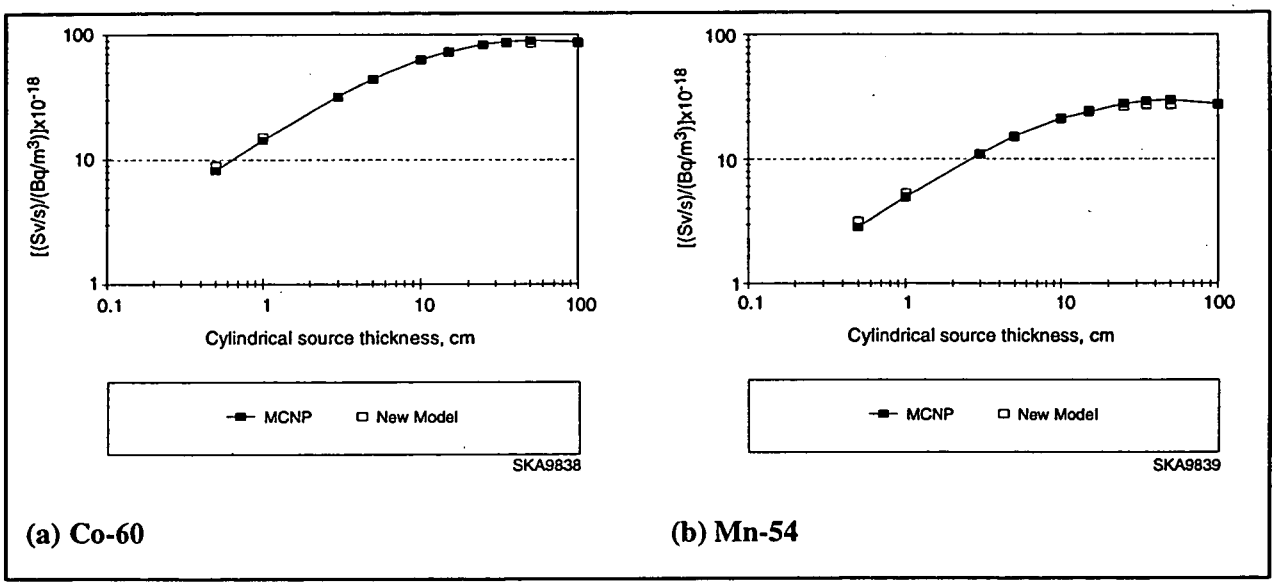

FIGURE A.3 Dose Comparison between MCNP and New RESRAD Model as a Function of Source Depth for Co-60 and Mn-54

TABLE A.7 Comparison of Dose Estimation between MCNP and the New RESRAD Model for Co-60 and Mn-54 Cylindrical Sources of Effectively Infinite Radius at Different Source Depths

Isotope	Source Depth (cm)	Dose Estimation [(Sv/s)/(Bq/m^3) × 10^{-18}] MCNP	Dose Estimation [(Sv/s)/(Bq/m^3) × 10^{-18}] New Model	Ratio New Model/MCNP
Co-60	0.5	8.17	9.09	1.11
	1.0	1.42×10^{1}	1.52×10^{1}	1.07
	3.0	3.18×10^{1}	3.17×10^{1}	1.00
	5.0	4.43×10^{1}	4.39×10^{1}	9.91×10^{-1}
	1.0×10^{1}	6.27×10^{1}	6.39×10^{1}	1.02
	1.5×10^{1}	7.25×10^{1}	7.46×10^{1}	1.03
	2.5×10^{1}	8.35×10^{1}	8.33×10^{1}	1.00
	3.5×10^{1}	8.79×10^{1}	8.58×10^{1}	9.76×10^{-1}
	5.0×10^{1}	8.95×10^{1}	8.66×10^{1}	9.68×10^{-1}
	1.0×10^{2}	8.73×10^{1}	8.68×10^{1}	9.94×10^{-1}
Mn-54	0.5	2.84	3.17	1.12
	1.0	4.96	5.33	1.07
	3.0	1.09×10^{1}	1.10×10^{1}	1.01
	5.0	1.51×10^{1}	1.51×10^{1}	1.00
	1.0×10^{1}	2.11×10^{1}	2.14×10^{1}	1.01
	1.5×10^{1}	2.38×10^{1}	2.45×10^{1}	1.03
	2.5×10^{1}	2.78×10^{1}	2.68×10^{1}	9.64×10^{-1}
	3.5×10^{1}	2.91×10^{1}	2.74×10^{1}	9.42×10^{-1}
	5.0×10^{1}	2.97×10^{1}	2.76×10^{1}	9.96×10^{-1}
	1.0×10^{2}	2.77×10^{1}	2.76×10^{1}	9.94×10^{-1}

TABLE A.8 Comparison of Dose (mrem/yr) Calculations for MCNP and the New RESRAD Model Using the Cover-and-Depth Factor for Co-60 and Mn-54

Cover Thickness (cm)	Source = 1 cm		Source = 5 cm		Source = 15 cm		Source = 50 cm	
	MCNP	New Model	MCNP	New Model	MCNP	New Model	MCNP	New Model
Co-60								
0.0	2.65	2.84	8.28	8.20	1.35×10^{1}	1.39×10^{1}	1.67×10^{1}	1.62×10^{1}
0.5	2.00	2.04	7.15	7.00	1.23×10^{1}	1.24×10^{1}	1.48×10^{1}	1.45×10^{1}
2.0	1.41	1.39	5.4	5.44	10.1	9.90	1.30×10^{1}	1.16×10^{1}
5.0	8.9×10^{-1}	9.43×10^{-1}	3.7	3.73	7.02	6.79	9.4	7.99
1.0×10^{1}	5.0×10^{-1}	5.04×10^{-1}	2.05	1.99	4.26	3.63	5.7	4.28
2.5×10^{1}	1.1×10^{-1}	7.70×10^{-2}	4.6×10^{-1}	3.05×10^{-1}	9.1×10^{-1}	5.54×10^{-1}	1.3	6.51×10^{-1}
Mn-54								
0.0	9.27×10^{-1}	9.96×10^{-1}	2.82	2.82	4.45	4.59	5.64	5.16
0.5	7.27×10^{-1}	7.22×10^{-1}	2.43	2.39	4.05	4.04	4.87	4.56
2.0	4.82×10^{-1}	4.76×10^{-1}	1.81	1.81	3.26	3.14	3.87	3.57
5.0	3.03×10^{-1}	3.07×10^{-1}	1.18	1.18	2.23	2.05	2.62	2.33
1.0×10^{1}	1.61×10^{-1}	1.52×10^{-1}	6.33×10^{-1}	5.83×10^{-1}	1.20	1.02	1.46	1.16
2.5×10^{1}	2.8×10^{-2}	1.84×10^{-2}	1.12×10^{-1}	7.07×10^{-2}	1.98×10^{-1}	1.23×10^{-1}	2.43×10^{-1}	1.40×10^{-1}

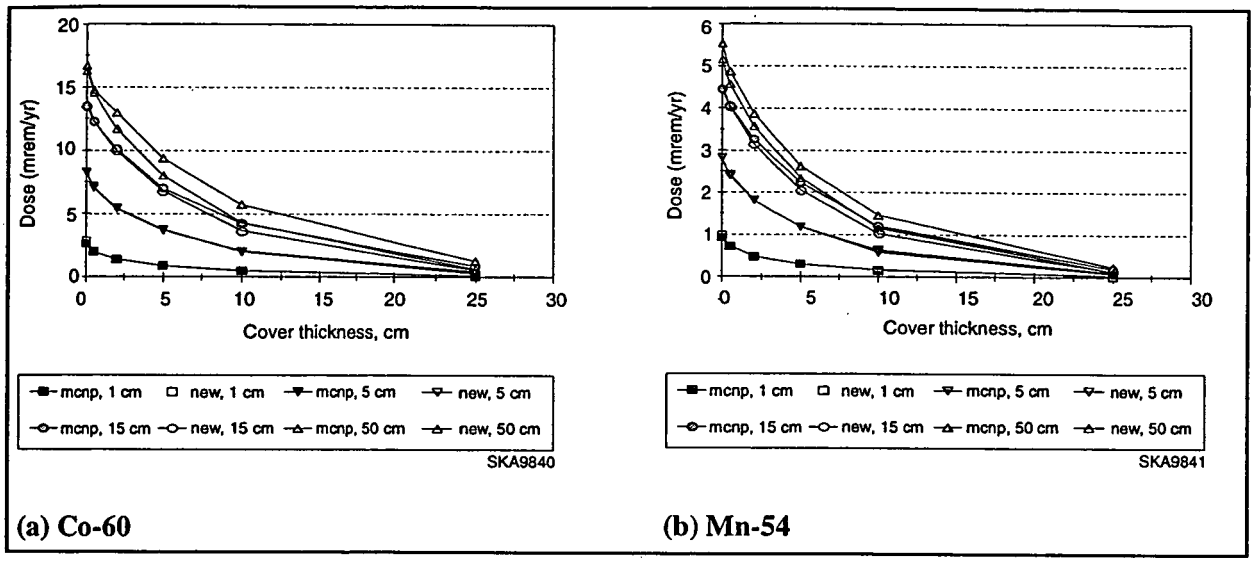

FIGURE A.4 Dose Comparison between MCNP and New RESRAD Model for Co-60 and Mn-54 as a Function of Cover Thickness for Different Source Depths

TABLE A.9 Ratio of New RESRAD Model/MCNP Dose Calculations as a Function of Cover Thickness for Different Source Depths for Co-60 and Mn-54

Cover Thickness (cm)	Ratio (New Model/MCNP) by Source Depth			
	1 cm	5 cm	15 cm	50 cm
Co-60				
0.0	1.07	9.90×10^{-1}	1.03	9.70×10^{-1}
0.5	1.02	9.79×10^{-1}	1.01	9.80×10^{-1}
2.0	9.86×10^{-1}	1.01	9.80×10^{-1}	8.92×10^{-1}
5.0	1.06	1.01	9.67×10^{-1}	8.50×10^{-1}
1.0×10^{1}	1.01	9.71×10^{-1}	8.52×10^{-1}	7.51×10^{-1}
2.5×10^{1}	7.00×10^{-1}	6.63×10^{-1}	6.09×10^{-1}	5.01×10^{-1}
Mn-54				
0.0	1.07	1.00	1.03	9.15×10^{-1}
0.5	9.93×10^{-1}	9.84×10^{-1}	9.98×10^{-1}	9.36×10^{-1}
2.0	9.88×10^{-1}	1.00	9.63×10^{-1}	9.22×10^{-1}
5.0	1.01	1.00	9.19×10^{-1}	8.89×10^{-1}
1.0×10^{1}	9.44×10^{-1}	9.21×10^{-1}	8.50×10^{-1}	7.95×10^{-1}
2.5×10^{1}	6.57×10^{-1}	6.31×10^{-1}	6.21×10^{-1}	5.76×10^{-1}

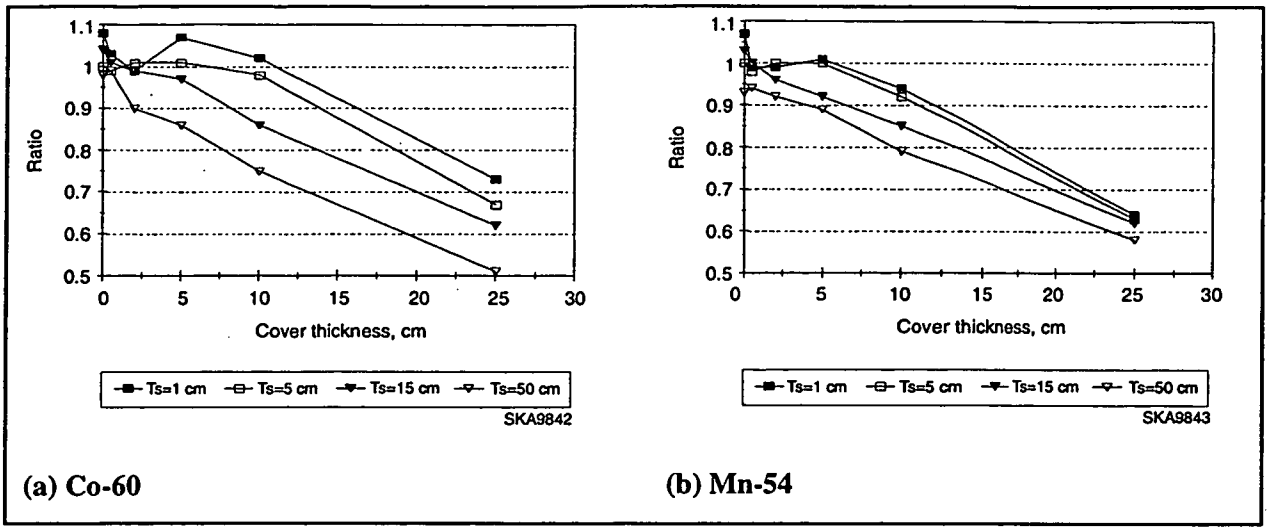

FIGURE A.5 Ratio of Cover-and-Depth Factor for Co-60 and Mn-54 at Different Source Depths

The above results could also arise from the use of different exposure models (rotational exposure [MCNP] and the actual field [FGR-12]) in effective dose equivalent calculations. An indication of support for this interpretation comes from FGR-12 (Figure II.16 in Eckerman and Ryman 1993), where the rotational exposures were 10-35% higher than actual fields, with the larger difference at greater source thicknesses.

A.4 REFERENCES FOR APPENDIX

Briesmeister, J.F. (editor), 1993, *MCNP — A General Monte Carlo N-Particle Transport Code, Version 4A*, LA-12625, Los Alamos National Laboratory, Los Alamos, N.M.

Eckerman, K.F., and J.C. Ryman, 1993, *External Exposure to Radionuclides in Air, Water, and Soil, Exposure to Dose Coefficients for General Application, Based on the 1987 Federal Radiation Protection Guidance*, EPA 402-R-93-081, Federal Guidance Report No. 12, prepared by Oak Ridge National Laboratory, Oak Ridge, Tenn., for U.S. Environmental Protection Agency, Office of Radiation and Indoor Air, Washington, D.C.

ICRP: See International Commission on Radiological Protection

International Commission on Radiological Protection, 1983, *Radionuclide Transformations: Energy and Intensity of Emissions*, ICRP Publication 38, Annals of the ICRP, Vols. 11-13, Pergamon Press, New York, N.Y.

77

International Commission on Radiological Protection, 1987, *Data for Use in Protection against External Radiation*, ICRP Publication 51, Annals of the ICRP, Vol. 17, No. 2/3, Pergamon Press, New York, N.Y.

ANL/EAD/TM-82

Evaluation of the Area Factor Used in the RESRAD Code for the Estimation of Airborne Contaminant Concentrations of Finite Area Sources

Environmental Assessment Division

Argonne National Laboratory

Operated by The University of Chicago,
under Contract W-31-109-Eng-38, for the

United States Department of Energy

79

Argonne National Laboratory

Argonne National Laboratory, with facilities in the states of Illinois and Idaho, is owned by the United States Government, and operated by the University of Chicago under the provisions of a contract with the Department of Energy.

This technical memo is a product of Argonne's Environmental Assessment Division (EAD). For information on the division's scientific and engineering activities, contact:

Director, Environmental Assessment Division
Argonne National Laboratory
Argonne, Illinois 60439-4815
Telephone (630) 252-3107

Presented in this technical memo are preliminary results of ongoing work or work that is more limited in scope and depth than that described in formal reports issued by the EAD.

Publishing support services were provided by Argonne's Information and Publishing Division (for more information, see IPD's home page: http://www.ipd.anl.gov/).

Disclaimer

80

ANL/EAD/TM-82

Evaluation of the Area Factor Used in the RESRAD Code for the Estimation of Airborne Contaminant Concentrations of Finite Area Sources

by Y.-S. Chang, C. Yu, and S.K. Wang*

Environmental Assessment Division,
Argonne National Laboratory, 9700 South Cass Avenue, Argonne, Illinois 60439

July 1998

Work sponsored by U.S. Department of Energy, Assistant Secretary for Environment, Safety and Health, Office of Environmental Policy and Assistance, and Assistant Secretary for Environmental Management, Office of Environmental Restoration

---

* S.K. Wang is currently associated with Kaohsiung Institute of Technology, Kaohsiung, Taiwan

81

This report is printed on recycled paper.

CONTENTS

FIGURES

82

TABLES

83

NOTATION

The following is a list of the acronyms and abbreviations, including units of measure, used in this report. Acronyms and abbreviations used only in equations, tables, or figures are defined in the respective equations, tables, or figures.

ACRONYMS AND ABBREVIATIONS

AMAD	activity median aerodynamic diameter
DOE	U.S. Department of Energy
EPA	U.S. Environmental Protection Agency
NOAA	National Oceanic and Atmospheric Administration
RESRAD	residual radioactive material code

UNITS OF MEASURE

cm	centimeter(s)
g	gram(s)
kg	kilogram(s)
m	meter(s)
m^2	square meter(s)
m^3	cubic meter(s)
µm	micrometer(s)
s	second(s)
yr	year(s)
°C	degree(s) Celsius

EVALUATION OF THE AREA FACTOR USED IN THE RESRAD CODE FOR THE ESTIMATION OF AIRBORNE CONTAMINANT CONCENTRATIONS OF FINITE AREA SOURCES

by

Y.-S. Chang, C. Yu, and S.K. Wang

ABSTRACT

The "area factor" is used in the RESRAD code to estimate the airborne contaminant concentrations for a finite area of contaminated soils. The area factor model used in RESRAD version 5.70 and earlier (referred to as the "old area factor") was a simple, but conservative, mixing model that tended to overestimate the airborne concentrations of radionuclide contaminants. An improved and more realistic model for the area factor (referred to here as the "new area factor") is described in this report. The new area factor model is designed to reflect site-specific soil characteristics and meteorological conditions. The site-specific parameters considered include the size of the source area, average particle diameter, and average wind speed. Other site-specific parameters (particle density, atmospheric stability, raindrop diameter, and annual precipitation rate) were assumed to be constant. The model uses the Gaussian plume model combined with contaminant removal processes, such as dry and wet deposition of particulates. Area factors estimated with the new model are compared with old area factors that were based on the simple mixing model. In addition, sensitivity analyses are conducted for parameters assumed to be constant. The new area factor model has been incorporated into RESRAD version 5.75 and later.

1 INTRODUCTION

The U.S. Department of Energy (DOE) residual radioactive material code (RESRAD) is a computer code developed at Argonne National Laboratory to calculate the radiological dose to which a hypothetical on-site resident or worker would be exposed when the soil over a particular site is radiologically contaminated (Yu et al. 1993). Various exposure pathways are considered in the RESRAD code, including the inhalation of contaminated airborne particulates. For an on-site receptor, the contaminated dust resulting from on-site activities such as mechanical disturbance or natural wind erosion would be diluted because of mixing with uncontaminated off-site dust. The

degree of dilution depends primarily on the soil characteristics and atmospheric conditions for the area of concern. For the inhalation and foliar deposition pathways in the RESRAD code, the fraction of the total ambient airborne particulate concentration that originates from the contaminated site is estimated from the monitored ambient particulate concentration data at the site or at a nearby location. This estimation involves the use of a parameter called the "area factor," which is defined as the ratio of the airborne concentration from a finite area source to the airborne concentration of an infinite area source. The area factor is less than or equal to unity because the airborne particulate concentration from a finite area source is always lower than that from an infinite area source. For example, for larger particles with high gravitational settling velocity under weak wind, emission sources upwind of some point within a square area source fail to contribute to a receptor at the downwind boundary of the site. In this case, the area factors for the area larger than the one mentioned become unity.

The area factor depends on wind speed and direction, location of receptor, particle size distribution, dry and wet deposition, and other atmospheric conditions. The area factor used in RESRAD version 5.70 and earlier, which was derived from a simple mixing model, depends only on the size of the contaminated surface area and fails to reflect any site-specific characteristics. To introduce important site-specific characteristics into the model, an alternative area factor formulation is presented. The new formulation is based on the concept of integrating airborne particulate contributions from multiple line sources that represent the area source, assuming the dispersion of the line source emissions as Gaussian. Site-specific parameters considered in the new formulation include average wind speed, the size of the contaminated site, and average particle size. The first two parameters are already incorporated into the RESRAD input database.

2 PROPOSED AREA SOURCE CONCENTRATION MODEL

To calculate for on-site receptor locations the airborne concentrations of particulate emissions from a contaminated site, the site is assumed to be a square area divided into a series of line sources oriented perpendicular to the wind direction (Figure 1). The receptor R_1, which is the basis for model formulation throughout this section, is assumed to be located at the center of the downwind edge of the contaminated site. The airborne concentration (χ_A, measured in grams per cubic meter) at the downwind receptor R_1 in Figure 1 resulting from the square area source can be estimated by combining concentration contributions from N line source segments as follows:

$$\chi_A = \sum_{i=1}^{N} \chi_{Li} \quad . \tag{1}$$

If each line source is situated on the y-axis (which moves with a line source being evaluated), airborne concentrations from the i^{th} line source emission at the downwind receptor R_1 can be calculated. The calculation is based on the generalized crosswind finite line source Gaussian formulation (Turner 1970, 1994) as follows:

$$\chi_{Li}\,(x,0,z;H_e) = \frac{q_{Li}^{eff}}{\sqrt{2\pi}u\sigma_z}\left\{\exp\left[-\frac{(z-H_e)^2}{2\sigma_z^{\,2}}\right] + \exp\left[-\frac{(z+H_e)^2}{2\sigma_z^{\,2}}\right]\right\} \cdot \int_{-L/2\sigma_y}^{L/2\sigma_y} \frac{1}{\sqrt{2\pi}}\exp\left(-\frac{p^2}{2}\right)dp \quad , \tag{2}$$

where

$\chi_{Li}\,(x,0,z;H_e)$ = concentration (g/m^3) at a receptor $R_1(x,0,z)$ resulting from the i^{th} line source with an effective release height H_e (m);

q_{Li}^{eff} = effective line source strength [g/(m·s)];

u = mean wind speed at effective release height (m/s);

σ_y, σ_z = standard deviation of lateral, vertical concentration distribution (m);

$p = y/\sigma_y$; and

L = side length of square area source (m).

88

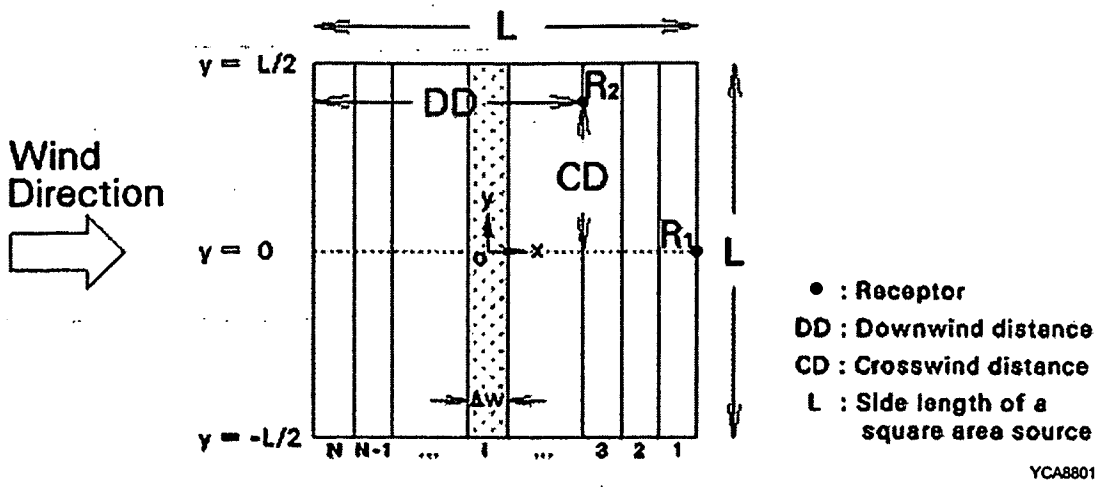

FIGURE 1 Representation of Area and Line Sources

To account for the gravitational settling of particulates, the effective release height of emission H_e in Equation 2 is replaced by the term $(H_e - H_v)$, where $H_v = v_g x/u$ and with v_g being the gravitational settling velocity. This substitution tilts the axis of the plume downward at an angle of $\tan^{-1}(v_g/u)$. (The effects of gravitational settling are further discussed later in this section.) The value of the integral in Equation 2, an area under the Gaussian curve, is determined with a fifth-order polynomial approximation (Abramowitz and Stegun 1964). If lower and upper limits in the integral approach $-\infty$ and $+\infty$, respectively, then the integral yields unity. Also, the particulate emission of concern is considered a ground-level or near-ground-level, nonbuoyant release; therefore, the contribution of reflection of the plume is relatively smaller at the top of the mixing layer than at the surface. In fact, this is not true for an extremely unstable condition (e.g., Pasquill Stability Class A) when vigorous vertical mixing occurs; however, over a long-term period, this condition accounts for far less time than the sum of other stability conditions. Accordingly, for simplicity, the reflection of the plume at the top of the mixing layer is not considered in this study.

The area source strength, q_A, at the point of emission will gradually decrease through dry deposition and rain scavenging as the plume disperses downwind. To account for the source depletion with downwind distance, the effective line source strength at the downwind receptor R_1 of particles emitted from the i^{th} line source shown in Figure 1 can be approximated as

$$q_{Li}^{eff} = q_{Ai}^{eff} \cdot \Delta w = [q_A - \sum_{i=1}^{i} (F_{Di} + F_{Wi})] \cdot \Delta w \quad , \tag{3}$$

89

where

q_{Ai}^{eff} = effective area source strength at the downwind receptor R_1 [g/(m^2· s)];

Δw = width of a line source, defined as the side length of square area source divided by the total number of line sources (m);

q_A = area source strength at the point of emission [g/(m^2 · s)]; and

F_{Di}, F_{Wi} = mass flux by dry and wet deposition on the surface of crosswind distances including downwind receptor R_1 of the i^{th} line source [g/(m^2· s)].

Mass fluxes F_{Di} and F_{Wi} can be estimated by integrating products of local concentration and deposition velocities from $-\infty$ to ∞ in the y direction. These fluxes can be approximated by multiplying the concentration at the center of the downwind edge by the deposition velocity, because the crosswind concentration profile forms a bell shape with a flat top, as shown in Figure 2. Also note that the concentration from an infinite area source should approach a finite value; the concentration from a finite area source is divided by this finite value to determine the area factor. Accordingly, in this study, the effective source strength concept as shown in Equation 3 was adopted rather than the source exponential decay term, which fails to approach zero until the downwind distance goes to infinity. Formulations for deriving dry and wet deposition fluxes F_D and F_W are discussed below.

In nature, air pollutants are ultimately removed from the atmosphere by (1) dry and/or wet deposition mechanisms onto the ground surface or (2) radioactive decay or chemical transformation while being transported downwind. In this study, only dry and wet deposition are considered, and the loss of material from the plume is approximated by assuming that the source strength decreases because of dry and wet deposition. Dry deposition of an airborne material onto the earth's surface can be caused by a combination of several natural processes, such as gravitational settling, inertial impaction, molecular and turbulent diffusion, and ground absorption (by soil, water, buildings, or vegetation). The dry deposition velocity is predicted to depend on particle density, friction velocity, and surface roughness. In general, large particles (D_p > 10 μm) are deposited predominantly by gravitational settling, whereas very small particles (D_p < 0.1 μm) are deposited mainly by Brownian diffusion. In this study, particles ranging from 1 to 30 μm in diameter are of interest; therefore, only the gravitational settling process is considered. Then, the rate of dry deposition as a result of gravitational settling, F_{Di} [g/(m^2 · s)], is given by

$$F_{Di}(x,z_d) = v_g \cdot \chi_{Li}(x,0,z_d;H_e) \quad , \tag{4}$$

90

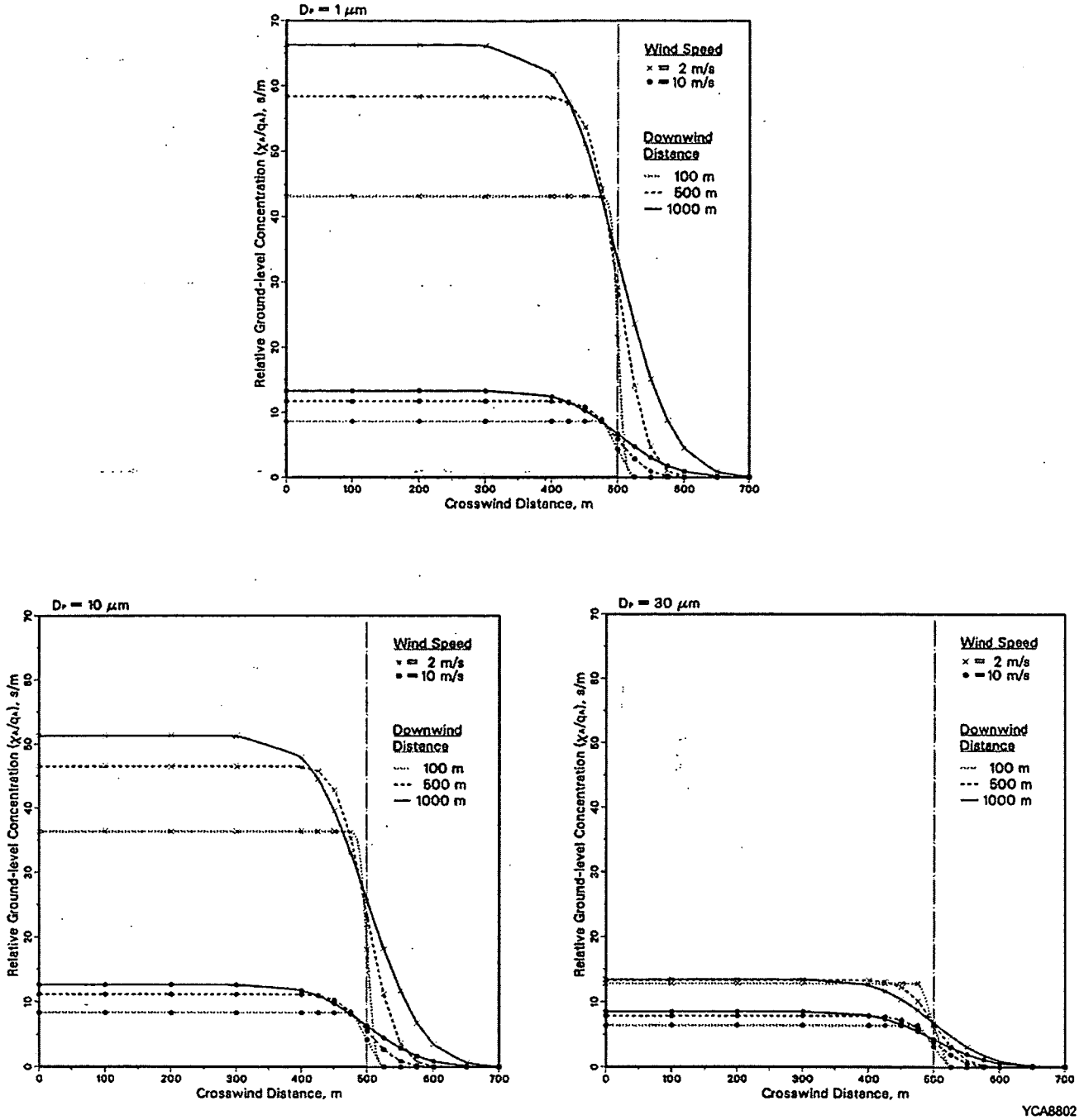

FIGURE 2 Relative Ground-Level Concentrations for L = 1,000 m and D_p = 1, 10, and 30 μm

where

v_g = gravitational settling velocity (m/s); and

$\chi_{Li}(x,0,z_d;H_e)$ = concentration (g/m^3) at a reference height z_d (m) above the surface.

For particles that follow the Stokes law, the terminal gravitational settling velocity v_g (m/s) can be expressed as

$$v_g = \frac{\rho_p \, g \, D_p^2}{18 \, \mu_a} \quad , \tag{5}$$

where

ρ_p = particle density (kg/m^3),

g = gravitational acceleration (9.8 m/s^2),

D_p = particle diameter (m), and

μ_a = absolute viscosity of air at sea level and 15°C [1.7894×10^{-5} kg/(m · s)].

Airborne particulates are also removed by wet deposition mechanisms, including rainout (in-cloud scavenging) and washout (below-cloud scavenging by falling rain, snow, etc.). In this study, only the washout process is considered. In many cases, the local rates of removal of particulates by wet deposition, in g/(m · s), can be represented as a first-order process:

$$Local\ rate\ of\ removal = \Lambda(D_p;z) \cdot \chi_{Li}(x,0,z;H_e) \quad , \tag{6}$$

where $\Lambda(D_p;z)$ = washout coefficient (s^{-1}). This first-order representation means that the scavenging is irreversible; that is, the rate of removal depends linearly on the airborne concentration and is independent of the quantity of material scavenged previously. The wet deposition flux is the sum of wet removal from all volume elements aloft, assuming that the scavenged materials fall down as precipitation. Similar to dry deposition, the rate of wet deposition, $F_{Wi}(x,z_d)$ in g/(m^2 · s) can be given by

$$F_{Wi}\, x\, z_d) = \int_0^H \Lambda(D_p;z) \cdot \chi_{Li}(x,0,z;H_e)\, dz = v_w \cdot \chi_{Li}(x,0,z_d;H_e) \quad , \tag{7}$$

92

where

H = average traveling distance of a raindrop (m), and

v_w = wet deposition velocity (m/s).

To formulate the wet deposition velocity, v_w, monodisperse raindrop size is assumed for simplicity. First, the number of raindrops falling onto the ground, N_r [number of droplets/(m^2 · s)], can be given by

$$N_r = 6.056 \times 10^{-10} \cdot R \,/\, D_r^3 \quad , \tag{8}$$

where

R = annual rainfall rate (cm/yr), and

D_r = diameter of a raindrop (m).

Also, the total mass of airborne particulates swept out by each raindrop, M (g), can be approximated by

$$M = A \cdot H \cdot \chi_{Li}^{av}(x,0;H_e) \quad , \tag{9}$$

where

A = cross-sectional area of a raindrop, given by $\pi D_r^2/4$ (m^2); and

$\chi_{Li}^{av}(x,0;H_e)$ = average airborne concentration in the volume swept by a raindrop (g/m^3).

This equation implies that all particles in the geometric volume swept out by a falling raindrop will be collected by the raindrop; that is, the value of the collection efficiency between droplets and particles is unity. Accordingly, combining Equations 8 and 9, the total flux, F_{Wi} [g/(m^2 · s)], can be given by

$$F_{Wi}(x,z_d) = 4.756 \times 10^{-10} \cdot R \cdot H \cdot \chi_{Li}^{av}(x,0;H_e) \,/\, D_r \quad . \tag{10}$$

It is reasonable to assume that the precipitation scavenging takes place from the point of $3\sigma_z$, where the concentration is approximately 1% of that of the plume centerline, to the surface. For convenience, the plume height, PH, to account for plume tilting is defined as

$$PH = 3\sigma_z - v_g \cdot x \,/\, u \quad . \tag{11}$$

93

Then, χ_{Li}^{av} can be expressed in terms of χ_{zd} in Equation 7:

$$\chi_{Li}^{av}(x,0;H_e) = \frac{\chi_{Li}(x,0,z_d;H_e) \int_0^{PH} [\exp(-\frac{p_1^2}{2}) + \exp(-\frac{p_2^2}{2})] \cdot dz}{PH \cdot [\exp(-\frac{q_1^2}{2}) + \exp(-\frac{q_2^2}{2})]} , \quad (12)$$

where

$$p_1 = (z - H_e + H_v)/\sigma_z,$$

$$p_2 = (z + H_e - H_v)/\sigma_z,$$

$$q_1 = (z_d - H_e + H_v)/\sigma_z, \text{ and}$$

$$q_2 = (z_d + H_e - H_v)/\sigma_z.$$

As in Equation 2, the value of the integral can be calculated with a fifth-order polynomial approximation. Combining Equations 11 and 12 into Equation 10, the rate of wet deposition can be rewritten in terms of wet deposition velocity v_w and concentration at the reference height z_d, as in the calculation for dry deposition.

Lateral and vertical dispersion coefficients σ_y and σ_z are estimated on the basis of the formulae used in the Industrial Source Complex model (EPA 1995). Equations that approximately fit the Pasquill-Gifford curves (Turner 1970, 1994) are introduced to calculate σ_y and σ_z (m) as a function of downwind distance (km) for the rural mode. The σ_y coefficient can be calculated by

$$\sigma_y = 465.11628 \cdot x \cdot \tan(TH) , \quad (13)$$

where

$$TH = 0.017453293 \cdot [c - d \cdot \ln(x)] .$$

Also, σ_z can be computed as

$$\sigma_z = a \cdot x^b . \quad (14)$$

For the above equations, the coefficients c and d for σ_y and a and b for σ_z are presented in Tables 1 and 2, respectively.

TABLE 1 Parameters Used to Calculate Pasquill-Gifford σ_y

$$\sigma_y = 465.11628\ (x)\ \tan\ (TH)^*$$

$$TH = 0.017453293\ [c - d \cdot \ln\ (x)]$$

Pasquill Stability Class	c	d
A	24.1670	2.5334
B	18.3330	1.8096
C	12.5000	1.0857
D	8.3330	0.72382
E	6.2500	0.54287
F	4.1667	0.36191

* σ_y is expressed in meters, and x is the downwind distance, in kilometers.

Source: EPA (1995).

Finally, numerical calculations were made after all components were incorporated into the model. Integrations were made in succession from the nearest line source to the farthest from the receptor R_1. If the receptor height (z) and the reference height (z_d) are the same, combining and rewriting Equations 2 and 3 shows that the concentration at the receptor R_1 resulting from the i^{th} line source appears in both sides, which can be readily solved by transposing,

From the first line source, $$\chi_{L1} = q_{L1}^{eff} \cdot RHS_1 = (q_A - \chi_{L1} v_{T1}) \cdot \Delta w \cdot RHS_1$$

From the second line source, $$\chi_{L2} = q_{L2}^{eff} \cdot RHS_2 = [q_A - (\chi_{L1} v_{T1} + \chi_{L2} v_{T2})] \cdot \Delta w \cdot RHS_2$$

.....

From the i^{th} line source, $$\chi_{Li} = q_{Li}^{eff} \cdot RHS_i = [q_A - (\chi_{L1} v_{T1} + \chi_{L2} v_{T2} \cdots + \chi_{Li} v_{Ti})] \cdot \Delta w \cdot RHS_i$$

where

$v_{Ti} = v_{gi} + v_{wi}$ (m/s); and

RHS_i = (right hand side of Equation 2) / q_{Li}^{eff}.

95

TABLE 2 Parameters Used to Calculate Pasquill-Gifford σ_z*

Pasquill Stability Class	x	$\sigma_z = a \cdot x^b$ a	b
A+	<0.10	122.800	0.94470
	0.10 - 0.15	158.080	1.05420
	0.16 - 0.20	170.220	1.09320
	0.21 - 0.25	179.520	1.12620
	0.26 - 0.30	217.410	1.26440
	0.31 - 0.40	258.890	1.40940
	0.41 - 0.50	346.750	1.72830
	0.51 - 3.11	453.850	2.11660
	>3.11	†	†
B+	<0.20	90.673	0.93198
	0.21 - 0.40	98.483	0.98332
	>0.40	109.300	1.09710
C+	All	61.141	0.91465
D	<0.30	34.459	0.86974
	0.31 - 1.00	32.093	0.81066
	1.01 - 3.00	32.093	0.64403
	3.01 - 10.00	33.504	0.60486
	10.01 - 30.00	36.650	0.56589
	>30.00	44.053	0.51179
E	<0.10	24.260	0.83660
	0.10 - 0.30	23.331	0.81956
	0.31 - 1.00	21.628	0.75660
	1.01 - 2.00	21.628	0.63077
	2.01 - 4.00	22.534	0.57154
	4.01 - 10.00	24.703	0.50527
	10.01 - 20.00	26.970	0.46713
	20.01 - 40.00	35.420	0.37615
	>40.00	47.618	0.29592
F	<0.20	15.209	0.81558
	0.21 - 0.70	14.457	0.78407
	0.71 - 1.00	13.953	0.68465
	1.01 - 2.00	13.953	0.63227
	2.01 - 3.00	14.823	0.54503
	3.01 - 7.00	16.187	0.46490
	7.01 - 15.00	17.836	0.41507
	15.01 - 30.00	22.651	0.32681
	30.01 - 60.00	27.074	0.27436
	>60.00	34.219	0.21716

* σ_z is expressed in meters, and x is expressed in kilometers.

+ If the calculated value of σ_z exceeds 5,000 m, σ_z is set to 5,000 m.

† σ_z is equal to 5,000 m.

Source: EPA (1995).

96

The model first divides an area source into 10- and 11-line sources, computes the concentration for each line (χ_{Li}) at the receptor R_1, and sums the concentrations to arrive at the total concentration (χ_A) resulting from the entire area source. Then, if the relative difference of concentrations between 10- and 11-line sources is within a given tolerance (e.g., 10^{-4}), the iterative procedures will be terminated. If not, successive iterations continue with further subdivisions in increments of 10 (e.g., 20/21, 30/31, 40/41) until the prescribed convergence condition is satisfied. For computational economy, the maximum number of line sources is limited to 10,000.

3 RESULTS AND DISCUSSION

The area factor can be defined as the ratio of the airborne concentration from a finite area source to that from an infinite area source. The methodology used to estimate the area factors is based on the notion that once released into the ambient air, all particulate matter would eventually be removed from the atmosphere by dry and/or wet deposition. The model first calculates the concentrations at the downwind receptor R_1 by increasing the square area source until concentration values are leveled off, that is, approach the maximum values. Then the area factors for square area sources are estimated by dividing their respective concentrations by the maximum concentrations. Some important factors that affect the airborne concentrations are area size, wind speed, wind direction, particle size, location of the receptor, stability class, rainfall rate, and raindrop size.

To illustrate the effects of these factors, the new model was implemented for four wind speeds (1, 2, 5, and 10 m/s at the measurement height [usually 10 m]) and six particle diameters (1, 2, 5, 10, 15, and 30 μm). Nine square area sources that have side lengths ranging from 1 to 100,000 m and that are oriented perpendicular to the wind direction are analyzed in this study. It is assumed that particles from a source area are emitted into the atmosphere by on-site activities such as mechanical disturbances or wind erosion. This assumption implies that particles are airborne, irrespective of the mechanism of dust generation, and are subsequently subject to a wind stream. For a finite source area, the average airborne concentration can be estimated by integrating the ground-level airborne concentrations over the entire source area. However, this value depends on the frequencies of occurrence of different wind directions and speeds. For simplicity, it is conservative to take the maximum local airborne concentration, that is, the concentration at the center of the downwind edge (receptor R_1 in Figure 1), as the average concentration. The airborne concentrations presented in the rest of the report are the values predicted for the locations at the center of the downwind edge, unless otherwise stated.

The depletion of emission sources associated with radionuclide decay is neglected in the current study. Also, the effective release height (H_e), receptor height (z), and reference height (z_r) are assumed to be zero, that is, at the surface. Parameter values used to estimate airborne concentrations and area factors were selected for typical sites in the United States, where possible (Table 3). On the basis of annual averages for more than 300 National Weather Service stations in the United States, the neutral conditions (represented by Pasquill Class D) occur almost one-half of the observations, while stable (Classes E and F) and unstable (Classes A, B, and C) conditions occur about one-third and one-sixth of the time, respectively (National Oceanic and Atmospheric Administration [NOAA] 1976). Therefore, in this study, neutral stability (Class D) was assumed.

To illustrate the effects of wind speed and particle size on the concentrations at various receptor locations within the site, the relative ground-level concentrations, χ_A/q_A, for a 1,000 × 1,000 m area source are shown in Figure 2 for various crosswind and downwind locations

98

TABLE 3 Parameter Values Used to Estimate Airborne Concentrations and Area Factors

Parameter	Values Used	Reference
Rainfall rate	R = 100 cm/yr	Miller and Thompson (1970)
Particle density	ρ_p = 2,650 kg/m^3	Brady (1974)
Stability class	D (Neutral)	NOAA (1976)
Diameter of raindrop	$D_r = 10^{-3}$ m	Miller and Thompson (1970)

(Figure 1). Concentrations at the off-axis receptor (e.g., receptor R_2 in Figure 1) can be estimated by integrating the area source upwind of the receptor with the modification of integration limits in Equation 2. Figure 2 shows relative ground-level concentrations for particle diameters of 1, 10, and 30 μm, respectively, for cases with wind speeds of 2 and 10 m/s. The downwind distances presented in the figure are 100, 500, and 1,000 m (i.e., downwind edge) from the upwind edge of the square source area. As shown in Figure 2, the airborne concentrations increase with the downwind distances and decrease with the crosswind distances from the centerline of the area source parallel to the wind direction. The airborne concentrations along the crosswind distance do not vary significantly except at the locations very close to the crosswind edges of the source area, where the airborne concentrations are predicted to be approximately 50% lower than those at the centerline locations. Also, concentration distributions show symmetry centering around the crosswind edge. (As mentioned in Equation 3, mass fluxes by depositions can be approximated only with concentration at the downwind receptor R_1 without integrating local concentrations along the crosswind distances because of the concentration profile described above.) The airborne concentrations near the crosswind edge are more affected by downwind distance associated with edge effects from the line source. In general, the particle suspension rate driven by wind erosion increases as the wind speed increases. However, the increase in emissions caused by higher wind speed is partially offset by the dilution by the higher wind speed.

To illustrate the effects of the size of the square source area on the airborne concentration, the relative ground-level concentrations χ_A/q_A resulting from square area sources of various sizes are shown in Figure 3 for particles 1, 10, and 30 μm in diameter. In general, the χ_A/q_A values increase monotonically with the size of the square area source and decrease with wind speed and particle diameter. If the source area is large enough, the airborne concentrations reach a maximum value and do not increase even if the size of the area source is further increased. This means that the airborne concentration thus calculated is similar to that of an area source of infinite size. For smaller particles (D_p = 1 μm), the airborne concentrations reach their maximums at side lengths of around 100,000 m or more, being primarily scavenged by precipitation. On the other hand, for particles of 30 μm in diameter and low wind speed, emissions from sources located more than 1,000 m upwind

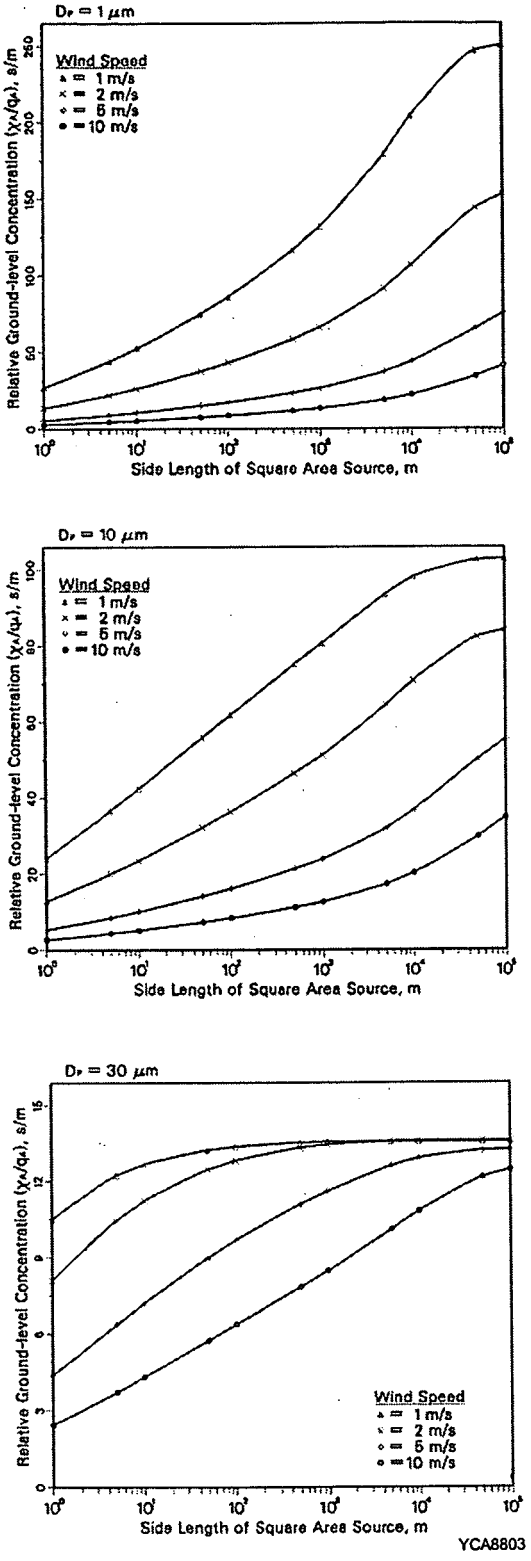

FIGURE 3 Relative Ground-Level Concentrations for D_p = 1, 10, and 30 μm

100

do not contribute to concentrations at the downwind receptor location because of high gravitational settling velocity.

To examine the relationship between virtual emissions and depositions within the area source, relative effective source strength and percentage deposited are depicted in Figure 4. The relative effective source strength, q_{eff}/q_A, is defined as the ratio of the effective source strength at the downwind edge to the source strength at the upwind edge of the square area. The percentage deposited is defined as the total mass deposited by dry and wet deposition up to the downwind edge divided by the total emissions within the site. Note that $q_{eff}/q_A = 0$ does not necessarily mean 100% deposition of particulates emitted, because airborne particulates still exist over the site. As shown in Figure 4, the wet deposition process is dominant over dry deposition for smaller particles ($D_p = 1$ μm). For particles of 10 μm or larger in diameter, gravitational settling is the major removal pathway. The side length of the square area source where emission from the upwind edge is almost depleted when the plume passes over the downwind edge is more than 100,000 m for a particle diameter of 1 μm and wind speed of 1 m/s. On the other hand, the side length size is approximately 1,000 m for the case of a particle diameter of 30 μm and wind speed of 1 m/s. More particles are deposited at lower wind speeds than at higher wind speeds because at lower wind speeds there are more chances for particles to be removed by dry or wet depositions before they pass over the downwind edge. It is interesting to note that for particles 1 μm in diameter, deposition can be ignored for area sources with side lengths of 1,000 m or less.

The area factors for cases with various wind speeds and particle diameters are shown in Figure 5. General trends for area factors are similar to those for relative ground-level concentrations expressed as χ_A/q_A (Figure 3). A physical interpretation for the small area factors is that dilution by the uncontaminated dust blown in from off-site is significant for the case of small particles and high wind speeds. On the other hand, for cases with large particles and low wind speeds, deposition becomes significant, and a maximum airborne concentration can be reached if the source area is sufficiently large. Accordingly, the larger the area factor, the more emitted particulates are removed before reaching the downwind edge.

The old area factors used in the RESRAD code are also plotted in Figure 5. The area factor is approximated by $A^{1/2}/(A^{1/2} + DL)$, where A is the area of contaminated site (m^2) and DL is the dilution length (m). Although DL depends on the wind speed, mixing height, resuspension rate, and thickness of the resuspendable dust layer (Appendix A in Gilbert et al. 1983), the geometric mean of the estimates of lower and upper bounds of DL is used as a default value. In the RESRAD code, the geometric mean (3 m) of 0.03 and 250 m (which correspond to the surface roughness and the height of the stable atmospheric layer, respectively) is assumed to be the default dilution length in predicting the airborne concentration from a finite source area. As shown in Figure 5, the old area factors used in the RESRAD code are larger than those obtained in the new model, except for the case of large particles ($D_p = 30$ μm) and low wind speed. Results show that the dilution length of

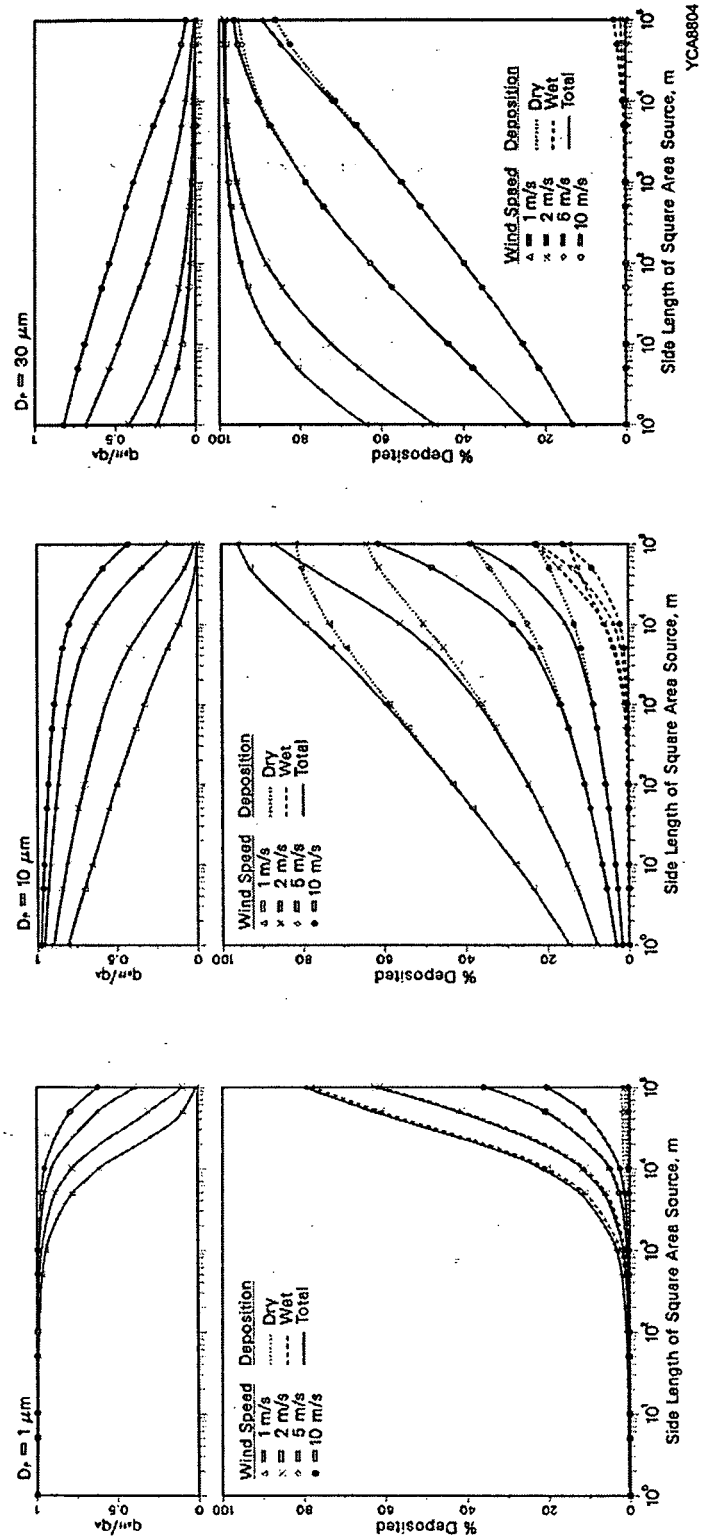

FIGURE 4 Relative Effective Source Strength and Percent Deposited over the Area Source for D_p = 1, 10, and 30 μm

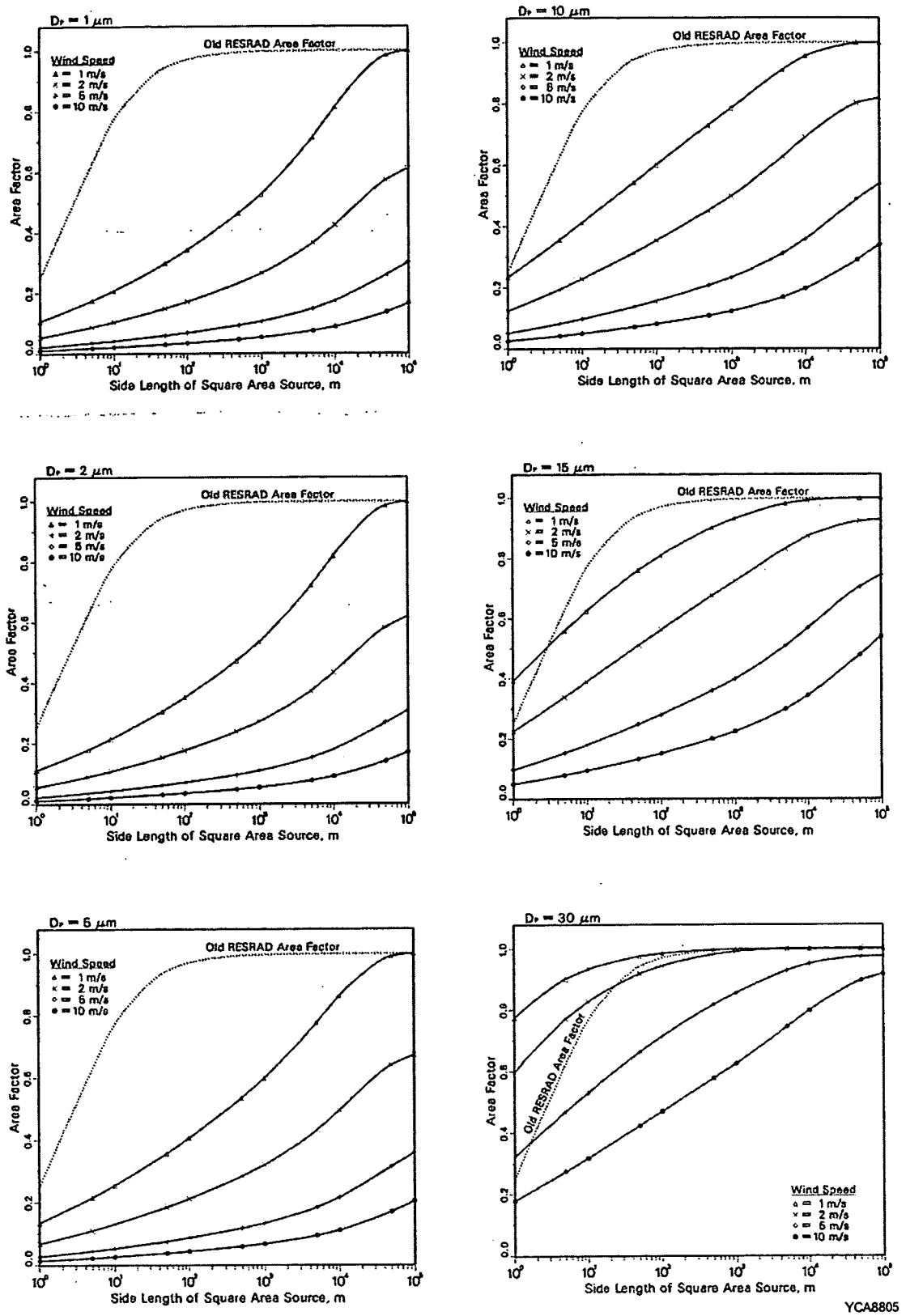

FIGURE 5 Area Factors for D_p = 1, 2, 5, 10, 15, and 30 μm

103

3 m as assumed in the RESRAD code provides a reasonably conservative estimate of the airborne concentrations for respirable particle sizes of 1-10 μm.

For direct use in the RESRAD code application, functional expressions are needed to compute the new area factor associated with a finite area source. The desired feature of the functional expression is a sigmoidal behavior with characteristics approaching 0 and 1 of area factors as the side length of source area varies from 0 m to ∞. Two candidates represented by the logistic growth rate function (Snedecor and Cochran 1980) and the hyperbolic tangent function were tested by regression. The former function was selected because it provides a remarkably good fit to the cases under study and a much better fit than the latter. The equation used to fit the new area factors can be written as

$$\text{Area Factor} = \frac{a}{1+b\ (\sqrt{A})^{c}} \tag{15}$$

where A = area of the contaminated zone. The coefficients a, b, and c for regression curves for the new area factors and related correlation coefficients are presented in Table 4. The regression curve fits very well for the side length $(\sqrt{A})$ of the square area source ranging from 1 to 10,000 m because more weights are assigned to points within that range.

TABLE 4 Coefficients Derived for the Least Square Regression Curves for Area Factors*

Particle Diameter (μm)	Wind Speed (m/s)	Area Factor+ = $\frac{a}{1 + b\ (\sqrt{A})^c}$			
		a	*b*	*c*	Correlation Coefficient
1	1	1.9005	14.1136	-0.2445	0.9978
	2	1.6819	25.5076	-0.2278	0.9991
	5	0.7837	31.5283	-0.2358	0.9946
	10	0.1846	14.6689	-0.2627	0.9732
2	1	1.8383	13.2106	-0.2451	0.9979
	2	1.6643	24.3606	-0.2273	0.9992
	5	0.8301	32.1641	-0.2339	0.9949
	10	0.1992	15.2539	-0.2598	0.9750
5	1	1.5112	8.7288	-0.2528	0.9982
	2	1.4913	17.2749	-0.2264	0.9992
	5	1.1050	33.8232	-0.2266	0.9966
	10	0.3174	19.9297	-0.2500	0.9838
10	1	1.1445	3.4160	-0.2891	0.9987
	2	1.1396	6.9377	-0.2451	0.9993
	5	1.6353	25.4614	-0.2112	0.9990
	10	1.2075	39.4658	-0.2212	0.9955
15	1	1.0273	1.6289	-0.3945	0.9996
	2	1.0469	3.1582	-0.2813	0.9993
	5	1.5252	11.8208	-0.2085	0.9995
	10	2.5496	40.9663	-0.2012	0.9988
30	1	1.0000	0.2656	-0.5937	0.9998
	2	1.0059	0.7305	-0.5352	0.9995
	5	1.0781	2.0215	-0.2979	0.9980
	10	1.1325	4.4736	-0.2483	0.9996

* The regression curve fits well for the side length ($\sqrt{A}$) of the square area source ranging from 1 to 10,000 m.

+ Where $\sqrt{A}$ is the length of the side of the square area source, in meters.

4 SENSITIVITY ANALYSIS

To perform sensitivity analyses for assumed parameters, four cases were simulated as follows (the Base Case is the original simulation):

- Case 1: Annual rainfall rate (R),
- Case 2: Diameter of a raindrop (D_r),
- Case 3: Particle density (D_p), and
- Case 4: Atmospheric stability class.

For Cases 1 to 3, 100% perturbation upward and downward for assumed parameter values was tested. For Case 4, the most unstable (Class A) and most stable (Class F) classes were tested. In fact, assuming 100% increase in annual rainfall rate for Case 1 provides identical results to 100% decrease in diameter of a raindrop for Case 2, or vice versa. This situation can be seen in Equation 10, where the annual rainfall rate (R) is inversely related to the raindrop diameter (D_r).

Relative area factors, which represent the ratio of area factor resulting from parameter perturbations to that for the Base Case, are presented in Figures 6 to 8 for perturbations in rainfall rate, particle density, and atmospheric stability class, respectively. Relative area factors are predicted to be relatively insensitive to changes in annual rainfall rate and, as shown in Figure 6, vary approximately 20, 5, and 0% for 1, 10, and 30 μm, respectively. This result suggests that for smaller particles, wet deposition plays an important role in removal, while for larger particles, gravitational settling is the major removal process. Perturbation of particle density for Case 3 is more sensitive than that of annual rainfall rate for Case 1. As shown in Figure 7, the sensitivity increases with particle size. Although considerable range in particle density may be observed, the values for most mineral soils usually vary between the narrow limits of 2,600 and 2,750 kg/m^3 (Brady 1974). Some mineral topsoils high in organic matter may drop to 2,400 kg/m^3 or lower. Nevertheless, for general calculations, the average arable surface soil may be considered to have a particle density of about 2,650 kg/m^3. For Case 4, the area factors are most sensitive, especially for smaller particles (Figure 8). This result means that smaller particles are more affected by atmospheric turbulence than larger particles. However, the most unstable (Class A) and most stable (Class F) cases are characterized by conditions under strong solar insolation and under clear nights, respectively, and for both cases, under weak wind. In general, these conditions prevail several hours per day at most, so the sum of the neutral and near-neutral conditions (Classes C, D, and E) is much greater than the sum of extreme conditions (Classes A and F). Therefore, over the long term (e.g., annual average concentrations), the use of neutral stability (Class D) in this study is reasonable because the area factor averaged over site-specific distributions of stability classes is believed to be close to the one calculated only from the neutral stability.

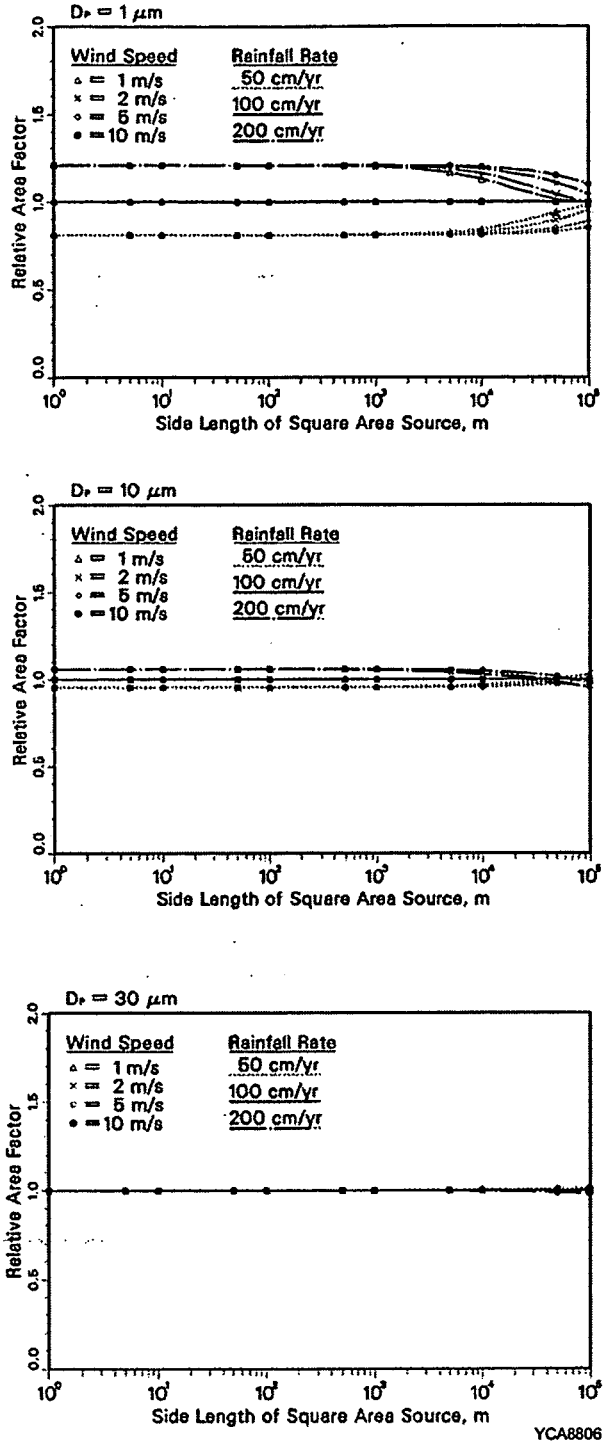

FIGURE 6 Relative Area Factors Associated with Perturbation of Rainfall Rate for D_p = 1, 10, and 30 μm

107

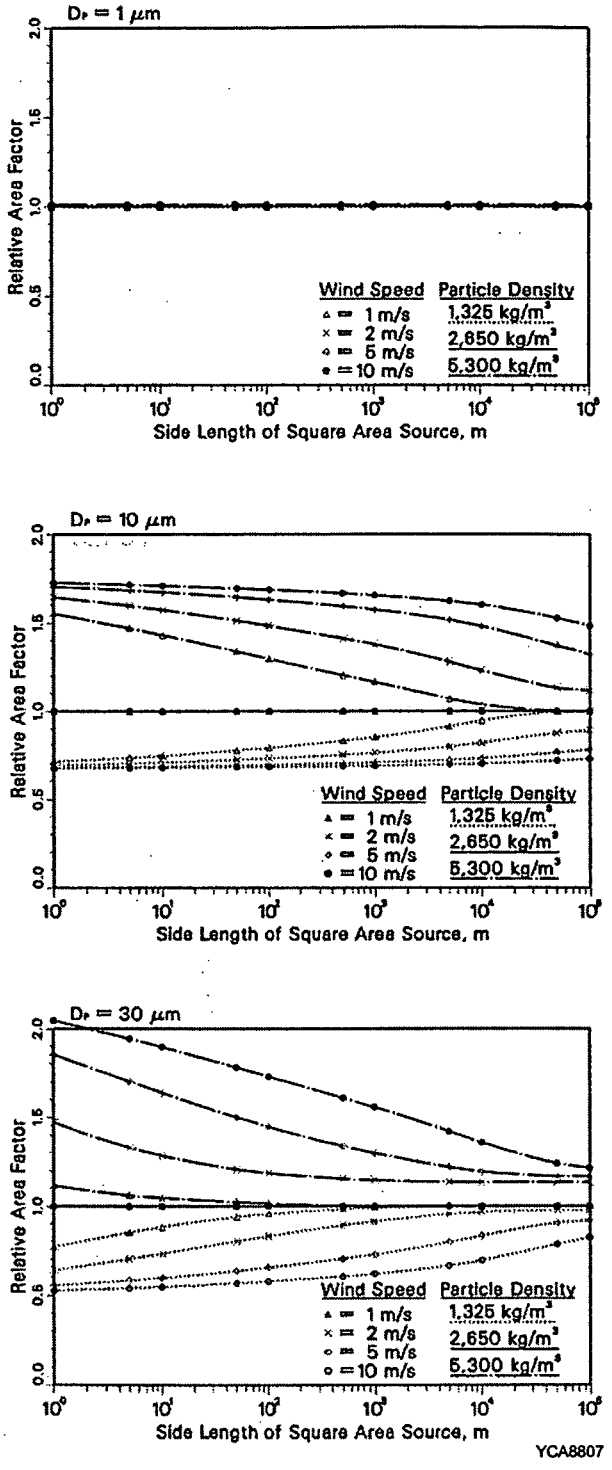

FIGURE 7 Relative Area Factors Associated with Perturbation of Particle Density for D_p = 1, 10, and 30 μm

108

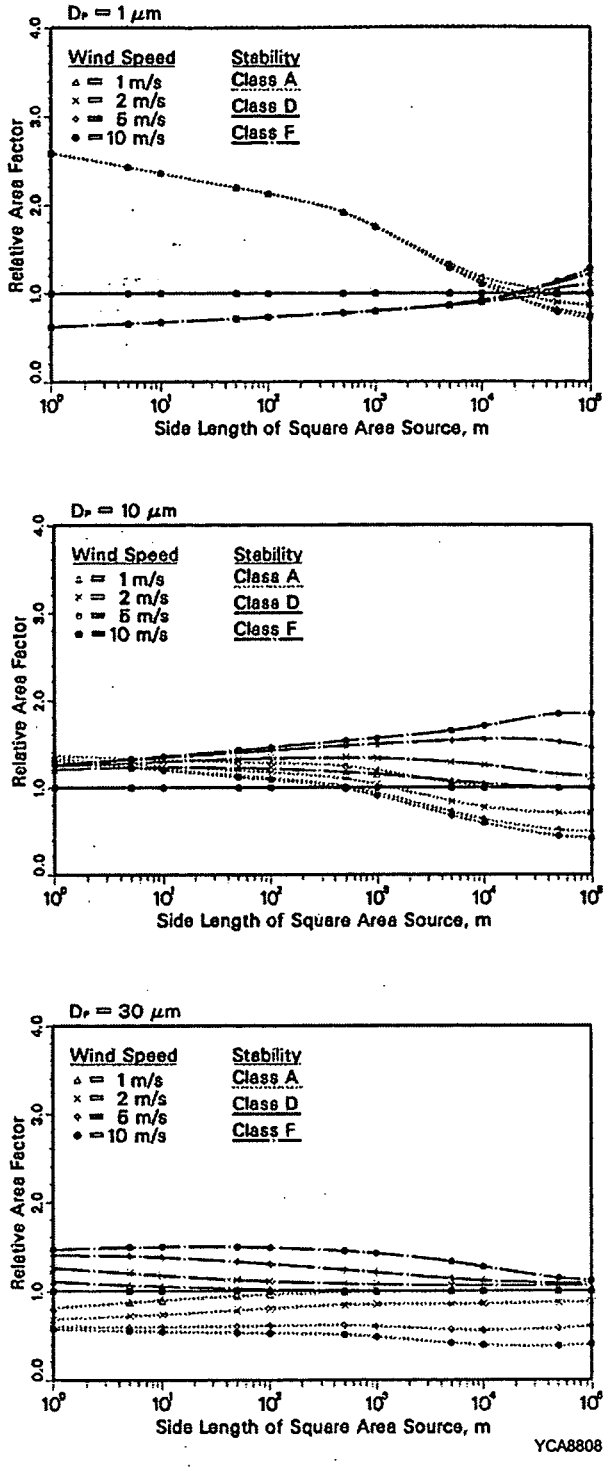

FIGURE 8 Relative Area Factors Associated with Perturbation of Stability Class for D_p = 1, 10, and 30 μm

5 SUMMARY AND DISCUSSION

The model described in this report was developed to improve the area factor used in older versions of the RESRAD code (Version 5.70 and older). The new model first approximates the on-site airborne concentrations of particulates emitted from an area source and subsequently calculates area factors as a function of particle diameter, wind speed, and side length of square area source. The assumptions made in developing the model include monodisperse particle size distributions, fixed particle density, fixed raindrop diameter, fixed annual rainfall rate, fixed atmospheric stability, and a neglect of the effect associated with radionuclide decay. Sensitivity analyses for the assumed fixed parameters indicate that the model provides reasonable results. Regression curves were developed for calculating area factors on the basis of the new model (Equation 15), which has been incorporated into RESRAD code version 5.75 and newer.

The new area factor is a function of particle size and wind speed. Because the inhalation dose conversion factors are for particles with an activity median aerodynamic diameter (AMAD) of 1 μm, the particle size is set to 1 μm in the current version of RESRAD. However, the area factor routine is written with the flexibility to use actual particle size data if available in later versions of the RESRAD code. Wind speed is an input parameter of RESRAD. The code will use interpolation based on Equation 15 to calculate the area factor for the user input wind speed and the size of the contaminated zone.

The RESRAD code uses a mass loading factor and an area factor to estimate contaminant concentration in the air suspended from finite area soil sources. The default mass loading factor used in RESRAD 5.70 and older is 0.0002 g/m^3. This mass loading factor takes into account short periods of high mass loading and sustained periods of normal farmyard activities for which the dust level may be somewhat higher than ambient. Anspaugh et al. (1974) and Healy and Rodgers (1979) used 0.0001 g/m^3 for predictive purposes and found that the predicted results and the real cases were comparable. The EPA (1977) has used 0.0001 g/m^3 for screening calculations. Average ambient concentrations of transportable particles range from 3.3×10^{-5} to 2.54×10^{-4} g/m^3 in urban locations and from 9×10^{-6} to 7.9×10^{-5} g/m^3 in nonurban locations. The mass loading value will fluctuate above its ambient level depending on human activities such as plowing and cultivating dry soil or driving on an unpaved road. A default value of 0.0002 g/m^3 seems to be overly conservative (perhaps by a factor of about 2 to 10). To reduce the over-conservatism in the RESRAD code, the default mass loading factor has been changed from 0.0002 g/m^3 to 0.0001 g/m^3 for more realistic (yet for most conditions still conservative) prediction of dust loading.

The new default mass loading factor and the area factor allow RESRAD to predict realistically conservative contaminant concentrations in the air. Hence, the inhalation doses estimated are more realistic. However, if measurement data are available, the measured air contaminant concentrations data should be used in RESRAD analysis.

6 REFERENCES

Abramowitz, M., and I.A. Stegun, 1964, *Handbook of Mathematical Functions with Formulas, Graphs, and Mathematical Tables*, National Bureau of Standards, Washington, D.C., June.

Anspaugh, L.R., et al., 1974, "Evaluation of the Resuspension Pathway toward Protective Guidelines for Soil Contamination with Radioactivity," presented at the *International Atomic Energy Agency/World Health Organization Symposium on Radiological Safety Evaluation of Population Doses and Application of Radiological Safety Standards to Man and the Environment*, Portoraz, Yugoslavia, May 20-24.

Brady, N.C., 1974, *The Nature and Properties of Soils*, 8th ed., Macmillan Publishing Co., Inc., New York, N.Y.

EPA — See U.S. Environmental Protection Agency.

Gilbert, T.L., et al., 1983, *Pathways Analysis and Radiation Dose Estimates for Radioactive Residues at Formerly Utilized MED/AEC Sites*, ORO-832 (Rev.), prepared by Argonne National Laboratory, Division of Environmental Impact Studies, Argonne, Ill., for U.S. Department of Energy, Oak Ridge Operations, Oak Ridge, Tenn., March (reprinted with corrections: Jan. 1984).

Healy, J.W., and J.C. Rodgers, 1979, *Limits for the Burial of the Department of Energy Transuranic Waste*, LA-UR-79-100, Los Alamos Scientific Laboratory, Los Alamos, N.M.

Miller, A., and J.C. Thompson, 1970, *Elements of Meteorology*, Charles E. Merrill Publishing Co., Columbus, Ohio.

National Oceanic and Atmospheric Administration (NOAA), 1976, *A Climatological Analysis of Pasquill Stability Categories Based on STAR Summaries,* Asheville, N.C., National Climatic Center, April.

NOAA — See National Oceanic and Atmospheric Administration.

Snedecor, G.W., and W.G. Cochran, 1980, *Statistical Methods*, 7th ed., The Iowa State University Press, Ames, Iowa.

Turner, D.B., 1970, *Workbook of Atmospheric Dispersion Estimates,* Office of Air Programs Publication Number AP-26, U.S. Environmental Protection Agency, Research Triangle Park, N.C.

111

Turner, D.D., 1994, *Workbook of Atmospheric Dispersion Estimates: An Introduction to Dispersion Modeling*, 2nd Ed., Lewis Publishers, Boca Raton, Fla.

U.S. Environmental Protection Agency, 1977, *Proposed Guidance on Dose Limits for Persons Exposed to Transuranium Elements in the General Environment*, Office of Radiation Programs, Criteria and Standards Division, Washington, D.C.

U.S. Environmental Protection Agency, 1995, *User's Guide for the Industrial Source Complex (ISC3) Dispersion Models: Volume II — Description of Model Algorithms*, Office of Air Quality Planning and Standards, Research Triangle Park, N.C., Sept.

Yu, C., et al., 1993, *Manual for Implementing Residual Radioactive Material Guidelines Using RESRAD, Version 5.0,* prepared by Argonne National Laboratory, Environmental Assessment Division, Argonne, Ill., for U.S. Department of Energy, Assistant Secretary for Environment, Safety, and Health, and Assistant Secretary for Environmental Restoration and Waste Management, Sept.

ANL/EAD/TM-24

RESRAD Benchmarking Against Six Radiation Exposure Pathway Models

Environmental Assessment Division
Argonne National Laboratory

Operated by The University of Chicago,
under Contract W-31-109-Eng-38, for the
United States Department of Energy

113

Argonne National Laboratory

Argonne National Laboratory, with facilities in the states of Illinois and Idaho, is owned by the United States Government, and operated by the University of Chicago under the provisions of a contract with the Department of Energy.

This technical memo is a product of Argonne's Environmental Assessment Division (EAD). For information on the division's scientific and engineering activities, contact:

Director, Environmental Assessment Division
Argonne National Laboratory
Argonne, Illinois 60439-4815
Telephone (708) 252-3107

Presented in this technical memo are preliminary results of ongoing work or work that is more limited in scope and depth than that described in formal reports issued by the EAD.

Disclaimer

Reproduced directly from the best available copy.

Available to DOE and DOE contractors from the Office of Scientific and Technical Information, P.O. Box 62, Oak Ridge, TN 37831; prices available from (615) 576-8401.

Available to the public from the National Technical Information Service, U.S. Department of Commerce, 5285 Port Royal Road, Springfield, VA 22161.

ANL/EAD/TM-24

RESRAD Benchmarking Against Six Radiation Exposure Pathway Models

by E.R. Faillace, J.-J. Cheng, and C. Yu

Environmental Assessment Division,
Argonne National Laboratory, 9700 South Cass Avenue, Argonne, Illinois 60439

October 1994

Work sponsored by United States Department of Energy,
Assistant Secretary for Environment, Safety and Health,
Office of Environmental Guidance, and
Assistant Secretary for Environmental Management,
Office of Environmental Restoration

115

This report is printed on recycled paper.

CONTENTS

116

CONTENTS (Cont.)

TABLES

117

TABLES (Cont.)

118

TABLES (Cont.)

ACKNOWLEDGMENTS

The authors would like to thank Eric Martell for compiling preliminary results, W. Alexander Williams, Hal Peterson, and Andy Wallo for reviewing the draft report, Bruce Napier for providing comments on GENII and GENII-S results, and Roger Seitz for providing copies of the DOE/LLW-188 report.

NOTATION

The following is a list of acronyms, initialisms, and abbreviations (including units of measure) used in this document. Some acronyms used in tables only are defined in the respective tables.

ACRONYMS, INITIALISMS, AND ABBREVIATIONS

Ac	actinium
Am	americium
C	carbon
Co	cobalt
Cs	cesium
DOE	U.S. Department of Energy
EPA	U.S. Environmental Protection Agency
H	hydrogen
I	iodine
Ni	nickel
Np	neptunium
NUREG/CR	U.S. Nuclear Regulatory Commission reports category
Pa	protactinium
Pb	lead
Pu	plutonium
Ra	radium
Sr	strontium
Tc	technetium
Th	thorium
U	uranium
Y	yttrium

UNITS OF MEASURE

Bq	becquerel(s)
Ci	curie(s)
pCi	picocurie(s)
µCi	microcurie(s)
cm	centimeter(s)
cm^3	cubic centimeter(s)
d	day(s)
g	gram(s)
mg	milligram(s)
h	hour(s)
kg	kilogram(s)
L	liter(s)
mL	milliliter(s)
m	meter(s)
m^2	square meter(s)
m^3	cubic meter(s)
mrem	millirem(s)
s	second(s)
Sv	sievert(s)
yr	year(s)

121

RESRAD BENCHMARKING AGAINST SIX RADIATION EXPOSURE PATHWAY MODELS

by

E.R. Faillace, J.-J. Cheng, and C. Yu

ABSTRACT

A series of benchmarking runs were conducted so that results obtained with the RESRAD code could be compared against those obtained with six pathway analysis models used to determine the radiation dose to an individual living on a radiologically contaminated site. The RESRAD computer code was benchmarked against five other computer codes — GENII-S, GENII, DECOM, PRESTO-EPA-CPG, and PATHRAE-EPA — and the uncodified methodology presented in the NUREG/CR-5512 report. Estimated doses for the external gamma pathway; the dust inhalation pathway; and the soil, food, and water ingestion pathways were calculated for each methodology by matching, to the extent possible, input parameters such as occupancy, shielding, and consumption factors.

1 INTRODUCTION

U.S. Department of Energy (DOE) Order 5400.5 (DOE 1990) requires that the methodology incorporated in the RESRAD computer code (Gilbert et al. 1989; Yu et al. 1993) be used to establish soil cleanup guidelines for radionuclide contamination at DOE sites. RESRAD is a pathway analysis code that calculates radiation doses to a hypothetical individual living on a contaminated site. Several other existing models can be used to perform similar tasks. Six of these models were selected for benchmark analyses of the RESRAD code: GENII-S, Version 1.485 (Leigh et al. 1992); GENII (Napier et al. 1988); DECOM, Version 2.2 (Till and Moore 1988); PRESTO-EPA-CPG (Hung 1989); PATHRAE-EPA (Rogers and Hung 1987); and NUREG/CR-5512 (Kennedy and Strenge 1992). The first five models have been codified for use on personal computers; the last model has not.

Two types of benchmark analyses were performed. In the first, as detailed in Section 2, the default residential-farmer scenario in RESRAD was used as a starting point, and the parameter values in the other computer codes were changed to match the RESRAD default scenario to the extent possible. Results obtained from the different methodologies were then compared with results from RESRAD for external gamma dose, dust inhalation dose, soil ingestion dose, food (plant, meat, and milk) ingestion dose, and drinking water

ingestion dose. Comparisons between RESRAD and GENII-S, DECOM, PRESTO-EPA-CPG, and NUREG/CR-5512 were tabulated.

The second type of benchmark analysis, as described in Section 3, involved comparison of RESRAD results with published results for the GENII and PATHRAE-EPA codes (Seitz et al. 1992, 1994). The parameter values used in RESRAD were adapted according to the published descriptions for GENII and PATHRAE-EPA so that a similar scenario was simulated by the three different computer codes. Results are presented in Section 3 and the Appendix.

2 BENCHMARKING AGAINST GENII-S, DECOM, PRESTO-EPA-CPG, AND NUREG/CR-5512 MODELS

2.1 MODEL DESCRIPTIONS

The RESRAD code and the four models against which it is benchmarked in this section are briefly described below. The four models are GENII-S, DECOM, PRESTO-EPA-CPG, and NUREG/CR-5512.

2.1.1 RESRAD Code

Version 4.6 of RESRAD (Gilbert et al. 1989) allows the user to define up to nine pathways and three exposure routes: external gamma radiation from radionuclides in soil; inhalation of contaminated dust and radon gas; and ingestion of contaminated plants, meat, milk, aquatic foods, water, and soil.[1] Several scenarios, including residential, industrial, and recreational, can be modeled by adding or suppressing pathways and entering appropriate values for occupancy and consumption rates.

Data input is carried out through an interactive menu system that is divided into several site- and pathway-specific parameter submenus. The code also includes user-accessible dose-factor and transfer-factor libraries. Conservative but realistic defaults, based on a residential scenario, are provided for all parameter values. Other features of the code include time-dependent dose calculations, graphical and text output, and parameter sensitivity analysis. The text output consists of dose estimates (in mrem/yr) for each radionuclide and pathway at the user-specified times. The maximum dose and the time at which it occurs are also calculated. In addition, guidelines are calculated for each radionuclide entered by the user. These guidelines are soil concentration values at which the receptor will not receive a radiation dose in excess of a user-specified limit.

Leaching of radionuclides from the contaminated layer may be calculated by directly inputting the leach rate, by entering the contaminated zone distribution coefficients, by entering the groundwater concentrations and time since disposal, or by having the code calculate the leach rate by using the plant transfer factors. A one-dimensional (nondispersion) groundwater transport model incorporated into the RESRAD code is used to model the transport of radionuclides through a maximum of five unsaturated layers down to the saturated zone and into a residential well or pond. In calculating the groundwater concentrations, the code takes into account the retardation of radionuclide transport and ingrowth and decay during transport, as well as any change in the contaminated zone concentration from leaching and radioactive ingrowth and decay. The code takes progeny radionuclides into account and considers them to be transported independently of their parents.

---

[1] Note: The calculations reported here were performed prior to the release of Version 5.0 of RESRAD (Yu et al. 1993).

2.1.2 GENII-S Code

The GENII-S code (Leigh et al. 1992) is a comprehensive package of models that address routine and accidental releases of radionuclides to air or water, as well as residual contamination from spills or decommissioning operations. Both population and individual doses can be calculated. The addition of a sensitivity and uncertainty analysis shell enables the user to perform stochastic as well as deterministic runs. For this report, only that portion of the code involving deterministic calculation of chronic individual doses from residual contamination in soil was considered.

The code allows the user to model up to two layers of contaminated soil: surface and deep soil. Surface contamination is contained in the first 15 cm of soil. Deep soil contamination may be located at any depth below the first 15 cm. The code calculates doses to a hypothetical receptor from the following pathways and exposure routes: external gamma dose from radionuclides in soil and air; inhalation dose from contaminated dust; and ingestion dose from intake of contaminated soil, plants, meat, milk, fish, and water. The code output options include printing tabulations of doses by radionuclide, pathway, and organ.

The GENII-S code includes a surface-water flow model for calculating radionuclide concentrations in surface water, but it does not include a groundwater model. The user can still assess the water ingestion dose, however, by explicitly entering the radionuclide concentrations in water.

2.1.3 DECOM Code

The DECOM code (Till and Moore 1988) allows the user to calculate doses from radionuclides with different concentrations in multiple soil layers (in 15-cm increments). The code calculates doses to a hypothetical receptor from the following pathways and exposure routes: external gamma dose from radionuclides in soil; inhalation dose from contaminated dust; and ingestion dose from intake of contaminated plants, meat, milk, and water. The code output is presented as total dose from all pathways; contributions by individual radionuclides and pathways are expressed as percentages of the total dose.

The code can be operated in one of two modes. In mode 1, the user enters the relative mix of radionuclides at the site and specifies an allowable dose limit. The code calculates the maximum total concentration allowable in each contaminated soil layer so that the dose limit will not be exceeded. In mode 2, the user specifies the radionuclide concentrations in each layer. The code then calculates the total dose and the percent contribution from each radionuclide and pathway. In mode 2, the user can also specify a soil removal option; the code will then calculate the amount of soil that needs to be removed so that the receptor dose will remain below the allowable limit.

Dose and soil concentration limits can be calculated only for one user-determined point in time each time the code is run. The code performs leaching and decay calculations to estimate the depletion of radionuclides from the contaminated zone at times other than

125

time zero, except when calculating the groundwater transport pathway. The groundwater transport model used in DECOM considers dispersion but does not take into account the depletion of radionuclides in the contaminated zone over time from leaching and radioactive decay. Thus, the model will overestimate the radionuclide concentrations in groundwater, particularly for short-lived radionuclides. The code does not take into account progeny ingrowth and transport.

2.1.4 PRESTO-EPA-CPG Code

The PRESTO-EPA-CPG (or simply PRESTO) code (Hung 1989) is designed to estimate radiation doses to individuals and critical population groups over a 1,000-year period from disposal of low-level radioactive waste. On-site doses resulting from farming and intrusion and off-site doses from exposure to contaminated air, surface water, and groundwater are considered. The code calculates doses to hypothetical individual receptors, both on-site and off-site, for the following pathways and exposure routes: external gamma dose from radionuclides in soil, water, and air; inhalation dose from contaminated dust; and ingestion dose from intake of contaminated plants, meat, milk, and water.

Data are input to PRESTO by creation or modification of two FORTRAN input files. Dose factors for external gamma radiation, inhalation, and ingestion are contained in another file that can be modified by the user. The default dose factors used by PRESTO are relatively old (1980) and are different from those used in RESRAD.

Code output options include printing doses by radionuclide, pathway, and organ. Doses summed by radionuclide and organ are provided for each user-specified time period. Dose contributions are itemized by pathway, radionuclide, and organ only for the time at which the maximum dose occurs. Separate doses are itemized for water ingestion and food ingestion; however, the separate contributions from the various food ingestion pathways are not itemized.

The PRESTO groundwater model considers dispersion of the contaminants during transport through the unsaturated zone and the aquifer. The user can select either a point source model or an area model. The area model, which divides the contaminated zone into nine point sources for calculational purposes, is recommended for the on-site well scenario (Section 2.2). The code does not take into account the ingrowth and transport of progeny radionuclides.

2.1.5 NUREG/CR-5512 Methodology

The methodology described in NUREG/CR-5512 (Kennedy and Strenge 1992) incorporates a set of generic screening models to calculate radiation doses received by an individual from residual contamination in buildings and soil, as well as from potential groundwater contamination. The methodology encompasses building occupancy and renovation scenarios and a residential scenario.

126

For the residential scenario, the contaminants are limited to the top 15 cm of soil. The potential pathways and exposure routes considered in NUREG/CR-5512 are external gamma dose from radionuclides in soil; inhalation dose from contaminated dust; and ingestion dose from intake of contaminated soil, plants, meat, milk, fish, and water.

Equations for each pathway and default parameter values are provided in the NUREG/CR-5512 document. Because the methodology has not been codified, the user must perform the calculations by hand. For these benchmarking efforts, the results of the NUREG/CR-5512 methodology were obtained by setting up the equations for each pathway on an electronic spreadsheet. Some of the equations are quite complex and require the user to calculate the time-integrated decay factor for each radionuclide over the exposure year. For the agricultural pathways, parameters such as growing times, harvest times, and holdup times are also required as input to the calculations. For long-lived radionuclides, these details add very little to the accuracy of the calculations. In such cases, the user can conservatively assume that no loss due to radioactive decay occurs during the year of exposure.

In the NUREG/CR-5512 methodology, a three-box model is used to calculate the transport of radionuclides in groundwater. The first box represents the contaminated zone, the second box the unsaturated zone, and the third box the aquifer. A leaching model is used to calculate contaminant movement from the first box to the second and then to the third. Contaminant removal and accumulation mechanisms include decay and ingrowth in all three boxes and water extraction in the third. To simplify calculations, the following conservative assumptions were made: groundwater flow in the unsaturated and saturated zones is not considered, no contaminant retardation occurs in the aquifer, and no dilution occurs with inflowing uncontaminated aquifer water.

2.2 SCENARIO DESCRIPTION

The default residential-farmer scenario in RESRAD was used as the starting point for the benchmark analysis. The pathways considered in that scenario are external gamma radiation from contaminated soil; inhalation of contaminated dust; and ingestion of contaminated water, soil, and food products. The radon (and progeny) inhalation pathway was not included because of all the models compared, RESRAD is the only one that considers the radon pathway. The assumptions made for this scenario were as follows:

- The contaminated zone covers an area of 10,000 m^2.
- The contaminated zone is 15 cm thick and has no cover (a special case was run, for the external pathway only, with a 1-m-thick contaminated zone and a 15-cm-thick cover).
- External gamma indoor exposure rates are 70% of outdoor levels.
- Mass loading of dust for the inhalation pathway is 0.2 mg/m^3.

127

- The inhalation rate is 8,520 m^3/yr.
- The soil ingestion rate is 36.5 g/yr.
- Indoor levels of dust are 40% of the outdoor levels.
- The fraction of soil ingested indoors that originates from outdoor soil is 40%.
- The resident spends 25% of the time outdoors on-site, 50% indoors on-site, and 25% off-site.
- The resident consumes 160 kg/yr of fruits, vegetables, and grains; 14 kg/yr of leafy vegetables; 63 kg/yr of meat; 92 L/yr of milk; and 510 L/yr of water.
- Fifty percent of the vegetables and all of the meat and milk consumed by the resident are produced on-site. (RESRAD uses an area factor to account for the fraction of grazing area that is contaminated; for a 10,000-m^2 area, a factor of 0.5 is applied by RESRAD to reduce the ingestion doses for meat and milk.)
- All the water consumed by the resident is drawn from an on-site well screened 10 m into the aquifer (10 m is also assumed to be the thickness of the aquifer in the other models that require this parameter).
- The unsaturated zone is 4 m thick.
- The exponential "b" parameter used by RESRAD to calculate the saturation ratio is assumed to be 5.3, resulting in an average moisture content in the contaminated and unsaturated zones of 0.3 mL/cm^3.
- Soil density, total porosity, and effective porosity in all soil layers are 1.6 g/cm^3, 0.4, and 0.2, respectively.
- The saturated hydraulic conductivity is 10 m/yr in the contaminated zone and 100 m/yr in both the unsaturated zone and the aquifer.
- The hydraulic gradient in the aquifer is 0.02, resulting in a groundwater velocity of 2 m/yr.
- Rainfall and irrigation rates are 1 and 0.2 m/yr, respectively, while the runoff and evapotranspiration coefficients are 0.2 and 0.6, respectively, resulting in a net infiltration rate of 0.4 m/yr.
- The distribution coefficients and biotic-transfer factors used are the RESRAD default values for each radionuclide.

- Seven representative radionuclides (including alpha, beta, and gamma emitters) were selected for the benchmark analyses. Soil concentrations of 1 pCi/g each of Co-60, Sr-90, I-129, Cs-137, U-234, U-238, and Pu-239 were assumed for all five models. When applicable, the short-lived progeny (half-life <6 months) were entered either explicitly or implicitly. The resulting doses take into account the contributions of progeny radionuclides. In DECOM, the dose from I-129 was not calculated because this radionuclide is not included in its database.

- To investigate the effects of radionuclide ingrowth, a special case was run entering a unit concentration of Pu-241, which decays to Am-241. Because of limitations in the other models, a comparison was only possible between RESRAD and GENII-S.

To the extent possible, the parameter values in the default file RESRAD.DEF were not altered (with the exception of the contaminated zone and cover thicknesses), and the parameter values in the other models were modified to reflect the RESRAD default values. However, in some cases, the model against which RESRAD was being benchmarked did not allow the user to match the parameter value used by RESRAD. Such was the case for the erosion rate in PRESTO and the inhalation rate in GENII-S. In those instances, the default parameter values in RESRAD and the remaining models were changed to match these fixed values. In some cases, a particular model incorporated a parameter not used by RESRAD. In those cases, the default value of that parameter was not changed.

In the NUREG/CR-5512 methodology, the activity initially present in soil must be integrated to account for decay, thus producing a time-averaged activity over the assessment year. To simplify calculations, the time-integrated activity factor over the assessment year was assumed to be 365 pCi-d/g per pCi/g of activity initially present in soil for all radionuclides (i.e., no decay). For even the shortest-lived radionuclide, Co-60, the activity present after one year of decay is 88% of the activity present at the beginning of the year. Thus, this simplification changes the results by less than 10% for all radionuclides.

2.3 BENCHMARKING RESULTS — TIME ZERO

2.3.1 Introduction

In the following sections, each pathway selected for analysis is discussed separately, and the results from RESRAD are compared with those from each of the other models. The results are presented as the ratio of the dose calculated by RESRAD to the dose calculated using one of the other four models. In this section, doses are compared at time zero for all pathways except the water ingestion pathway. To compare how each model treats radionuclide decay, leaching, and groundwater transport, the doses from the dust inhalation (a representative water-independent pathway) and water ingestion pathways are compared for an elapsed time of 500 years in Section 2.4.

129

Annual dose contributions from water-independent external gamma, dust inhalation, soil ingestion, and food ingestion pathways were calculated for the first year. The water ingestion pathway is not a contributor to this initial dose because groundwater transport is assumed to start at time zero, with no prior groundwater contamination.

For the PRESTO code, the dose comparison is made for the second year because the external gamma pathway (referred to as the basement residence model in that code) cannot be activated during the first year. Because of the additional year of radioactive decay and leaching, the dose contributions calculated by PRESTO are slightly reduced from those calculated by RESRAD. However, the radionuclides considered have half-lives that are long compared to one year, so this limitation of the PRESTO code does not significantly affect the results.

2.3.2 External Gamma Pathway

The first series of benchmarking runs was performed for the external dose pathway. One case was run for radionuclides present in the top 15 cm of soil. To account for the effects of a cover material, a second case was run with a 1-m-thick contaminated zone covered by 15 cm of uncontaminated soil. The NUREG/CR-5512 model considers only contamination in the top 15 cm of soil; therefore, only results for the first case were calculated with that model.

The RESRAD default values for area of contamination and soil density (10,000 m^2 and 1.6 g/cm^3, respectively) were input in the first four models. The NUREG/CR-5512 methodology does not permit the user to adjust for area and density factors; instead, they are included by default in the dose factors used. Occupancy and shielding factors were adjusted to the RESRAD default value of 0.6, which was derived by assuming 25% outdoor occupancy, 50% indoor occupancy with 70% of outside gamma levels, and 25% off-site occupancy.

2.3.2.1 RESRAD vs. GENII-S

In GENII-S, the user has the option of considering a surface or a deep contaminated zone. In the first case, the surface zone (top 15 cm) was activated and the radionuclide concentrations were entered in units of pCi/kg. The soil density of this surface zone was changed from the default 225 to 240 kg/m^2, which is equivalent to a density of 1.6 g/cm^3 over a thickness of 15 cm. GENII-S does not have a provision for shielding during indoor occupancy. To obtain a value equivalent to the shielding and occupancy factor used by RESRAD, the exposure time to ground contamination in GENII-S was changed from the default value of 8,760 to 5,256 h/yr, or 60% of a full year.

The two codes were then compared by calculating the external dose in the presence of an uncontaminated cover. In GENII-S, a concentration of 1.6×10^6 pCi/m^3 was entered for each radionuclide in the deep contaminated zone. This value is equivalent to a concentration of 1.0 pCi/g in soil with a density of 1.6 g/cm^3. The presence of a 15-cm uncontaminated surface layer was assumed.

As shown in Table 1, the results in the first case (surface soil contamination) indicate that the external doses calculated by RESRAD tend to be higher (by factors in the range of 1.5 to 4.4) than those for GENII-S. Exceptions are I-129, a factor of 2.6 lower, and U-238, for which RESRAD calculates a dose that is 94 times lower. In the case of deep soil contamination, RESRAD calculates doses ranging from 1.9 to 49,000 times higher than those calculated by GENII-S (except for the U-238 dose, which is 50 times smaller).

2.3.2.2 RESRAD vs. DECOM

In the RESRAD code, the depth of the contaminated zone was set to 15 cm, and all pathways except the external radiation pathway were suppressed. In DECOM, the surface soil depth was set to 15 cm, and the soil density was set to 240 kg/m^2 (1.6 g/cm^3) for a surface area of 10,000 m^2. In DECOM, the percentage of time spent on-site was changed from 100% to 60% to simulate the RESRAD default value of 0.6 for the shielding and occupancy factor.

The two codes were then compared by considering the external dose in the presence of an uncontaminated cover. All of the above parameters were kept the same, except that a 15-cm cover was added on top of a 1-m-thick contaminated zone. The DECOM code only

TABLE 1 Comparison of External Dose Calculations, RESRAD vs. GENII-S (time zero)

	Doses (mrem/yr)		
Radionuclide	GENII-S	RESRAD	Dose Ratio, RESRAD/GENII-S
Surface soil			
Co-60	7.5	1.1×10^{1}	1.5
Sr-90	1.9×10^{-2}	0.0	NC[a]
I-129	5.3×10^{-3}	2.0×10^{-3}	3.8×10^{-1}
Cs-137	1.8	2.7	1.5
U-234	1.8×10^{-4}	8.0×10^{-4}	4.4
U-238	6.2	6.6×10^{-2}	1.1×10^{-2}
Pu-239	1.3×10^{-4}	4.3×10^{-4}	3.3
Deep soil			
Co-60	1.4	2.6	1.9
Sr-90	1.4×10^{-3}	0.0	NC
I-129	2.0×10^{-9}	9.8×10^{-5}	4.9×10^{4}
Cs-137	1.9×10^{-1}	4.2×10^{-1}	2.2
U-234	9.9×10^{-7}	2.1×10^{-5}	2.1×10^{1}
U-238	5.5×10^{-1}	1.1×10^{-2}	2.0×10^{-2}
Pu-239	1.2×10^{-6}	8.8×10^{-6}	7.3

[a] NC = not calculated.

131

allows for the input of concentrations in 15-cm layers. Thus, the doses calculated by DECOM were based on one uncontaminated 15-cm layer plus seven contaminated soil layers between 15 and 120 cm. Table 2 compares the results for surface soil and deep soil doses.

Because Sr-90 and its decay product Y-90 are pure beta-emitters, no external gamma dose conversion factors are available for Sr-90. DECOM does not include a Pu-239 gamma dose conversion factor in its database.

In both cases, RESRAD calculates a dose for Co-60 and Cs-137 that is within a factor of 2 higher than the dose calculated by DECOM. For the uranium isotopes, a much greater discrepancy occurs; DECOM calculates significantly higher doses than RESRAD. In fact, the U-234 dose calculated by DECOM is three to four times higher than the Cs-137 dose. These large discrepancies may result from erroneous dose-factor values used by DECOM to calculate external doses from the uranium isotopes. Also, RESRAD uses a volumetric dose conversion factor for a contaminated slab of infinite thickness; this factor is corrected for the actual thickness of the contaminated layer and shielding by an uncontaminated layer. DECOM uses surface dose factors distributed over 5-cm intervals to simulate a volume source.

2.3.2.3 RESRAD vs. PRESTO

With PRESTO, the user can consider a surface and/or a deep contaminated zone by changing the thickness of the trench overburden and the depth of the trench. For the surface contamination case, a 15-cm-deep trench with no overburden and a total inventory of

TABLE 2 Comparison of External Dose Calculations, RESRAD vs. DECOM (time zero)

Radionuclide	Doses (mrem/yr) DECOM	Doses (mrem/yr) RESRAD	Dose Ratio, RESRAD/DECOM
Surface soil			
Co-60	7.3	1.1×10^{1}	1.5
Sr-90	0.0	0.0	NC[a]
Cs-137	1.8	2.7	1.5
U-234	4.7	8.0×10^{-4}	1.7×10^{-4}
U-238	2.1×10^{1}	6.6×10^{-2}	3.1×10^{-3}
Pu-239	0.0	4.3×10^{-4}	NC
Deep soil			
Co-60	1.6	2.6	1.6
Sr-90	0.0	0.0	NC
Cs-137	2.4×10^{-1}	4.2×10^{-1}	1.8
U-234	9.7×10^{-1}	2.1×10^{-5}	2.2×10^{-5}
U-238	4.2	1.1×10^{-2}	2.6×10^{-3}
Pu-239	0.0	8.8×10^{-6}	NC

[a] NC = not calculated.

132

2.4×10^{-3} Ci for each radionuclide were entered. The external gamma pathway can only be activated by assuming that the resident lives in a basement for part of the year. As mentioned earlier, this pathway can be activated only at one year after time zero. To obtain a value equivalent to the shielding and occupancy factor used by RESRAD, the factor in PRESTO characterizing the intensity and duration of gamma exposure from the basement scenario was set to 0.6. For the deep contaminated soil case, a trench depth of 1.15 m with a 15-cm overburden thickness and an inventory of 1.6×10^{-2} Ci per radionuclide were entered. Table 3 compares the results for the two codes.

In both cases, PRESTO calculates a dose from U-238 that is significantly lower than the dose calculated by RESRAD; this may be due in part to failure of PRESTO to account for the ingrowth of short-lived U-238 progeny. The Co-60 and Cs-137 doses are also somewhat lower in the PRESTO calculations for the surface soil case (and deep soil case for Co-60). For all other radionuclides, the doses calculated by PRESTO are higher than those from RESRAD by up to a factor of 190. The doses calculated by PRESTO are not significantly lower in the deep soil case when compared with the surface soil case. In addition, it is not clear why the I-129 dose is zero for the surface soil case but non-zero in the deep soil case.

TABLE 3 Comparison of External Dose Calculations, RESRAD vs. PRESTO (time zero)

Radionuclide	Doses (mrem/yr)		Dose Ratio, RESRAD/PRESTO
	PRESTO	RESRAD	
Surface soil			
Co-60	2.7	1.1×10^{1}	4.1
Sr-90	0.0	0.0	NC[a]
I-129	0.0	2.0×10^{-3}	NC
Cs-137	8.0×10^{-1}	2.7	3.4
U-234	8.4×10^{-4}	8.0×10^{-4}	9.5×10^{-1}
U-238	6.7×10^{-4}	6.6×10^{-2}	9.9×10^{1}
Pu-239	4.4×10^{-4}	4.3×10^{-4}	9.8×10^{-1}
Deep soil			
Co-60	2.3	2.6	1.1
Sr-90	0.0	0.0	NC
I-129	1.9×10^{-2}	9.8×10^{-5}	5.2×10^{-3}
Cs-137	6.8×10^{-1}	4.2×10^{-1}	6.2×10^{-1}
U-234	8.1×10^{-4}	2.1×10^{-5}	2.6×10^{-2}
U-238	6.4×10^{-4}	1.1×10^{-2}	1.7×10^{1}
Pu-239	3.8×10^{-4}	8.8×10^{-6}	2.3×10^{-2}

[a] NC = not calculated.

2.3.2.4 RESRAD vs. NUREG/CR-5512

The equation in NUREG/CR-5512 that is used to calculate external exposure (Equation 5.69) requires the user to input the number of days during the assessment year spent gardening, outdoors on-site, and indoors on-site. The NUREG/CR-5512 default values of 4.17 days gardening, 71.83 days outdoors, and 200 days indoors were changed to 0, 91.25, and 182.5 days, respectively, to obtain the same occupancy factors used by RESRAD. The shielding factor for indoor occupancy was changed from the NUREG/CR-5512 default of 0.33 to the RESRAD default of 0.7. The dose factors for external radiation exposure were obtained from Table E.2 of the report after converting from units of Sv/d per Bq/m^3 to units of mrem/h per pCi/g. Table 4 shows the results for the surface soil case. The deep soil case is not compared because the NUREG/CR-5512 methodology only simulates a 15-cm soil layer.

With the exception of I-129 and U-238, the doses calculated by RESRAD are higher than those from NUREG/CR-5512 by factors ranging from 1.3 to 3.3. The I-129 and U-238 doses calculated by RESRAD are approximately 0.25 and 0.5, respectively, of the dose calculated with the NUREG/CR-5512 methodology.

2.3.2.5 Summary of the External Gamma Pathway

Table 5 summarizes the external gamma pathway doses at time zero that were calculated by using each of the five models.

For high energy gamma emitters in soil (Co-60 and Cs-137), the calculated doses are within a factor of 5 for all models; RESRAD calculated the highest doses in all cases except the deep soil dose from Cs-137 calculated by PRESTO.

TABLE 4 Comparison of External Dose Calculations (surface soil only), RESRAD vs. NUREG/CR-5512 (time zero)

	Doses (mrem/yr)		
Radionuclide	NUREG	RESRAD	Dose Ratio, RESRAD/NUREG
Co-60	8.7	1.1×10^{1}	1.3
Sr-90	0.0	0.0	NC[a]
I-129	7.9×10^{-3}	2.0×10^{-3}	2.5×10^{-1}
Cs-137	1.9	2.7	1.4
U-234	2.4×10^{-4}	8.0×10^{-4}	3.3
U-238	1.3×10^{-1}	6.6×10^{-2}	5.3×10^{-1}
Pu-239	1.7×10^{-4}	4.3×10^{-4}	2.5

[a] NC = not calculated.

TABLE 5 Comparison of External Dose Calculations, All Models (time zero)

	Doses (mrem/yr)				
Radionuclide	RESRAD	GENII-S	DECOM	PRESTO	NUREG
Surface soil					
Co-60	1.1×10^{1}	7.5	7.3	2.7	8.7
Sr-90	0.0	1.9×10^{-2}	0.0	0.0	0.0
I-129	2.0×10^{-3}	5.3×10^{-3}	NC[a]	0.0	7.9×10^{-3}
Cs-137	2.7	1.8	1.8	8.0×10^{-1}	1.9
U-234	8.0×10^{-4}	1.8×10^{-4}	4.7	8.4×10^{-4}	2.4×10^{-4}
U-238	6.6×10^{-2}	6.2	2.1×10^{1}	6.7×10^{-4}	1.3×10^{-1}
Pu-239	4.3×10^{-4}	1.3×10^{-4}	0.0	4.4×10^{-4}	1.7×10^{-4}
Deep soil					
Co-60	2.6	1.4	1.6	2.3	NC
Sr-90	0.0	1.4×10^{-3}	0.0	0.0	NC
I-129	9.8×10^{-5}	2.0×10^{-9}	NC	1.9×10^{-2}	NC
Cs-137	4.2×10^{-1}	1.9×10^{-1}	2.4×10^{-1}	6.8×10^{-1}	NC
U-234	2.1×10^{-5}	9.9×10^{-7}	9.7×10^{-1}	8.1×10^{-4}	NC
U-238	1.1×10^{-2}	5.5×10^{-1}	4.2	6.4×10^{-4}	NC
Pu-239	8.8×10^{-6}	1.2×10^{-6}	0.0	3.8×10^{-4}	NC

[a] NC = not calculated.

Only GENII-S calculated an external gamma dose from Sr-90. External dose calculations for I-129 varied significantly between models when surface soil and deep soil cases were compared. It is not clear why PRESTO calculated a zero dose from I-129 for the surface soil case but calculated a non-zero dose for the deep soil case; this is physically impossible. Also, GENII-S calculated an I-129 dose for the deep soil case that is more than six orders of magnitude lower than the surface soil case. This appears to be inconsistent with the calculations for U-234 and Pu-239, both of which had lower doses than I-129 in the surface soil case but higher doses in the deep soil case.

The doses calculated by DECOM for U-234 and U-238 were significantly higher than the doses calculated by all other models because of the high dose conversion factors assumed by DECOM for these two radionuclides. The PRESTO calculations for U-238 underestimated the external dose since they do not include the contributions from the short-lived progeny of U-238.

With the exception of DECOM, which assumes a zero external dose from Pu-239, all other models calculated Pu-239 doses within a factor of four in the surface soil case. In the deep soil case, however, PRESTO calculated a dose that is significantly higher than the dose calculated by RESRAD or GENII-S.

135

All models appear to account for the shielding properties of a clean surface soil layer (except PRESTO with I-129 and NUREG/CR-5512, which considers only surface soil) since the calculated doses are lower for the deep soil case than for the surface soil case. However, the relative attenuation factors vary (in some cases, significantly) between models.

2.3.3 Dust Inhalation Pathway

The second series of benchmarking runs was performed for the dust inhalation dose pathway from radionuclides present in the top 15 cm of soil. In the RESRAD, GENII-S, DECOM, and PRESTO models, all pathways except the dust inhalation pathway were suppressed. Equation 5.70 in NUREG/CR-5512 was used to calculate the dose from the inhalation pathway.

The RESRAD default value for mass loading of dust in air (2×10^{-4} g/m^3) was entered in the four other models. The RESRAD code is the only model that considers the size of the contaminated area when adjusting doses; however, the area factor for inhalation calculated by RESRAD is very close to one (0.97) for an area of 10,000 m^2 and will not significantly affect the results. Because the inhalation rate in GENII-S is fixed at 270 mL/s (8,520 m^3/yr), the inhalation rates in RESRAD, DECOM, PRESTO, and NUREG/CR-5512 were adjusted to this value. Occupancy and shielding factors were adjusted to the RESRAD default value of 0.45, which was derived by assuming 25% outdoor occupancy, 50% indoor occupancy with 40% of dust originating from contaminated soil, and 25% off-site occupancy.

2.3.3.1 RESRAD vs. GENII-S

To adjust for the occupancy and shielding factor used by RESRAD, the inhalation exposure time in GENII-S was reduced from the default value of 8,760 to 3,942 h/yr. As mentioned previously, the inhalation rate in RESRAD was adjusted from the default value of 8,400 to 8,520 m^3/yr. Table 6 compares the inhalation doses obtained by using the two codes.

RESRAD calculated a higher inhalation dose for all radionuclides except Co-60. The doses calculated by GENII-S and RESRAD agree within a factor of two, with the exception of Sr-90 (RESRAD calculated a dose that is seven times higher). These discrepancies may be attributed to differences in the dose factor method used by GENII-S to calculate the committed effective dose equivalent.

2.3.3.2 RESRAD vs. DECOM

The DECOM default mass loading factor for dust (7×10^{-5} g/m^3) was changed to 2×10^{-4} g/m^3. To account for the RESRAD default occupancy and shielding factor of 0.45, the parameter in DECOM for percentage of time on-site was changed from the default value of 100% to 45%. The DECOM default inhalation rate of 8,300 m^3/yr was increased to 8,520 m^3/yr. Table 7 lists the inhalation doses obtained by using the two codes.

TABLE 6 Comparison of Dust Inhalation Dose Calculations, RESRAD vs. GENII-S (time zero)

Radionuclide	Doses (mrem/yr) GENII-S	Doses (mrem/yr) RESRAD	Dose Ratio, RESRAD/GENII-S
Co-60	1.4×10^{-4}	1.1×10^{-4}	7.9×10^{-1}
Sr-90	1.4×10^{-4}	9.7×10^{-4}	6.9
I-129	1.1×10^{-4}	1.3×10^{-4}	1.2
Cs-137	2.1×10^{-5}	2.4×10^{-5}	1.1
U-234	9.3×10^{-2}	9.7×10^{-2}	1.0
U-238	8.3×10^{-2}	8.9×10^{-2}	1.1
Pu-239	2.1×10^{-1}	3.8×10^{-1}	1.8

TABLE 7 Comparison of Dust Inhalation Dose Calculations, RESRAD vs. DECOM (time zero)

Radionuclide	Doses (mrem/yr) DECOM	Doses (mrem/yr) RESRAD	Dose Ratio, RESRAD/DECOM
Co-60	1.1×10^{-4}	1.1×10^{-4}	1.0
Sr-90	1.0×10^{-3}	9.7×10^{-4}	9.7×10^{-1}
Cs-137	2.5×10^{-5}	2.4×10^{-5}	9.6×10^{-1}
U-234	8.5×10^{-2}	9.7×10^{-2}	1.1
U-238	9.2×10^{-2}	8.9×10^{-2}	9.7×10^{-1}
Pu-239	3.9×10^{-1}	3.8×10^{-1}	9.7×10^{-1}

The RESRAD and DECOM results for the dust inhalation pathway were in excellent agreement. The area factor used accounts for the slightly lower doses calculated by RESRAD.

2.3.3.3 RESRAD vs. PRESTO

The default PRESTO scenario does not consider the on-site inhalation pathway. To activate this pathway, the mass loading for dust inhalation was changed in the PRESTO default file from 0.0 to 2×10^{-4} g/m^3, and the fraction of year that the on-site resident is exposed to dust was changed from 0.0 to 0.45. The PRESTO inhalation rate was changed from the default value of 8,035 to 8,520 m^3/yr. Table 8 lists the inhalation doses obtained by using the two codes.

The inhalation doses for Co-60, I-129, and the uranium isotopes calculated with the PRESTO code were higher than those calculated with RESRAD by factors ranging from 1.5 to 3.3. The Sr-90 and Pu-239 doses calculated by RESRAD were 1.3 and 6.5 times higher, respectively. The use of different dose factors may account for this variability.

137

TABLE 8 Comparison of Dust Inhalation Dose Calculations, RESRAD vs. PRESTO (time zero)

Radionuclide	Doses (mrem/yr) PRESTO	RESRAD	Dose Ratio, RESRAD/PRESTO
Co-60	2.9×10^{-4}	1.1×10^{-4}	3.8×10^{-1}
Sr-90	1.5×10^{-4}	9.7×10^{-4}	6.5
I-129	4.4×10^{-4}	1.3×10^{-4}	3.0×10^{-1}
Cs-137	2.3×10^{-5}	2.4×10^{-5}	1.0
U-234	1.5×10^{-1}	9.7×10^{-2}	6.5×10^{-1}
U-238	1.3×10^{-1}	8.9×10^{-2}	6.8×10^{-1}
Pu-239	2.9×10^{-1}	3.8×10^{-1}	1.3

2.3.3.4 RESRAD vs. NUREG/CR-5512

As in the case for external exposure, the equation used in NUREG/CR-5512 to calculate inhalation doses (Equation 5.70) requires the user to input the number of days during the assessment year spent gardening and the number of days spent on-site, both indoors and outdoors. The NUREG/CR-5512 default values of 4.17 days gardening, 71.83 days outdoors, and 200 days indoors were changed to 0, 91.25, and 182.5 days, respectively, to obtain the same occupancy factors used by RESRAD. In Equation 5.70, different mass loading factors are used for outdoor and indoor occupancy. For outdoor occupancy, this factor was changed from the default 1×10^{-4} g/m^3 to 2×10^{-4} g/m^3. The default indoor mass loading factor is calculated as 5×10^{-5} g/m^3, plus a resuspension factor of 0.4/m times a surface dust loading of 5×10^{-5} g/m^2, totaling 7×10^{-5} g/m^3. This indoor default was changed to 8×10^{-5} g/m^3, which is equal to the RESRAD assumption that indoor dust levels are 40% of outdoor levels. The dose factors for inhalation were obtained from Table E.2 of the NUREG/CR-5512 report after converting from units of Sv/Bq to units of mrem/pCi.

Table 9 lists the inhalation doses obtained by using the two codes. For all radionuclides, the doses calculated by the two codes were equal within a factor of 1.5.

2.3.3.5 Summary of the Inhalation Pathway

Table 10 summarizes the inhalation pathway doses at time zero calculated by using each of the five models.

With few exceptions, dust inhalation doses calculated by all models were within a factor of 2 for all radionuclides. Both GENII-S and PRESTO calculated Sr-90 doses that were an order of magnitude lower than Sr-90 doses calculated by the other models. The I-129 dose calculated by PRESTO was a factor of 3 higher than the dose calculated by the other models. These discrepancies are due in large part to differences in the dose factors used by each code.

TABLE 9 Comparison of Dust Inhalation Dose Calculations, RESRAD vs. NUREG/CR-5512 (time zero)

Radionuclide	Doses (mrem/yr) NUREG	Doses (mrem/yr) RESRAD	Dose Ratio, RESRAD/NUREG
Co-60	1.7×10^{-4}	1.1×10^{-4}	6.6×10^{-1}
Sr-90	1.0×10^{-3}	9.7×10^{-4}	9.7×10^{-1}
I-129	1.3×10^{-4}	1.3×10^{-4}	1.0
Cs-137	2.4×10^{-5}	2.4×10^{-5}	1.0
U-234	1.0×10^{-1}	9.7×10^{-2}	9.6×10^{-1}
U-238	9.1×10^{-2}	8.9×10^{-2}	9.8×10^{-1}
Pu-239	3.3×10^{-1}	3.8×10^{-1}	1.2

TABLE 10 Comparison of Dust Inhalation Dose Calculations, All Models (time zero)

Radionuclide	Doses (mrem/yr) RESRAD	GENII-S	DECOM	PRESTO	NUREG
Co-60	1.1×10^{-4}	1.4×10^{-4}	1.1×10^{-4}	2.9×10^{-4}	1.7×10^{-4}
Sr-90	9.7×10^{-4}	1.4×10^{-4}	1.0×10^{-3}	1.5×10^{-4}	1.0×10^{-3}
I-129	1.3×10^{-4}	1.1×10^{-4}	NC[a]	4.4×10^{-4}	1.3×10^{-4}
Cs-137	2.4×10^{-5}	2.1×10^{-5}	2.5×10^{-5}	2.3×10^{-5}	2.4×10^{-5}
U-234	9.7×10^{-2}	9.3×10^{-2}	8.5×10^{-2}	1.5×10^{-1}	1.0×10^{-1}
U-238	8.9×10^{-2}	8.3×10^{-2}	9.2×10^{-2}	1.3×10^{-1}	9.1×10^{-2}
Pu-239	3.8×10^{-1}	2.1×10^{-1}	3.9×10^{-1}	2.9×10^{-1}	3.3×10^{-1}

[a] NC = not calculated.

2.3.4 Soil Ingestion Pathway

The third series of benchmarking runs was performed for the soil ingestion dose pathway for radionuclides present in the top 15 cm of soil. Because the DECOM and PRESTO codes do not consider the soil ingestion pathway, RESRAD could not be compared with those codes.

The RESRAD default value for the annual ingestion rate of soil (36.5 g/yr) was used as the baseline ingestion rate in the other models. This baseline ingestion rate was adjusted to account for occupancy factors and dilution with uncontaminated materials. The RESRAD default adjustment value is 0.45, which was derived by assuming 25% outdoor occupancy, 50% indoor occupancy with 40% of ingested material originating from contaminated soil, and 25% off-site occupancy.

2.3.4.1 RESRAD vs. GENII-S

To adjust for the soil ingestion rate and the occupancy and dilution factors used by RESRAD, the soil ingestion rate in GENII-S was reduced from the default value of 410 to 45 mg/d. Table 11 compares the soil ingestion doses obtained with the two codes.

RESRAD calculated a higher ingestion dose for all cases. The doses calculated by GENII-S and RESRAD agreed within a factor of 1.2 to 2.9, with the exception of the uranium isotopes and Pu-239 (RESRAD calculated doses that were more than 10 times higher). These discrepancies may be attributed to differences in the dose factor method used by GENII-S to calculate the committed effective dose equivalent, as well as the less conservative dose factors for uranium and plutonium used by GENII-S.

2.3.4.2 RESRAD vs. NUREG/CR-5512

Equation 5.73 in NUREG/CR-5512 was used to calculate the soil ingestion dose. This equation does not account for the fraction of soil or dust ingested that originates from uncontaminated sources. Therefore, the effective transfer rate for ingestion of soil was reduced from the default value of 5×10^{-2} to 4.5×10^{-2} g/d to be consistent with the occupancy and dilution factor used in RESRAD. The dose factors for ingestion were obtained from Table E.2 of the NUREG report after converting from units of Sv/Bq to units of mrem/pCi. Table 12 lists the soil ingestion doses obtained with the two codes. For all radionuclides, the doses calculated by the two models were the same within a factor of 1.2.

2.3.4.3 Summary of the Soil Ingestion Pathway

Table 13 summarizes the soil ingestion pathway doses at time zero calculated by using three of the five models.

TABLE 11 Comparison of Soil Ingestion Dose Calculations, RESRAD vs. GENII-S (time zero)

	Doses (mrem/yr)		
Radionuclide	GENII-S	RESRAD	Dose Ratio, RESRAD/GENII-S
Co-60	1.5×10^{-4}	4.3×10^{-4}	2.9
Sr-90	1.8×10^{-3}	2.3×10^{-3}	1.3
I-129	3.7×10^{-3}	4.6×10^{-3}	1.2
Cs-137	7.1×10^{-4}	8.2×10^{-4}	1.2
U-234	3.9×10^{-4}	4.3×10^{-3}	1.1×10^{1}
U-238	3.5×10^{-4}	4.1×10^{-3}	1.2×10^{1}
Pu-239	7.5×10^{-4}	7.1×10^{-2}	9.5×10^{1}

TABLE 12 Comparison of Soil Ingestion Dose Calculations, RESRAD vs. NUREG/CR-5512 (time zero)

Radionuclide	Doses (mrem/yr) NUREG	Doses (mrem/yr) RESRAD	Dose Ratio, RESRAD/NUREG
Co-60	4.4×10^{-4}	4.3×10^{-4}	9.7×10^{-1}
Sr-90	2.5×10^{-3}	2.3×10^{-3}	9.1×10^{-1}
I-129	4.5×10^{-3}	4.6×10^{-3}	1.0
Cs-137	8.2×10^{-4}	8.2×10^{-4}	1.0
U-234	4.7×10^{-3}	4.3×10^{-3}	9.2×10^{-1}
U-238	4.4×10^{-3}	4.1×10^{-3}	9.3×10^{-1}
Pu-239	5.8×10^{-2}	7.1×10^{-2}	1.2

TABLE 13 Comparison of Soil Ingestion Dose Calculations, All Models (time zero)

Radionuclide	Doses (mrem/yr) RESRAD	GENII-S	DECOM	PRESTO	NUREG
Co-60	4.3×10^{-4}	1.5×10^{-4}	NC[a]	NC	4.4×10^{-4}
Sr-90	2.3×10^{-3}	1.8×10^{-3}	NC	NC	2.5×10^{-3}
I-129	4.6×10^{-3}	3.7×10^{-3}	NC	NC	4.5×10^{-3}
Cs-137	8.2×10^{-4}	7.1×10^{-4}	NC	NC	8.2×10^{-4}
U-234	4.3×10^{-3}	3.9×10^{-4}	NC	NC	4.7×10^{-3}
U-238	4.1×10^{-3}	3.5×10^{-4}	NC	NC	4.4×10^{-3}
Pu-239	7.1×10^{-2}	7.5×10^{-4}	NC	NC	5.8×10^{-2}

[a] NC = not calculated.

A dose comparison for the soil ingestion pathway was possible for only three of the five models: RESRAD, GENII-S, and NUREG/CR-5512. Excellent agreement was obtained between RESRAD and NUREG/CR-5512, where doses from all radionuclides were within a factor of 1.2. The doses from U-234 and U-238 calculated by GENII-S were one order of magnitude lower, while the Pu-239 dose was two orders of magnitude lower. The doses calculated by GENII-S for the other radionuclide were in much better agreement with doses calculated by RESRAD and NUREG/CR-5512. The dose conversion factors used by GENII-S probably account for these differences.

2.3.5 Food Ingestion Pathways

The fourth series of benchmarking runs was performed for the food ingestion pathway for radionuclides present in the top 15 cm of soil. Ingestion doses were calculated

for the consumption of plants, meat, and milk produced on a contaminated site. In the RESRAD model, all pathways except the plant, meat, and milk pathway were suppressed. In GENII-S, these pathways are identified as terrestrial food and animal food ingestion pathways. In DECOM, the plant, meat, and milk pathways are all included within the food ingestion pathway. In PRESTO, the doses from the food ingestion pathways are summed. Several equations in Chapter 5.0 of NUREG/CR-5512 were used to calculate the dose from the food ingestion pathways.

The RESRAD default values for the annual ingestion rates of leafy vegetables (14 kg/yr); other vegetables, fruits, and grains (160 kg/yr); meat (63 kg/yr); and milk (92 L/yr) were used as the baseline consumption rates in the other models. The baseline rates are adjusted automatically in the RESRAD code to account for the fraction obtained off-site (50% of plant products) or the fraction raised on uncontaminated soil (50% of meat and milk products). In the other models, the fraction of contaminated food was adjusted either explicitly or by dividing the doses obtained by a factor of two.

The method for treatment of the food ingestion pathways by the various models ranges from use of relatively few parameters (DECOM) to use of a large number of parameters (GENII-S, PRESTO, and NUREG/CR-5512); RESRAD is between the two extremes. DECOM accounts for root uptake but not foliar deposition in the plant ingestion pathway, and fodder ingestion rates by cattle are incorporated directly into the transfer factors. GENII-S, PRESTO, and NUREG/CR-5512, however, include such parameters as plant growing times, food storage times before consumption, and fraction of animal feed that is fresh pasture. For long-lived radionuclides, the parameters that will have a more significant impact on the ingestion doses are the transfer factors, consumption rates, and dose factors.

2.3.5.1 RESRAD vs. GENII-S

Table 14 compares doses calculated by RESRAD and GENII-S for ingestion pathways. For calculation of the dose from ingestion of plants grown on contaminated soil, the default consumption rates in GENII-S were changed from 15 to 14 kg/yr for leafy vegetables. The GENII-S code allows the user to specify the consumption of other vegetables, fruits, and grains separately, with defaults of 140, 64, and 72 kg/yr, respectively. Because RESRAD uses a single consumption rate, the RESRAD default value of 160 kg/yr was allocated equally among these three plant types (53.3 kg/yr each). Also, because the RESRAD code assumes that 50% of plant products consumed are imported, the results obtained with the GENII-S code (which considers all products to be grown on-site) had to be divided by 2. The transfer factors for leafy vegetables, other vegetables, fruits, and grains included in GENII-S were changed to the single default value used by RESRAD for soil-to-plant transfer for each radionuclide. By dividing the RESRAD transfer factors by the moisture content in each plant type (from NUREG/CR-5512, Table 6.17), these transfer factors were converted from a wet-weight basis to the dry-weight basis used in GENII-S. In GENII-S, the fraction of roots in contaminated surface soil was set to 0.167 by taking the ratio of contaminated soil thickness (15 cm) to the RESRAD default root depth (90 cm).

TABLE 14 Comparison of Food Ingestion Dose Calculations, RESRAD vs. GENII-S (time zero)

Radionuclide	Doses (mrem/yr) GENII-S	Doses (mrem/yr) RESRAD	Dose Ratio, RESRAD/GENII-S
Plant ingestion			
Co-60	1.9×10^{-3}	3.6×10^{-3}	1.9
Sr-90	2.4×10^{-1}	4.1×10^{-1}	1.7
I-129	4.7×10^{-2}	8.3×10^{-2}	1.8
Cs-137	4.4×10^{-3}	1.5×10^{-3}	3.4×10^{-1}
U-234	6.5×10^{-4}	9.6×10^{-3}	1.5×10^{1}
U-238	6.8×10^{-4}	9.2×10^{-3}	1.4×10^{1}
Pu-239	2.1×10^{-4}	1.8×10^{-2}	8.9×10^{1}
Meat ingestion			
Co-60	4.7×10^{-5}	8.9×10^{-5}	1.9
Sr-90	2.7×10^{-3}	3.0×10^{-3}	1.1
I-129	3.6×10^{-2}	4.3×10^{-2}	1.2
Cs-137	1.5×10^{-3}	1.2×10^{-3}	8.0×10^{-1}
U-234	1.6×10^{-4}	1.2×10^{-3}	8.0
U-238	2.2×10^{-4}	1.2×10^{-3}	5.4
Pu-239	1.1×10^{-4}	3.2×10^{-3}	3.0×10^{1}
Milk ingestion			
Co-60	2.8×10^{-5}	5.2×10^{-5}	1.9
Sr-90	1.5×10^{-2}	1.8×10^{-2}	1.2
I-129	2.1×10^{-2}	2.6×10^{-2}	1.2
Cs-137	2.6×10^{-4}	2.3×10^{-4}	8.8×10^{-1}
U-234	2.1×10^{-5}	1.8×10^{-4}	8.6
U-238	1.9×10^{-5}	1.7×10^{-4}	8.7
Pu-239	5.0×10^{-10}	1.9×10^{-8}	3.8×10^{1}

As shown in Table 14, for all radionuclides except Cs-137, doses calculated by RESRAD were higher by factors ranging from 1.8 to 89. The Cs-137 dose was three times lower. The ratios calculated for the plant pathway for each radionuclide were very close to the ratios calculated for the soil ingestion pathway for the same radionuclides. This similarity indicates that dose factor differences account for most of the discrepancies between the two models.

To calculate the dose from ingestion of meat, the default value for beef consumption in GENII-S was changed from 70 to 63 kg/yr. The consumption rate for poultry and eggs in GENII-S was set to 0. The fraction of feed from fresh pasture was set to 1.0 (i.e., no stored feed). In GENII-S, the code's default values for plant-to-meat transfer factors were replaced with RESRAD default values. The GENII-S code does not allow the user to specify the cattle's intake rate of fodder; it is not clear how this value differs from the RESRAD default value. Because RESRAD assumes that an area of at least 20,000 m^2 is needed to raise cattle,

an area factor of 0.5 is automatically calculated by the code. Therefore, the meat ingestion doses calculated by GENII-S were divided by 2 to obtain the doses listed in Table 14.

For all radionuclides except Cs-137, the doses calculated by RESRAD were higher by factors of 1.1 to 30. The Cs-137 dose was 20% lower. As was the case for the plant ingestion pathway, much of the discrepancy between the two models can be attributed to dose factor differences.

To calculate the dose from ingestion of milk, the default value for milk consumption in GENII-S was changed from 230 to 92 L/yr. The fraction of feed from fresh pasture was set at 1.0. Because RESRAD assumes an area factor of 0.5, the milk ingestion doses calculated by GENII-S were divided by 2 to obtain the doses listed in Table 14. For all radionuclides except Cs-137, the doses calculated by RESRAD were higher than the GENII-S doses by factors ranging from 1.2 to 38. The Cs-137 dose was slightly lower.

2.3.5.2 RESRAD vs. DECOM

Table 15 compares ingestion dose results computed by RESRAD and DECOM. To calculate the dose from ingestion of plants grown on contaminated soil, the default consumption rates in DECOM were changed from 18 to 14 kg/yr for leafy vegetables and from 176 to 160 kg/yr for other vegetables, fruits, and grains. The soil-to-plant transfer factors were changed to the RESRAD defaults. Because the RESRAD code assumes that 50% of the plant products consumed are imported, the percentage of leafy vegetables and produce grown on-site was changed from the DECOM default of 100% to 50%.

In all cases, except for U-234 and Pu-239, the plant ingestion doses obtained with RESRAD were about 5 times lower than the DECOM doses. The RESRAD-calculated U-234 and Pu-239 doses were approximately 2 times higher than those calculated by DECOM (Table 15).

To calculate the dose from ingestion of meat, the default value for meat consumption in DECOM was changed from 94 to 63 kg/yr. For DECOM, the percentage of meat produced on-site was changed from the default value of 100% to 50% to account for the area factor applied by RESRAD. The transfer factor used by DECOM for pasture feed was converted to the required dry-weight basis by dividing the RESRAD default soil-to-plant transfer factor (wet-weight basis) by 0.22 to account for the moisture content in pasture grass. This value is the same one recommended in NUREG/CR-5512 to convert from dry-weight to wet-weight transfer factors. The DECOM code also uses soil-to-meat transfer factors that account for the ingestion of soil by animals, a subpathway not considered by RESRAD Version 4.6. The DECOM code also includes another parameter not used by RESRAD Version 4.6 — the quantity of soil ingested by a cow.[2] The DECOM default value for this parameter

[2] Ingestion of soil by animals is considered in Version 5.0 of RESRAD (Yu et al. 1993).

TABLE 15 Comparison of Food Ingestion Dose Calculations, RESRAD vs. DECOM (time zero)

Radionuclide	Doses (mrem/yr) DECOM	Doses (mrem/yr) RESRAD	Dose Ratio, RESRAD/DECOM
Plant ingestion			
Co-60	2.0×10^{-2}	3.6×10^{-3}	1.8×10^{-1}
Sr-90	2.1	4.1×10^{-1}	1.9×10^{-1}
Cs-137	8.2×10^{-3}	1.5×10^{-3}	1.8×10^{-1}
U-234	5.2×10^{-3}	9.6×10^{-3}	1.9
U-238	4.7×10^{-2}	9.2×10^{-3}	2.0×10^{-1}
Pu-239	8.8×10^{-3}	1.8×10^{-2}	2.1
Meat ingestion			
Co-60	8.9×10^{-3}	8.9×10^{-5}	1.0×10^{-2}
Sr-90	5.0×10^{-2}	3.0×10^{-3}	6.0×10^{-2}
Cs-137	1.8×10^{-1}	1.2×10^{-3}	6.6×10^{-3}
U-234	8.2×10^{-5}	1.2×10^{-3}	1.5×10^{1}
U-238	7.5×10^{-4}	1.2×10^{-3}	1.5
Pu-239	1.4×10^{-6}	3.2×10^{-3}	2.2×10^{3}
Milk ingestion			
Co-60	1.3×10^{-3}	5.2×10^{-5}	4.0×10^{-2}
Sr-90	3.6×10^{-1}	1.8×10^{-2}	4.9×10^{-2}
Cs-137	9.0×10^{-2}	2.3×10^{-4}	2.5×10^{-3}
U-234	3.6×10^{-4}	1.8×10^{-4}	4.9×10^{-1}
U-238	3.3×10^{-3}	1.7×10^{-4}	5.1×10^{-2}
Pu-239	4.2×10^{-7}	1.9×10^{-8}	4.5×10^{-2}

(500 g/d) and the soil-to-meat transfer factors were left unchanged. The DECOM code does not allow the user to specify the cattle's intake rate of fodder; it is not clear how this value differs from the RESRAD default value.

As shown in Table 15, for Co-60, Sr-90, and Cs-137, the doses obtained with RESRAD were lower than the DECOM doses by factors ranging from 16 to 150. For the uranium isotopes and Pu-239, the doses calculated by RESRAD were 1.5 to 2,200 times higher than the DECOM doses. Differences in the transfer factor methods used, rather than dose factor differences, account for most of the differences in the results.

To calculate the dose from ingestion of milk, the default value for milk consumption in DECOM was changed from 112 to 92 L/yr. The percentage of milk produced on-site was changed from the default value of 100% to 50% to account for the area factor applied by RESRAD. Similar issues regarding parameters used by DECOM to calculate the meat ingestion dose were encountered with the milk ingestion pathway; as with the meat ingestion pathway, DECOM default soil-to-meat transfer factors and soil ingestion rates were not

145

changed. For all radionuclides, the doses obtained by using RESRAD were lower than the DECOM doses by factors ranging from 2 to 400 (Table 15).

2.3.5.3 RESRAD vs. PRESTO

Table 16 compares ingestion doses calculated by RESRAD and PRESTO. To calculate the dose from ingestion of plants grown on contaminated soil, the default consumption rates in PRESTO were changed from 88.5 to 160 kg/yr for other vegetables, fruits, and grains (in both RESRAD and PRESTO, the default for leafy vegetable consumption is 14 kg/yr). Because the RESRAD code assumes that 50% of plant products consumed are imported, the results obtained with the PRESTO code were divided by 2. The soil-to-plant transfer factors for leafy vegetables and for other vegetables, fruits, and grains included in PRESTO were changed to the single default value used by RESRAD.

TABLE 16 Comparison of Food Ingestion Dose Calculations, RESRAD vs. PRESTO (time zero)

Radionuclide	Doses (mrem/yr) PRESTO	Doses (mrem/yr) RESRAD	Dose Ratio, RESRAD/PRESTO
Plant ingestion			
Co-60	1.9×10^{-4}	3.6×10^{-3}	1.8×10^{1}
Sr-90	3.1×10^{-3}	4.1×10^{-1}	1.3×10^{2}
I-129	4.2×10^{-3}	8.3×10^{-2}	2.0×10^{-1}
Cs-137	5.1×10^{-4}	1.5×10^{-3}	2.9
U-234	1.1×10^{-4}	9.6×10^{-3}	9.1×10^{1}
U-238	9.9×10^{-5}	9.2×10^{-3}	9.3×10^{1}
Pu-239	1.7×10^{-3}	1.8×10^{-2}	1.1×10^{1}
Meat ingestion			
Co-60	8.7×10^{-6}	8.9×10^{-5}	1.0×10^{1}
Sr-90	3.3×10^{-5}	3.0×10^{-3}	9.1×10^{1}
I-129	9.4×10^{-3}	4.3×10^{-2}	4.6
Cs-137	1.0×10^{-3}	1.2×10^{-3}	1.1
U-234	3.4×10^{-5}	1.2×10^{-3}	3.6×10^{1}
U-238	3.2×10^{-5}	1.2×10^{-3}	3.7×10^{1}
Pu-239	9.9×10^{-4}	3.2×10^{-3}	3.2
Milk ingestion			
Co-60	7.3×10^{-6}	5.2×10^{-5}	7.2
Sr-90	3.1×10^{-4}	1.8×10^{-2}	5.7×10^{1}
I-129	5.8×10^{-3}	2.6×10^{-2}	4.4
Cs-137	2.4×10^{-4}	2.3×10^{-4}	9.4×10^{-1}
U-234	5.9×10^{-6}	1.8×10^{-4}	3.0×10^{1}
U-238	5.6×10^{-6}	1.7×10^{-4}	3.0×10^{1}
Pu-239	6.2×10^{-9}	1.9×10^{-8}	3.0

As shown in Table 16, for all radionuclides, RESRAD calculated higher plant ingestion doses than PRESTO by factors ranging from 2.9 to 130.

To calculate the meat ingestion dose, the default value for beef consumption in PRESTO was changed from 62.8 to 63 kg/yr, and the fraction of feed from fresh pasture was set to 1.0 (i.e., no stored feed). RESRAD default values for plant-to-meat transfer factors were used. The cattle's intake rate of fodder was changed from the PRESTO default of 50 kg/d to the RESRAD default of 68 kg/d. As with the other codes, the meat ingestion doses calculated by PRESTO were divided by 2 to account for the area factor calculated by RESRAD. As with the plant ingestion pathway, RESRAD calculated higher doses than PRESTO by factors of 1.1 to 91 (Table 16).

Milk ingestion doses were calculated by changing the PRESTO default value for consumption of cow's milk from 89.4 to 92 L/yr. The ingestion rate of goat's milk was set to 0. The fraction of feed from fresh pasture was set to 1.0. Because RESRAD assumes an area factor of 0.5, the milk ingestion doses calculated by PRESTO were divided by 2 to obtain the doses listed in Table 16. RESRAD calculated higher doses for all radionuclides except Cs-137 (1.1 times lower). In all three ingestion pathways, the best agreement was obtained for Cs-137 doses, while the largest differences were for the Sr-90 doses.

2.3.5.4 RESRAD vs. NUREG/CR-5512

Table 17 compares ingestion doses from RESRAD and NUREG/CR-5512. Equation 5.5 in NUREG/CR-5512 was used to calculate the radionuclide concentrations in edible parts of plants. The results were entered in Equations 5.9, 5.10, 5.67, 5.71, and 5.72 of NUREG/CR-5512 to calculate the produce ingestion dose. The transfer factors for root uptake used in NUREG/CR-5512 require conversion from a dry-weight to a wet-weight basis. This conversion was not required when entering the RESRAD default transfer factors because they are already based on wet weight. The mass loading transfer factor (referred to as the foliar deposition model in RESRAD) used by NUREG/CR-5512 was set to 0.1 for leafy vegetables and 0.01 for all other vegetables, fruits, and grains after reviewing the values reported in Table 6.9 of NUREG/CR-5512. Because of the long half-life of all radionuclides used in this report, all factors involving radiological decay functions were set to 0 decay over one year to simplify the calculations. The annual ingestion rate of leafy vegetables listed in Table 6.15 of NUREG/CR-5512 (11 kg/yr) was replaced with the RESRAD default of 14 kg/yr. The values reported in the same table for other vegetables, fruits, and grains are 51, 46, and 69 kg/yr, respectively; the total of 166 kg/yr was replaced with the RESRAD default of 160 kg/yr (apportioned equally among the three produce categories). The dose factors for ingestion were obtained from Table E.2 of the NUREG report after converting from units of Sv/Bq to units of mrem/pCi. The diet fraction parameter was set to 0.5 to account for the fraction of produce grown on-site.

The doses calculated by NUREG/CR-5512 were 6.3 to 100 times higher than those calculated by RESRAD (Table 17). Differences in the foliar deposition model may account for these discrepancies.

TABLE 17 Comparison of Food Ingestion Dose Calculations, RESRAD vs. NUREG/CR-5512 (time zero)

Radionuclide	Doses (mrem/yr) NUREG	Doses (mrem/yr) RESRAD	Dose Ratio, RESRAD/NUREG
Plant ingestion			
Co-60	3.5×10^{-2}	3.6×10^{-3}	1.0×10^{-1}
Sr-90	2.6	4.1×10^{-1}	1.6×10^{-1}
I-129	6.2×10^{-1}	8.3×10^{-2}	1.3×10^{-1}
Cs-137	3.4×10^{-2}	1.5×10^{-3}	4.4×10^{-2}
U-234	2.0×10^{-1}	9.6×10^{-3}	4.7×10^{-2}
U-238	1.9×10^{-1}	9.2×10^{-3}	4.8×10^{-2}
Pu-239	1.8	1.8×10^{-2}	9.9×10^{-3}
Meat ingestion			
Co-60	1.7×10^{-3}	8.9×10^{-5}	5.3×10^{-2}
Sr-90	2.3×10^{-2}	3.0×10^{-3}	1.3×10^{-1}
I-129	4.7×10^{-1}	4.3×10^{-2}	9.2×10^{-2}
Cs-137	7.0×10^{-2}	1.2×10^{-3}	1.7×10^{-2}
U-234	6.8×10^{-2}	1.2×10^{-3}	1.8×10^{-2}
U-238	6.4×10^{-2}	1.2×10^{-3}	1.9×10^{-2}
Pu-239	7.6×10^{-1}	3.2×10^{-3}	4.2×10^{-3}
Milk ingestion			
Co-60	1.0×10^{-3}	5.2×10^{-5}	5.1×10^{-2}
Sr-90	1.2×10^{-1}	1.8×10^{-2}	1.5×10^{-1}
I-129	2.9×10^{-1}	2.6×10^{-2}	9.0×10^{-2}
Cs-137	1.4×10^{-2}	2.3×10^{-4}	1.6×10^{-2}
U-234	1.0×10^{-2}	1.8×10^{-4}	1.7×10^{-2}
U-238	9.0×10^{-3}	1.7×10^{-4}	1.9×10^{-2}
Pu-239	4.7×10^{-6}	1.9×10^{-8}	4.0×10^{-3}

Equations 5.15, 5.18, 5.19, 5.20, 5.67, 5.71, and 5.72 in NUREG/CR-5512 were used to calculate the concentrations in meat and the meat ingestion dose. As with the plant ingestion pathway, transfer factors for root uptake used in NUREG/CR-5512 for fodder require conversion from a dry-weight basis to a wet-weight basis. No conversion was required when entering the RESRAD default transfer factors. The mass loading transfer factor used by NUREG/CR-5512 was set to 0.07 for pasture grasses after reviewing the values reported in Table 6.9. The consumption rate of fresh forage listed in Table 6.23 of NUREG/CR-5512 for beef cattle was changed from 27 kg/d to the RESRAD default of 68 kg/d. As in the DECOM code, the NUREG/CR-5512 methodology includes the transfer of contaminants from soil to meat as the result of ingestion of soil by cattle during foraging. The parameter in NUREG/CR-5512 for this process is the fraction of forage intake that is made up of contaminated soil. The default value for this parameter is listed as 0.02 in Table 6.23 of NUREG/CR-5512. The fraction of pasture forage eaten by a cow that is grown on uncontaminated soil was set to 0.5. All factors involving radiological decay functions were

set to 0 decay over one year to simplify the calculations. The annual ingestion rates of beef and poultry listed in Table 6.15 of NUREG/CR-5512 total 68 kg/yr; this was replaced with the RESRAD default of 63 kg/yr. The dose factors for ingestion were obtained from Table E.2 of the report after converting from units of Sv/Bq to units of mrem/pCi.

As shown in Table 17, the doses calculated with NUREG/CR-5512 are 7.6 to 240 times higher than those calculated by RESRAD. These differences may result in large part from model differences, including the foliar deposition transfer model and the direct soil-to-cow transfer model.

The equations used to calculate the milk ingestion dose in NUREG/CR-5512 are the same as those used for the meat ingestion pathway. The only differences are the plant-to-milk transfer factors and the fodder and milk consumption rates. RESRAD default values were used for the transfer factors. The fodder ingestion rate for milk cattle was changed from 36 kg/d (Table 6.23 in NUREG/CR-5512) to the RESRAD default value of 55 kg/d. The milk consumption rate was changed from 100 L/yr (Table 6.15 in NUREG/CR-5512) to the RESRAD default value of 92 L/yr. All other parameters were the same as for the meat ingestion pathway.

The doses calculated with NUREG/CR-5512 were 6.7 to 250 times higher than doses calculated by RESRAD (Table 17). These differences are similar in magnitude when compared to ratios calculated for the meat ingestion doses.

2.3.5.5 Summary of the Food Ingestion Pathways

Table 18 summarizes the inhalation pathway doses at time zero calculated by using each of the five models.

For all radionuclides in the plant ingestion pathway, the doses calculated by using the NUREG/CR-5512 methodology were consistently higher than the doses calculated by all other models. The PRESTO code calculated the lowest plant ingestion doses for all radionuclides except Pu-239 (GENII-S calculated a lower dose). The difference between the highest and lowest calculated dose exceeded two orders of magnitude for most radionuclides but approached four orders of magnitude for Pu-239.

For the meat ingestion pathway, the highest doses calculated by using the NUREG/CR-5512 methodology were the highest doses calculated from the actinides; DECOM calculated the highest dose from the fission and activation products. As with the plant ingestion pathway, PRESTO calculated the lowest doses for all radionuclides except Pu-239 (in this case, DECOM calculated a lower dose). A large range of variability occurred between high and low doses, ranging from less than two orders of magnitude for I-129 to greater than five orders of magnitude for Pu-239.

TABLE 18 Comparison of Food Ingestion Dose Calculations, All Models (time zero)

	Doses (mrem/yr)				
Radionuclide	RESRAD	GENII-S	DECOM	PRESTO	NUREG
Plant ingestion					
Co-60	3.6×10^{-3}	1.9×10^{-3}	2.0×10^{-2}	1.9×10^{-4}	3.5×10^{-2}
Sr-90	4.1×10^{-1}	2.4×10^{-1}	2.1	3.1×10^{-3}	2.6
I-129	8.3×10^{-2}	4.7×10^{-2}	NC[a]	4.2×10^{-3}	6.2×10^{-1}
Cs-137	1.5×10^{-3}	4.4×10^{-3}	8.2×10^{-3}	5.1×10^{-4}	3.4×10^{-2}
U-234	9.6×10^{-3}	6.5×10^{-4}	5.2×10^{-3}	1.1×10^{-4}	2.0×10^{-1}
U-238	9.2×10^{-3}	6.8×10^{-4}	4.7×10^{-2}	9.9×10^{-5}	1.9×10^{-1}
Pu-239	1.8×10^{-2}	2.1×10^{-4}	8.8×10^{-3}	1.7×10^{-3}	1.8
Meat ingestion					
Co-60	8.9×10^{-5}	4.7×10^{-5}	8.9×10^{-3}	8.7×10^{-6}	1.7×10^{-3}
Sr-90	3.0×10^{-3}	2.7×10^{-3}	5.0×10^{-2}	3.3×10^{-5}	2.3×10^{-2}
I-129	4.3×10^{-2}	3.6×10^{-2}	NC	9.4×10^{-3}	4.7×10^{-1}
Cs-137	1.2×10^{-3}	1.5×10^{-3}	1.8×10^{-1}	1.0×10^{-3}	7.0×10^{-2}
U-234	1.2×10^{-3}	1.6×10^{-4}	8.2×10^{-5}	3.4×10^{-5}	6.8×10^{-2}
U-238	1.2×10^{-3}	2.2×10^{-4}	7.5×10^{-4}	3.2×10^{-5}	6.4×10^{-2}
Pu-239	3.2×10^{-3}	1.1×10^{-4}	1.4×10^{-6}	9.9×10^{-4}	7.6×10^{-1}
Milk ingestion					
Co-60	5.2×10^{-5}	2.8×10^{-5}	1.3×10^{-3}	7.3×10^{-6}	1.0×10^{-3}
Sr-90	1.8×10^{-2}	1.5×10^{-2}	3.6×10^{-1}	3.1×10^{-4}	1.2×10^{-1}
I-129	2.6×10^{-2}	2.1×10^{-2}	NC	5.8×10^{-3}	2.9×10^{-1}
Cs-137	2.3×10^{-4}	2.6×10^{-4}	9.0×10^{-2}	2.4×10^{-4}	1.4×10^{-2}
U-234	1.8×10^{-4}	2.1×10^{-5}	3.6×10^{-4}	5.9×10^{-6}	1.0×10^{-2}
U-238	1.7×10^{-4}	1.9×10^{-5}	3.3×10^{-3}	5.6×10^{-6}	9.0×10^{-3}
Pu-239	1.9×10^{-8}	5.0×10^{-10}	4.2×10^{-7}	6.2×10^{-9}	4.7×10^{-6}

[a] NC = not calculated.

For the milk ingestion pathway, use of the NUREG/CR-5512 methodology once again resulted in the highest doses from the actinides; DECOM calculated the highest dose from the fission and activation products. While PRESTO still calculated the lowest doses for most radionuclides, RESRAD calculated the lowest dose for Cs-137 and GENII-S calculated the lowest dose for Pu-239. As in the previous two pathways, a large variability was found in the calculated doses, ranging from two to three orders of magnitude for all radionuclides except Pu-239 (four orders of magnitude).

Such a large variability in the food ingestion doses can be attributed primarily to differences in the mathematical formulae used by each code to model these pathways. Some additional variability is due to differences in the dose factors, as was the case for the soil ingestion pathway.

150

2.4 BENCHMARKING RESULTS — AFTER 500 YEARS

Additional runs were performed for the point in time 500 years after time zero to investigate the effect of time on the calculated doses. Of the five models being used, only RESRAD and PRESTO calculate doses at more than one time over a user-selected time interval. PRESTO limits the user to a 1,000-year interval; the RESRAD default is 10,000 years. In GENII-S and DECOM, only one time can be calculated per run. For water-independent pathways, NUREG/CR-5512 does not explicitly indicate how doses at future times are to be calculated; for the groundwater pathway, the user is instructed to iterate the model once per year until a maximum dose is reached. Because of these considerations, a complete set of comparisons between RESRAD and the other five models could not be performed.

2.4.1 Dust Inhalation Pathway

To determine the effects of time on dose, the dust inhalation pathway was selected as representative of the water-independent pathways. All parameters that affect the leach rate from the 15-cm contaminated zone (including soil properties, meteorological parameters, and distribution coefficients) were set to the RESRAD defaults. One exception was the erosion rate, which was calculated with the PRESTO default file as 0.0002 m/yr. This value was used in the RESRAD run (the other three models do not account for erosion over time). The infiltration rate calculated by RESRAD is 0.4 m/yr (precipitation plus irrigation corrected for runoff and evapotranspiration). GENII-S requires the user to enter leach rates in the transfer factor library. Leach rates were obtained from the values calculated by RESRAD on the basis of default distribution coefficients, soil density and porosity, saturation ratio, and infiltration rate. All other parameters applicable to time zero calculations (inhalation rates, mass loading, area dimensions, and occupancy and shielding factors) were not changed.

2.4.1.1 RESRAD vs. GENII-S

Table 19 compares the dust inhalation doses calculated by GENII-S and RESRAD after 500 years. For both codes, the dose from Co-60 and I-129 is effectively 0, primarily because of the radioactive decay of Co-60 and leaching of I-129. GENII-S calculated a Sr-90 dose that was five orders of magnitude higher than the RESRAD dose. However, RESRAD calculated doses from all other radionuclides that were five to nine orders of magnitude higher than GENII-S doses. The reason for such large differences is not clear. The much larger differences in the U-234 values could be due in part to the ingrowth of U-234 decay products. This ingrowth is accounted for by RESRAD but not by GENII-S. These U-234 progeny have much higher default distribution coefficients than uranium and are retained in the contaminated zone.

151

TABLE 19 Comparison of Dust Inhalation Dose Calculations, RESRAD vs. GENII-S (500 years)

Radionuclide	Doses (mrem/yr) GENII-S	RESRAD	Dose Ratio, RESRAD/GENII-S
Co-60	1.3×10^{-39}	0.0	NC[a]
Sr-90	2.0×10^{-16}	2.0×10^{-21}	1.0×10^{-5}
I-129	0.0	0.0	NC
Cs-137	9.0×10^{-17}	3.5×10^{-11}	3.9×10^{5}
U-234	6.4×10^{-15}	2.1×10^{-5}	3.4×10^{9}
U-238	5.7×10^{-15}	3.6×10^{-9}	6.3×10^{5}
Pu-239	1.4×10^{-7}	8.2×10^{-2}	5.9×10^{5}

[a] NC = not calculated.

2.4.1.2 RESRAD vs. DECOM

Table 20 compares the dust inhalation doses calculated by DECOM after 500 years with those calculated by RESRAD.

In both cases, the Co-60 and Sr-90 doses were essentially 0. DECOM calculated a higher dose for all other radionuclides except U-234. This difference is due in part to the erosion of 67% of the contaminated zone over 500 years, a factor not taken into account in the DECOM code. Once again, the U-234 dose calculated by RESRAD was higher because of decay product ingrowth.

2.4.1.3 RESRAD vs. PRESTO

Table 21 shows the dust inhalation doses calculated by PRESTO for after 500 years. The I-129 dose calculated by PRESTO was the same as the inhalation dose calculated at time zero, despite the very low distribution coefficient (resulting in a high leach rate) and the erosion of the contaminated zone, both factors accounted for in PRESTO. The reason for this situation is not clear, but it could be related to vertical migration assumptions incorporated into PRESTO for wastes buried in disposal trenches. PRESTO calculated a zero dose for Co-60, Sr-90, and the uranium isotopes. The doses calculated by the two codes for Cs-137 and Pu-239 were the same within a factor of 3.

2.4.1.4 RESRAD vs. NUREG/CR-5512

No explicit formula for the calculation of future dust inhalation doses is provided in NUREG/CR-5512. For sake of comparison, Table 22 shows the doses by NUREG/CR-5512 at time zero corrected only for radioactive decay. In all cases, the NUREG/CR-5512 doses

TABLE 20 Comparison of Dust Inhalation Dose Calculations, RESRAD vs. DECOM (500 years)

Radionuclide	Doses (mrem/yr)		Dose Ratio, RESRAD/DECOM
	DECOM	RESRAD	
Co-60	0.0	0.0	NC[a]
Sr-90	0.0	2.0×10^{-21}	NC
Cs-137	1.1×10^{-10}	3.5×10^{-11}	3.2×10^{-1}
U-234	5.2×10^{-9}	2.1×10^{-5}	4.0×10^{3}
U-238	5.7×10^{-9}	3.6×10^{-9}	6.3×10^{-1}
Pu-239	2.5×10^{-1}	8.2×10^{-2}	3.3×10^{-1}

[a] NC = not calculated.

TABLE 21 Comparison of Dust Inhalation Dose Calculations, RESRAD vs. PRESTO (500 years)

Radionuclide	Doses (mrem/yr)		Dose Ratio, RESRAD/PRESTO
	PRESTO	RESRAD	
Co-60	0.0	0.0	NC[a]
Sr-90	0.0	2.0×10^{-21}	NC
I-129	4.4×10^{-4}	0.0	NC
Cs-137	1.1×10^{-11}	3.5×10^{-11}	3.2
U-234	0.0	2.1×10^{-5}	NC
U-238	0.0	3.6×10^{-9}	NC
Pu-239	1.1×10^{-1}	8.2×10^{-2}	7.5×10^{-1}

[a] NC = not calculated.

TABLE 22 Comparison of Dust Inhalation Dose Calculations, RESRAD vs. NUREG/CR-5512 (500 years)

Radionuclide	Doses (mrem/yr)		Dose Ratio, RESRAD/NUREG
	NUREG	RESRAD	
Co-60	3.9×10^{-33}	0.0	NC[a]
Sr-90	6.5×10^{-9}	2.0×10^{-21}	3.1×10^{-13}
I-129	1.3×10^{-4}	0.0	NC
Cs-137	2.5×10^{-10}	3.5×10^{-11}	1.4×10^{-1}
U-234	1.0×10^{-1}	2.1×10^{-5}	2.1×10^{-4}
U-238	9.1×10^{-2}	3.6×10^{-9}	4.0×10^{-8}
Pu-239	3.3×10^{-1}	8.2×10^{-2}	2.5×10^{-1}

[a] NC = not calculated.

153

were higher. The best agreement was obtained for radionuclides with the lowest default leach rates (Cs-137 and Pu-239). For these nuclides, the differences are due to the erosion of the contaminated zone as calculated by RESRAD.

2.4.1.5 Summary of the Inhalation Pathway after 500 Years

Table 23 summarizes the inhalation pathway doses after 500 years calculated by using each of the five models.

While large differences were generally found between models, some agreement was obtained in a few cases. Of the non-zero doses, the best agreement was found between RESRAD, DECOM, PRESTO, and NUREG/CR-5512 for Cs-137 and Pu-239; the calculated doses fall within a factor of 20. The Cs-137 and Pu-239 doses calculated by GENII-S were five orders of magnitude smaller.

2.4.2 Water Ingestion Pathway

The default scenario in RESRAD assumes that the on-site resident ingests 510 L/yr of water drawn from a well located at the downgradient edge of the contaminated zone. The RESRAD water ingestion doses could be compared only with DECOM and PRESTO. GENII-S does not have a groundwater transport pathway; ingestion doses are calculated following direct user input of groundwater radionuclide concentrations. The NUREG/CR-5512 calculations for the groundwater pathway are not easily performed by hand because they require iterations representing many years to obtain the maximum dose. The methodology uses first order leaching and decay rate equations to calculate radionuclide movement between compartments, but no groundwater transport or dispersion model is used. Because no groundwater movement is considered, the aquifer is assumed to be contaminated in the

TABLE 23 Comparison of Dust Inhalation Dose Calculations, All Models (500 years)

	Doses (mrem/yr)				
Radionuclide	RESRAD	GENII-S	DECOM	PRESTO	NUREG
Co-60	0.0	1.3×10^{-39}	0.0	0.0	3.9×10^{-33}
Sr-90	2.0×10^{-21}	2.0×10^{-16}	0.0	0.0	6.5×10^{-9}
I-129	0.0	0.0	NC[a]	4.4×10^{-4}	1.3×10^{-4}
Cs-137	3.5×10^{-11}	9.0×10^{-17}	1.1×10^{-10}	1.1×10^{-11}	2.5×10^{-10}
U-234	2.1×10^{-5}	6.4×10^{-15}	5.2×10^{-9}	0.0	1.0×10^{-1}
U-238	3.6×10^{-9}	5.7×10^{-15}	5.7×10^{-9}	0.0	9.1×10^{-2}
Pu-239	8.2×10^{-2}	1.4×10^{-7}	2.5×10^{-1}	1.1×10^{-1}	3.3×10^{-1}

[a] NC = not calculated.

first year following the release. The model also assumes that the dilution volume is the larger of the volume of water percolating through the contaminated zone or the household usage volume. Therefore, the NUREG/CR-5512 methodology is expected to produce more conservative groundwater concentrations than RESRAD, especially for large area sources.

2.4.2.1 RESRAD vs. DECOM

The groundwater model used in DECOM assumes a steady-state release from the contaminated zone because of leaching and does not consider radioactive decay over time. Therefore, the groundwater ingestion doses calculated by DECOM will be independent of time. Because RESRAD accounts for the time dependency of the source, the maximum concentrations in groundwater of radionuclides with different decay constants, leach rates, and retardation coefficients will be reached at different times. DECOM considers the dispersion of contaminants; RESRAD uses a nondispersion model. The DECOM defaults for the longitudinal and transverse dispersivities were not changed (10 and 1 m, respectively). The infiltration rate was set to the value calculated by RESRAD (40 cm/yr). All distribution coefficients were set to the RESRAD defaults. The volumetric water fraction in the contaminated zone in DECOM was set to the average value (0.3) calculated by RESRAD for the contaminated and unsaturated zones. The groundwater seepage velocity was set to 6.3×10^{-8} m/s, which corresponds to the groundwater velocity calculated by RESRAD for a hydraulic gradient of 0.02 and a hydraulic conductivity of 100 m/yr. The aquifer depth in DECOM was set to 10 m, the RESRAD default depth of the well in the aquifer. The fraction of water consumed that is drawn from the well was set to 100% for both codes. Results of the two runs are compared in Table 24. As expected from the difference in the code approaches, the groundwater ingestion doses calculated by DECOM were one to six orders of magnitude higher than the doses calculated by RESRAD after 500 years.

TABLE 24 Comparison of Water Ingestion Dose Calculations, RESRAD vs. DECOM (500 years)

Radionuclide	Doses (mrem/yr)		Dose Ratio, RESRAD/DECOM
	DECOM	RESRAD	
Co-60	5.6×10^{-5}	0.0	NC[a]
Sr-90	1.3×10^{-1}	1.5×10^{-4}	1.2×10^{-3}
Cs-137	2.6×10^{-4}	0.0	NC
U-234	4.9×10^{-1}	7.4×10^{-2}	1.5×10^{-1}
U-238	4.7	7.2×10^{-2}	1.5×10^{-2}
Pu-239	1.8×10^{-2}	4.3×10^{-8}	2.4×10^{-6}

[a] NC = not calculated.

2.4.2.2 RESRAD vs. PRESTO

The PRESTO groundwater model assumes that the contaminated zone is divided into nine equivalent point sources. The contaminant leach rate from these point sources is a function of the infiltration rate and distribution coefficients, both of which were set equal to the RESRAD defaults for this comparison. For the transport of contaminants in groundwater, all soil and hydrogeological parameters were set equal to the RESRAD defaults. Because PRESTO takes into consideration the dispersion of contaminants during groundwater transport, while RESRAD does not, PRESTO defaults for dispersivity were used (0.3 m in both the unsaturated zone and the aquifer). To estimate dilution in the aquifer, the PRESTO default plume dispersion angle was used (0.3 radians). The aquifer was assumed to be 10-m thick, and the well was assumed to be located 50 m from the center of the site (assuming the site was 100 m × 100 m).

A zero dose was calculated by PRESTO for all radionuclides after 500 years. During the 1,000-year interval allowed in PRESTO, the only radionuclide contributing to a non-zero dose was Sr-90, which would reach a maximum concentration in water after 577 years. No clear explanation can be given for the zero groundwater dose from I-129 between time zero and 500 years; this situation is unusual since the I-129 dose should reach a peak before Sr-90 because of the lower distribution coefficient (0.1 mL/g for I-129 compared with 30 mL/g for Sr-90). By trial-and-error, it was determined that a minimum distribution coefficient of 5 mL/g was required for PRESTO to calculate a groundwater ingestion dose. However, inspection of the annual doses for the 1,000-year period indicated a uniform cycle of periods of elevated water ingestion doses with intervening periods of zero dose. Increasing the distribution coefficient has the effect of decreasing the number of cycles. The reason for this behavior could not be ascertained, but may be related to the method used by PRESTO to simulate an area source (i.e., nine equivalent point sources).

2.5 RADIONUCLIDE DECAY AND INGROWTH — RESRAD vs. GENII-S

The ingrowth of radioactive progeny from an initially present parent radionuclide can result in higher doses than would be contributed by the parent alone. To investigate how the other models account for ingrowth of progeny, a comparison was made using the Pu-241/Am-241 decay chain. This pair was selected because the short half-life of Pu-241 (14.4 yr) relative to Am-241 (432.2 yr) results in a rapid decay of the parent, leaving only the progeny behind. This test was possible only between RESRAD and GENII-S. Neither DECOM or PRESTO consider progeny ingrowth, and NUREG/CR-5512 considers only the dose from ingrowth during the first year of exposure.

A relatively simple pathway, the inhalation of contaminated dust, was selected. With the exception of the inhalation rate, which is fixed in GENII-S (see Section 2.3.3), and the erosion rate (set to zero in RESRAD), the parameter values used by RESRAD were the defaults for the residential farmer scenario. With the exception of the inhalation dose factors, the parameter values used in GENII-S to calculate inhalation doses were the same as those used by RESRAD. A concentration of 1 pCi/g of Pu-241 (1,000 pCi/kg in GENII-S) was

entered in the top 15 cm of soil. The leach rates for Pu-241 and Am-241 were calculated by RESRAD to be 8.3×10^{-4} and 8.3×10^{-2} per year, respectively. These values were entered in the FTRANS.DAT file in GENII-S. Because the default americium leach rate is two orders of magnitude higher than the plutonium leach rate, the americium is not retained in the surface soil as strongly as the plutonium. The calculated doses should reflect the competing effects of ingrowth and the leaching of Am-241.

Considering the radionuclide half-lives and leach rates, a 100-year time horizon was sufficient to encompass the peak dose from ingrowth of Am-241. In RESRAD, the year in which doses are calculated was set to 1, 2, 5, 10, 20, 50, and 100 years. Because GENII-S allows the user to calculate doses only at one user-specified year, multiple runs were executed by changing the inventory disposal time for each run.

Table 25 lists the time-dependent inhalation doses calculated by GENII-S and RESRAD and shows the contributions from parent (Pu-241) and progeny (Am-241) radionuclides.

The doses from Pu-241 calculated by RESRAD were approximately 2.2 times higher than the Pu-241 doses calculated by GENII-S. The doses from Am-241 calculated by RESRAD were approximately 1.3 times higher than the Am-241 doses calculated by GENII-S. For both radionuclides, this ratio remains constant over the time span considered. Despite the higher leach rate, the dose from Am-241 becomes the dominant contributor as the Pu-241 decays; when considering the total dose, the RESRAD/GENII-S ratio decreases from 2.2 at time zero to 1.3 after 100 years. In RESRAD, the peak inhalation dose occurs after 5 years; in GENII-S, the peak dose occurs after 10 years. This discrepancy is the result of differences in the dose ratios for each radionuclide as discussed previously. Because the dose ratios for the individual radionuclides remain constant over time, the discrepancy is primarily due to differences in the dose factors used in RESRAD and GENII-S. It appears that both models account for the effects of radionuclide decay, ingrowth, and leaching in a consistent manner.

TABLE 25 Comparison of Inhalation Doses due to Ingrowth of Am-241 from Pu-241, RESRAD vs. GENII-S

	Doses (mrem/yr)			
Year	Pu-241 GENII-S	Am-241 GENII-S	Pu-241 RESRAD	Am-241 RESRAD
0	3.4×10^{-3}	0.0	7.4×10^{-3}	0.0
1	3.3×10^{-3}	4.4×10^{-4}	7.1×10^{-3}	5.8×10^{-4}
2	3.1×10^{-3}	8.9×10^{-4}	6.8×10^{-3}	1.1×10^{-3}
5	2.7×10^{-3}	1.8×10^{-3}	5.8×10^{-3}	2.2×10^{-3}
10	2.1×10^{-3}	2.6×10^{-3}	4.6×10^{-3}	3.2×10^{-3}
20	1.3×10^{-3}	2.7×10^{-3}	2.8×10^{-3}	3.3×10^{-3}
50	3.0×10^{-4}	1.0×10^{-3}	6.4×10^{-4}	1.3×10^{-3}
100	2.6×10^{-5}	1.0×10^{-4}	5.5×10^{-5}	1.3×10^{-4}

157

2.6 CONCLUSIONS

Conclusions reached from the comparison of results presented in Tables 1 through 25 can be summarized as follows:

- For the external dose pathway, the best agreement with RESRAD results was obtained with the NUREG/CR-5512 methodology. The discrepancies with the other codes spanned several orders of magnitude for some radionuclides, particularly the low-energy gamma emitters.

- The results from the dust inhalation pathway agreed within less than a factor of 10 for all models; DECOM exhibited the closest agreement to RESRAD.

- Good agreement was found between the soil ingestion doses calculated by RESRAD and NUREG/CR-5512. The actinide ingestion doses calculated by RESRAD and GENII-S were in poor agreement.

- Results of the food ingestion pathway calculations indicated considerable variability among the various models, sometimes spanning two or more orders of magnitude.

- With the exception of U-234, the best agreement for the dust inhalation dose after 500 years was obtained between RESRAD and DECOM. Results from the other models spanned several orders of magnitude.

- Because of significantly different groundwater models, no agreement was found at 500 years among doses calculated by RESRAD, DECOM, and PRESTO.

- Other than modeling differences, some of the discrepancies were due to differences (and possible errors) in the dose factor libraries used. The possibility of errors in data entry or code errors and bugs cannot be excluded as potential causes for some of these discrepancies.

3 BENCHMARKING AGAINST GENII AND PATHRAE

This section summarizes a benchmarking effort to compare results from RESRAD with those of the PATHRAE and GENII computer codes. The results of PATHRAE and GENII were taken directly from a paper presented at the 1992 Waste Management Symposium (Seitz et al. 1992) in which the authors compared the PATHRAE and GENII computer codes.

3.1 MODEL DESCRIPTIONS

3.1.1 GENII

The GENII code (Napier et al. 1988) was the predecessor of the GENII-S code developed by Pacific Northwest Laboratory. The function of the GENII code is similar to that of GENII-S except it does not have the capability to perform uncertainty analysis for the input parameters. Section 2.1.2 summarizes the applications of the GENII-S code.

3.1.2 PATHRAE-EPA

The PATHRAE-EPA code (Rogers and Hung 1987) was designed to calculate average annual and maximum annual effective doses and cancer risks to an on-site critical population group and an off-site population at risk. Cancer risks are calculated from the effective dose equivalent and a constant risk/dose conversion factor. This approach is different from that used in RESRAD, which uses EPA slope factors to obtain lifetime excess cancer risks.

The approach used in PATHRAE is similar to that used in PRESTO. The scenarios by which radioactivity can reach humans are as follows: groundwater migration with discharge to a river or to a well; surface erosion of the cover material and waste and subsequent contamination of surface water; saturation of waste with subsequent overflows to a stream; ingestion of food grown on the contaminated site either with or without associated disturbance of the waste material; direct gamma exposure; inhalation of radioactive dust on-site and off-site; and inhalation of radon while inside a structure built on the waste site. Annual doses are obtained by performing food chain analyses for ingestion of produce, meat, milk, fish, and drinking water. Inhalation doses are obtained directly with an inhalation rate and a time fraction input parameter. Dispersion is considered in the transport of nuclides in the groundwater system. However, the ingrowth of progeny nuclides is considered only for three-member decay chains. When a decay chain includes more than three members, some of the progeny nuclides are represented by using identical transport parameters and by assuming that the chain member is in equilibrium with its parent.

Five input files with specific names and input parameters are required to run the PATHRAE code. The code generates a text output file that tabulates input summary and

calculational results, including concentrations in different environmental media and annual doses and risks at different time periods for individual radionuclides and pathways.

3.2 SCENARIO DESCRIPTION

In the paper by Seitz et al. (1992), an intruder scenario was assumed, and the calculational results for three exposure pathways — external gamma, dust inhalation, and plant food ingestion — were compared. Because the meat and milk pathways involve more complicated food chain analyses, the methodologies implemented in different computer codes to calculate annual doses vary considerably. Therefore, annual doses from these two pathways were not compared in the Seitz et al. (1992) paper. Because the intrusion scenario considered did not involve a groundwater contribution, leaching of contaminants from the waste site was not taken into account, and that feature of RESRAD was disabled for these comparisons. Table 26 lists the input parameters used for that comparison. An effort was made to maintain as much consistency as possible in the input data when using the RESRAD code. Table 27 lists the RESRAD input parameters (default values were used for the RESRAD parameters not listed in Table 27).

3.3 COMPARISON OF INPUT PARAMETERS

The soil concentration used in the RESRAD code was 1 pCi/g, versus 1 Ci/m^3 in the GENII and PATHRAE codes. With a soil density of 1.6 g/cm^3, the concentration of 1 Ci/m^3 converts to 625,000 pCi/g. Therefore, the doses calculated with the RESRAD code were

TABLE 26 Parameter Values Used in the GENII and PATHRAE Codes

Parameters	Values
Soil concentration	1 Ci/m^3
Soil density	1.6 g/cm^3
Exposure time	8,760 h/yr
Breathing rate	8,400 m^3/yr
Dust loading	5.53×10^{-8} kg/m^3
Time of dose occurrence	1 year after disposal
Leafy vegetable consumption	18 kg/yr
Produce consumption	176 kg/yr
Fraction of consumed food that is contaminated	25%
Dry-to-wet ratios	
Leafy vegetable	0.066 (PATHRAE)
Produce	0.187 (PATHRAE)
Internal dose conversion factors	GENII default values

TABLE 27. Parameter Values Used in the RESRAD Code

Parameters	Values
Soil concentration	1 pCi/g
Soil density	1.6 g/cm^3
Time fraction spent outdoors	1
Inhalation rate	8,400 m^3/yr
Mass loading factor for dust inhalation	5.53 × 10^{-5} g/m^3
Mass loading factor for foliar deposition	5.53 × 10^{-5} g/m^3
Time of dose occurrence	1 year after disposal
Leafy vegetable consumption	18 kg/yr
Vegetables, fruits, and grain consumption	176 kg/yr
Dose conversion factors	RESRAD default values
Thickness of contaminated zone[a]	0.15 m
Area of contaminated zone[a]	2,500 m^2
Thickness of cover material	0 m
Distribution coefficients, all zones	1 × 10^6 cm^3/g
Irrigation rate	1 × 10^{-4} m/yr
Precipitation rate	1 × 10^{-4} m/yr
Contaminated zone erosion rate	0 m/yr

[a] Data from Wood (1992).

multiplied by 625,000 so that they could be compared with those of PATHRAE and GENII. The exposure time of 8,760 h/yr listed in Table 26 corresponds to a value of 1 for the "time fraction spent outdoors" parameter in the RESRAD code. The dust loading of 5.53 × 10^{-8} kg/m^3 listed in Table 26 is equivalent to 5.53 × 10^{-5} g/m^3, after a conversion factor is applied. This value was used in the RESRAD code for the mass loading factors for both dust inhalation and foliar deposition. The produce consumption rate listed in Table 26 can be represented by the fruits, vegetables, and grain consumption rate parameter in the RESRAD code. Seitz et al. (1992) assumed that 25% of the consumed food was contaminated, (i.e., was from the contaminated site). The version of the RESRAD code used in this study has a built-in capability to automatically estimate the fraction of consumed food grown on-site. With a contaminated area of 2,500 m^2 (Wood 1992), the fraction estimated by RESRAD was 50%. Because that value was different from the 25% used in the other two codes, the RESRAD doses for the plant food ingestion pathway were divided by 2.

The food/soil transfer factors used in the RESRAD code are on the weight basis of dry soil and wet plant; therefore, the results do not have to be converted to account for the dry-to-wet plant food ratio. The soil/water distribution coefficients used in the RESRAD code for all radionuclides were set to 1,000,000 cm^3/g. Such a large value will suppress the influence of leaching from the waste. Furthermore, both the irrigation and precipitation rate

parameters were set to 0.0001 m/yr to reduce the magnitude of the water infiltration rate. These two selections result in an estimated leaching of 3.0×10^{-11} (1/yr), which is negligible in the dose calculation, and provide consistency in the simulated conditions between the RESRAD code and the GENII and PATHRAE codes. The contaminated zone erosion rate used in the RESRAD code was set to 0 since this input parameter was not mentioned in the Seitz et al. (1992) paper. Delay times between harvest and consumption were not considered in the version of the RESRAD code used in this study; however, because all of the radionuclides in the comparison have much longer half-lives than the possible delay times between harvest and consumption, the influence of the delay on the calculated doses should be insignificant. The default soil-to-plant transfer factors and dose conversion factors were used in the RESRAD calculation.

3.4 RESULTS AND DISCUSSION

Table 28 lists the radiation doses calculated by the three computer codes. Table 29 lists the relative doses after normalization with the ingestion dose of Sr-90 from GENII, that is, 2.4×10^5 mrem/yr. The relative doses predicted by GENII and PATHRAE are almost identical to those published by Seitz et al. (1992). In general, good agreement was obtained for the ingestion and inhalation pathways. The differences arise primarily from differences in the soil-to-plant transfer factors and the dose conversion factors. The excellent agreement between the GENII and PATHRAE codes may be explained by the intention to obtain results that agree within 10%, as mentioned in the Seitz et al. (1992) paper. To attain this goal, the primary inputs of the GENII and PATHRAE codes were set to identical values, and a number of secondary inputs for the two codes were also made consistent.

In Table 28, the major differences lie in the direct gamma doses. Implementation of different dose conversion factors and methodologies may explain these large inconsistencies. Theoretically, Co-60 (a gamma emitter) should impart a larger external dose than Sr-90 (both Sr-90 and its decay product Y-90 are beta emitters); however, GENII predicts a Sr-90 dose greater than the Co-60 dose. PATHRAE predicts little difference in the external doses for Co-60 and Sr-90. Significant differences in the doses from these two radionuclides can only be observed from the RESRAD results. Another gamma emitter, Cs-137, was estimated to give external doses of 4.2×10^4 and 1.0×10^5 mrem/yr by GENII and PATHRAE, respectively. Both of the numbers are greater than the doses estimated by the two codes for Co-60. Cobalt-60 has a stronger penetration capability than Cs-137. This situation is consistent with the prediction by RESRAD, which yields a Co-60 dose that is approximately 4 times higher than the Cs-137 dose. The relatively closer magnitudes of 1.0×10^7 and 2.7×10^6 for Co-60 and Cs-137 reported by RESRAD versus differences of four to five orders in the GENII and PATHRAE results suggests that the Co-60 dose estimated by RESRAD is more reasonable. Furthermore, examination of the external doses discussed in Section 2.3.2 shows that the GENII-S results were close to the RESRAD results for both Co-60 and Cs-137. This suggests that the results presented in Seitz et al. (1992) for external

TABLE 28 Comparison of RESRAD Results with GENII and PATHRAE Code Results[a]

Radionuclide	Doses (mrem/yr)			Dose Ratios	
	GENII	PATHRAE	RESRAD	RESRAD/ GENII	RESRAD/ PATHRAE
Plant ingestion[b]					
Sr-90	2.4×10^5	2.2×10^5	1.4×10^5	5.8×10^{-1}	6.4×10^{-1}
Tc-99	2.1×10^4	2.1×10^4	1.6×10^3	7.6×10^{-2}	7.6×10^{-1}
I-129	6.9×10^4	7.2×10^4	2.9×10^4	4.2×10^{-1}	4.0×10^{-1}
Cs-137	8.0×10^3	7.8×10^3	4.9×10^2	6.1×10^{-2}	6.3×10^{-2}
Pu-239	1.4×10^3	1.4×10^3	5.9×10^3	4.2	4.2
Dust inhalation					
Sr-90	6.2×10^1	5.9×10^1	3.5×10^2	5.6	5.9
Tc-99	2.6	2.5	2.1	8.0×10^{-1}	8.0×10^{-1}
I-129	4.5×10^1	4.4×10^1	4.9×10^1	1.1	1.1
Cs-137	8.6	8.7	8.6	1.0	1.0
Pu-239	1.5×10^5	1.5×10^5	1.4×10^5	9.3×10^{-1}	9.3×10^{-1}
External gamma					
Co-60	3.1	6.8	1.0×10^7	3.2×10^6	1.5×10^6
Sr-90	6.8	0.0	0.0	NC[c]	NC
I-129	5.3×10^2	1.0×10^5	2.0×10^4	3.8×10^1	2.0×10^{-1}
Cs-137	4.2×10^4	1.0×10^5	2.7×10^6	6.4×10^1	2.7×10^1
Pu-239	3.1×10^1	1.4×10^3	4.5×10^2	1.5×10^1	3.2×10^{-1}

[a] GENII and PATHRAE results were taken from Wood (1992); these results were subsequently published in Seitz et al. (1992) as relative doses and are presented in Table 29.

[b] From leafy vegetables and produce.

[c] NC = not calculated.

dose may be erroneous. (Recent communication with R. Seitz indicated that an error was made in the initial calculations; this error has been corrected. The corrected results have been published in a recent report [Seitz et al. 1994]. Benchmarking of RESRAD with the corrected results is presented in Appendix A.)

3.5 CONCLUSIONS

The doses predicted by the RESRAD, GENII, and PATHRAE codes for the inhalation and ingestion pathways were in relatively good agreement. Differences were caused primarily by the transfer factors and dose conversion factors used in the dose calculation.

Predicted effective doses for external radiation differed considerably among the three codes. The external doses for Co-60 estimated by the GENII and PATHRAE codes were much

TABLE 29 Comparison of RESRAD, GENII, and PATHRAE Relative Radiation Doses[a]

Radionuclide	Relative Doses		
	GENII[b]	PATHRAE[c]	RESRAD
Plant ingestion			
Sr-90	1.0	9.2×10^{-1}	5.8×10^{-1}
Tc-99	8.7×10^{-2}	8.7×10^{-2}	6.7×10^{-3}
I-129	2.9×10^{-1}	3.0×10^{-1}	1.2×10^{-1}
Cs-137	3.3×10^{-2}	3.2×10^{-2}	2.0×10^{-3}
Pu-239	5.8×10^{-3}	5.8×10^{-3}	2.5×10^{-2}
Dust inhalation			
Sr-90	2.6×10^{-4}	2.5×10^{-4}	1.5×10^{-3}
Tc-99	1.1×10^{-5}	1.0×10^{-5}	8.8×10^{-6}
I-129	1.9×10^{-4}	1.8×10^{-4}	2.0×10^{-4}
Cs-137	3.6×10^{-5}	3.6×10^{-5}	3.6×10^{-5}
Pu-239	6.2×10^{-1}	6.2×10^{-1}	5.8×10^{-1}
External gamma			
Co-60	1.3×10^{-5}	2.8×10^{-5}	4.2×10^{1}
Sr-90	2.8×10^{-5}	0.0	0.0
I-129	2.2×10^{-3}	4.2×10^{-1}	8.3×10^{-2}
Cs-137	1.7×10^{-1}	4.2×10^{-1}	1.1×10^{-1}
Pu-239	1.3×10^{-4}	5.8×10^{-3}	1.9×10^{-3}

[a] The relative doses were the radiation doses listed in Table 28 and normalized by 2.4×10^{5} (mrem/yr).

[b] The relative doses for GENII were the same as those published by Seitz et al. (1992).

[c] The relative doses for PATHRAE were the same as those published by Seitz et al. (1992) except for the external gamma dose for Sr-90, which was 1.6×10^{-3} in the Seitz paper and converted to a radiation dose of 3.8×10^{2} (mrem/yr).

closer to each other than they were to the RESRAD results. However, judging by the radiation properties of the other radionuclides, the results indicate that the RESRAD estimation of Co-60 dose is more reasonable. This benchmarking exercise has demonstrated that in judging the validity of risk assessment models, comparison of the results from different models is not enough — professional judgment and the availability of the real data should play important roles in assessing the results.

4 REFERENCES

Gilbert, T.L., et al., 1989, *A Manual for Implementing Residual Radioactive Material Guidelines*, ANL/ES-160, DOE/CH/8901, prepared by Argonne National Laboratory, Argonne, Ill., for U.S. Department of Energy, Washington, D.C.

Hung, C.Y., 1989, *User's Guide for the SYSCPG Program — A PC Version of the PRESTO-EPA-CPG Operation System,* EPA 520/1-89-017, U.S. Environmental Protection Agency, Washington, D.C.

Kennedy, W.E., and D.L. Strenge, 1992, *Residual Radioactive Contamination from Decommissioning; Volume 1; Technical Basis for Translating Contamination Levels to Annual Total Effective Dose Equivalent*, NUREG/CR-5512, prepared by Pacific Northwest Laboratory, Richland, Wash., for U.S. Nuclear Regulatory Commission, Washington, D.C.

Leigh, C.D., et al., 1992, *User's Guide for GENII-S: A Code for Statistical and Deterministic Simulations for Radiation Doses to Humans from Radionuclides in the Environment*, SAND91-0561A, Sandia National Laboratories, Albuquerque, N.M.

Napier, B.A., et al., 1988, *GENII — The Hanford Environmental Radiation Dosimetry Software System,* vols. 1 and 2, PNL-6584, Pacific Northwest Laboratory, Richland, Wash.

Rogers, V.C., and C. Hung, 1987, *PATHRAE-EPA: A Low-Level Radioactive Waste Environmental Transport and Risk Assessment Code — Methodology and Users Manual*, EPA 520/1-87-028, prepared by Rogers and Associates, Salt Lake City, Utah, for U.S. Environmental Protection Agency, Washington, D.C.

Seitz, R.R., et al., 1992, "Comparison of Computer Codes and Approaches Used at DOE Sites to Model Intrusion Scenarios," proceedings of the Symposium on Waste Management, Tucson, Ariz., March 1-5, vol. 1, p. 509.

Seitz, R.R., et al., 1994, *Benchmarking of Computer Codes and Approaches for Modeling Exposure Scenarios*, DOE/LLW-188, prepared by Idaho National Engineering Laboratory, EG&G Idaho, Inc., Idaho Falls, Idaho, for U.S. Department of Energy, Washington, D.C.

Till, J.E., and R.E. Moore, 1988, "A Pathway Analysis Approach for Determining Acceptable Levels of Contamination of Radionuclides in Soil," *Health Physics* 55(3):541.

U.S. Department of Energy, 1990, "Radiation Protection of the Public and the Environment," DOE Order 5400.5, Washington, D.C.

Wood, M.I., 1992, personal communication from Wood (Westinghouse Hanford Company, Richland, Wash.) to C. Yu (Argonne National Laboratory, Argonne, Ill.), July 22.

Yu, C., et al., 1993, *Manual for Implementing Residual Radioactive Material Guidelines Using RESRAD, Version 5.0*, Working Draft, ANL/EAD/LD-2, Argonne National Laboratory, Argonne, Ill.

165

APPENDIX:

BENCHMARKING RESRAD RADIATION DOSE RESULTS AGAINST DATA FROM DOE/LLW-188

APPENDIX:

BENCHMARKING RESRAD RADIATION DOSE RESULTS AGAINST DATA FROM DOE/LLW-188

This appendix compares radiation dose results from RESRAD and those from DOE/LLW-188 (Seitz et al. 1994) for GENII and PATHRAE. As mentioned in Section 3, the external doses for Co-60 calculated by Seitz et al. (1992) with GENII and PATHRAE were much lower (approximately six orders less) than those calculated by RESRAD. Argonne National Laboratory (ANL) documented the rationale for the RESRAD results and forwarded this information to Seitz for review. Subsequently, Seitz issued a report (Seitz et al. 1994) that contains more extensive comparisons between the GENII and PATHRAE codes by including more radionuclides and pathways. This appendix presents benchmarking results using the latest version of the RESRAD code (Version 5.191) and the results from GENII and PATHRAE as presented in the recent report of Seitz et al. (1994).

A.1 METHODOLOGY

In the report by Seitz et al. (1994), the benchmarking was limited to comparisons of external, plant ingestion, and inhalation doses from a unit soil concentration (1 Ci/m^3) and plant, meat, milk, and water ingestion doses from a unit water concentration (1 μCi/L). Because radiation doses at a future time were not compared, discrepancies in environmental transport models (such as the air dispersion model and groundwater model) used by the different computer codes could not be identified. However, excluding the influence of the fate and transport models, a direct comparison of the food transfer models for radionuclides can easily be made.

Radionuclides in the soil phase constitute the original source of contamination considered in the RESRAD model. Theoretically, water contamination cannot be observed at time zero (when the radioactive material is placed in the soil phase) since it takes some time for the radionuclides to be transported through the vadose zone (unsaturated zone) and reach the groundwater table, unless the contaminated zone is located in the saturated zone. RESRAD allows for the input of groundwater concentrations only in cases in which the waste material was placed on-site a specific period of time prior to the radiological survey. During this time, the radionuclides would have already penetrated the unsaturated zone and reached the groundwater table. In this case, the input groundwater concentrations should be those measured at the same time as the soil concentrations. RESRAD will derive the soil/water distribution coefficients for the radionuclides on the basis of the input concentrations and soil property, meteorological, and hydrological parameters. This particular feature of RESRAD was used in this benchmarking effort to generate a unit water concentration (1 μCi/L) and to calculate the food concentrations from the contaminated irrigation water. In Seitz et al. (1994), the leaching factor for the GENII code was set to zero. In order to make the leaching effect negligible, the time since material placement parameter and the unsaturated zone thickness parameter used in the RESRAD code were tuned so that the leaching constant was

small enough to match the setting in the other comparison, yet still yield valid distribution coefficients.

In Seitz et al. (1994), different plant transfer factors were used for leafy and nonleafy vegetables. In RESRAD, both types of plant food have the same transfer factors. The same situation applies to livestock fodder. In Seitz et al. (1994), different storage times and root uptake factors were used for fresh and stored fodder. In RESRAD, only one type of fodder is considered in each calculation. To generate comparable results, multiple RESRAD runs were performed with different input values for food consumption rates and livestock fodder consumption rates by using the corresponding transfer factors and storage times. The results were then summed to give total doses for comparison. The root uptake transfer factors used in the RESRAD code are the plant/soil concentration ratios for wet plants and dry soil. The transfer factors used in the GENII and PATHRAE codes are based on the ratio of dry plants to dry soil. The values used by Seitz et al. (1994) must be adjusted by the dry-to-wet ratios to comply with RESRAD's definition of the transfer factor.

Because the purpose of the Seitz et al. report (1994) is to compare the food transfer models rather than the environmental fate models, the number of input parameters required is far less than the total number of parameters used in the RESRAD code. In the comparison reported here, the same input values were used as in Seitz et al. (1994) whenever possible. For those parameters that were not used or specified in the report, the RESRAD default values were selected.

A.2 RESRAD INPUT PARAMETERS

The soil concentration for each of the radionuclides considered in this comparison was 666,667 pCi/g. This value is equivalent to a soil concentration of 1 Ci/m^3, with a soil density of 1.5 g/cm^3. The groundwater concentration for each of the radionuclides was 1,000,000 pCi/L, which is equivalent to 1 μCi/L as specified in Seitz et al. (1994). The time since material placement parameter was set to 300 years. The cover thickness was set to 0 m. Erosion was not considered. The irrigation rate was 0.914 m/yr, which converts to 36 in./yr, as mentioned in Seitz et al. (1994). The precipitation rate was 0.11 m/yr. The runoff coefficient and evapotranspiration coefficient were set to the default values. The values of these parameters were not mentioned in Seitz et al. (1994); however, they are needed in the RESRAD code to derive the soil/water distribution coefficients. The thickness of the unsaturated zone parameter was set to 0.1 m after several trials with the time since material placement parameter to reduce the leaching effect. The input distribution coefficients for parent radionuclides were ignored by RESRAD during dose calculations because of the nonzero input groundwater concentrations. The distribution coefficients for progeny radionuclides were all set to 1.0×10^9 cm^3/g so that the progeny groundwater concentrations were much smaller than their parent concentrations, and their contributions to the total doses were negligible. The derived K_d values for parent radionuclides were 213.6 cm^3/g, and the leaching constants were 8.3×10^{-3} (1/yr). Table A.1 lists the groundwater concentrations for all radionuclides at time zero. Principal decay progeny (with

half-lives greater than 0.5 year) were Ac-227, Pa-231, Pb-210, Th-229, Th-230, U-233, U-234, and U-235. Lead-210 is the decay progeny of Ra-226 and U-238. Its groundwater concentration of 8.5×10^1 pCi/L comes primarily from Ra-226. Uranium-233 is the decay progeny of Np-237; its groundwater concentration is 1.21 pCi/L. The progeny concentrations were all small compared to their parent concentrations — 1,000,000 pCi/L. Their contributions to the total doses, as confirmed by the dose/source ratios for the water-dependent components of the plant, meat, and milk pathways in the detailed report generated by RESRAD, were negligible.

TABLE A.1 Groundwater Concentrations (time zero)

Radionuclide	Concentration (pCi/L)
Co-60	1.0×10^6
Ni-59	1.0×10^6
Sr-90	1.0×10^6
Tc-99	1.0×10^6
I-129	1.0×10^6
Cs-137	1.0×10^6
Pb-210	8.5×10^1
Ra-226	1.0×10^6
Ac-227	3.8×10^{-7}
Th-229	1.6×10^{-4}
Th-230	9.5×10^{-8}
Pa-231	5.3×10^{-9}
U-233	1.2
U-234	7.9×10^{-3}
U-235	2.7×10^{-6}
Np-237	1.0×10^6
U-238	1.0×10^6
Pu-239	1.0×10^6
Am-241	1.0×10^6

Several RESRAD runs were performed to simulate the conditions in Seitz et al. (1994). To use different root uptake transfer factors for plants and fodder, the plant, meat, and milk pathways cannot be considered simultaneously in a single run. Even for the plant pathway, two separate calculations have to be performed by RESRAD to consider different root transfer factors for leafy and nonleafy vegetables. Six input data files with their own databases were created to duplicate the exposure scenarios assumed in Seitz et al. (1994) (Table A.2 lists the input parameters). The first input data file (BENCH1.DAT) considered the external, inhalation, plant, and drinking water pathways. The inhalation rate was 8,500 m^3/yr. Mass loading factors were 0.0001 g/m^3 for both inhalation and foliar deposition. The exposed individual spent 100% of the time outdoors on-site. The plant consumption rates were 172 kg/yr for fruits, vegetables, and grain, and 0 kg/yr for leafy vegetables. The contamination fraction for plant food was 25%. The root uptake factors for nonleafy vegetables in Seitz et al. (1994) were multiplied by a dry-to-wet ratio of 0.187 and used with BENCH1.DAT in the RESRAD calculation. The inhalation and ingestion internal dose conversion factors used in the RESRAD calculation were also from Seitz et al. (1994).

Table A.3 lists the input parameters used in BENCH1.DAT. The results generated by using this input data file are listed in Table A.4 for external radiation doses, in Table A.5 for inhalation doses, and in Table A.6 for drinking water doses and can be compared directly with GENII and PATHRAE results. The second input data file (BENCH2.DAT) used by RESRAD considered only the plant pathway. It had the same input parameters as BENCH1.DAT except that the plant consumption rates were 0 kg/yr for fruits, vegetables,

TABLE A.2 Input Parameters Used in the Seitz et al. 1994 Benchmarking Report

General Parameters

Parameter	Value
Breathing rate (m^3/h)	0.97
Exposure time (h)	8,800
Indoor dust loading (g/m^3)	0.001
Leafy vegetables consumed (kg/yr)	20
Other vegetables consumed (kg/yr)	172
Fraction of contaminated food	0.25

Vegetation Parameters

Parameter	Garden Produce		Cattle Feed	
	Leafy	Other	Fresh	Stored
Yield (kg/m^2)	2.0	2.0	1.0	1.0
Dry-to-wet ratio	0.066	0.187	0.243	0.68
Growing period (d)	60	60	30	30
Delay: harvest-consumption (d)	1	60	0	90
Fraction of cattle diet[a]	NA[b]	NA	0.75	0.25
Fraction using Bv[c] (PATHRAE)	NA	NA	1.00	0.622
Fraction using Br[d] (PATHRAE)	NA	NA	0.0	0.378
Fraction using Bv (GENII)	NA	NA	1.00	0.0
Fraction using Br (GENII)	NA	NA	0.0	1.00

Milk and Meat Pathway Parameters

Parameter	Milk	Beef
Daily water consumption by cow (L)	55	55
Daily fodder consumption by cow (kg)	50	50
Annual human intake of milk (L) and meat (kg)	110	95
Storage time prior to consumption (d)	2	20

Source: Seitz et al. (1994).

[a] The cattle diet fractions are hardwired in the computer programs and cannot be changed by the user.

[b] NA = not applicable.

[c] Bv = soil-to-plant transfer factor for leafy vegetables (from PATHRAE).

[d] Br = soil-to-plant transfer factor for nonleafy vegetables (from PATHRAE).

TABLE A.3 Input Parameters Used in BENCH1.DAT for RESRAD[a]

Parameter	Value
Area of contaminated zone (m^2)	1,250
Thickness of contaminated zone (m)	0.15
Time since placement of material (yr)	300
Initial principal radionuclide concentration (pCi/g) for Co-60, Ni-59, Sr-90, Tc-99, I-129, Cs-137, Ra-226, U-238, Np-237, Pu-239, and Am-241	666,667
Concentration in groundwater (pCi/L) for Co-60, Ni-59, Sr-90, Tc-99, I-129, Cs-137, Ra-226, U-238, Np-237, Pu-239, and Am-241	1,000,000
Cover depth (m)	0
Density of contaminated zone (g/cm^3)	1.5
Contaminated zone erosion rate (m/yr)	0
Precipitation rate (m/yr)	0.11
Irrigation rate (m/yr)	0.941
Irrigation mode	Overhead
Unsaturated zone thickness (m)	0.1
Distribution coefficient (cm^3/g) for Pb-210, Ac-227, Th-229, Th-230, Pa-231, U-233, U-234, and U-235	1.0×10^9
Inhalation rate (m^3/yr)	8,500
Mass loading for inhalation (g/m^3)	0.0001
Fraction of time spent outdoors	1.0
Fruit, vegetable, and grain consumption (kg/yr)	172
Leafy vegetable consumption (kg/yr)	0
Drinking water intake (L/yr)	730
Contamination fraction of plant food	0.25
Contamination fraction of drinking water	1.0
Mass loading for foliar deposition (g/m^3)	0.0001
Depth of roots (m)	0.15
Storage times of contaminated foodstuffs (d)	
Fruits, nonleafy vegetables, and grain	60
Leafy vegetables	1

[a] Default values were used for parameters not listed in this table.

and grain and 20 kg/yr for leafy vegetables. The root uptake factors used in BENCH2.DAT were those for leafy vegetables in Seitz et al. (1994) multiplied by a dry-to-wet ratio of 0.066. The plant ingestion doses for BENCH1.DAT and BENCH2.DAT were summed to give the total ingestion doses for the plant pathway and are given in Tables A.7 and A.8 for the water-independent and water-dependent components, respectively.

The radiation doses from ingestion of meat and milk were obtained from two separate runs. In the RESRAD input data files BENCH3.DAT and BENCH4.DAT, meat and milk ingestion were the only pathways considered. Most of the input parameters were the

TABLE A.4 Comparison of External Radiation Doses (mrem/yr) from a Unit Soil Concentration (1 Ci/m^3)

Radionuclide	RESRAD	GENII	PATHRAE	RESRAD/ GENII	RESRAD/ PATHRAE
Co-60	1.2×10^7	8.7×10^6	3.9×10^7	1.38	0.31
Ni-59	3.7	1.5×10^2	0	0.02	NC[a]
Sr-90	0	2.2×10^4	0	0	NC
Tc-99	1.1	5.6×10^1	0	0.02	NC
I-129	2.2×10^4	6.1×10^3	6.1×10^5	3.61	0.04
Cs-137	2.9×10^6	2.1×10^6	1.1×10^7	1.38	0.26
Ra-226	8.2×10^6	6.5×10^6	3.2×10^7	1.26	0.26
U-238	7.3×10^4	8.3×10^4	1.3×10^6	0.88	0.06
Np-237	9.8×10^5	8.1×10^5	1.3×10^7	1.21	0.08
Pu-239	4.9×10^2	1.5×10^2	1.8×10^4	3.27	0.03
Am-241	3.2×10^4	1.6×10^4	1.1×10^6	2.00	0.03

[a] NC = not calculated.

TABLE A.5 Comparison of Inhalation Radiation Doses (mrem/yr) from a Unit Soil Concentration (1 Ci/m^3)

Radionuclide	RESRAD	GENII	PATHRAE	RESRAD/ GENII	RESRAD/ PATHRAE
Co-60	1.1×10^2	1.1×10^2	1.1×10^2	1.00	1.00
Ni-59	6.7×10^{-1}	7.3×10^{-1}	7.1×10^{-1}	0.92	0.94
Sr-90	1.1×10^2	1.2×10^2	1.2×10^2	0.92	0.92
Tc-99	4.7	5.1×10^0	5.0×10^0	0.92	0.94
I-129	7.9×10^1	8.6×10^1	8.4×10^1	0.92	0.94
Cs-137	1.6×10^1	1.7×10^1	1.7×10^1	0.94	0.94
Ra-226	4.3×10^3	4.7×10^3	4.6×10^3	0.91	0.93
U-238	6.2×10^4	6.7×10^4	6.5×10^4	0.93	0.95
Np-237	3.3×10^5	3.6×10^5	3.5×10^5	0.92	0.94
Pu-239	2.3×10^5	2.5×10^5	2.4×10^5	0.92	0.96
Am-241	2.3×10^5	2.5×10^5	2.5×10^5	0.92	0.92

same as BENCH1.DAT except for a few parameters related to the meat and milk consumption. The annual milk consumption was 110 L/yr. The annual meat consumption was 95 kg/yr. Storage times were 2 days for milk and 20 days for meat. In BENCH3.DAT, the livestock fodder intake for meat and milk was 37.5 kg/d, and the livestock water intake for meat and milk was 55 L/d. Storage time for livestock fodder was not considered. The root uptake transfer factors were those for leafy vegetables in Seitz et al. (1994) multiplied by a dry-to-wet ratio of 0.243. In BENCH4.DAT, the livestock fodder intake for meat and milk was 12.5 kg/d, and the livestock water intake for meat and milk was 0 L/d. The storage time

TABLE A.6 Comparison of Drinking Water Ingestion Doses (mrem/yr) from a Unit Water Concentration (1 μCi/L)

Radionuclide	RESRAD	GENII	PATHRAE	RESRAD/ GENII	RESRAD/ PATHRAE
Co-60	2.0×10^4	1.9×10^4	1.9×10^4	1.00	1.00
Ni-59	1.5×10^2	1.5×10^2	1.5×10^2	1.00	1.00
Sr-90	9.9×10^4	9.7×10^4	9.6×10^4	1.02	1.03
Tc-99	1.7×10^3	1.6×10^3	1.6×10^3	1.06	1.06
I-129	1.9×10^5	1.8×10^5	1.8×10^5	1.06	1.06
Cs-137	3.6×10^4	3.5×10^4	3.5×10^4	1.03	1.03
Ra-226	7.2×10^5	7.0×10^5	7.0×10^5	1.03	1.03
U-238	2.0×10^5	2.0×10^5	2.0×10^5	1.00	1.00
Np-237	4.0×10^6	3.8×10^6	3.8×10^6	1.05	1.05
Pu-239	2.7×10^6	2.6×10^6	2.6×10^6	1.04	1.04
Am-241	2.7×10^6	2.7×10^6	2.7×10^6	1.00	1.00

TABLE A.7 Comparison of Plant Ingestion Doses (mrem/yr) from a Unit Soil Concentration (1 Ci/m^3)

Radionuclide	RESRAD	GENII	PATHRAE	RESRAD/ GENII	RESRAD/ PATHRAE
Co-60	1.1×10^3	1.1×10^3	1.1×10^3	1.00	1.00
Ni-59	6.9×10^1	6.8×10^1	6.9×10^1	1.01	1.00
Sr-90	2.5×10^5	2.4×10^5	2.5×10^5	1.04	1.00
Tc-99	2.3×10^4	2.3×10^4	2.3×10^4	1.00	1.00
I-129	7.6×10^4	7.6×10^4	7.5×10^4	1.00	1.01
Cs-137	8.5×10^3	8.5×10^3	8.5×10^3	1.00	1.00
Ra-226	1.1×10^4	1.1×10^4	1.1×10^4	1.00	1.00
U-238	6.4×10^3	6.4×10^3	6.3×10^3	1.00	1.02
Np-237	4.0×10^5	4.0×10^5	4.0×10^5	1.00	1.00
Pu-239	2.0×10^3	1.2×10^3	1.2×10^3	1.67	1.67
Am-241	1.0×10^4	9.1×10^3	9.3×10^3	1.10	1.08

for fodder was 90 days. The root uptake transfer factors were those for nonleafy vegetables in Seitz et al. (1994) multiplied by a dry-to-wet ratio of 0.68. Results for BENCH3.DAT and BENCH4.DAT were summed to give the total doses (comparable to the GENII results) from meat and milk ingestion and are listed in Tables A.9 and A.10, respectively. The water-dependent components for the meat and milk pathways were compared with results from Seitz et al. (1994) since irrigation water was the only source for the meat and milk contamination. Another two input data files (BENCH5.DAT and BENCH6.DAT) were generated to obtain meat and milk ingestion doses comparable to the PATHRAE results. This was performed because in the PATHRAE code, different root uptake factors were used

TABLE A.8 Comparison of Plant Ingestion Doses (mrem/yr) from a Unit Water Concentration (1 μCi/L)

Radionuclide	RESRAD	GENII	PATHRAE	RESRAD/ GENII	RESRAD/ PATHRAE
Co-60	2.8×10^3	2.9×10^3	2.9×10^3	0.97	0.97
Ni-59	2.2×10^1	2.3×10^1	2.3×10^1	0.96	0.96
Sr-90	1.4×10^4	1.6×10^4	1.6×10^4	0.88	0.88
Tc-99	2.5×10^2	3.9×10^2	3.9×10^2	0.64	0.64
I-129	2.6×10^4	2.8×10^4	2.8×10^4	0.93	0.93
Cs-137	5.1×10^3	5.4×10^3	5.4×10^3	0.94	0.94
Ra-226	1.0×10^5	1.1×10^5	1.1×10^5	0.91	0.91
U-238	2.9×10^4	3.0×10^4	3.1×10^4	0.97	0.94
Np-237	5.6×10^5	5.9×10^5	5.9×10^5	0.95	0.95
Pu-239	3.8×10^5	4.0×10^5	4.0×10^5	0.95	0.95
Am-241	3.8×10^5	4.1×10^5	4.1×10^5	0.93	0.93

TABLE A.9 Comparison of Meat Ingestion Doses (mrem/yr) from a Unit Water Concentration (1 μCi/L)

Radionuclide	RESRAD[a]	RESRAD[b]	GENII	PATHRAE	RESRAD[a]/ GENII	RESRAD[b]/ PATHRAE
Co-60	2.3×10^4	2.3×10^4	4.0×10^4	4.1×10^4	0.58	0.56
Ni-59	5.5×10^1	5.5×10^1	9.6×10^1	9.6×10^1	0.57	0.57
Sr-90	1.8×10^3	1.8×10^3	3.4×10^3	3.6×10^3	0.53	0.50
Tc-99	8.9×10^2	9.0×10^2	2.2×10^3	2.5×10^3	0.40	0.36
I-129	7.8×10^4	7.8×10^4	1.4×10^5	1.4×10^5	0.56	0.56
Cs-137	4.3×10^4	4.3×10^4	7.2×10^4	7.5×10^4	0.60	0.57
Ra-226	1.1×10^4	1.1×10^4	1.8×10^4	1.9×10^4	0.61	0.58
U-238	2.4×10^3	2.4×10^3	4.0×10^3	4.2×10^3	0.60	0.57
Np-237	1.3×10^4	1.3×10^4	2.3×10^4	2.3×10^4	0.57	0.57
Pu-239	8.0×10^1	8.0×10^1	1.4×10^2	1.4×10^2	0.57	0.57
Am-241	5.7×10^2	5.7×10^2	9.8×10^2	9.8×10^2	0.58	0.58

[a] RESRAD results were obtained by using leafy vegetable transfer factors for 100% fresh fodder and nonleafy vegetable transfer factors for 100% stored fodder.

[b] RESRAD results were obtained by using leafy vegetable transfer factors for 100% fresh fodder and 62.2% stored fodder and nonleafy vegetable transfer factors for 37.8% stored fodder.

TABLE A.10 Comparison of Milk Ingestion Doses (mrem/yr) from a Unit Water Concentration (1 μCi/L)

Radionuclide	RESRAD[a]	RESRAD[b]	GENII	PATHRAE	RESRAD[a]/ GENII	RESRAD[b]/ PATHRAE
Co-60	2.7×10^3	2.7×10^3	4.8×10^3	4.7×10^3	0.56	0.57
Ni-59	1.1×10^1	1.1×10^1	1.8×10^1	1.9×10^1	0.61	0.58
Sr-90	1.0×10^4	1.0×10^4	1.9×10^4	2.1×10^4	0.53	0.48
Tc-99	1.2×10^3	1.2×10^3	2.9×10^3	3.4×10^3	0.41	0.35
I-129	1.3×10^5	1.3×10^5	2.2×10^5	2.3×10^5	0.59	0.57
Cs-137	1.7×10^4	1.7×10^4	3.0×10^4	3.0×10^4	0.57	0.57
Ra-226	2.3×10^4	2.3×10^4	3.8×10^4	3.9×10^4	0.61	0.59
U-238	8.4×10^3	8.4×10^3	1.4×10^4	1.5×10^4	0.60	0.60
Np-237	1.4×10^3	1.4×10^3	2.4×10^3	2.4×10^3	0.58	0.58
Pu-239	1.8×10^1	1.8×10^1	3.2×10^1	3.2×10^1	0.56	0.56
Am-241	7.5×10^1	7.5×10^1	1.3×10^2	1.3×10^2	0.58	0.58

[a] RESRAD results were obtained by using leafy vegetable transfer factors for 100% fresh fodder and nonleafy vegetable transfer factors for 100% stored fodder.

[b] RESRAD results were obtained by using leafy vegetable transfer factors for 100% fresh fodder and 62.2% stored fodder and nonleafy vegetable transfer factors for 37.8% stored fodder.

for certain fractions of the stored fodder, and these diet fractions cannot be changed by the user. In BENCH5.DAT, the livestock fodder consumption rate was 4.725 kg/d, which was 37.8% of the consumed stored fodder; the water consumption rate was 0 L/d. The root uptake factors were the same as used in BENCH4.DAT. In BENCH6.DAT, the livestock fodder consumption rate was 7.775 kg/d (62.2% of the consumed stored fodder), and the water consumption rate was also 0 L/d. The root uptake factors for leafy vegetables in Seitz et al. (1994) were multiplied by a dry-to-wet ratio of 0.68 and used in the RESRAD calculation. Results for BENCH3.DAT, BENCH5.DAT, and BENCH6.DAT were summed to give meat and milk (water-dependent component) doses comparable to the PATHRAE results. These results are given in Tables A.9 and A.10.

A.3 RESULTS AND DISCUSSION

Table A.4 compares the external radiation doses from the three computer codes. The GENII and PATHRAE codes took into account the ingrowth and decay of radionuclides within the one-year exposure period and calculated the accumulated doses. The RESRAD code also considered the ingrowth and decay of radionuclides and adjusted the soil concentrations at the calculation time periods. However, RESRAD does not integrate the radiation doses within the one-year exposure period; the radiation doses are assumed to be constant and to correspond to the soil concentrations at the beginning of the one-year period. To obtain the accumulated doses, decimal numbers can be entered at user-specified times, and then radiation doses at different times can be summed and averaged. The more time periods

selected within the one-year duration, the better the average doses agree with the integrated doses. The RESRAD results listed in Table A.4 are averages of the radiation doses at t = 0 yr and t = 1 yr. Radiation doses for t = 0 yr and t = 1 yr were about the same because all of the radionuclides considered have half-lives much greater than 1 yr except Co-60, for which the radiation dose at t = 1 yr was about 13% less than that at t = 0 yr. Because of the different methodologies used, the external doses from RESRAD, GENII, and PATHRAE, did not agree with each other; however, the RESRAD results were much closer to the GENII results than to the PATHRAE results.

The inhalation (Table A.5) and drinking water (Table A.6) doses compare very well among the three codes. The slightly smaller inhalation doses predicted by RESRAD were caused by the area factor, which with a value of 0.92 for an area of 1,250 m^2 was used to adjust the radiation doses for the finite size of the contaminated area.

The plant ingestion doses (Table A.7) from a unit soil concentration agree very well among the three computer codes, except for Pu-239. The plant contamination comes from direct root uptake and foliar deposition of the airborne particulates. For all of the radionuclides excluding Pu-239, the root uptake is the dominant source of contamination. For Pu-239, foliar deposition is more important since the root uptake transfer factors are small. The wet-weight crop yield, weathering removal constant, and growing period parameters used in the RESRAD foliar deposition model have hard-wired values and cannot be changed without modifying the source codes. These hard-wired parameters are different from those used by Seitz et al. (1994) and are the cause of discrepancies in the calculated doses, particularly for Pu-239.

The plant food could become contaminated by irrigation water. This contamination is caused by direct deposition of radionuclides through overhead irrigation. The radionuclides are intercepted by plant leaves and then absorbed and transferred to the edible portion, or they are deposited in the soil phase with subsequent root uptake. These two components were taken into account by all three computer codes and, in fact, the models used by the three computer codes are very similar. For the soil deposition, the RESRAD methodology takes into account the leaching loss of the deposited radionuclides during the growing period and balances the soil deposition with the amount of radionuclides intercepted by foliage (Equation D.14, Yu et al. 1993). The effective surface density of soil and the growing period used for the soil deposition model are hard-wired in the RESRAD code. For the foliar deposition model, the growing period, weathering removal constant, and wet-weight crop yield are hard-wired numbers. Treatment of the irrigation rate differs among the three computer codes. In RESRAD, the annual irrigation water is assumed to be applied evenly throughout the year; however, in the GENII code, the irrigation water can be applied within the user-specified duration (six months was used by Seitz et al. [1994]). In this benchmarking study, the average annual irrigation rate of 36 in./yr in Seitz et al. (1994) was used. For all of the radionuclides except Tc-99, foliar deposition is the dominant source for plant contamination. The radiation doses for plant ingestion (Table A.8) agree fairly well among the three codes. The close ratios between the RESRAD doses and the GENII (or PATHRAE) doses for different radionuclides appear to be an aggregated effect of the hard-wired

parameters and the irrigation rate. For Tc-99, which has large root uptake transfer factors, the root uptake contribution to the ingestion dose cannot be neglected. Therefore, the RESRAD/GENII (or RESRAD/PATHRAE) ratio also includes the effect from the effective surface density of soil.

Tables A.9 and A.10 compare the radiation doses of the meat and milk ingestion pathways resulting from a unit groundwater concentration (1 μCi/L). The meat and milk cows ingest fodder irrigated by contaminated water and drink contaminated water directly. Therefore, except for the two sources (root uptake and foliar deposition) mentioned previously that contaminate fodder, the third source is the drinking water itself. The magnitude of influence on the radiation doses from the ingestion of drinking water was a little less than that from foliar deposition. Influence from the meat and milk transfer factors can be excluded since the RESRAD results were obtained by using the same numbers that Seitz et al. (1994) used. Using different root uptake factors rather than the same for all stored fodder does not significantly affect the results. The radiation doses predicted by RESRAD, as shown in the second and third columns of Tables A.9 and A.10, are almost identical. The close ratios for the different radionuclides are mainly an aggregated effect of the hard-wired parameters for the irrigation model.

A.4 CONCLUSIONS

The RESRAD results agreed very well with the GENII and PATHRAE results for inhalation and drinking water doses. The radiation doses for the plant, meat, and milk ingestion pathways also agreed favorably among the RESRAD, GENII, and PATHRAE codes. The differences were primarily caused by the hard-wired parameters in the RESRAD code (the values of which could not be changed unless the source code was modified) and the way the irrigation rate was treated among the three codes. Using the same values for the hard-wired parameters and the assumption that the irrigation water was evenly applied throughout the year, the RESRAD results should match those of GENII and PATHRAE even better. The comparisons confirmed that the food transfer models implemented in the RESRAD code are similar to those used in the GENII and PATHRAE codes. The major differences were observed in the external radiation doses because of the use of different methodologies. The RESRAD external doses agreed better with the GENII doses than with the PATHRAE doses.

Although the RESRAD code uses the same root uptake factors for different types of plants (leafy vegetables, nonleafy vegetables, and fodder) and considers only one type of fodder for meat and milk cows, more than one type of plant and fodder with different transfer factors can be simulated by RESRAD with multiple runs. The groundwater contamination at the beginning of the time period can be considered in the RESRAD code through the groundwater contamination input and the time since material placement parameter. However, caution should be taken to fine tune the time since material placement and the thickness of the unsaturated zone parameters to allow for derivation of a valid distribution coefficient while matching the assumed leaching condition.

A.5 REFERENCES

Seitz, R.R., et al., 1994, *Benchmarking of Computer Codes and Approaches for Modeling Exposure Scenarios*, DOE/LLW-188, prepared by Idaho National Engineering Laboratory, EG&G Idaho, Inc., Idaho Falls, Idaho, for U.S. Department of Energy, Washington, D.C.

Yu, C., et al., 1993, *Manual for Implementing Residual Radioactive Material Guidelines Using RESRAD, Version 5.0,* Working Draft, ANL/EAD/LD-2, Argonne National Laboratory, Argonne, Ill.

178

ANL/EAIS/TM-103

A Compilation of Radionuclide Transfer Factors for the Plant, Meat, Milk, and Aquatic Food Pathways and the Suggested Default Values for the RESRAD Code

Environmental Assessment and Information Sciences Division

Argonne National Laboratory

Operated by The University of Chicago,
under Contract W-31-109-Eng-38, for the

United States Department of Energy

179

Argonne National Laboratory

Argonne National Laboratory, with facilities in the states of Illinois and Idaho, is owned by the United States government, and operated by the University of Chicago under the provisions of a contract with the Department of Energy.

This technical memo is a product of Argonne's Environmental Assessment and Information Sciences (EAIS) Division. For information on the division's scientific and engineering activities, contact:

Director, Environmental Assessment and
Information Sciences Division
Argonne National Laboratory
Argonne, Illinois 60439-4815
Telephone (708) 252-3759

Presented in this technical memo are preliminary results of ongoing work or work that is more limited in scope and depth than that described in formal reports issued by the EAIS Division.

Disclaimer

Reproduced directly from the best available copy.

Available to DOE and DOE contractors from the Office of Scientific and Technical Information, P.O. Box 62, Oak Ridge, TN 37831; prices available from (615) 576-8401.

Available to the public from the National Technical Information Service, U.S. Department of Commerce, 5285 Port Royal Road, Springfield, VA 22161.

ANL/EAIS/TM-103

A Compilation of Radionuclide Transfer Factors for the Plant, Meat, Milk, and Aquatic Food Pathways and the Suggested Default Values for the RESRAD Code

by Y.-Y. Wang, B.M. Biwer, and C. Yu

Environmental Assessment and Information Sciences Division,
Argonne National Laboratory, 9700 South Cass Avenue, Argonne, Illinois 60439

August 1993

Work sponsored by United States Department of Energy,
Assistant Secretary for Environment, Safety and Health,
Office of Environmental Guidance

and

Assistant Secretary for Environmental Restoration and Waste Management,
Office of Environmental Restoration

181

CONTENTS

TABLES

183

TABLES (Cont.)

A COMPILATION OF RADIONUCLIDE TRANSFER FACTORS FOR THE PLANT, MEAT, MILK, AND AQUATIC FOOD PATHWAYS AND THE SUGGESTED DEFAULT VALUES FOR THE RESRAD CODE

by

Y.-Y. Wang, B.M. Biwer, and C. Yu

ABSTRACT

The ongoing development and revision of the RESRAD computer code at Argonne National Laboratory requires update of radionuclide transfer factors for the plant, meat, milk, and aquatic food pathways. Default values for these transfer factors used in published radiological assessment reports are compiled and compared with values used in RESRAD. The differences among the reported default values used in different radiological assessment codes and reports are also discussed. In data comparisons, values used in more recent reports are given more weight because more recent experimental work tends to be conducted under better-defined laboratory or field conditions. A new default value is suggested for RESRAD if one of the following conditions is met: (1) values used in recent reports are an order of magnitude higher or lower than the default value currently used in RESRAD, or (2) the same default value is used in several recent radiological assessment reports.

1 INTRODUCTION

The radionuclide transfer factors for the plant, meat, milk, and aquatic food pathways used in the current version of the RESRAD computer code (Gilbert et al. 1989) are derived primarily from a handbook compiled by Ng et al. (1968). These factors are being updated at Argonne National Laboratory as part of the ongoing RESRAD development and revision effort. In Section 2 of this report, values of transfer factors used in the literature are compiled and compared with default values used in the current version of RESRAD. In Section 3, on the basis of these comparisons, new default values are suggested for future application of RESRAD.

2 DATA COMPILATION AND COMPARISON

Data from several published radiological assessment reports, listed in Table 1, are used as the sources for the transfer factors compiled in this report. The vegetable/soil, beef/feed, milk/feed, and aquatic food bioaccumulation transfer factors are compiled and compared in the following subsections.

2.1 VEGETABLE/SOIL TRANSFER FACTORS FOR ROOT UPTAKE

Comparison of vegetable/soil transfer factors for root uptake used in RESRAD with those used in other published radiological assessment models can be difficult because the parameters are generally reported in one of two different formats. In RESRAD (Gilbert et al. 1989), the food transfer coefficient for plants is expressed as the ratio: pCi per gram plant (wet)/pCi per gram soil (dry). In other published radiological assessment reports, the plant/soil concentration ratios have been reported on the basis of either the fresh (wet) weight or the dry weight of the vegetation. Dry-to-wet weight conversion factors must be estimated to make comparison possible. An overall average value of 0.428 for this parameter has been estimated by Baes et al. (1984) by the following processes: (1) calculation of the dry-to-wet weight conversion factors for exposed produce, protected produce, and grains on the basis of relative importance of various nonleafy vegetables in the United States; and (2) calculation of the average dry-to-wet conversion factor by weighing these calculated values by the relative importance (based on production in kilograms) of each vegetable category in the United States. Baes et al. (1984) caution, however, that unnecessary uncertainty might be introduced into the estimated parameter, and thus the adoption of dry-weight concentration ratios is preferred so as to reduce additional imprecision in parameter estimates.

A similar recommendation has been made by the IAEA (1982). For vegetation consumed by animals, expressing the vegetation biomass on a dry-weight basis is preferred so as to reduce both the large variability associated with the moisture content of fresh vegetation and the difficulties in accurately determining the fresh weight. In addition, animal consumption rates are most frequently reported on a dry-weight basis. On the other hand, for vegetation consumed by humans, it is more convenient to refer to the harvest yield or standing crop biomass on a fresh-weight basis because human consumption is most frequently reported in fresh weight. To aid in converting between the two bases of measurement, representative dry-to-wet weight ratios for food crops and forage plants that have been presented by Baes et al. (1984) and NRC (1983) are summarized in Table 2.

The vegetable/soil transfer factor of a radionuclide varies in a complex manner with soil properties and the geochemical properties of the radionuclide in soil. After entering the transpiration stream, radionuclides may not be uniformly distributed within a plant, but instead tend to concentrate in certain organs (Grogan 1985). Many studies have shown that

TABLE 1 Transfer Factors and References Cited in Each Radiological Assessment Report Used as a Source for Data Compilation

Radiological Assessment Report	Transfer Factor	References
NCRP (1991)	Vegetable/soil, beef/feed, and milk/feed transfer factors Aquatic bioaccumulation factor	Baes et al. (1984); Frissel (1989); IAEA (1982); Ng et al. (1977, 1982a) Copeland et al. (1973); Hoffman and Baes (1979); IAEA (1982); Killough and McKay (1976); Newman (1985); Poston and Klopfer (1986); Thompson et al. (1972)
NRC (1977)	Vegetable/soil transfer factor Beef/feed transfer factor Milk/feed transfer factor	Ng et al. (1968) Booth et al. (1971); Garner (1972); Ng et al. (1968) Booth et al. (1971); Garner (1972); Ng et al. (1968)
NRC (1983)	Milk/feed transfer factor Beef/feed transfer factor Aquatic bioaccumulation factor	Ng et al. (1977) Ng et al. (1979a,b, 1982b) Davis and Foster (1958); Friend et al. (1965); Harvey (1964); IAEA (1975); NAS (1971); Vanderploeg (1975)
Ng et al. (1982a) (NUREG/CR-2975)	Vegetable/soil transfer factor	Baker et al. (1976); Fletcher and Dotson (1971); McDowell-Boyer and Baes (1980); Moore et al. (1979); NRPB/CEA (1979)
Baes et al. (1984) (ORNL-5786)	Vegetable/soil transfer factor Beef/feed transfer factor Milk/feed transfer factor	Ng et al. (1968); NRC (1977) Ng et al. (1968, 1979a,b) Ng et al. (1977, 1979b)
IAEA (1982)	Vegetable/soil transfer factor Beef/feed transfer factor Milk/feed transfer factor Aquatic bioaccumulation factor	McDowell-Boyer et al. (1979); Ng et al. (1982a) Little (1979); Ng et al. (1977, 1979a,b) McDowell-Boyer et al. (1979); Ng et al. (1977, 1979a,b) Hoffman and Baes (1979); IAEA (1978); Thompson et al. (1972); Vanderploeg et al. (1975)

TABLE 1 (Cont.)

Radiological Assessment Report	Transfer Factor	References
IAEA (1985)	Aquatic bioaccumulation factor	Coughtrey et al (1983); Coughtrey and Thorne (1983); Eisler (1981)
IAEA (1993)	Milk/feed transfer factor	Coughtrey and Thorne (1983); Johnson et al. (1988); Morgan and Beetham (1990); Ng et al. (1977, 1982b); Van Bruwaene et al. (1982)
	Beef/feed transfer factor	Bishop et al. (1989); IAEA (1982); Johnson et al. (1988); Morgan and Beetham (1990); Ng et al. (1982b); Van Bruwaene et al. (1982)
	Aquatic bioaccumulation factor	Blaylock (1982); Copeland et al. (1973); IAEA (1982); Killough and McKay (1976); Newman (1985); Onishi et al. (1981); Poston and Klopfer (1986); Thompson et al. (1972); Vanderploeg et al. (1975)
Kennedy and Strenge (1992) (NUREG/ CR-5512)	Vegetable/soil transfer factor	Baes et al. (1984); IUR (1989)
	Beef/feed transfer factor	Baes et al. (1984); Napier et al. (1988)
	Milk/feed transfer factor	Baes et al. (1984); Napier et al. (1988)

TABLE 2 Dry-to-Wet Weight Conversion Factors for Food Crops and Forage Plants

Crop	Baes et al. (1984)	NRC (1983)	Crop	Baes et al. (1984)	NRC (1983)
Leafy Vegetables			Fruits (Cont.)		
Asparagus	0.070	0.083	Raspberry	-	0.175
Cabbage	-[a]	0.077	Cucumber	0.039	0.050
Cauliflower	-	0.083	Eggplant	0.073	0.077
Celery	-	0.063	Pepper	-	0.067
Lettuce	-	0.050	Pumpkin	-	0.084
Rhubarb	-	0.053	Squash	0.082	0.060
Spinach	-	0.083	Tomato	0.059	0.067
Broccoli	-	0.110	Grapefruit	0.112	0.116
Brussels sprout	-	0.147	Orange	0.128	0.141
Kale	-	0.125	Peach	0.131	0.109
Turnip green	-	0.100	Strawberry	0.101	0.101
			Cantaloupe	0.060	-
Root Vegetables			Watermelon	0.079	-
Potato	0.222	0.222	Lemon	0.107	-
Sweet potato	0.315	0.294			
Yam	-	0.263	Grains		
Beet	-	0.127	Barley	0.889	0.926
Carrot	0.118	0.118	Rice	-	0.877
Onion	0.125	0.116	Wheat	0.875	0.870
Radish	-	0.056	Corn	0.895	0.263
Turnip	-	0.085			
			Forage		
Fruits			Alfalfa	-	0.227
Apple	0.159	0.149	Clover	-	0.200
Apricot	-	0.147	Grass	-	0.182
Banana	-	0.244	Silage	-	0.238
Blackberry	-	0.156			
Blueberry	-	0.167	Others		
Cherry	0.170	0.196	Lima bean	-	0.322
Fig	-	0.227	Pea	0.257	0.169
Pear	0.173	0.167	Green bean	-	0.100
Pineapple	-	0.147	Chestnut	-	0.476
Plum	0.540	0.189	Peanut	0.920	0.943

[a] No conversion factor is given by the source.

the vegetable/soil transfer factor also varies with crop type and variety, stage of growth, and plant part, as well as with subsoil characteristics and agriculture practices (Baes et al. 1984; IAEA 1993; Ng et al. 1982a). Comprehensive data on transfer factors in different crops grown on various soils are available in the literature for relatively few radionuclides. Data for radionuclides for which little or no experimental information exists have been customarily estimated on the basis of the assumption that chemically similar elements act similarly in the soil-plant environment (Baes et al. 1984). Relationships between transfer factors for an element and those for other elements of the same or adjacent periods or groups were established and examined for possible trends. Such trends were extrapolated to the element in question.

In published radiological assessment models, default values for vegetable/soil transfer factors are reported as composite values from various food and feed crops or as separate values for forage vegetation and edible portions of various vegetables and produce. The current version of the RESRAD computer code uses composite values of vegetable/soil transfer factors. Differences among food crops (such as leafy vegetables, root vegetables, fruits, grain, and forage plants) and consumption groups (such as humans and animals) are not considered. To take any such differences into account, categorization of crop plants into different food classes is required. Four food classes (k=0, 1, 2, and 3) are used in this report to present data collected from different food crops. Food class descriptions and radiological assessment models used as the data source for vegetable/soil transfer factors are listed in Table 3.

Values of vegetable/soil transfer factors for root uptake compiled from published radiological assessment models are listed in Table 4 for the food classes defined in Table 3.

TABLE 3 Descriptions of Food Classes for Human and Animal Food Consumption and Associated Data Sources

Food Class	Class Description	Assessment Models Used as Data Sources
k=0	Composite	IAEA (1982); NCRP (1991); Ng et al. (1982a); NRC (1977)
k=1	Root vegetables, fruits, and grain for human consumption	Baes et al (1984); IAEA (1993); Kennedy and Strenge (1992); Napier et al. (1988); Ng et al. (1982a)
k=2	Leafy vegetables for human consumption	Baes et al. (1984); IAEA (1993); Kennedy and Strenge (1992); Napier et al. (1988); Ng et al. (1982a)
k=3	Forage plants for pasture vegetation and other animal feeds	IAEA (1982, 1993); NCRP (1991); Ng et al (1982a)

TABLE 4 Compilation of Vegetable/Soil Transfer Factors for Plant Foods

Part I: Composite (k=0) and Root Vegetables, Fruits, and Grain (k=1)

	Composite, k=0 (pCi/kg wet weight per pCi/kg dry soil)					Root Vegetables, Fruits, and Grain, k=1 (pCi/kg dry weight per pCi/kg dry soil)				
Element	RESRAD	NCRP (1991)	NRC (1977)	Ng et al. (1982a)	IAEA (1982)	Napier et al. (1988)	Kennedy and Strenge (1992)	Baes et al. (1984)	Ng et al.[a] (1982a)	IAEA[a] (1993)
H	0	-[b]	4.8	-	-	0.0	-	-	-	-
Be	4.7×10^{-4}	0.004	-	-	-	6.4×10^{-3}	1.5×10^{-3}	1.5×10^{-3}	-	-
C	5.5	-	5.5	-	-	0.0	7.0×10^{-1}	-	-	-
N	7.5	7.5	-	-	-	7.5	3.0×10^{-1}	3.0×10	-	-
F	2.0×10^{-2}	0.02	-	-	-	2.0×10^{-2}	6.0×10^{-3}	6.0×10^{-3}	-	-
Na	5.0×10^{-2}	0.05	5.2×10^{-2}	5.0×10^{-2} - 5.2×10^{-2}	5×10^{-2}	1.0×10	5.5×10^{-2}	5.5×10^{-2}	4.6×10^{-2}	-
P	5.0×10^{-1}	1	1.1	1.1×10^{0} - 5.0×10^{1}	1	4.0	3.5	3.5	-	-
Cl	5.0	20	-	-	-	3.3×10	7.0×10	7.0×10	-	-
Ar	0	0	-	-	-	0.0	-	-	-	-
K	3.0×10^{-1}	0.3	-	-	-	3.3	5.5×10^{-1}	5.5×10^{-1}	-	-
Ca	4.0×10^{-2}	0.5	-	-	-	2.0	3.5×10^{-1}	3.5×10^{-1}	-	-
Sc	1.1×10^{-3}	0.002	-	-	-	1.0×10^{-2}	1.0×10^{-3}	1.0×10^{-3}	-	-
Cr	2.5×10^{-4}	0.01	2.5×10^{-4}	2.5×10^{-4}	8×10^{-4}	2.8×10^{-2}	4.5×10^{-3}	4.5×10^{-3}	1.5×10^{-2}	-
Mn	3.0×10^{-2}	0.3	2.9×10^{-2}	2.9×10^{-2} - 3.0×10^{-2}	5×10^{-1}	5.3×10^{-1}	1.6×10^{-1}	5.0×10^{-2}	2.1×10^{-1}	3.0×10^{-1}
Fe	4.0×10^{-4}	0.001	6.6×10^{-4}	1.5×10^{-4} - 6.6×10^{-4}	7×10^{-4}	1.5×10^{-2}	1.0×10^{-3}	1.0×10^{-3}	4.3×10^{-3}	-
Co	9.4×10^{-3}	0.08	9.4×10^{-3}	1.0×10^{-3} - 1.0×10^{-2}	3×10^{-2}	8.0×10^{-3}	1.7×10^{-2}	7.0×10^{-3}	8.9×10^{-2}	2.2×10^{-2}
Ni	1.9×10^{-2}	0.05	1.9×10^{-2}	1.9×10^{-2} - 1.9×10^{0}	2×10^{-2}	8.3×10^{-2}	6.0×10^{-2}	6.0×10^{-2}	5.0×10^{-2}	1.4×10^{-1}
Cu	1.3×10^{-1}	0.005	1.2×10^{-1}	1.3×10^{-1}	-	3.5×10^{-2}	2.5×10^{-1}	2.5×10^{-1}	1.7×10^{-1}	-
Zn	4.0×10^{-1}	0.4	4.0×10^{-1}	4.1×10^{-1}	4×10^{-1}	2.0	9.3×10^{-1}	9.0×10^{-1}	5.6×10^{-1}	8.1×10^{-1}
As	1.0×10^{-2}	0.08	-	-	-	1.0×10^{-2}	6.0×10^{-3}	6.0×10^{-3}	-	-
Se	1.3	0.1	-	-	-	3.5×10^{-1}	2.5×10^{-2}	-	-	-
Br	7.6×10^{-1}	0.4	-	-	-	7.6×10^{-1}	1.5	1.5	-	-
Kr	0	0	-	-	-	0.0	-	-	-	-
Rb	1.3×10^{-1}	0.2	1.3×10^{-1}	1.3×10^{-1}	-	3.0×10^{-1}	7.0×10^{-2}	7.0×10^{-2}	-	-
Sr	2.0×10^{-1}	0.3	1.7×10^{-2}	2.0×10^{-2} - 1.0×10^{0}	3×10^{-1}	1.4	3.7×10^{-1}	2.5×10^{-1}	4.0×10^{-1}	2.6×10^{-1}
Y	2.5×10^{-3}	0.002	2.6×10^{-3}	2.5×10^{-3} - 4.3×10^{-3}	2×10^{-3}	7.0×10^{-3}	6.0×10^{-3}	6.0×10^{-3}	-	-
Zr	1.7×10^{-4}	0.001	1.7×10^{-4}	1.7×10^{-4}	5×10^{-3}	4.0×10^{-2}	5.0×10^{-4}	5.0×10^{-4}	1.8×10^{-3}	-
Nb	9.4×10^{-3}	0.01	9.4×10^{-3}	9.4×10^{-3}	1×10^{-2}	2.9×10^{-2}	5.0×10^{-3}	5.0×10^{-3}	-	-
Mo	1.3×10^{-1}	0.1	1.2×10^{-1}	1.3×10^{-1}	-	7.0×10^{-1}	6.0×10^{-2}	6.0×10^{-2}	-	-
Tc	2.5×10^{-1}	5	2.5×10^{-1}	2.5×10^{-1} - 5.0×10^{1}	5	4.0×10	1.1	1.5	-	5.8
Ru	1.0×10^{-2}	0.03	5.0×10^{-2}	3.8×10^{-3} - 6.0×10^{-2}	8×10^{-3}	2.0×10^{-1}	1.5×10^{-2}	2.0×10^{-2}	9.4×10^{-3}	-
Rh	1.3×10^{-1}	0.03	1.3×10^{1}	1.3×10^{1}	-	3.5×10	4.0×10^{-2}	4.0×10^{-2}	-	-
Pd	5.0	0.1	-	-	-	3.2×10^{-1}	4.0×10^{-2}	4.0×10^{-2}	-	-
Ag	1.5×10^{-1}	0.004	1.5×10^{-1}	1.5×10^{-1}	2×10^{-1}	4.2×10^{-1}	3.4×10^{-3}	1.0×10^{-1}	-	-
Cd	3.0×10^{-1}	0.5	-	-	-	1.5	1.5×10^{-1}	1.5×10^{-1}	-	-
Sn	2.5×10^{-3}	0.3	-	-	-	7.0×10^{-2}	6.0×10^{-3}	6.0×10^{-3}	-	-

TABLE 4, Part I (Cont.)

Element	Composite, k=0 (pCi/kg wet weight per pCi/kg dry soil)					Root Vegetables, Fruits, and Grain, k=1 (pCi/kg dry weight per pCi/kg dry soil)				
	RESRAD	NCRP (1991)	NRC (1977)	Ng et al. (1982a)	IAEA (1982)	Napier et al. (1988)	Kennedy and Strenge (1992)	Baes et al. (1984)	Ng et al.[a] (1982a)	IAEA[a] (1993)
Sb	1.1×10^{-2}	0.01	-	-	1×10^{-2}	5.0×10^{-2}	1.0×10^{-2}	3.0×10^{-2}	-	-
Te	1.3	0.1	1.3	1.3	6×10^{-1}	3.5	4.0×10^{-3}	4.0×10^{-3}	-	-
I	2.0×10^{-2}	0.02	2.0×10^{-2}	2.0×10^{-2} - 5.5×10^{-2}	2.0×10^{-2}	4.0×10^{-1}	5.0×10^{-2}	5.0×10^{-2}	3.8×10^{-2}	
Xe	0	0	-	-	-	0.0	-	-	-	-
Cs	2.0×10^{-3}	0.04	1.0×10^{-2}	6.4×10^{-4} - 7.8×10^{-2}	3×10^{-2}	1.7×10^{-2}	9.8×10^{-2}	3.0×10^{-2}	1.9×10^{-2}	4.4×10^{-2}
Ba	5.0×10^{-3}	0.01	5.0×10^{-3}	5.0×10^{-3}	5×10^{-3}	2.8×10^{-2}	1.5×10^{-2}	1.5×10^{-2}	-	-
La	2.5×10^{-3}	0.002	2.5×10^{-3}	2.5×10^{-3}	2×10^{-3}	1.7×10^{-2}	6.4×10^{-4}	4.0×10^{-3}	-	6.6×10^{-4}
Ce	5.0×10^{-4}	0.002	2.5×10^{-3}	5.0×10^{-4} - 7.0×10^{-3}	2×10^{-3}	2.8×10^{-2}	4.0×10^{-3}	4.0×10^{-3}	4.6×10^{-3}	-
Pr	2.5×10^{-3}	0.002	2.5×10^{-3}	2.5×10^{-3}	-	7.0×10^{-3}	4.0×10^{-3}	4.0×10^{-3}	-	-
Nd	2.4×10^{-3}	0.002	2.4×10^{-3}	2.4×10^{-3}	-	7.0×10^{-3}	4.0×10^{-3}	4.0×10^{-3}	-	-
Pm	2.5×10^{-3}	0.002	-	-	2×10^{-3}	7.0×10^{-3}	4.0×10^{-3}	4.0×10^{-3}	-	-
Sm	2.5×10^{-3}	0.002	-	-	2×10^{-3}	7.3×10^{-3}	4.0×10^{-3}	4.0×10^{-3}	-	-
Eu	2.5×10^{-3}	0.002	-	-	2×10^{-3}	7.3×10^{-3}	4.0×10^{-3}	4.0×10^{-3}	-	-
Gd	2.5×10^{-3}	0.002	-	-	-	3.5×10^{-2}	4.0×10^{-3}	4.0×10^{-3}	-	-
Tb	2.6×10^{-3}	0.002	-	-	-	2.6×10^{-3}	4.0×10^{-3}	4.0×10^{-3}	-	-
Ho	2.6×10^{-3}	0.002	-	-	-	1.1×10^{-2}	4.0×10^{-3}	4.0×10^{-3}	-	-
W	1.8×10^{-2}	0.8	1.8×10^{-2}	1.8×10^{-2}	-	2.1	1.0×10^{-2}	1.0×10^{-2}	-	-
Ir	9.9×10^{-4}	0.03	-	-	-	6.8×10^{-2}	1.5×10^{-2}	1.5×10^{-2}	-	-
Hg	3.8×10^{-1}	0.3	-	-	-	7.0×10^{-1}	2.0×10^{-1}	2.0×10^{-1}	-	-
Pb	6.8×10^{-2}	0.004	-	-	1×10^{-2}	7.0×10^{-2}	5.6×10^{-3}	9.0×10^{-3}	-	5.0×10^{-3}
Bi	1.5×10^{-1}	0.1	-	-	1×10^{-1}	6.0×10^{-1}	5.0×10^{-3}	5.0×10^{-3}	-	-
Po	9.0×10^{-3}	0.001	-	-	2×10^{-4}	7.0×10^{-3}	3.3×10^{-4}	4.0×10^{-4}	-	-
Rn	0	0	-	-	-	0.0	-	-	-	-
Ra	1.4×10^{-3}	0.04	-	-	4×10^{-2}	7.0×10^{-3}	3.5×10^{-3}	1.5×10^{-3}	-	4.9×10^{-3}
Ac	2.5×10^{-3}	0.001	-	-	1×10^{-3}	4.4×10^{-3}	3.5×10^{-4}	3.5×10^{-4}	-	-
Th	4.2×10^{-3}	0.001	-	-	5×10^{-4}	2.8×10^{-3}	8.0×10^{-5}	8.5×10^{-3}	-	2.1×10^{-4}
Pa	2.5×10^{-3}	0.01	-	-	4×10^{-2}	4.0×10^{-2}	2.5×10^{-4}	2.5×10^{-4}	-	-
U	2.5×10^{-3}	0.002	-	-	2×10^{-3}	2.7×10^{-3}	6.4×10^{-3}	4.0×10^{-3}	-	5.8×10^{-3}
Np	2.5×10^{-3}	0.02	2.5×10^{-3}	1.0×10^{-6} - 2.5×10^{-3}	4×10^{-2}	7.0×10^{-1}	7.4×10^{-3}	1.0×10^{-2}	1.4×10^{-1}	1.7×10^{-2}
Pu	2.5×10^{-4}	0.001	-	-	5×10^{-4}	2.8×10^{-4}	9.0×10^{-4}	4.5×10^{-5}	-	1.9×10^{-4}
Am	2.5×10^{-4}	0.001	-	-	1×10^{-3}	1.4×10^{-3}	2.4×10^{-4}	2.5×10^{-4}	-	4.1×10^{-4}
Cm	2.5×10^{-3}	0.001	-	-	1×10^{-3}	1.4×10^{-3}	9.2×10^{-4}	1.5×10^{-5}	-	2.4×10^{-4}
Cf	2.5×10^{-3}	0.001	-	-	-	2.5×10^{-3}	1.0×10^{-2}	-	-	-

[a] Values are calculated as the geometric means of data presented in original document.

[b] Data not listed.

TABLE 4 (Cont.)

Part II: Leafy Vegetables (k=2) and Forage Plants (k=3)

Element	Leafy Vegetables, k=2 (pCi/kg dry weight per pCi/kg dry soil)					Forage Plants, k=3 (pCi/kg dry weight per pCi/kg dry soil)			
	Napier et al. (1988)	Kennedy and Strenge (1992)	Baes et al. (1984)	Ng et al.[a] (1982a)	IAEA[a] (1993)	NCRP (1991)	IAEA (1982)	Ng et al.[a] (1982a)	IAEA[a] (1993)
H	0.0	-[b]	-	-	-	-	-	-	-
Be	8.0×10^{-3}	1.0×10^{-2}	1.0×10^{-2}	-	-	0.1	-	-	-
C	0.0	7.0×10^{-1}	-	-	-	-	-	-	-
N	7.5	3.0×10	3.0×10	-	-	20	-	-	-
F	2.0×10^{-2}	6.0×10^{-2}	6.0×10^{-2}	-	-	0.1	-	-	-
Na	1.0×10	7.5×10^{-2}	7.5×10^{-2}	3.5×10^{-1}	-	0.2	2×10^{-1}	-	-
P	4.0	3.5	3.5	-	-	3	3	-	-
Cl	5.0×10	7.0×10	7.0×10	-	-	100	-	-	-
Ar	0.0	-	-	-	-	0	-	-	-
K	3.0	1.0	1.0	-	-	3	-	-	-
Ca	2.0	3.5	3.5	-	-	5	-	-	-
Sc	1.0×10^{-2}	6.0×10^{-3}	6.0×10^{-3}	-	-	0.1	-	-	-
Cr	4.0×10^{-2}	7.5×10^{-3}	7.5×10^{-3}	-	-	0.1	3×10^{-3}	2.0×10^{-2}	-
Mn	7.0×10^{-1}	5.6×10^{-1}	2.5×10^{-1}	2.1	4.9×10^{-1}	10	3×10^{-1}	6.7×10^{-1}	9.2×10^{-1}
Fe	2.0×10^{-2}	4.0×10^{-3}	4.0×10^{-3}	-	-	0.1	3×10^{-3}	3.0×10^{-3}	-
Co	1.0×10^{-1}	8.1×10^{-2}	2.0×10^{-2}	-	1.6×10^{-1}	2	4×10^{-1}	1.1×10^{-1}	8.8×10^{-2}
Ni	1.0×10^{-1}	2.8×10^{-1}	6.0×10^{-2}	-	-	1	4×10^{-2}	1.1×10^{-1}	-
Cu	5.0×10^{-1}	4.0×10^{-1}	4.0×10^{-1}	6.4×10^{-2}	-	0.8	-	5.3×10^{-1}	-
Zn	2.0	1.4	1.5	8.3×10^{-1}	1.6	1	5×10^{-1}	6.4×10^{-1}	5.6×10^{-1}
As	1.0×10^{-2}	4.0×10^{-2}	4.0×10^{-2}	-	-	0.2	-	-	-
Se	5.0×10^{-1}	2.5×10^{-2}	2.5×10^{-2}	-	-	0.5	-	-	-
Br	7.6×10^{-1}	1.5	1.5	-	-	2	-	-	-
Kr	0.0	-	-	-	-	0	-	-	-
Rb	3.0×10^{-1}	1.5×10^{-1}	1.5×10^{-1}	-	-	2	-	8.1×10^{-1}	-
Sr	2.0	1.6	2.5	1.8	1.3	4	2	1.9	0.86
Y	1.0×10^{-2}	1.5×10^{-2}	1.5×10^{-2}	-	-	0.1	1×10^{-2}	-	-
Zr	4.0×10^{-2}	2.0×10^{-3}	2.0×10^{-3}	1.4×10^{-2}	-	0.1	2×10^{-2}	7.2×10^{-2}	-
Nb	4.0×10^{-2}	2.0×10^{-2}	2.0×10^{-2}	-	-	0.1	4×10^{-2}	-	-
Mo	1.0	2.5×10^{-1}	2.5×10^{-1}	-	-	0.4	-	-	-
Tc	4.0×10	4.4×10^{-1}	9.5	-	1.8×10^{2}	40	20	-	-
Ru	2.0×10^{-1}	5.2×10^{-1}	7.5×10^{-2}	4.7×10^{-2}	-	0.2	9×10^{-2}	1.1×10^{-1}	-
Rh	5.0×10	1.5×10^{-1}	1.5×10^{-1}	-	-	0.2	-	-	-
Pd	3.0×10^{-1}	1.5×10^{-1}	1.5×10^{-1}	-	-	0.5	-	-	-
Ag	6.0×10^{-1}	2.7×10^{-4}	4.0×10^{-1}	-	-	0.1	1	-	-
Cd	2.0	5.5×10^{-1}	5.5×10^{-1}	-	-	1	-	-	-
Sn	1.0×10^{-1}	3.0×10^{-2}	3.0×10^{-2}	-	-	1	-	-	-

TABLE 4, Part II (Cont.)

Element	Leafy Vegetables, k=2 (pCi/kg dry weight per pCi/kg dry soil)					Forage Plants, k=3 (pCi/kg dry weight per pCi/kg dry soil)			
	Napier et al. (1988)	Kennedy and Strenge (1992)	Baes et al. (1984)	Ng et al.[a] (1982a)	IAEA[a] (1993)	NCRP (1991)	IAEA (1982)	Ng et al.[a] (1982a)	IAEA[a] (1993)
Sb	5.0×10^{-2}	1.3×10^{-4}	2.0×10^{-1}	-	-	0.1	4×10^{-2}	-	-
Te	5.0	2.5×10^{-2}	2.5×10^{-2}	-	-	40	2	-	-
I	4.0×10^{-1}	3.4×10^{-3}	1.5×10^{-1}	1.6×10^{-1}	-	0.1	9×10^{-1}	1.7×10^{-1}	-
Xe	0.0	-	-	-	-	0	-	-	-
Cs	2.0×10^{-2}	1.3×10^{-1}	8.0×10^{-2}	1.1×10^{-1}	2.8×10^{-1}	0.2	1×10^{-1}	1.4×10^{-1}	1.7×10^{-1}
Ba	4.0×10^{-2}	1.5×10^{-1}	1.5×10^{-1}	-	-	0.1	2×10^{-2}	3.9×10^{-2}	-
La	1.0×10^{-2}	5.7×10^{-4}	1.0×10^{-2}	-	-	0.1	4×10^{-2}	-	-
Ce	4.0×10^{-2}	1.0×10^{-2}	1.0×10^{-2}	3.0×10^{-2}	-	0.1	4×10^{-2}	5.8×10^{-2}	-
Pr	1.0×10^{-2}	1.0×10^{-2}	1.0×10^{-2}	-	-	0.1	-	-	-
Nd	1.0×10^{-2}	1.0×10^{-2}	1.0×10^{-2}	-	-	0.1	-	-	-
Pm	1.0×10^{-2}	1.0×10^{-2}	1.0×10^{-2}	-	-	0.1	4×10^{-2}	-	-
Sm	1.0×10^{-2}	1.0×10^{-2}	1.0×10^{-2}	-	-	0.1	4×10^{-2}	-	-
Eu	1.0×10^{-2}	1.0×10^{-2}	1.0×10^{-2}	-	-	0.1	4×10^{-2}	-	-
Gd	5.0×10^{-2}	1.0×10^{-2}	1.0×10^{-2}	-	-	0.1	-	-	-
Tb	2.6×10^{-3}	1.0×10^{-2}	1.0×10^{-2}	-	-	0.1	-	-	-
Ho	1.0×10^{-2}	1.0×10^{-2}	1.0×10^{-2}	-	-	0.1	-	-	-
W	3.0	4.5×10^{-2}	4.5×10^{-2}	-	-	3	-	-	-
Ir	1.0×10^{-1}	5.5×10^{-2}	5.5×10^{-2}	-	-	0.2	-	-	-
Hg	1.0	9.0×10^{-1}	9.0×10^{-1}	-	-	1	-	-	-
Pb	1.0×10^{-1}	5.8×10^{-3}	4.5×10^{-2}	-	-	0.1	9×10^{-2}	-	-
Bi	6.0×10^{-1}	3.5×10^{-2}	3.5×10^{-2}	-	-	0.5	5×10^{-1}	-	-
Po	1.0×10^{-2}	2.5×10^{-3}	2.5×10^{-3}	-	-	0.1	4×10^{-3}	-	-
Rn	0.0	-	-	-	-	0	-	-	-
Ra	1.0×10^{-1}	7.5×10^{-2}	1.5×10^{-2}	-	-	0.2	2×10^{-1}	-	-
Ac	1.0×10^{-2}	3.5×10^{-3}	3.5×10^{-3}	-	-	0.1	4×10^{-3}	-	-
Th	4.0×10^{-3}	6.6×10^{-3}	8.5×10^{-4}	-	-	0.1	1×10^{-3}	-	9.0×10^{-3}
Pa	5.0×10^{-2}	2.5×10^{-3}	2.5×10^{-3}	-	-	0.1	1×10^{-1}	-	-
U	4.0×10^{-3}	1.7×10^{-2}	8.5×10^{-3}	-	-	0.1	1×10^{-2}	-	-
Np	1.0	1.3×10^{-2}	1.0×10^{-1}	-	5.1×10^{-2}	0.1	1×10^{-1}	1.1	2.3×10^{-2}
Pu	4.0×10^{-4}	3.9×10^{-4}	4.5×10^{-4}	-	1.2×10^{-4}	0.1	1×10^{-3}	-	2.7×10^{-4}
Am	2.0×10^{-3}	5.8×10^{-4}	5.5×10^{-3}	-	2.0×10^{-4}	0.1	4×10^{-3}	-	1.0×10^{-3}
Cm	2.0×10^{-3}	3.0×10^{-4}	8.5×10^{-4}	-	-	0.1	4×10^{-3}	-	4.8×10^{-4}
Cf	2.5×10^{-3}	1.0×10^{-2}	-	-	-	0.1	-	-	-

[a] Values are calculated as the geometric means of data presented in original document.

[b] Data not listed.

The data are intended to reflect only uptake of radionuclides from plant roots and to exclude the effects of deposition of radionuclides on plant surfaces following resuspension from soil. Comparison of these data is subjective, depending on the number of references available for an element. When many references are available for an element, data comparison can be conducted with reasonable confidence to suggest an appropriate value for future use.

In comparing data, we do not consider a twofold or threefold difference between default values in published reports and those used in RESRAD to be significant. When the difference is greater than an order of magnitude, the values from more recent reports are recommended for use in RESRAD (Section 3). This procedure is based on the assumption that the more recent experimental work has been conducted under better-defined laboratory or field conditions. In addition, a new default value is suggested for RESRAD when the new value, regardless of the magnitude of the difference, is used in several other reports that are based on independent work.

2.2 BEEF/FEED TRANSFER FACTORS

A beef/feed transfer factor represents the fraction of the daily intake of a radionuclide by beef cattle that is transferred to and remains in 1 kg of meat at equilibrium or at the time of slaughter. It is reported that this transfer factor is perhaps the least well documented in the literature because of the obvious practical difficulty — the need to sacrifice the meat-producing animals to collect the required experimental data (IAEA 1982).

For many elements and/or radionuclides, the beef/feed transfer factor is derived from other sources, such as stable element concentrations in feed and animal tissues, extrapolations from single-dose tracer experiments, and comparison of elemental concentrations in associated or unassociated meat, or milk, and feed (Ng et al. 1982b). Some of the difficulties in deriving the beef/feed transfer factor include the following:

- *The need for equilibrium* — With a few exceptions, the time required for a radionuclide to reach equilibrium in many animal products (e.g., beef) is so long that few experiments can be conducted sufficiently long to approach equilibrium conditions (IAEA 1993). Hence, a transfer factor derived from comparatively short experiments will underestimate the equilibrium transfer factor.

- *Effect of chemical and physical forms of diet and composition* — The availability of a radionuclide for gut uptake differs markedly, depending on the chemical and physical forms of the radionuclide and on the constituents of the diet (Beresford et al. 1989; Howard et al. 1989; Johnson et al. 1968). Higher radionuclide concentrations are often found in tissues other than muscle, particularly liver (e.g., for Pu, Am, Co, Ag, Ru) and bone (e.g., Pu, Am) (IAEA 1993). Radionuclide transfer models often underestimate soil adhesion on vegetation ingested by animals. The extent of soil ingestion will be influenced by the species of animal,

season, soil type, stocking rates, and pasture management. Consequently, values for soil ingestion will be highly site specific.

- *Influence of age* — The intake of radionuclides by an animal is dependent on the animal's species, mass, age, and growth rate, as well as on the digestibility of the feed. Young animals often have enhanced gut uptake and, hence, higher transfer coefficients than adults. Few available transfer coefficient data take these factors into account.

Published radiological assessments used for comparison of beef/feed transfer factors are Baes et al. (1984), IAEA (1982, 1993), Kennedy and Strenge (1992), Napier et al. (1988), NCRP (1991), Ng et al. (1982b), and NRC (1977, 1983). Table 5 lists default values of beef/feed transfer factors compiled from these sources. The same criteria used to compare plant uptake transfer factors were applied.

2.3 MILK/FEED TRANSFER FACTORS

A milk/feed transfer factor for milk cows is expressed as the fraction of the daily elemental intake in feed that is transferred to a kilogram of milk. Ng et al. (1977) report that radionuclide concentrations in animal food products depend on the relationship between intake, turnover in animal tissue, and excretion. The biological availability of a radionuclide in feed for uptake by dairy cattle depends on the physical and chemical forms of that radionuclide. In addition, the secretion of isotopes in milk is influenced by many factors besides physical and chemical states. For example, breed of dairy cow, age, nutritional status, stage of lactation, and feed and management practices are some of the important parameters that must be considered.

Reports reviewed for compilation and comparison of milk/feed transfer factors are Baes et al. (1984), IAEA (1982, 1993), Kennedy and Strenge (1992), Napier et al. (1988), NCRP (1991), and NRC (1977, 1983). The milk/feed transfer factors from these sources are compiled in Table 6. The criteria used for comparing the plant uptake transfer factors were applied.

2.4 AQUATIC BIOACCUMULATION FACTORS

A bioaccumulation factor is used to calculate the transfer of a radionuclide from contaminated water through various trophic levels of aquatic foodstuffs consumed by humans. The factor is normally expressed as the ratio of radioactivity in animal tissue to that in water at equilibrium conditions (Bq/kg wet or dry weight organism per Bq/kg or L water).

The physicochemical form of the radionuclide is generally more important in aquatic ecosystems than in terrestrial ecosystems. In terrestrial ecosystems, most of the food products are produced in situations where most of the factors can be controlled. In aquatic

TABLE 5 Compilation of Beef/Feed Transfer Factors (pCi/kg beef per pCi/daily intake)

Element	RESRAD	NCRP (1991)	Baes et al. (1984)	Napier et al. (1988)	IAEA (1993)	IAEA (1982)	Kennedy & Strenge (1992)	Ng et al. (1982b)	NRC (1977)	NRC (1983)
H	0	-[a]	-	0.0	-	-	-	-	0.012	-
Be	8.0×10^{-4}	0.005	1.0×10^{-3}	8.0×10^{-4}	-	-	1.0×10^{-3}	-	-	-
C	0	-	-	0.0	-	-	-	-	0.031	-
N	9.9×10^{-4}	0.01	0.075	9.9×10^{-4}	-	-	0.075	-	-	-
F	2.0×10^{-2}	0.02	0.15	2.0×10^{-2}	-	-	0.15	-	-	-
Na	5.0×10^{-2}	0.08	0.055	-	8×10^{-2}	2×10^{-1}	0.055	8.3×10^{-2}	0.03	8.3×10^{-3}
P	5.0×10^{-2}	0.05	0.055	-	5×10^{-2}	8×10^{-2}	0.055	4.9×10^{-2}	0.046	4.9×10^{-2}
Cl	6.0×10^{-2}	0.04	0.080	3.0×10^{-2}	1.7×10^{-2}	-	0.080	-	-	-
Ar	0	0	-	0.0	-	-	-	-	-	-
K	2.0×10^{-2}	0.02	2.0×10^{-2}	1.8×10^{-2}	1.8×10^{-2}	-	2.0×10^{-2}	1.8×10^{-2}	-	1.8×10^{-2}
Ca	3.3×10^{-3}	0.002	7.0×10^{-4}	1.6×10^{-3}	2×10^{-3}	-	7.0×10^{-4}	1.6×10^{-3}	-	1.6×10^{-3}
Sc	6.0×10^{-3}	0.002	0.015	6.0×10^{-3}	-	-	0.015	-	-	-
Cr	9.9×10^{-4}	0.03	5.5×10^{-3}	9.0×10^{-3}	9×10^{-3}	3×10^{-2}	5.5×10^{-3}	9.2×10^{-3}	2.4×10^{-3}	9.2×10^{-3}
Mn	5.0×10^{-3}	0.001	4.0×10^{-4}	5.0×10^{-4}	5×10^{-4}	1×10^{-3}	4.0×10^{-4}	5.0×10^{-4}	8.0×10^{-4}	5.0×10^{-4}
Fe	2.0×10^{-2}	0.03	0.020	2.0×10^{-2}	2×10^{-2}	3×10^{-2}	0.020	2.1×10^{-2}	0.04	2.1×10^{-2}
Co	1.0×10^{-3}	0.03	0.020	2.0×10^{-2}	1×10^{-2}	3×10^{-2}	0.020	2.0×10^{-3}	0.013	1.2×10^{-2}
Ni	1.0×10^{-3}	0.005	6.0×10^{-3}	2.0×10^{-3}	5.2×10^{-3}	5×10^{-3}	6.0×10^{-3}	2.0×10^{-3}	0.053	2.0×10^{-3}
Cu	1.0×10^{-2}	0.01	0.010	9.0×10^{-3}	9×10^{-3}	-	0.010	9.0×10^{-3}	8.0×10^{-3}	1.3×10^{-2}
Zn	5.0×10^{-2}	0.1	0.10	1.0×10^{-1}	1×10^{-1}	-	0.10	9.8×10^{-2}	0.03	-
As	1.5×10^{-3}	0.02	2.0×10^{-3}	1.5×10^{-3}	-	-	2.0×10^{-3}	-	-	-
Se	1.0	0.1	0.015	1.0	-	-	0.015	-	-	-
Br	2.0×10^{-2}	0.05	0.025	2.0×10^{-2}	-	-	0.025	-	-	-
Kr	0	0	-	0.0	-	-	-	-	-	-
Rb	1.5×10^{-1}	0.03	0.015	1.0×10^{-2}	1×10^{-2}	-	0.015	1.1×10^{-2}	0.031	1.1×10^{-2}
Sr	3.0×10^{-4}	0.01	3.0×10^{-4}	8.0×10^{-4}	8×10^{-3}	6×10^{-4}	3.0×10^{-4}	8.1×10^{-4}	6.0×10^{-4}	8.1×10^{-4}
Y	5.0×10^{-3}	0.002	3.0×10^{-4}	1.0×10^{-3}	1×10^{-3}	2×10^{-3}	3.0×10^{-4}	1.0×10^{-3}	4.6×10^{-3}	1.0×10^{-3}
Zr	5.0×10^{-4}	1×10^{-6}	5.5×10^{-3}	1.2×10^{-6}	1×10^{-6}	2×10^{-2}	5.5×10^{-3}	2.0×10^{-2}	0.034	2.1×10^{-2}
Nb	5.0×10^{-4}	3×10^{-7}	0.25	2.6×10^{-7}	3×10^{-7}	3×10^{-1}	0.25	2.5×10^{-1}	0.28	2.0×10^{-3}
Mo	1.0×10^{-2}	0.001	6.0×10^{-3}	1.2×10^{-3}	1×10^{-3}	-	6.0×10^{-3}	6.8×10^{-3}	8.0×10^{-3}	6.8×10^{-3}
Tc	9.9×10^{-4}	1×10^{-4}	8.5×10^{-3}	9.9×10^{-4}	1×10^{-4}	1×10^{-2}	8.5×10^{-3}	-	0.4	8.7×10^{-3}
Ru	1.0×10^{-3}	0.002	2.0×10^{-3}	2.0×10^{-3}	5.1×10^{-2}	2×10^{-3}	2.0×10^{-3}	2.0×10^{-3}	0.4	2.0×10^{-3}
Rh	1.0×10^{-3}	0.002	2.0×10^{-3}	1.0×10^{-3}	-	-	2.0×10^{-3}	-	1.5×10^{-3}	-
Pd	1.0×10^{-3}	0.0002	4.0×10^{-3}	1.0×10^{-3}	-	-	4.0×10^{-3}	-	-	-
Ag	9.9×10^{-4}	0.003	3.0×10^{-3}	2.0×10^{-3}	3×10^{-3}	5×10^{-3}	3.0×10^{-3}	2.0×10^{-3}	0.017	-
Cd	1.6×10^{-2}	0.001	5.5×10^{-4}	4.0×10^{-4}	4×10^{-4}	-	5.5×10^{-4}	3.5×10^{-4}	-	-

TABLE 5 (Cont.)

Element	RESRAD	NCRP (1991)	Baes et al. (1984)	Napier et al. (1988)	IAEA (1993)	IAEA (1982)	Kennedy & Strenge (1992)	Ng et al. (1982b)	NRC (1977)	NRC (1983)
Sn	9.9×10^{-4}	0.01	0.080	1.0×10^{-2}	-	-	0.080	-	-	-
Sb	3.0×10^{-3}	0.001	1.0×10^{-3}	1.0×10^{-3}	4×10^{-5}	1×10^{-3}	1.0×10^{-3}	9.2×10^{-4}	-	1.2×10^{-3}
Te	5.0×10^{-2}	0.007	0.015	7.0×10^{-3}	7×10^{-3}	2×10^{-2}	0.015	-	0.077	1.5×10^{-2}
I	2.0×10^{-2}	0.004	7.0×10^{-3}	2.0×10^{-3}	3.8×10^{-2}	1×10^{-2}	7.0×10^{-3}	3.6×10^{-3}	2.9×10^{-3}	7.2×10^{-3}
Xe	0	0	-	0.0	-	-	-	-	-	-
Cs	3.0×10^{-2}	0.05	0.020	3.0×10^{-2}	5.1×10^{-2}	2×10^{-2}	0.020	2.6×10^{-2}	4.0×10^{-3}	2.0×10^{-3}
Ba	5.0×10^{-4}	0.0002	1.5×10^{-4}	5.0×10^{-4}	2.3×10^{-4}	2×10^{-4}	1.5×10^{-4}	9.7×10^{-5}	3.2×10^{-3}	-
La	5.0×10^{-3}	0.002	3.0×10^{-4}	5.0×10^{-3}	-	2×10^{-3}	3.0×10^{-4}	-	2.0×10^{-4}	-
Ce	1.0×10^{-3}	2×10^{-5}	7.5×10^{-4}	2.0×10^{-3}	2×10^{-5}	2×10^{-3}	7.5×10^{-4}	2.0×10^{-3}	1.2×10^{-3}	-
Pr	5.0×10^{-3}	0.002	3.0×10^{-4}	5.0×10^{-3}	-	-	3.0×10^{-4}	-	4.7×10^{-3}	-
Nd	5.0×10^{-3}	0.002	3.0×10^{-4}	5.0×10^{-3}	-	-	3.0×10^{-4}	-	3.3×10^{-3}	-
Pm	5.0×10^{-3}	0.002	5.0×10^{-3}	5.0×10^{-3}	-	2×10^{-3}	5.0×10^{-3}	-	-	-
Sm	5.0×10^{-3}	0.002	5.0×10^{-3}	5.0×10^{-3}	-	2×10^{-3}	5.0×10^{-3}	-	-	-
Eu	5.0×10^{-3}	0.002	5.0×10^{-3}	6.0×10^{-3}	-	2×10^{-3}	5.0×10^{-3}	-	-	-
Gd	5.0×10^{-3}	0.002	3.5×10^{-3}	2.0×10^{-3}	-	-	3.5×10^{-3}	-	-	-
Tb	5.0×10^{-3}	0.002	4.5×10^{-3}	5.0×10^{-3}	-	-	4.5×10^{-3}	-	-	-
Ho	5.0×10^{-3}	0.002	4.5×10^{-3}	5.0×10^{-3}	-	-	4.5×10^{-3}	-	-	-
W	9.9×10^{-4}	0.04	0.045	3.7×10^{-2}	4×10^{-2}	-	0.045	3.7×10^{-2}	1.3×10^{-3}	3.7×10^{-2}
Ir	9.9×10^{-4}	0.002	1.5×10^{-3}	2.0×10^{-3}	-	-	1.5×10^{-3}	-	-	-
Hg	1.0×10^{-1}	0.01	0.25	1.0×10^{-1}	-	-	0.25	-	-	-
Pb	9.9×10^{-4}	0.0008	3.0×10^{-4}	4.0×10^{-4}	4×10^{-4}	8×10^{-4}	3.0×10^{-4}	4.0×10^{-4}	-	4.0×10^{-4}
Bi	9.9×10^{-4}	0.002	4.0×10^{-4}	1.7×10^{-2}	-	2×10^{-2}	4.0×10^{-4}	-	-	-
Po	9.9×10^{-4}	0.005	9.5×10^{-5}	4.5×10^{-3}	5×10^{-3}	3×10^{-3}	3.0×10^{-4}	4.5×10^{-3}	-	4.5×10^{-3}
Rn	0	0	-	0.0	-	-	-	-	-	-
Ra	9.9×10^{-4}	0.001	2.5×10^{-4}	9.0×10^{-4}	9×10^{-4}	5×10^{-4}	2.5×10^{-4}	9.0×10^{-4}	-	5.1×10^{-4}
Ac	5.0×10^{-3}	2×10^{-5}	2.5×10^{-5}	4.0×10^{-4}	-	2×10^{-5}	2.5×10^{-5}	-	-	-
Th	5.0×10^{-3}	0.0001	6.0×10^{-6}	5.0×10^{-3}	-	1×10^{-4}	6.0×10^{-6}	-	-	2.0×10^{-4}
Pa	5.0×10^{-3}	5×10^{-6}	1.0×10^{-5}	5.0×10^{-3}	-	1×10^{-3}	1.0×10^{-5}	-	-	-
U	5.0×10^{-3}	0.0008	2.0×10^{-4}	2.0×10^{-4}	3.4×10^{-4}	3×10^{-2}	2.0×10^{-4}	-	-	3.4×10^{-4}
Np	5.0×10^{-3}	0.001	5.5×10^{-5}	1.0×10^{-3}	1×10^{-3}	1×10^{-3}	5.5×10^{-5}	-	2.0×10^{-4}	-
Pu	5.0×10^{-3}	0.0001	5.0×10^{-7}	2.0×10^{-6}	1.8×10^{-5}	1×10^{-5}	5.0×10^{-7}	2.0×10^{-6}	-	1.0×10^{-6}
Am	5.0×10^{-3}	5×10^{-5}	3.5×10^{-6}	2.0×10^{-5}	4×10^{-5}	2×10^{-5}	3.5×10^{-6}	-	-	-
Cm	5.0×10^{-3}	2×10^{-5}	3.5×10^{-6}	5.0×10^{-3}	-	2×10^{-5}	3.5×10^{-6}	-	-	-
Cf	5.0×10^{-3}	6×10^{-5}	-	5.0×10^{-3}	-	-	5.0×10^{-3}	-	-	-

[a] Data not listed.

TABLE 6 Compilation of Milk/Feed Transfer Factors (pCi/L milk per pCi/daily intake)

Element	RESRAD	NCRP (1991)	Baes et al. (1984)	Napier et al. (1988)	IAEA (1993)	IAEA (1982)	Kennedy & Strenge (1992)	NRC (1983)	NRC (1977)
H	0	-[a]	-	0.0	-	-	-	1.4×10^{-2}	0.01
Be	2.0×10^{-6}	2×10^{-6}	9.0×10^{-7}	2.0×10^{-6}	-	-	9.0×10^{-7}	-	-
C	0	-	-	0.0	-	-	-	1.5×10^{-2}	0.012
N	1.0×10^{-2}	0.01	0.025	1.1×10^{-2}	-	-	0.025	-	-
F	7.0×10^{-3}	0.007	1.0×10^{-3}	7.0×10^{-3}	-	-	1.0×10^{-3}	-	-
Na	4.0×10^{-2}	0.04	0.035	2.0×10^{-2}	1.6×10^{-2}	4×10^{-2}	0.035	3.5×10^{-2}	0.04
P	1.2×10^{-2}	0.02	0.015	1.5×10^{-2}	1.6×10^{-2}	2×10^{-2}	0.015	1.6×10^{-2}	0.025
Cl	8.0×10^{-2}	0.02	0.015	2.0×10^{-2}	1.7×10^{-2}	-	0.015	-	-
Ar	0	0	-	0.0	-	-	-	-	-
K	7.0×10^{-3}	0.007	7.0×10^{-3}	7.0×10^{-3}	7.2×10^{-3}	-	7.0×10^{-3}	7.2×10^{-3}	-
Ca	8.0×10^{-3}	0.003	0.010	8.0×10^{-3}	3×10^{-3}	-	0.010	1.1×10^{-2}	-
Sc	2.5×10^{-6}	6×10^{-5}	5.0×10^{-6}	2.5×10^{-6}	-	-	5.0×10^{-6}	-	-
Cr	1.1×10^{-3}	0.002	1.5×10^{-3}	1.0×10^{-5}	1×10^{-5}	2×10^{-3}	1.5×10^{-3}	2.0×10^{-3}	2.5×10^{-3}
Mn	1.0×10^{-4}	0.0003	3.5×10^{-4}	3.0×10^{-4}	3×10^{-5}	3×10^{-4}	3.5×10^{-4}	8.4×10^{-5}	2.5×10^{-4}
Fe	6.0×10^{-4}	0.0003	2.5×10^{-4}	5.0×10^{-5}	3×10^{-5}	3×10^{-4}	2.5×10^{-4}	5.9×10^{-5}	1.2×10^{-3}
Co	5.0×10^{-4}	0.002	2.0×10^{-3}	1.0×10^{-4}	-[b]	2×10^{-3}	2.0×10^{-3}	2.0×10^{-3}	1.0×10^{-3}
Ni	3.4×10^{-3}	0.02	1.0×10^{-3}	1.0×10^{-3}	1.6×10^{-2}	1×10^{-2}	1.0×10^{-3}	1.0×10^{-2}	6.7×10^{-3}
Cu	7.0×10^{-3}	0.002	1.5×10^{-3}	2.0×10^{-3}	-	-	1.5×10^{-3}	1.7×10^{-3}	0.014
Zn	6.0×10^{-3}	0.01	0.010	1.0×10^{-2}	-	1×10^{-2}	0.010	1.0×10^{-2}	0.039
As	3.0×10^{-3}	1×10^{-4}	6.0×10^{-3}	8.0×10^{-5}	-	-	6.0×10^{-5}	-	-
Se	2.3×10^{-2}	0.01	4.0×10^{-3}	2.3×10^{-2}	-	-	4.0×10^{-3}	-	-
Br	2.5×10^{-2}	0.02	0.020	2.0×10^{-2}	-	-	0.020	2.0×10^{-2}	-
Kr	0	0	-	0.0	-	-	-	2.0×10^{-2}	-
Rb	1.0×10^{-2}	0.01	0.010	1.0×10^{-2}	1.2×10^{-2}	-	0.010	1.2×10^{-2}	0.03
Sr	1.5×10^{-3}	0.002	1.5×10^{-3}	1.3×10^{-3}	2.8×10^{-3}	1×10^{-3}	1.5×10^{-3}	1.4×10^{-3}	8.0×10^{-4}
Y	5.0×10^{-6}	6×10^{-5}	2.0×10^{-5}	5.0×10^{-6}	-	2×10^{-5}	2.0×10^{-5}	2.0×10^{-5}	1.0×10^{-5}
Zr	2.5×10^{-6}	6×10^{-7}	3.0×10^{-5}	5.5×10^{-7}	5.5×10^{-7}	3×10^{-5}	3.0×10^{-5}	8.0×10^{-2}	5.0×10^{-6}
Nb	1.2×10^{-3}	2×10^{-6}	0.020	4.1×10^{-7}	4.1×10^{-7}	2×10^{-2}	0.020	2.0×10^{-2}	2.5×10^{-3}
Mo	4.0×10^{-3}	0.002	1.5×10^{-3}	1.7×10^{-3}	1.7×10^{-3}	-	1.5×10^{-3}	1.4×10^{-3}	7.5×10^{-3}
Tc	1.2×10^{-2}	0.001	0.010	3.0×10^{-4}	1.1×10^{-3}	1×10^{-2}	0.010	9.9×10^{-3}	0.025
Ru	5.0×10^{-7}	2×10^{-5}	6.0×10^{-7}	6.0×10^{-7}	3.3×10^{-6}	5×10^{-7}	6.0×10^{-7}	6.1×10^{-7}	1.0×10^{-6}
Rh	5.0×10^{-3}	0.0005	0.010	5.0×10^{-3}	-	-	0.010	-	0.01
Pd	5.0×10^{-3}	0.0001	0.010	5.0×10^{-3}	-	-	0.010	-	-
Ag	2.5×10^{-2}	0.006	0.020	2.5×10^{-2}	5×10^{-5}	3×10^{-2}	0.020	-	0.05
Cd	6.2×10^{-5}	0.002	1.0×10^{-3}	1.2×10^{-4}	-	-	1.0×10^{-3}	-	-
Sn	1.3×10^{-3}	0.001	1.0×10^{-3}	1.0×10^{-3}	-	-	1.0×10^{-3}	-	-

TABLE 6 (Cont.)

Element	RESRAD	NCRP (1991)	Baes et al. (1984)	Napier et al. (1988)	IAEA (1993)	IAEA (1982)	Kennedy & Strenge (1992)	NRC (1983)	NRC (1977)
Sb	7.5×10^{-4}	0.0001	1.0×10^{-4}	7.5×10^{-4}	2.5×10^{-5}	2×10^{-5}	1.0×10^{-4}	2.0×10^{-5}	-
Te	5.0×10^{-4}	0.0005	2.0×10^{-4}	4.5×10^{-4}	4.5×10^{-4}	2×10^{-4}	2.0×10^{-4}	2.0×10^{-4}	1.3
I	1.0×10^{-2}	0.01	0.010	1.2×10^{-2}	1×10^{-2}	1×10^{-2}	0.010	9.9×10^{-3}	2.0×10^{-2}
Xe	0	0	-	0.0	-	-	-	-	-
Cs	5.0×10^{-3}	0.01	7.0×10^{-3}	7.0×10^{-3}	7.9×10^{-3}	8×10^{-3}	7.0×10^{-3}	7.1×10^{-3}	1.0×10^{-2}
Ba	4.0×10^{-4}	0.0005	3.5×10^{-4}	4.8×10^{-4}	4.8×10^{-4}	4×10^{-4}	3.5×10^{-4}	-	5.0×10^{-3}
La	2.5×10^{-6}	6×10^{-5}	2.0×10^{-5}	2.5×10^{-6}	-	2×10^{-5}	2.0×10^{-5}	-	2.5×10^{-3}
Ce	1.0×10^{-5}	6×10^{-5}	2.0×10^{-5}	4.0×10^{-5}	3×10^{-5}	2×10^{-5}	2.0×10^{-5}	2.0×10^{-5}	2.5×10^{-3}
Pr	2.5×10^{-6}	6×10^{-5}	2.0×10^{-5}	2.5×10^{-6}	-	-	2.0×10^{-5}	-	2.5×10^{-3}
Nd	2.5×10^{-6}	6×10^{-5}	2.0×10^{-5}	2.0×10^{-5}	-	-	2.0×10^{-5}	-	2.4×10^{-3}
Pm	2.5×10^{-6}	6×10^{-5}	2.0×10^{-5}	2.5×10^{-6}	-	2×10^{-5}	2.0×10^{-5}	-	-
Sm	2.5×10^{-6}	6×10^{-5}	2.0×10^{-5}	2.0×10^{-5}	-	2×10^{-5}	2.0×10^{-5}	-	-
Eu	2.5×10^{-6}	6×10^{-5}	2.0×10^{-5}	2.0×10^{-5}	-	2×10^{-5}	2.0×10^{-5}	-	-
Gd	2.5×10^{-6}	6×10^{-5}	2.0×10^{-5}	6.0×10^{-5}	-	-	2.0×10^{-5}	-	-
Tb	2.5×10^{-6}	6×10^{-5}	2.0×10^{-5}	2.5×10^{-6}	-	-	2.0×10^{-5}	-	-
Ho	2.5×10^{-6}	6×10^{-5}	2.0×10^{-5}	2.5×10^{-6}	-	-	2.0×10^{-5}	-	-
W	2.5×10^{-4}	0.0003	3.0×10^{-4}	3.0×10^{-4}	-	-	3.0×10^{-4}	2.9×10^{-4}	1.8×10^{-2}
Ir	9.9×10^{-4}	2×10^{-6}	2.0×10^{-6}	2.0×10^{-6}	-	-	2.0×10^{-6}	5.0×10^{-6}	-
Hg	1.9×10^{-2}	0.0005	4.5×10^{-4}	4.0×10^{-4}	4.7×10^{-4}	-	4.5×10^{-4}	9.7×10^{-6}	-
Pb	1.0×10^{-5}	0.0003	2.5×10^{-4}	3.0×10^{-5}	-	3×10^{-4}	2.5×10^{-4}	2.6×10^{-4}	-
Bi	2.5×10^{-4}	0.001	5.0×10^{-4}	5.0×10^{-4}	-	5×10^{-4}	5.0×10^{-4}	5.0×10^{-4}	-
Po	1.2×10^{-4}	0.0004	3.5×10^{-4}	1.2×10^{-4}	3.4×10^{-4}	1×10^{-4}	3.5×10^{-4}	1.4×10^{-2}	-
Rn	0	0	-	0.0	-	-	-	3.0×10^{-2}	-
Ra	2.0×10^{-4}	0.001	4.5×10^{-4}	2.0×10^{-4}	1.3×10^{-3}	6×10^{-4}	4.5×10^{-4}	4.5×10^{-4}	-
Ac	2.5×10^{-6}	2×10^{-6}	2.0×10^{-5}	2.0×10^{-5}	-	2×10^{-5}	2.0×10^{-5}	2.0×10^{-5}	-
Th	2.5×10^{-6}	5×10^{-6}	5.0×10^{-6}	2.5×10^{-6}	-	5×10^{-6}	5.0×10^{-6}	5.0×10^{-6}	-
Pa	2.5×10^{-6}	5×10^{-6}	5.0×10^{-6}	2.5×10^{-6}	-	5×10^{-6}	5.0×10^{-6}	5.0×10^{-6}	-
U	6.0×10^{-4}	0.0004	6.0×10^{-4}	6.0×10^{-4}	4×10^{-4}	6×10^{-4}	6.0×10^{-4}	6.1×10^{-4}	-
Np	2.5×10^{-6}	1×10^{-5}	5.0×10^{-6}	1.0×10^{-5}	5×10^{-6}	5×10^{-6}	5.0×10^{-6}	5.0×10^{-6}	2.5×10^{-3}
Pu	2.5×10^{-8}	1×10^{-6}	1.0×10^{-7}	1.0×10^{-7}	1.1×10^{-6}	1×10^{-7}	1.0×10^{-7}	2.7×10^{-9}	-
Am	2.5×10^{-6}	2×10^{-6}	4.0×10^{-7}	3.0×10^{-7}	1.5×10^{-6}	4×10^{-7}	4.0×10^{-7}	-	-
Cm	2.5×10^{-6}	2×10^{-6}	2.0×10^{-5}	3.0×10^{-7}	-	2×10^{-5}	2.0×10^{-5}	-	-
Cf	7.5×10^{-7}	2×10^{-6}	-	7.5×10^{-7}	-	-	7.5×10^{-7}	-	-

[a] Data not listed.

[b] Cobalt transfer differs according to its chemical form. For organically bound cobalt, a higher value of 3×10^{-4} is expected; for inorganic forms, a lower value of 7×10^{-5} is appropriate.

and marine environments, numerous species in the food chain are mobile and can move over considerable distances. Therefore, the concentration of a radionuclide can change much faster with time in aquatic ecosystems than in terrestrial systems, and an equilibrium condition is less likely to be achieved in the former. A radionuclide may exist in water in a truly dissolved state or in an undissolved state as a colloid or sorbed to particulate matter. Reactions between radionuclide and chemical species present in the water determine the biological availability of a radionuclide for uptake in aquatic environments. A dissolved radionuclide might precipitate out of solution and become less available for uptake if the concentrations of ligands in the water system are sufficiently high that the corresponding solubility product is exceeded. A radionuclide that is adsorbed to particulate matter might dissolve and become available for uptake if the concentrations of ligands and stable isotopes of the radionuclide are such that the solubility product is not exceeded.

The physiological status of fish also plays an important role in their uptake of radionuclides. Young, rapidly growing fish may accumulate higher levels of biologically active radionuclides than fish in a stationary growth period. The osmoregulatory problem faced by freshwater fish and marine fish also determines the difference in the route of radionuclide uptake (Poston and Klopfer 1986). In seawater, the salt concentration is high, and marine fish drink large amounts of water and expend considerable energy to excrete salt against a concentration gradient. In freshwater, fish retain salt and excrete a large amount of water. Therefore, radionuclides found in the water column, either as dissolved species or sorbed to particulate matter, are more prone to gastrointestinal (GI) absorption in marine species than in freshwater species (Poston and Klopfer 1986).

In the literature, bioaccumulation factors are derived by a number of methods, and the reported values vary widely. Historically, radioactivity in animal tissue is estimated on the basis of ash weight, dry weight, wet weight, whole body burdens, and/or muscle tissue. Radioactivity in water is estimated on the basis of filtered or unfiltered water. Wet weight to dry weight and dry weight to ash weight ratios can vary as a function of the age, size, and species of fish. To make comparisons possible, Poston and Klopfer (1986) listed the values summarized by Vinogradov (1953) for conversion as follows: ash weights ranged from 0.11 to 6.82%, with most in the range of 1-2%; water content ranged from 52.78 to 89.94%; and dry weights ranged from 20 to 40%. For radionuclides that partition into soluble and particulate phases, the degree of partitioning must be considered. A high transfer factor will be obtained if the radioactivity of the soluble (filtrate) fraction is measured. For instance, if 1% of a radionuclide is present as a soluble species, and the rest is in the solid phase, the transfer factor for a filtered water sample would be estimated to be 100 times greater than the factor for an unfiltered water sample (Poston and Klopfer 1986).

Published radiological assessments used for comparison of bioaccumulation transfer through the freshwater pathway are IAEA (1982, 1993), Kennedy and Strenge (1992), NCRP (1991), NRC (1977, 1983), and Thompson et al. (1972). Values for freshwater fish compiled from these reports are listed in Table 7. Aquatic bioaccumulation factors for crustacea and mollusks in freshwater, presented in NRC (1983), are listed in Table 8. The criteria used for comparing plant uptake transfer factors were applied.

TABLE 7 Compilation of Aquatic Bioaccumulation Factors for Freshwater Fish (Bq/kg freshwater fish per Bq/L water)

Element	RESRAD	Thompson et al. (1972)	NCRP (1991)	IAEA (1993)	IAEA (1982)	Kennedy & Strenge (1992)	NRC (1983)	NRC (1977)
H	9.0×10^{-1}	-[a]	1	1	-	1	-	0.9
Be	2.0	-	1.0×10^{2}	100	-	2	-	-
C	4.6×10^{3}	-	5.0×10^{4}	5.0×10^{4}	-	4.6×10^{3}	-	4.6×10^{3}
N	0	-	1.5×10^{5}	2.0×10^{5}	-	1.5×10^{5}	-	-
F	1.0×10^{1}	-	10	-	-	10	-	-
Na	1.0×10^{2}	20	20	20	20	1.0×10^{2}	1.3×10^{2}	1×10^{2}
P	1.0×10^{5}	1.0×10^{5}	5.0×10^{4}	5.0×10^{4}	1×10^{5}	7.0×10^{4}	3.8×10^{5}	1×10^{5}
Cl	1.3×10^{2}	-	1.0×10^{3}	-	-	50	-	-
Ar	1.0	-	0	-	-	-	-	-
K	1.0×10^{3}	-	1.0×10^{4}	-	-	1.0×10^{3}	-	-
Ca	4.0×10^{1}	-	1.0×10^{3}	-	-	40	-	-
Sc	2.0	100	1.0×10^{2}	1.0×10^{2}	-	1.0×10^{2}	-	-
Cr	2.0×10^{1}	-	2.0×10^{2}	2.0×10^{2}	2×10^{2}	2.0×10^{2}	1.2×10^{2}	2.0×10^{2}
Mn	4.0×10^{2}	100	5.0×10^{2}	4.0×10^{2}	4×10^{2}	4.0×10^{2}	1.6×10^{2}	4.0×10^{2}
Fe	1.0×10^{2}	100	2.0×10^{2}	2.0×10^{2}	1×10^{2}	2.0×10^{3}	2.0×10^{3}	1.0×10^{2}
Co	5.0×10^{1}	20	3.0×10^{2}	3.0×10^{2}	3×10^{2}	3.3×10^{2}	1.3×10^{2}	50
Ni	1.0×10^{2}	100	1.0×10^{2}	1.0×10^{2}	1×10^{2}	1.0×10^{2}	-	1.0×10^{2}
Cu	5.0×10^{1}	-	2.0×10^{2}	2.0×10^{2}	-	50	9.2	50
Zn	2.0×10^{3}	1000	1.0×10^{3}	1.0×10^{3}	1×10^{3}	2.5×10^{3}	8.3×10^{2}	2.0×10^{3}
As	3.0×10^{2}	-	4.0×10^{2}	-	-	1.0×10^{2}	-	-
Se	1.7×10^{2}	-	2.0×10^{2}	-	-	1.7×10^{2}	-	-
Br	4.2×10^{2}	-	4.0×10^{2}	4.0×10^{2}	-	4.2×10^{2}	-	4.2×10^{2}
Kr	1.0	-	0	-	-	-	-	-
Rb	2.0×10^{3}	-	2.0×10^{3}	2×10^{3}	-	2.0×10^{3}	-	2.0×10^{3}
Sr	3.0×10^{1}	5	60	60	60	50	2.8×10^{1}	30
Y	2.5×10^{1}	-	30	30	30	25	-	25
Zr	3.3	3.33	3.0×10^{2}	3.0×10^{2}	3×10^{2}	2.0×10^{2}	2.6	3.3
Nb	3.0×10^{4}	30,000	3.0×10^{2}	3.0×10^{2}	3×10^{2}	2.0×10^{2}	-	3×10^{4}
Mo	1.0×10^{1}	10	10	10	-	10	10	10
Tc	1.5×10^{1}	15	20	20	20	15	7.8×10^{1}	15
Ru	1.0×10^{1}	10	10	10	10	1.0×10^{2}	1.9×10^{1}	10
Rh	1.0×10^{1}	-	3.0×10^{2}	10	-	10	-	10
Pd	1.0×10^{1}	-	10	-	-	10	-	-
Ag	2.3	-	10	5	2	2.3	-	-
Cd	2.0×10^{2}	-	2.0×10^{2}	-	-	2.0×10^{2}	-	-

TABLE 7 (Cont.)

Element	RESRAD	Thompson et al. (1972)	NCRP (1991)	IAEA (1993)	IAEA (1982)	Kennedy & Strenge (1992)	NRC (1983)	NRC (1977)
Sn	3.0×10^3	-	3.0×10^3	3×10^3	-	3.0×10^3	1.0×10^2	-
Sb	1.0	1	1.0×10^2	1×10^2	1	2.0×10^2	-	-
Te	4.0×10^2	-	4.0×10^2	4×10^2	4×10^2	4.0×10^2	-	4.0×10^2
I	1.5×10^1	15	40	40	40	5.0×10^2	40	15
Xe	1.0	-	0	-	-	-	-	-
Cs	2.0×10^3	400	2.0×10^3	2×10^3	2×10^3	2.0×10^3	5.6×10^3	2.0×10^3
Ba	4.0	25	4	4	4	2.0×10^2	-	4
La	2.5×10^1	-	30	30	30	25	-	25
Ce	1.0	-	30	30	30	5.0×10^2	1.6×10^2	1
Pr	2.5×10^1	-	1.0×10^2	1×10^2	-	25	-	25
Nd	2.5×10^1	-	1.0×10^2	1×10^2	-	25	-	25
Pm	2.5×10^1	-	30	30	30	25	-	-
Sm	2.5×10^1	-	25	-	-	25	-	-
Eu	2.5×10^1	-	50	50	-	25	-	-
Gd	2.5×10^1	-	30	-	-	25	-	-
Tb	2.5×10^1	-	25	-	-	25	-	-
Ho	2.5×10^1	-	1.2×10^4	-	-	25	-	-
W	1.2×10^3	-	1.2×10^4	10	-	1.2×10^3	-	1.2×10^3
Ir	5.0×10^1	-	10	-	-	10	-	-
Hg	2.0×10^4	-	1.0×10^3	1×10^3	-	1.0×10^3	-	-
Pb	1.0×10^2	-	3.0×10^2	3×10^2	3×10^2	1.0×10^2	-	-
Bi	1.5×10^1	-	15	10	20	15	-	-
Po	5.0×10^2	-	1.0×10^2	50	50	5.0×10^2	-	-
Rn	5.7×10^1	-	0	-	-	-	-	-
Ra	5.0×10^1	50	50	50	50	70	5.2×10^2	-
Ac	2.5×10^1	-	15	-	-	25	-	-
Th	3.0×10^1	30	1.0×10^2	1×10^2	30	1.0×10^2	8.0×10^1	-
Pa	1.1×10^1	-	10	10	10	11	-	-
U	2.0	10	10	10	10	50	7.5	-
Np	1.0×10^1	10	30	30	10	2.5×10^2	-	10
Pu	3.5	3.5	30	30	4	2.5×10^2	8.0	-
Am	2.5×10^1	25	30	30	30	2.5×10^2	-	-
Cm	2.5×10^1	25	30	30	30	2.5×10^2	-	-
Cf	2.5×10^1	-	25	-	-	25	-	-

[a] Data not listed.

TABLE 8 Compilation of Aquatic Bioaccumulation Factors for Crustacea and Mollusks in Freshwater (Bq/kg organism per Bq/L water)

Element	RESRAD	NRC (1983)		Element	RESRAD	NRC (1983)	
	Crustacea and Mollusks	Crustaceans	Mollusks		Crustacea and Mollusks	Crustaceans	Mollusks
H	9.0×10^{-1}	-[a]	-	Cd	2.0×10^{3}	-	-
Be	1.0×10^{1}	-	-	Sn	1.0×10^{3}	-	-
C	9.1×10^{3}	-	-	Sb	1.0×10^{1}	-	-
N	0	-	-	Te	7.5×10^{1}	-	-
F	1.0×10^{2}	-	-	I	5.0	4.0×10	2.2×10^{2}
Na	2.0×10^{2}	2.3×10^{3}	2.0×10^{2}	Xe	1.0	-	-
P	2.0×10^{4}	1.3×10^{4}	6.0×10^{4}	Cs	1.0×10^{2}	2.2×10^{4}	2.2×10^{2}
Cl	1.9×10^{2}	-	-	Ba	2.0×10^{2}	-	-
Ar	1.0	-	-	La	1.0×10^{3}	-	-
K	2.0×10^{2}	-	-	Ce	1.0×10^{3}	9.8×10^{2}	9.0×10^{3}
Ca	3.3×10^{2}	-	-	Pr	1.0×10^{3}	-	-
Sc	1.0×10^{3}	-	-	Nd	1.0×10^{3}	-	-
Cr	2.0×10^{3}	2.9×10^{2}	4.4×10^{2}	Pm	1.0×10^{3}	-	-
Mn	9.0×10^{4}	1.9×10^{3}	9.2×10^{3}	Sm	1.0×10^{3}	-	-
Fe	3.2×10^{3}	2.4×10^{3}	9.6×10^{3}	Eu	1.0×10^{3}	-	-
Co	2.0×10^{2}	8.8×10^{2}	1.9×10^{3}	Gd	1.0×10^{3}	-	-
Ni	1.0×10^{2}	-	-	Tb	1.0×10^{3}	-	-
Cu	4.0×10^{2}	3.0×10	5.6×10^{2}	Ho	1.0×10^{3}	-	-
Zn	1.0×10^{4}	4.1×10^{3}	1.7×10^{4}	W	1.0×10^{1}	-	-
As	3.0×10^{2}	-	-	Ir	2.0×10^{2}	-	-
Se	1.7×10^{2}	-	-	Hg	2.0×10^{4}	-	-
Br	3.3×10^{2}	-	-	Pb	1.0×10^{2}	-	-
Kr	1.0	-	-	Bi	1.0×10^{1}	-	-
Rb	1.0×10^{3}	-	-	Po	2.0×10^{4}	-	-
Sr	1.0×10^{2}	-	3.2×10^{2}	Rn	1.0	-	-
Y	1.0×10^{3}	-	-	Ra	2.5×10^{2}	3.2×10^{3}	-
Zr	6.7	1.6×10^{3}	1.6×10^{2}	Ac	1.0×10^{3}	-	-
Nb	1.0×10^{2}	-	-	Th	5.0×10^{2}	-	-
Mo	1.0×10^{1}	1.0×10^{2}	6.0×10	Pa	1.1×10^{2}	-	-
Tc	5.0	-	-	U	6.0×10^{1}	1.6×10	-
Ru	3.0×10^{2}	2.3×10^{2}	3.6	Np	4.0×10^{2}	-	-

TABLE 8 (Cont.)

Element	RESRAD Crustacea and Mollusks	NRC (1983) Crustaceans	NRC (1983) Mollusks	Element	RESRAD Crustacea and Mollusks	NRC (1983) Crustaceans	NRC (1983) Mollusks
Rh	3.0×10^2	-	-	Pu	1.0×10^2	1.0×10^3	-
Pd	3.0×10^2	-	-	Am	1.0×10^3	-	-
Ag	7.7×10^2	-	-	Cm	1.0×10^3	-	-
				Cf	1.0×10^3	-	-

[a] Data not listed.

3 SUGGESTED VALUES FOR RESRAD REVISION

Summary tables of current and suggested elemental transfer factors for vegetable/soil, beef/feed, milk/feed, and aquatic food bioaccumulation pathways are presented in this section. For future application of RESRAD, suggested default values of vegetable/soil transfer factors for root uptake are presented in Tables 9 and 10. Suggested default values of beef/feed and milk/feed transfer factors are presented in Tables 11 and 12, respectively. Suggested default values of aquatic bioaccumulation factors for freshwater fish are presented in Table 13. Each table lists the current value, the suggested value, the change ([suggested value - default value]/[default value]), and the assessment models on which the suggested changes are based.

4 SUGGESTIONS FOR FUTURE WORK

The aquatic bioaccumulation factors used in RESRAD for pathways involving crustacea and mollusks in freshwater are listed in Table D.5 of Gilbert et al. (1989) and are compiled with data reported from NRC (1983) in Table 8. As indicated by the IAEA (1982, 1993), freshwater mollusks and crustacea are minor components of the human food chain. Default values for bioaccumulation factors for freshwater mollusks and crustacea are lacking in most radiological reports reviewed. To provide an overview of possible values of transfer factors for these species, bioaccumulation factors for mollusks and crustacea in marine are listed in Table 14 for future use. Appropriate bioaccumulation factors for freshwater mollusks and crustacea are not suggested in this report because the NRC (1983) report is the only source for data comparison. Update of RESRAD bioaccumulation factors for mollusks and crustacea is recommended for future work.

TABLE 9 Current RESRAD Default Values and Suggested Values for Vegetable/Soil Transfer Factors for Composite Plant Foods (k=0) (pCi/kg wet weight per pCi/kg dry soil)

Element	Current Default Value	Suggested Value	Change[a]	Radiological Assessment Model Source
H	0	4.8	-[b]	NRC (1977)
Be	4.7×10^{-4}	4.0×10^{-3}	7.5	NCRP (1991)
C	5.5	NC	NC[c]	NRC (1977)
N	7.5	NC	NC	NCRP (1991)
F	2.0×10^{-2}	NC	NC	NCRP (1991)
Na	5.0×10^{-2}	NC	NC	IAEA (1982); NCRP (1991)
P	5.0×10^{-1}	1	1.0	IAEA (1982); NCRP (1991)
Cl	5.0	20	3.0	NCRP (1991)
Ar	0	NC	NC	NCRP (1991)
K	3.0×10^{-1}	NC	NC	NCRP (1991)
Ca	4.0×10^{-2}	5.0×10^{-1}	11.5	NCRP (1991)
Sc	1.1×10^{-3}	2.0×10^{-3}	0.82	NCRP (1991)
Cr	2.5×10^{-4}	NC	NC	Ng et al. (1982a); NRC (1977)
Mn	3.0×10^{-2}	3.0×10^{-1}	9.0	NCRP (1991)
Fe	4.0×10^{-4}	1.0×10^{-3}	1.5	NCRP (1991)
Co	9.4×10^{-3}	8.0×10^{-2}	7.5	NCRP (1991)
Ni	1.9×10^{-2}	5.0×10^{-2}	1.6	NCRP (1991)
Cu	1.3×10^{-1}	NC	NC	Ng et al. (1982a)
Zn	4.0×10^{-1}	NC	NC	IAEA (1982); NCRP (1991); Ng et al. (1982a); NRC (1977)
As	1.0×10^{-2}	8.0×10^{-2}	7.0	NCRP (1991)
Se	1.3	1.0×10^{-1}	-0.92	NCRP (1991)
Br	7.6×10^{-1}	NC	NC	
Kr	0	NC	NC	NCRP (1991)
Rb	1.3×10^{-1}	NC	NC	Ng et al. (1982a); NRC (1977)
Sr	2.0×10^{-1}	3.0×10^{-1}	0.50	IAEA (1982); NCRP (1991)
Y	2.5×10^{-3}	NC	NC	
Zr	1.7×10^{-4}	1.0×10^{-3}	4.9	NCRP (1991)
Nb	9.4×10^{-3}	1.0×10^{-2}	0.06	IAEA (1982); NCRP (1991)
Mo	1.3×10^{-1}	NC	NC	Ng et al. (1982a); NRC (1977)
Tc	2.5×10^{-1}	5	19	IAEA (1982); NCRP (1991)
Ru	1.0×10^{-2}	3.0×10^{-2}	2.0	NCRP (1991)
Rh	1.3×10^{-1}	NC	NC	Ng et al. (1982a); NRC (1977)
Pd	5.0	1.0×10^{-1}	-0.98	NCRP (1991)
Ag	1.5×10^{-1}	NC	NC	Ng et al. (1982a); NRC (1977)
Cd	3.0×10^{-1}	NC	NC	
Sn	2.5×10^{-3}	NC	NC	
Sb	1.1×10^{-2}	1.0×10^{-2}	-0.09	IAEA (1982); NCRP (1991)
Te	1.3	6.0×10^{-1}	-0.54	IAEA (1982)
I	2.0×10^{-2}	NC	NC	IAEA (1982); NCRP (1991); Ng et al. (1982a), NRC (1977)
Xe	0	NC	NC	NCRP (1991)
Cs	2.0×10^{-3}	4.0×10^{-2}	19	NCRP (1991)
Ba	5.0×10^{-3}	NC	NC	IAEA (1982); Ng et al. (1982a); NRC (1977)

TABLE 9 (Cont.)

Element	Current Default Value	Suggested Value	Change[a]	Radiological Assessment Model Source
La	2.5×10^{-3}	NC	NC	Ng et al. (1982a); NRC (1977)
Ce	5.0×10^{-4}	2.0×10^{-3}	3.0	IAEA (1982); NCRP (1991)
Pr	2.5×10^{-3}	NC	NC	Ng et al. (1982a); NRC (1977)
Nd	2.4×10^{-3}	NC	NC	Ng et al. (1982a); NRC (1977)
Pm	2.5×10^{-3}	NC	NC	
Sm	2.5×10^{-3}	NC	NC	
Eu	2.5×10^{-3}	NC	NC	
Gd	2.5×10^{-3}	NC	NC	
Tb	2.6×10^{-3}	NC	NC	
Ho	2.6×10^{-3}	NC	NC	
W	1.8×10^{-2}	NC	NC	
Ir	9.9×10^{-4}	3.0×10^{-2}	29	NCRP (1991)
Hg	3.8×10^{-1}	NC	NC	
Pb	6.8×10^{-2}	1.0×10^{-2}	-0.85	IAEA (1982)
Bi	1.5×10^{-1}	1.0×10^{-1}	-0.33	IAEA (1982); NCRP (1991)
Po	9.0×10^{-3}	1.0×10^{-3}	-0.89	NCRP (1991)
Rn	0	NC	NC	NCRP (1991)
Ra	1.4×10^{-3}	4.0×10^{-2}	28	IAEA (1982); NCRP (1991)
Ac	2.5×10^{-3}	NC	NC	
Th	4.2×10^{-3}	1.0×10^{-3}	-0.76	NCRP (1991)
Pa	2.5×10^{-3}	1.0×10^{-2}	3.0	NCRP (1991)
U	2.5×10^{-3}	NC	NC	
Np	2.5×10^{-3}	2.0×10^{-2}	7	NCRP (1991)
Pu	2.5×10^{-4}	1.0×10^{-3}	3	NCRP (1991)
Am	2.5×10^{-4}	1.0×10^{-3}	3	NCRP (1991)
Cm	2.5×10^{-3}	1.0×10^{-3}	-0.60	NCRP (1991)
Cf	2.5×10^{-3}	1.0×10^{-3}	-0.60	NCRP (1991)

[a] Change = (suggested value - default value)/(default value).

[b] Not calculated.

[c] No change.

208

TABLE 10 Suggested RESRAD Default Values for Specific Plant Foods (k=1, 2, and 3; for root vegetables, fruit, and grain; leafy vegetables; and forage plants, respectively) (pCi/kg dry weight per pCi/kg dry soil)[a]

Element	k=1	Radiological Assessment Model Source	k=2	Radiological Assessment Model Source	k=3	Radiological Assessment Model Source
H	0.0	b	0.0	b	-[i]	NA[j]
Be	1.5×10^{-3}	c; d	1.0×10^{-2}	c; d	1.0×10^{-1}	g
C	7.0×10^{-1}	c	7.0×10^{-1}	c	-	NA
N	7.5	b	3.0×10	c; d	2.0×10	g
F	6.0×10^{-3}	c; d	6.0×10^{-2}	c; d	1.0×10^{-1}	g
Na	5.5×10^{-2}	c; d	7.5×10^{-2}	c; d	2.0×10^{-1}	g; h
P	3.5	c; d	3.5	c; d	3	g; h
Cl	7.0×10	c; d	7.0×10	c; d	1.0×10^{2}	g
Ar	0.0	b	0.0	b	0	g
K	5.5×10^{-1}	c; d	1.0	c; d	3	g
Ca	3.5×10^{-1}	c; d	3.5	c; d	5	g
Sc	1.0×10^{-3}	c; d	6.0×10^{-3}	c; d	1.0×10^{-1}	g
Cr	1.5×10^{-2}	e	7.5×10^{-3}	c; d	1.0×10^{-1}	g
Mn	1.6×10^{-1}	c	5.6×10^{-1}	c	9.2×10^{-1}	f
Fe	1.0×10^{-3}	c; d	4.0×10^{-3}	c; d	3.0×10^{-3}	e; h
Co	1.7×10^{-2}	c	8.1×10^{-2}	c	4.0×10^{-1}	h
Ni	6.0×10^{-2}	c; d	2.8×10^{-1}	c	1.1×10^{-1}	e
Cu	2.5×10^{-1}	c; d	4.0×10^{-1}	c; d	8.0×10^{-1}	g
Zn	9.3×10^{-1}	c; d	1.5	d	5.0×10^{-1}	h
As	6.0×10^{-3}	c; d	4.0×10^{-2}	c; d	2.0×10^{-1}	g
Se	2.5×10^{-2}	c	2.5×10^{-2}	c; d	5.0×10^{-1}	g
Br	1.5	c; d	1.5	c; d	2	g
Kr	0.0	b	0.0	b	0	g
Rb	7.0×10^{-2}	c; d	1.5×10^{-1}	c; d	2	g
Sr	3.7×10^{-1}	c	1.6	c	2	h
Y	6.0×10^{-3}	c; d	1.5×10^{-2}	c; d	1.0×10^{-1}	g
Zr	1.8×10^{-3}	e	2.0×10^{-3}	c; d	1.0×10^{-1}	g
Nb	5.0×10^{-3}	c; d	2.0×10^{-2}	c; d	1.0×10^{-1}	g
Mo	6.0×10^{-2}	c; d	2.5×10^{-1}	c; d	4.0×10^{-1}	g
Tc	1.5	d	4.0×10	b	4.0×10	g
Ru	1.5×10^{-2}	c	2.0×10^{-1}	b	2.0×10^{-1}	g
Rh	4.0×10^{-2}	c; d	1.5×10^{-1}	c; d	2.0×10^{-1}	g
Pd	4.0×10^{-2}	c; d	1.5×10^{-1}	c; d	5.0×10^{-1}	g
Ag	1.0×10^{-1}	d	4.0×10^{-1}	d	1.0×10^{-1}	g
Cd	1.5×10^{-1}	c; d	5.5×10^{-1}	c; d	1	g
Sn	6.0×10^{-3}	c; d	3.0×10^{-2}	c; d	1	g
Sb	3.0×10^{-2}	d	5.0×10^{-2}	b	1.0×10^{-1}	g
Te	4.0×10^{-3}	c; d	2.5×10^{-2}	c; d	4.0×10	g
I	5.0×10^{-2}	c; d	1.5×10^{-1}	d	1.7×10^{-1}	e
Xe	0.0	b	0.0	b	0	g
Cs	9.8×10^{-2}	c	1.3×10^{-1}	c	2.0×10^{-1}	g
Ba	1.5×10^{-2}	c; d	1.5×10^{-1}	c; d	1.0×10^{-1}	g
La	6.4×10^{-4}	c	1.0×10^{-2}	c; d	1.0×10^{-1}	g
Ce	4.0×10^{-3}	c; d	1.0×10^{-2}	c; d	1.0×10^{-1}	g

TABLE 10 (Cont.)

Element	k=1	Radiological Assessment Model Source	k=2	Radiological Assessment Model Source	k=3	Radiological Assessment Model Source
Pr	4.0×10^{-3}	c; d	1.0×10^{-2}	b; c; d	1.0×10^{-1}	g
Nd	4.0×10^{-3}	c; d	1.0×10^{-2}	b; c; d	1.0×10^{-1}	g
Pm	4.0×10^{-3}	c; d	1.0×10^{-2}	b; c; d	1.0×10^{-1}	g
Sm	4.0×10^{-3}	c; d	1.0×10^{-2}	b; c; d	1.0×10^{-1}	g
Eu	4.0×10^{-3}	c; d	1.0×10^{-2}	b; c; d	1.0×10^{-1}	g
Gd	4.0×10^{-3}	c; d	1.0×10^{-2}	c; d	1.0×10^{-1}	g
Tb	4.0×10^{-3}	c; d	1.0×10^{-2}	c; d	1.0×10^{-1}	g
Ho	4.0×10^{-3}	c; d	1.0×10^{-2}	b; c; d	1.0×10^{-1}	g
W	1.0×10^{-2}	c; d	4.5×10^{-2}	c; d	3	g
Ir	1.5×10^{-2}	c; d	5.5×10^{-2}	c; d	2.0×10^{-1}	g
Hg	2.0×10^{-1}	c; d	9.0×10^{-1}	c; d	1	g
Pb	5.6×10^{-3}	c	4.5×10^{-2}	d	1.0×10^{-1}	g
Bi	5.0×10^{-3}	c; d	3.5×10^{-2}	c; d	5.0×10^{-1}	g; h
Po	3.3×10^{-4}	c	2.5×10^{-3}	c; d	1.0×10^{-1}	g
Rn	0.0	b	0.0	b	0	g
Ra	3.5×10^{-3}	c	7.5×10^{-2}	c	2.0×10^{-1}	g; h
Ac	3.5×10^{-4}	c; d	3.5×10^{-3}	c; d	1.0×10^{-1}	g
Th	2.1×10^{-4}	f	4.0×10^{-3}	b	9.0×10^{-3}	f
Pa	2.5×10^{-4}	c; d	2.5×10^{-3}	c; d	1.0×10^{-1}	g; h
U	6.4×10^{-3}	c	8.5×10^{-3}	d	1.0×10^{-1}	g
Np	1.7×10^{-2}	f	1.3×10^{-2}	c	1.0×10^{-1}	g; h
Pu	1.9×10^{-4}	f	3.9×10^{-4}	c	2.7×10^{-4}	f
Am	4.1×10^{-4}	f	2.0×10^{-3}	b	4.0×10^{-3}	h
Cm	9.2×10^{-4}	c	8.5×10^{-4}	d	4.0×10^{-3}	h
Cf	1.0×10^{-2}	c	1.0×10^{-2}	c	1.0×10^{-1}	g

[a] Use dry-to-wet weight conversion factors listed in Table 2 to apply these suggested values for RESRAD input.

[b] Napier et al. (1988).

[c] Kennedy and Strenge (1992).

[d] Baes et al. (1984).

[e] Ng et al. (1982a).

[f] IAEA (1993).

[g] NCRP (1991).

[h] IAEA (1982).

[i] Data not listed.

[j] Not applicable.

210

TABLE 11 Current RESRAD Default Values and Suggested Values for Beef/Feed Transfer Factors (pCi/kg beef per pCi/daily intake)

Element	Current Default Value	Suggested Value	Change[a]	Radiological Assessment Model Source
H	0	1.2×10^{-2}	-[b]	NRC (1977)
Be	8.0×10^{-4}	1.0×10^{-3}	0.25	Baes et al. (1984); Kennedy and Strenge (1992)
C	0	3.1×10^{-2}	-	NRC (1977)
N	9.9×10^{-4}	1.0×10^{-2}	9.10	NCRP (1991)
F	2.0×10^{-2}	NC[c]	NC	Napier et al. (1988); NCRP (1991)
Na	5.0×10^{-2}	8.0×10^{-2}	0.60	IAEA (1993); NCRP (1991)
P	5.0×10^{-2}	NC	NC	IAEA (1993); NCRP (1991)
Cl	6.0×10^{-2}	NC	NC	
Ar	0	NC	NC	Napier et al. (1988); NCRP (1991)
K	2.0×10^{-2}	NC	-	Baes et al. (1984); Kennedy and Strenge (1992); NCRP (1991)
Ca	3.3×10^{-3}	1.6×10^{-3}	-0.52	Napier et al. (1988); Ng (1982b); NRC (1983)
Sc	6.0×10^{-3}	1.5×10^{-2}	1.5	Baes et al. (1984); Kennedy and Strenge (1992)
Cr	9.9×10^{-4}	9.0×10^{-3}	8.1	IAEA (1993); Napier et al. (1988)
Mn	5.0×10^{-3}	5.0×10^{-4}	-0.90	IAEA (1993); Napier et al. (1988); Ng (1982b); NRC (1983)
Fe	2.0×10^{-2}	NC	NC	Baes et al. (1984); IAEA (1993); Kennedy and Strenge (1992); Napier et al. (1988)
Co	1.0×10^{-3}	2.0×10^{-2}	19	Baes et al. (1984); Kennedy and Strenge (1992); Napier et al. (1984)
Ni	1.0×10^{-3}	5.0×10^{-3}	4	IAEA (1982); NCRP (1991)
Cu	1.0×10^{-2}	NC	NC	Baes et al. (1984); Kennedy and Strenge (1992); NCRP (1991)
Zn	5.0×10^{-2}	1.0×10^{-1}	1	Baes et al. (1984); IAEA (1993); Kennedy and Strenge (1992); Napier et al. (1988); NCRP (1991)
As	1.5×10^{-3}	NC	NC	Napier et al. (1988)
Se	1.0	1.0×10^{-1}	-0.90	NCRP (1991)
Br	2.0×10^{-2}	NC	NC	Napier et al. (1988)
Kr	0	NC	NC	Napier et al. (1988); NCRP (1991)
Rb	1.5×10^{-1}	1.5×10^{-2}	-0.9	Baes et al. (1984); Kennedy and Strenge (1992)
Sr	3.0×10^{-4}	8.0×10^{-3}	26	IAEA (1993)
Y	5.0×10^{-3}	2.0×10^{-3}	-0.6	IAEA (1982); NCRP (1991)
Zr	5.0×10^{-4}	1.0×10^{-6}	-1.0	IAEA (1993); NCRP (1991)
Nb	5.0×10^{-4}	3.0×10^{-7}	-1.0	IAEA (1993); NCRP (1991)
Mo	1.0×10^{-2}	1.0×10^{-3}	-0.90	IAEA (1993); NCRP (1991)

TABLE 11 (Cont.)

Element	Current Default Value	Suggested Value	Change[a]	Radiological Assessment Model Source
Tc	9.9×10^{-4}	1.0×10^{-4}	-0.90	IAEA (1993); NCRP (1991)
Ru	1.0×10^{-3}	2.0×10^{-3}	1.0	Baes et al. (1984); IAEA (1982); Kennedy and Strenge (1992); Napier et al. (1988); NCRP (1991); Ng (1982b); NRC (1983)
Rh	1.0×10^{-3}	NC	NC	Napier et al. (1988)
Pd	1.0×10^{-3}	NC	NC	Napier et al. (1988)
Ag	9.9×10^{-4}	3.0×10^{-3}	2.0	Baes et al. (1984); IAEA (1993); Kennedy and Strenge (1992); NCRP (1991)
Cd	1.6×10^{-2}	4.0×10^{-4}	-1.0	IAEA (1993); Napier et al. (1988)
Sn	9.9×10^{-4}	1.0×10^{-2}	9.1	Napier et al. (1988); NCRP (1991)
Sb	3.0×10^{-3}	1.0×10^{-3}	-0.67	Baes et al. (1984); IAEA (1982); Kennedy and Strenge (1992); Napier et al. (1988); NCRP (1991)
Te	5.0×10^{-2}	7.0×10^{-3}	-0.86	IAEA (1993); Napier et al. (1988); NCRP (1991)
I	2.0×10^{-2}	7.0×10^{-3}	-0.65	Baes et al. (1984); Kennedy and Strenge (1992)
Xe	0	NC	NC	Napier et al. (1988); NCRP (1991);
Cs	3.0×10^{-2}	NC	NC	Napier et al. (1988)
Ba	5.0×10^{-4}	2.0×10^{-4}	-0.60	IAEA (1982); NCRP (1991)
La	5.0×10^{-3}	2.0×10^{-3}	-0.60	IAEA (1982); NCRP (1991)
Ce	1.0×10^{-3}	2.0×10^{-5}	-0.98	IAEA (1993); NCRP (1991)
Pr	5.0×10^{-3}	2.0×10^{-3}	-0.60	NCRP (1991)
Nd	5.0×10^{-3}	2.0×10^{-3}	-0.60	NCRP (1991)
Pm	5.0×10^{-3}	2.0×10^{-3}	-0.60	IAEA (1982); NCRP (1991)
Sm	5.0×10^{-3}	2.0×10^{-3}	-0.60	IAEA (1982); NCRP (1991)
Eu	5.0×10^{-3}	2.0×10^{-3}	-0.60	IAEA (1982); NCRP (1991)
Gd	5.0×10^{-3}	2.0×10^{-3}	-0.60	Napier et al. (1988); NCRP (1991)
Tb	5.0×10^{-3}	2.0×10^{-3}	-0.60	NCRP (1991)
Ho	5.0×10^{-3}	2.0×10^{-3}	-0.60	NCRP (1991)
W	9.9×10^{-4}	4.0×10^{-2}	39	IAEA (1993); NCRP (1991)
Ir	9.9×10^{-4}	2.0×10^{-3}	1.0	Napier et al. (1988); NCRP (1991)
Hg	1.0×10^{-1}	NC	NC	Napier et al. (1988)
Pb	9.9×10^{-4}	8.0×10^{-4}	-0.19	IAEA (1982); NCRP (1991)
Bi	9.9×10^{-4}	2.0×10^{-3}	1.0	NCRP (1991)
Po	9.9×10^{-4}	5.0×10^{-3}	4.1	IAEA (1993); NCRP (1991)
Rn	0	NC	NC	Napier et al. (1988); NCRP (1991)

TABLE 11 (Cont.)

Element	Current Default Value	Suggested Value	Change[a]	Radiological Assessment Model Source
Ra	9.9×10^{-4}	1.0×10^{-3}	0.01	NCRP (1991)
Ac	5.0×10^{-3}	2.0×10^{-5}	-1.0	IAEA (1982); NCRP (1991)
Th	5.0×10^{-3}	1.0×10^{-4}	-1.0	IAEA (1982); NCRP (1991)
Pa	5.0×10^{-3}	NC	NC	Napier et al. (1988)
U	5.0×10^{-3}	3.4×10^{-4}	-0.93	IAEA (1993); NRC (1983)
Np	5.0×10^{-3}	1.0×10^{-3}	-0.80	IAEA (1982, 1993); Napier et al. (1988); NCRP (1991)
Pu	5.0×10^{-3}	1.0×10^{-4}	-1.0	NCRP (1991)
Am	5.0×10^{-3}	5.0×10^{-5}	-1.0	NCRP (1991)
Cm	5.0×10^{-3}	2.0×10^{-5}	-1.0	IAEA (1982); NCRP (1991)
Cf	5.0×10^{-3}	6.0×10^{-5}	-1.0	NCRP (1991)

[a] Change = (suggested value - default)/(default value).

[b] Not calculated.

[c] No change.

TABLE 12 Current RESRAD Default Values and Suggested Values for Milk/Feed Transfer Factors (pCi/L milk per pCi/daily intake)

Element	Current Default Value	Suggested Value	Change[a]	Radiological Assessment Model Source
H	0	1.0×10^{-2}	-[b]	NRC (1977)
Be	2.0×10^{-6}	NC[c]	NC	Napier et al. (1988); NCRP (1991)
C	0	1.2×10^{-2}	-	NRC (1977)
N	1.0×10^{-2}	NC	NC	NCRP (1991)
F	7.0×10^{-3}	NC	NC	Napier et al. (1988); NCRP (1991)
Na	4.0×10^{-2}	NC	NC	IAEA (1982); NCRP (1991); NRC (1977)
P	1.2×10^{-2}	1.6×10^{-2}	0.33	IAEA (1993); NRC (1983)
Cl	8.0×10^{-2}	2.0×10^{-2}	-0.75	Napier et al. (1988); NCRP (1991)
Ar	0	NC	NC	Napier et al. (1988); NCRP (1991)
K	7.0×10^{-3}	NC	NC	Baes et al. (1984); Kennedy and Strenge (1992); Napier et al. (1988); NCRP (1991)
Ca	8.0×10^{-3}	3.0×10^{-3}	-0.63	IAEA (1993); NCRP (1991)
Sc	2.5×10^{-6}	5.0×10^{-6}	1.0	Baes et al. (1984); Kennedy and Strenge (1992)
Cr	1.1×10^{-3}	2.0×10^{-3}	0.82	IAEA (1982); NCRP (1991); NRC (1983)
Mn	1.0×10^{-4}	3.0×10^{-4}	2.0	IAEA (1982); Napier et al. (1988); NCRP (1991)
Fe	6.0×10^{-4}	3.0×10^{-4}	-0.5	IAEA (1982); NCRP (1991)
Co	5.0×10^{-4}	2.0×10^{-3}	3	Baes et al. (1984); IAEA (1982); Kennedy and Strenge (1992); NCRP (1991); NRC (1983)
Ni	3.4×10^{-3}	2.0×10^{-2}	4.89	NCRP (1991)
Cu	7.0×10^{-3}	2.0×10^{-3}	-0.71	Napier et al. (1988); NCRP (1991)
Zn	6.0×10^{-3}	1.0×10^{-2}	0.67	Baes et al. (1984); IAEA (1982); Kennedy and Strenge (1992); Napier et al. (1988); NCRP (1991); NRC (1983)
As	3.0×10^{-3}	1.0×10^{-4}	-1.0	NCRP (1991)
Se	2.3×10^{-2}	1.0×10^{-2}	-0.57	NCRP (1991)
Br	2.5×10^{-2}	2.0×10^{-2}	-0.20	Baes et al. (1984); Kennedy and Strenge (1992); Napier et al. (1988); NCRP (1991); NRC (1983)
Kr	0	NC	NC	Napier et al. (1988); NCRP (1991)
Rb	1.0×10^{-2}	NC	NC	Baes et al. (1984); Kennedy and Strenge (1992); Napier et al. (1988); NCRP (1991)
Sr	1.5×10^{-3}	2.0×10^{-3}	0.33	NCRP (1991)

TABLE 12 (Cont.)

Element	Current Default Value	Suggested Value	Change[a]	Radiological Assessment Model Source
Y	5.0×10^{-6}	2.0×10^{-5}	3.0	Baes et al. (1984); IAEA (1982); Kennedy and Strenge (1992); NRC (1983)
Zr	2.5×10^{-6}	6.0×10^{-7}	-0.76	NCRP (1991)
Nb	1.2×10^{-3}	2.0×10^{-6}	-1.0	NCRP (1991)
Mo	4.0×10^{-3}	1.7×10^{-3}	-0.58	IAEA (1993); Napier et al. (1988)
Tc	1.2×10^{-2}	1.0×10^{-3}	-0.92	IAEA (1993); NCRP (1991)
Ru	5.0×10^{-7}	3.3×10^{-6}	5.6	IAEA (1993)
Rh	5.0×10^{-3}	NC	NC	Napier et al. (1988)
Pd	5.0×10^{-3}	NC	NC	Napier et al. (1988)
Ag	2.5×10^{-2}	NC	NC	Napier et al. (1988)
Cd	6.2×10^{-5}	1.0×10^{-3}	15	Baes et al. (1984); Kennedy and Strenge (1992)
Sn	1.3×10^{-3}	1.0×10^{-3}	-0.23	Baes et al. (1984); Kennedy and Strenge (1992); Napier et al. (1988); NCRP (1991)
Sb	7.5×10^{-4}	1.0×10^{-4}	-0.87	Baes et al. (1984); Kennedy and Strenge (1992); Napier et al. (1988); NCRP (1991)
Te	5.0×10^{-4}	NC	NC	NCRP (1991)
I	1.0×10^{-2}	NC	NC	Baes et al. (1984); IAEA (1982, 1993); Kennedy and Strenge (1992); NCRP (1991)
Xe	0	NC	NC	Napier et al. (1988); NCRP (1991)
Cs	5.0×10^{-3}	8.0×10^{-3}	0.60	IAEA (1982, 1993)
Ba	4.0×10^{-4}	5.0×10^{-4}	0.25	NCRP (1991)
La	2.5×10^{-6}	2.0×10^{-5}	7.0	Baes et al. (1984); IAEA (1982); Kennedy and Strenge (1992)
Ce	1.0×10^{-5}	3.0×10^{-5}	2.0	IAEA (1993)
Pr	2.5×10^{-6}	2.0×10^{-5}	7.0	Baes et al. (1984); Kennedy and Strenge (1992)
Nd	2.5×10^{-6}	2.0×10^{-5}	7.0	Baes et al. (1984); Kennedy and Strenge (1992); Napier et al. (1988)
Pm	2.5×10^{-6}	2.0×10^{-5}	7.0	Baes et al. (1984); IAEA (1982); Kennedy and Strenge (1992)
Sm	2.5×10^{-6}	2.0×10^{-5}	7.0	Baes et al. (1984); IAEA (1982); Kennedy and Strenge (1992); Napier et al. (1988);
Eu	2.5×10^{-6}	2.0×10^{-5}	7.0	Baes et al. (1984); IAEA (1982); Kennedy and Strenge (1992); Napier et al. (1988);
Gd	2.5×10^{-6}	2.0×10^{-5}	7.0	Baes et al. (1984); Kennedy and Strenge (1992)
Tb	2.5×10^{-6}	2.0×10^{-5}	7.0	Baes et al. (1984); Kennedy and Strenge (1992)

TABLE 12 (Cont.)

Element	Current Default Value	Suggested Value	Change[a]	Radiological Assessment Model Source
Ho	2.5×10^{-6}	2.0×10^{-5}	7.0	Baes et al. (1984); Kennedy and Strenge (1992)
W	2.5×10^{-4}	3.0×10^{-4}	0.20	Baes et al. (1984); Kennedy and Strenge (1992); Napier et al. (1988); NCRP (1991)
Ir	9.9×10^{-4}	2.0×10^{-6}	-1.0	Baes et al. (1984); Kennedy and Strenge (1992); Napier et al. (1988); NCRP (1991)
Hg	1.9×10^{-2}	5.0×10^{-4}	-1.0	NCRP (1991)
Pb	1.0×10^{-5}	3.0×10^{-4}	29	IAEA (1982); NCRP (1991)
Bi	2.5×10^{-4}	5.0×10^{-4}	1.0	Baes et al. (1984); IAEA (1982); Kennedy and Strenge (1992); Napier et al. (1988); NRC (1983)
Po	1.2×10^{-4}	3.4×10^{-4}	1.8	Baes et al. (1984); IAEA (1993); Kennedy and Strenge (1992)
Rn	0	NC	NC	Napier et al. (1988); NCRP (1991)
Ra	2.0×10^{-4}	1.0×10^{-3}	4.0	NCRP (1991)
Ac	2.5×10^{-6}	2.0×10^{-5}	7	Baes et al. (1984); IAEA (1982); Kennedy and Strenge (1992); Napier et al. (1988); NRC (1983)
Th	2.5×10^{-6}	5.0×10^{-6}	1.0	Baes et al. (1984); IAEA (1982); Kennedy and Strenge (1992); NCRP (1991); NRC (1983)
Pa	2.5×10^{-6}	5.0×10^{-6}	1.0	Baes et al. (1984); IAEA (1982); Kennedy and Strenge (1992); NCRP (1991); NRC (1983)
U	6.0×10^{-4}	NC	NC	Baes et al. (1984); IAEA (1982); Kennedy and Strenge (1992); Napier et al. (1988); NRC (1983)
Np	2.5×10^{-6}	5.0×10^{-6}	1.0	Baes et al. (1984); IAEA (1982, 1993); Kennedy and Strenge (1992); NRC (1983)
Pu	2.5×10^{-8}	1.0×10^{-6}	39	IAEA (1993); NCRP (1991)
Am	2.5×10^{-6}	2.0×10^{-6}	-0.20	NCRP (1991)
Cm	2.5×10^{-6}	2.0×10^{-6}	-0.20	NCRP (1991)
Cf	7.5×10^{-7}	NC	NC	Kennedy and Strenge (1992); Napier et al. (1988)

[a] Change = (suggested value - default)/(default value).

[b] Not calculated.

[c] No change.

TABLE 13 Current RESRAD Default Values and Suggested Values for Aquatic Bioaccumulation Factors for Freshwater Fish (Bq/kg freshwater fish per Bq/L water)

Element	Current Default Value	Suggested Value	Change[a]	Radiological Assessment Model Source
H	9.0×10^{-1}	1	0.11	IAEA (1993); Kennedy and Strenge (1992); NCRP (1991)
Be	2.0	1.0×10^{2}	49	IAEA (1993); NCRP (1991)
C	4.6×10^{3}	5.0×10^{4}	9.9	IAEA (1993); NCRP (1991)
N	0	1.5×10^{5}	-[b]	Kennedy and Strenge (1992); NCRP (1991)
F	1.0×10^{1}	NC[c]	NC	Kennedy and Strenge (1992); NCRP (1991)
Na	1.0×10^{2}	2.0×10^{1}	-0.80	IAEA (1982, 1993); NCRP (1991); Thompson et al. (1972)
P	1.0×10^{5}	5.0×10^{4}	-0.50	IAEA (1993); NCRP (1991)
Cl	1.3×10^{2}	1.0×10^{3}	6.7	NCRP (1991)
Ar	1.0	0	-1.0	NCRP (1991)
K	1.0×10^{3}	NC	NC	Kennedy and Strenge (1992)
Ca	4.0×10^{1}	1.0×10^{3}	24	NCRP (1991)
Sc	2.0	1.0×10^{2}	49	IAEA (1993); Kennedy and Strenge (1992); NCRP (1991); Thompson et al. (1972)
Cr	2.0×10^{1}	2.0×10^{2}	9.0	IAEA (1982, 1993); Kennedy and Strenge (1992); NCRP (1991); NRC (1977)
Mn	4.0×10^{2}	NC	NC	IAEA (1982, 1993); Kennedy and Strenge (1992); NRC (1977)
Fe	1.0×10^{2}	2.0×10^{2}	1.0	IAEA (1993); NCRP (1991)
Co	5.0×10^{1}	3.0×10^{2}	5.0	IAEA (1982, 1993); NCRP (1991)
Ni	1.0×10^{2}	NC	NC	IAEA (1982, 1993); Kennedy and Strenge (1992); NCRP (1991); NRC (1977); Thompson et al. (1972)
Cu	5.0×10^{1}	2.0×10^{2}	3.0	IAEA (1993); NCRP (1991)
Zn	2.0×10^{3}	1.0×10^{3}	-0.50	IAEA (1982, 1993); NCRP (1991); Thompson et al. (1972)
As	3.0×10^{2}	NC	NC	
Se	1.7×10^{2}	2.0×10^{2}	0.2	NCRP (1991)
Br	4.2×10^{2}	NC	NC	Kennedy and Strenge (1992); NRC (1977)
Kr	1.0	0	-1.0	NCRP (1991)
Rb	2.0×10^{3}	NC	NC	IAEA (1993); Kennedy and Strenge (1992); NCRP (1991); NRC (1977)
Sr	3.0×10^{1}	6.0×10^{1}	1.0	IAEA (1982, 1993); NCRP (1991)
Y	2.5×10^{1}	3.0×10^{1}	0.20	IAEA (1982, 1993); NCRP (1991)
Zr	3.3	3.0×10^{2}	90	IAEA (1982, 1993); NCRP (1991)
Nb	3.0×10^{4}	3.0×10^{2}	-0.99	IAEA (1982, 1993); NCRP (1991)

812

TABLE 13 (Cont.)

Element	Current Default Value	Suggested Value	Change[a]	Radiological Assessment Model Source
Mo	1.0×10^1	NC	NC	IAEA (1993); Kennedy and Strenge (1992); NCRP (1991); NRC (1977, 1983); Thompson et al. (1972)
Tc	1.5×10^1	2.0×10^1	0.33	IAEA (1982, 1993); NCRP (1991)
Ru	1.0×10^1	NC	NC	IAEA (1982, 1993); NCRP (1991); NRC (1977); Thompson et al. (1972)
Rh	1.0×10^1	NC	NC	IAEA (1993); Kennedy and Strenge (1992); NRC (1977)
Pd	1.0×10^1	NC	NC	Kennedy and Strenge (1992); NCRP (1991)
Ag	2.3	5	1.20	IAEA (1993)
Cd	2.0×10^2	NC	NC	Kennedy and Strenge (1992); NCRP (1991)
Sn	3.0×10^3	NC	NC	IAEA (1993); Kennedy and Strenge (1992); NCRP (1991)
Sb	1.0	1.0×10^2	99	IAEA (1993); NCRP (1991)
Te	4.0×10^2	NC	NC	IAEA (1982, 1993); Kennedy and Strenge (1992); NCRP (1991); NRC (1977)
I	1.5×10^1	4.0×10^1	1.7	IAEA (1982, 1993); NCRP (1991); NRC (1983)
Xe	1.0	0	-1.0	NCRP (1991)
Cs	2.0×10^3	NC	NC	IAEA (1982, 1993); Kennedy and Strenge (1992); NCRP (1991); NRC (1977)
Ba	4.0	NC	NC	IAEA (1982, 1993); NCRP (1991); NRC (1977)
La	2.5×10^1	3.0×10^1	0.20	IAEA (1982, 1993); NCRP (1991)
Ce	1.0	3.0×10^1	29	IAEA (1982, 1993); NCRP (1991)
Pr	2.5×10^1	1.0×10^2	3.0	IAEA (1993); NCRP (1991)
Nd	2.5×10^1	1.0×10^2	3.0	IAEA (1993); NCRP (1991)
Pm	2.5×10^1	3.0×10^1	0.20	IAEA (1982, 1993); NCRP (1991)
Sm	2.5×10^1	NC	NC	Kennedy and Strenge (1992); NCRP (1991)
Eu	2.5×10^1	5.0×10^1	1.0	IAEA (1993); NCRP (1991)
Gd	2.5×10^1	NC	NC	Kennedy and Strenge (1992)
Tb	2.5×10^1	NC	NC	Kennedy and Strenge (1992); NCRP (1991)
Ho	2.5×10^1	NC	NC	Kennedy and Strenge (1992)
W	1.2×10^3	NC	NC	Kennedy and Strenge (1992); NRC (1977)
Ir	5.0×10^1	1.0×10^1	-0.80	Kennedy and Strenge (1992); NCRP (1991)
Hg	2.0×10^4	1.0×10^3	-0.95	IAEA (1993); Kennedy and Strenge (1992); NCRP (1991)
Pb	1.0×10^2	3.0×10^2	2.0	IAEA (1982, 1993); NCRP (1991)
Bi	1.5×10^1	NC	NC	Kennedy and Strenge (1992); NCRP (1991)
Po	5.0×10^2	1.0×10^2	-0.80	NCRP (1991)
Rn	5.7×10^1	0	-1.0	NCRP (1991)

TABLE 13 (Cont.)

Element	Current Default Value	Suggested Value	Change[a]	Radiological Assessment Model Source
Ra	5.0×10^1	NC	NC	IAEA (1982, 1993); NCRP (1991); Thompson et al. (1972)
Ac	2.5×10^1	1.5×10^1	-0.40	NCRP (1991)
Th	3.0×10^1	1.0×10^2	2.3	IAEA (1993); Kennedy and Strenge (1992); NCRP (1991)
Pa	1.1×10^1	1.0×10^1	-0.09	IAEA (1982, 1993); NCRP (1991)
U	2.0	1.0×10^1	4.0	IAEA (1982, 1993); NCRP (1991); Thompson et al. (1972)
Np	1.0×10^1	3.0×10^1	2.0	IAEA (1993); NCRP (1991)
Pu	3.5	3.0×10^1	7.6	IAEA (1993); NCRP (1991)
Am	2.5×10^1	3.0×10^1	0.20	IAEA (1982, 1993); NCRP (1991)
Cm	2.5×10^1	3.0×10^1	0.20	IAEA (1982, 1993); NCRP (1991)
Cf	2.5×10^1	NC	NC	Kennedy and Strenge (1992); NCRP (1991)

[a] Change = (suggested value - default value)/(default value).

[b] Not calculated.

[c] No change.

TABLE 14 Compilation of Aquatic Bioaccumulation Factors for Crustacea and Mollusks in Marine Environments (Bq/kg organism per Bq/L water)

	Crustacea			Mollusks			Shellfish
Element	IAEA (1982)	IAEA (1985)	NRC (1983)	IAEA (1982)	IAEA (1985)	NRC (1983)	NCRP (1991)
H	-[a]	1	-	-	1	-	1
Be	-	-	-	-	-	-	2.0×10^2
C	-	2.0×10^4	-	-	2.0×10^4	-	2.0×10^3
N	-	-	-	-	-	-	6.0×10^4
F	-	-	-	-	-	-	4
Na	1	1.0×10^{-1}	3.0×10^{-1}	1	3.0×10^{-1}	2.0×10^{-1}	1.0×10^1
P	1×10^4	-	2.4×10^4	1×10^4	-	6.0×10^3	2.0×10^4
Cl	-	5.0×10^{-2}	-	-	5.0×10^{-2}	-	1
Ar	-	0	-	-	0	-	0
Ca	-	5.0	-	-	1.0×10^0	-	1
Sc	-	3.0×10^2	-	-	1.0×10^5	-	1.0×10^4
Cr	5×10^2	5.0×10^2	1.9×10^3	5×10^2	8.0×10^2	6.4×10^3	5.0×10^2
Mn	1×10^4	5.0×10^2	9.4×10^2	1×10^4	5.0×10^3	2.3×10^3	1.0×10^3
Fe	1×10^3	5.0×10^3	1.8×10^3	1×10^3	3.0×10^4	2.1×10^4	1.0×10^4
Co	1×10^3	5.0×10^3	2.2×10^2	1×10^3	5.0×10^3	2.4×10^3	1.0×10^3
Ni	1×10^2	1.0×10^3	-	1×10^2	2.0×10^3	-	1.0×10^2
Cu	-	-	-	-	-	-	1.7×10^3
Zn	4×10^3	5.0×10^4	1.3×10^4	1×10^5	3.0×10^4	1.5×10^4	2.0×10^4
As	-	-	-	-	-	-	1.0×10^3
Se	-	5.0×10^3	-	-	6.0×10^3	-	1.0×10^3
Br	-	-	-	-	-	-	1.0×10^1
Kr	-	1	-	-	1	-	0
Rb	-	-	-	-	-	-	2.0×10^1
Sr	1×10^1	2	1.5	1×10^1	1	9.6	1.0×10^1
Y	1×10^3	1.0×10^3	-	1×10^3	1.0×10^3	-	1.0×10^3
Zr	1×10^2	2.0×10^2	-	1×10^3	5.0×10^3	-	-
Nb	1×10^2	2.0×10^2	-	1×10^3	1.0×10^3	-	-
Mo	-	-	-	-	-	-	-
Tc	1×10^3	1.0×10^3	-	1×10^2	1.0×10^3	-	-
Ru	6×10^2	1.0×10^2	4.0×10^2	2×10^3	2.0×10^3	3.8×10^2	3.8×10^2
Rh	-	-	-	-	-	-	-

TABLE 14 (Cont.)

	Crustacea			Mollusks			Shellfish
Element	IAEA (1982)	IAEA (1985)	NRC (1983)	IAEA (1982)	IAEA (1985)	NRC (1983)	NCRP (1991)
Pd	-	3.0×10^2	-	-	3.0×10^2	-	2.0×10^3
Ag	5×10^3	5.0×10^3	9.5×10^2	1×10^5	1.0×10^4	5.9×10^3	5.0×10^3
Cd	-	1.0×104	-	-	2.0×10^4	-	2.5×10^5
Sn	-	5.0×10^4	1.7×10^2	-	5.0×10^2	4.4×10^2	3.0×10^2
Sb	3×10^2	4.0×10^2	-	1×10^2	2.0×10^2	-	3.0×10^2
Te	1×10^3	1.0×10^3	-	1×10^4	1.0×10^3	-	1.0×10^4
I	1×10^2	1.0×10^1	5.0×10	1×10^2	1.0×10^1	3.0×10	1.0×10^2
Xe	-	1	-	-	1	-	0
Cs	3×10^1	3.0×10^1	5.7×10	1×10^1	3.0×10^1	3.5×10	3.0×10^1
Ba	1×10^2	1	-	1×10^2	2.0×10^1	-	1.0×10^2
La	1×10^3	-	-	1×10^3	-	-	1.0×10^3
Ce	1×10^1	1.0×10^3	1.4×10^3	1×10^1	5.0×10^3	8.6×10^2	1.0×10^1
Pr	-	-	-	-	-	-	1.0×10^1
Nd	-	-	-	-	-	-	1.0×10^3
Pm	1×10^3	1.0×10^3	-	1×10^3	5.0×10^3	-	1.0×10^3
Sm	-	1.0×10^3	-	-	5.0×10^3	-	1.0×10^3
Eu	-	1.0×10^3	-	-	7.0×10^3	-	1.0×10^3
Gd	-	2.0×10^3	-	-	5.0×10^3	-	1.0×10^3
Tb	-	1.0×10^3	-	-	3.0×10^3	-	1.0×10^3
Ho	-	-	-	-	-	-	3.0×10^1
W	-	1.0×10^1	-	-	1.0×10^2	-	3.0×10^1
Ir	-	1.0×10^2	-	-	1.0×10^2	-	2.0×10^3
Hg	-	2.0×10^4	-	-	1.0×10^4	-	1.0×10^3
Pb	1×10^2	1.0×10^3	-	1×10^2	1.0×10^3	4.0×10	1.0×10^2
Bi	1×10^3	-	-	1×10^3	-	-	1.0×10^3
Po	2×10^4	5.0×10^4	-	2×10^4	1.0×10^4	-	2.0×10^4
Rn	-	-	-	-	-	-	0
Ra	1×10^2	1.0×10^2	1.4×10^2	1×10^2	1.0×10^3	1.3×10^3	1.0×10^2
Ac	-	1.0×10^3	-	-	1.0×10^3	-	5.0×10^1
Th	1×10^3	1.0×10^3	-	1×10^3	1.0×10^3	-	1.0×10^3
Pa	1×10^1	1.0×10^1	-	1×10^1	5.0×10^2	-	1.0×10^1
U	1×10^1	1.0×10^1	-	1×10^1	3.0×10^1	-	1.0×10^1
Np	1×10^2	1.0×10^2	-	1×10^3	4.0×10^2	-	1.0×10^3

TABLE 14 (Cont.)

	Crustacea			Mollusks			Shellfish
Element	IAEA (1982)	IAEA (1985)	NRC (1983)	IAEA (1982)	IAEA (1985)	NRC (1983)	NCRP (1991)
Pu	1×10^2	3.0×10^2	1.9×10^2	1×10^3	3.0×10^3	2.6×10^2	1.0×10^2
Am	2×10^2	5.0×10^2	2.0×10^2	2×10^3	2.0×10^4	-	2.0×10^3
Cm	2×10^2	5.0×10^2	-	2×10^3	3.0×10^4	-	2.0×10^2
Cf	-	5.0×10^2	-	-	2.0×10^4	-	1.0×10^3

[a] Data not listed.

5 REFERENCES

Baes, C.F., III, et al., 1984, *A Review and Analysis of Parameters for Assessing Transport of Environmentally Released Radionuclides through Agriculture,* report ORNL-5786, Oak Ridge National Laboratory, Oak Ridge, Tenn.

Baker, D.A., et al., 1976, *Food — An Interactive Code to Calculate Internal Radiation Doses from Contaminated Food Products*, report BNWL-SA-5523, Pacific Northwest Laboratory, Richland, Wash.

Beresford, N.A., et al., 1989, "The Effect of Treating Pastures with Bentonite on the Transfer of Cs-137 from Grazed Herbage to Sheep," *Journal of Environmental Radiation* 9:251-264.

Bishop, G.P., et al., 1989, *Review of Literature for Chlorine, Technetium, Iodine and Neptunium,* report NSS/R193, Nirex Radioactive Waste Disposal Safety Studies, U.K. Nirex Ltd., Harwell, England.

Blaylock, B.G., 1982, "Radionuclide Data Bases Available for Bioaccumulation Factors for Freshwater Biota," *Nuclear Safety* 23(4):427-438.

Booth, R.S., et al., 1971, "A Systems Analysis Methodology for Predicting Dose to Man from a Radioactivity Contaminated Terrestrial Environment," *Proceedings of the Third National Symposium on Radioecology,* report CONF-710501, U.S. Atomic Energy Commission, Oak Ridge, Tenn.

Copeland, R.A., et al., 1973, *Trace Element Distributions in Lake Michigan Fish: A Baseline Study with Calculations of Concentration Factors and Equilibrium Radioisotope Distributions,* REG Special Report No. 2, University of Michigan, Ann Arbor, Mich.

Coughtrey, P.C., and M.C. Thorne, 1983, *Radionuclide Distribution and Transport in Terrestrial and Aquatic Ecosystems, A Critical Review of Data*, Vol. 2, A.A. Balkema, Rotterdam.

Coughtrey, P.C., et al., 1983, *Radionuclide Distribution and Transport in Terrestrial and Aquatic Ecosystems,* Vol. 1, A.A. Balkema, Rotterdam.

Davis, J.J., and R.F. Foster, 1958, "Bioaccumulation of Radioisotopes through Aquatic Food Chains," *Ecology* 39(3):530-535.

Eisler, R., 1981, *Trace Metal Concentrations in Marine Organisms*, Pergamon Press, New York.

Fletcher, J.F., and W.L. Dotson, 1971, *HERMES - A Digital Computer Code for Estimating Regional Radiological Effects from the Nuclear Power Industry*, report HEDL-TME-71-168, Hanford Engineering Development Laboratory, Richland, Wash.

223

Friend, A.G., et al., 1965, *Behavior of Certain Radionuclides Released into Fresh-Water Environments*, Publication 999-RH-13, U.S. Public Health Service, Washington, D.C., June.

Frissel, M. (ed.), 1989, *VIth Report of the Working Group Soil-to-Plant Transfer Factors,* Report of the Working Group Meeting in Guttannen, Grimselpass, Switzerland, May 24-26, 1968, International Union of Radioecologists, Commission of European Communities.

Garner, R.J., 1972, *Transfer of Radioactive Materials from the Terrestrial Environment to Animals and Man,* CRC Press, Cleveland, Ohio.

Gilbert, T.L., et al., 1989, *A Manual for Implementing Residual Radioactive Material Guidelines,* report ANL/ES-160 (DOE/CH/8901), prepared by Argonne National Laboratory, Energy and Environmental Systems Division, Argonne, Ill., for U.S. Department of Energy, Assistant Secretary for Nuclear Energy, Washington, D.C., June.

Grogan, H.A., 1985, *Concentration Ratios for BIOPATH: Selection of the Soil-to-Plant Concentration Ratio Database,* report EIR-Bericht Nr. 575, Swiss Federal Institute for Reactor Research, Geneva, Switzerland.

Harvey, R.S., 1964, "Uptake of Radionuclides by Freshwater Algae and Fish," *Health Physics* 10(4):243-247.

Hoffman, F.O., and C.F. Baes III (eds.), 1979, *A Statistical Analysis of Selected Parameters for Predicting Food Chain Transport and Internal Dose of Radionuclides,* report NUREG/CR-1004, ORNL/NUREG/TM-282, Oak Ridge National Laboratory, Oak Ridge, Tenn.

Howard, B.J., et al., 1989, "Transfer of Radiocesium from Different Environmental Sources to Ewes and Suckling Lambs," *Health Physics* 57:579-586.

IAEA (International Atomic Energy Agency), 1975, *Impacts of Nuclear Releases into the Aquatic Environment*, Proceedings of the IAEA Symposium, Otaniemi, Finland, 30 June-4 July, 1975, IAEA, Vienna, Austria.

IAEA, 1978, *The Radiological Basis of the IAEA Revised Definition and Recommendations Concerning High-Level Radioactive Waste Unsuitable for Dumping at Sea*, Technical Document 211, Vienna, Austria.

IAEA, 1982, *Generic Models and Parameters for Assessing the Environmental Transfer of Radionuclides from Routine Releases; Exposure of Critical Groups,* Safety Series No. 57, Vienna, Austria.

IAEA, 1985, *Sediment Kds and Concentration Factors for Radionuclides in the Marine Environment,* Technical Report Series No. 247, Vienna, Austria.

IAEA, 1993, Unpublished data, Vienna, Austria.

IUR (International Union of Radioecologists), 1989, *Sixth Report of the Working Groups on Soil-to-Plant Transfer Factors*, RIVM, Bilthoven, The Netherlands.

Johnson, J.E., et al., 1968, "Metabolism of Radioactive Cesium (Cs-134 and Cs-137) and Potassium of Dairy Cattle as Influenced by High and Lower Forage Diets," *Journal of Nutrition* 94:282-288.

Johnson, J.E., et al., 1988, "Transfer Coefficients of Selected Radionuclides to Animal Products, 1. Comparison of Milk and Meat from Dairy Cows and Goats," *Health Physics* 54: 161-166.

Kennedy, W.E., Jr., and D.L. Strange, 1992, *Residual Radioactive Contamination from Decommissioning; Volume 1: Technical Basis for Translating Contamination Levels to Annual Total Effective Dose Equivalent*, report NUREG/CR-5512, Pacific Northwest Laboratory, Richland, Washington.

Killough, G., and L. McKay, 1976, *BIORA2 Bioaccumulation Factors for Freshwater Biota,* report ORNL-4992, Oak Ridge National Laboratory, Oak Ridge, Tenn.

Little, C.A., 1979, "The Coefficient for the Transfer of Radionuclides from Annual Intake to Meat, F_f," in *A Statistical Analysis of Selected Parameters for Predicting Food Chain Transport and Internal Dose of Radionuclides,* report ORNL/NUREG/TM-282, Oak Ridge National Laboratory, Oak Ridge, Tenn.

McDowell-Boyer, L.M., et al., 1979, *Review and Recommendations of Dose Conversion Factors and Environmental Transport Parameters for ^{210}Pb and ^{226}Ra,* report NUREG/CR-0574, U.S. Nuclear Regulatory Commission, Washington, D.C.

McDowell-Boyer, L.M., and C.F. Baes III, 1980, "Terrestrial Food Chain Transport," in *Recommendations Concerning Models and Parameters Best Suited to Breeder Reactor Environmental Radiological Assessments*, report ORNL-5592, Oak Ridge National Laboratory, Oak Ridge, Tenn.

Moore, R.E., et al., 1979, *AIRDOS-EPA: A Computerized Methodology for Estimating Environmental Concentrations and Dose to Man from Airborne Releases of Radionuclides*, report ORNL-5532, Oak Ridge National Laboratory, Oak Ridge, Tenn.

Morgan, J.E., and C.J. Beetham, 1990, *Review of Literature for Radium, Protactinium, Tin, and Carbon*, Nirex Radioactive Waste Disposal Safety Studies, U.K. Nirex Ltd., Harwell, England.

Napier, B.A., et al., 1988, *GENII — The Hanford Environmental Radiation Dosimetry Software System; Volume 2: Users' Manual*, report PNL-6584, Vol. 2, Pacific Northwest Laboratory, Richland, Wash., Nov.

NAS (National Academy of Sciences-National Research Council), 1971, *Radioactivity in the Marine Environments*, Washington, D.C.

225

NCRP (National Council on Radiation Protection and Measurements), 1991, unpublished data, Washington, D.C.

Newman, G., 1985, *Concentration Factors for Stable Metals and Radionuclides in Fish, Mussels, and Crustaceans — A Literature Survey*, report SNUPM 1976E, National Swedish Environmental Protection Board, Solna, Sweden.

Ng, Y.C., et al., 1968, *Prediction of the Maximum Dosage to Man from the Fallout of Nuclear Devices; IV: Handbook for Estimating the Maximum Internal Dose from Radionuclides Released to the Biosphere*, report UCRL-50163, Part IV, Lawrence Livermore National Laboratory, Livermore, Calif.

Ng, Y.C., et al., 1977, *Transfer Coefficients for the Prediction of the Dose to Man Via the Forage-Cow-Milk Pathway from Radionuclides Released to the Biosphere,* report UCRL-51939, Lawrence Livermore National Laboratory, Livermore, Calif.

Ng, Y.C., et al., 1979a, "Transfer Coefficients for Terrestrial Food Chain — Their Derivation and Limitations," in *Radioaktivitat and Umwelt*, Proceedings of the 12th Annual Conference of the Fachverband fur Strahlenchutz, Norderney, West Germany, pp. 455-481.

Ng, Y.C., et al., 1979b, "Transfer Factors for Assessing the Dose from Radionuclides in Agriculture Products," in *Biological Implications of Radionuclides Released from Nuclear Industries*, Vol. 2, International Atomic Energy Agency, Vienna, Austria.

Ng, Y.C., et al., 1982a, *Soil-to-Plant Concentration Factors for Radiological Assessments,* report NUREG/CR-2975, UCID-19463, Lawrence Livermore National Laboratory, Livermore, Calif.

Ng, Y.C., et al., 1982b, *Transfer Coefficients for Assessing the Dose from Radionuclides in Meat and Eggs,* report NUREG/CR-2976, UCID-19464, Lawrence Livermore National Laboratory, Livermore, Calif.

NRC (U.S. Nuclear Regulatory Commission), 1977, *Regulatory Guide 1.109, Rev. 1, Calculation of Annual Doses to Man from Routine Releases of Reactor Effluents for the Purpose of Evaluating Compliance with 10 CFR Part 50, Appendix I*, Washington, D.C.

NRC, 1983, *Radiological Assessment: A Textbook on Environmental Dose Analysis,* report NUREG/CR-3332 (ORNL-5968), prepared by Oak Ridge National Laboratory, Oak Ridge, Tenn., for U.S. Nuclear Regulatory Commission, Washington, D.C.

NRPB/CEA (National Radiological Board/Commissariat a l' Energie Atomique), 1979, *Methodology for Evaluating the Radiological Consequences of Radioactive Effluents Released in Normal Operations,* report U/386579e, Commission of the European Communities, Brussels.

226

Onishi, Y., et al., 1981, *Critical Review: Radionuclide Transport, Sediment Transport, and Water Quality Mathematical Modeling; and Radionuclide Adsorption / Desorption Mechanisms,* report NUREG/CR-1322, PNL-2901, Pacific Northwest Laboratory, Richland, Wash.

Poston, T.M., and D.C. Klopfer, 1986, *A Literature Review of the Concentration Ratios of Selected Radionuclides in Freshwater and Marine Fish,* report PNL-5484, Pacific Northwest Laboratory, Richland, Wash.

Thompson, S.E., et al., 1972, *Concentration Factors of Chemical Elements in Edible Aquatic Organisms,* report UCRL-50567, Lawrence Livermore National Laboratory, Livermore, Calif.

Van Bruwaene, R., et al., 1982, "Metabolism of Antimony-124 in Lactating Dairy Cows," *Health Physics* 43:733-738.

Vanderploeg, H.A., et al., 1975, *Bioaccumulation Factors for Radionuclides in Freshwater Biota,* report ORNL-5002, ESD Publication No. 783, Oak Ridge National Laboratory, Oak Ridge, Tenn.

Vinogradov, A.P., 1953, *The Elementary Chemical Composition of Marine Organisms,* Sears Foundation for Marine Research, Yale University, New Haven, Conn.

227
227